Using traditional modelling approaches for a MBR system to investigate alternate approaches based on system identification procedures for improved design and control of a wastewater treatment process

Parneet Paul

September 2011

A thesis submitted in partial fulfilment of the requirements for the Degree of
Doctor of Philosophy
Awarded by
De Montfort University

Process Control - Water Software Systems, Dept. of Engineering, De Montfort University
in collaboration with Aquabio Ltd, ITT Sanitaire Ltd and Northern Ireland Water

This work was sponsored by the Technology Programme of the TSB (Technology Strategy Board)
TP/3/DSM/6/I/15123

Abstract

The specific research work described in this thesis forms part of a much larger research project that was funded by the Technology Programme of the UK Government. This larger project considered improving the design and efficiency of membrane bioreactor (MBR) plant by using modelling, simulation and laboratory methods.

This research work uses phenomenological mechanistic models based on MBR filtration and biochemical processes to measure the effectiveness of alternative behavioural models based upon input-output system identification methods. Both model types are calibrated and validated using similar plant layouts and data sets derived for this purpose.

Results prove that although both approaches have their advantages, they also have specific disadvantages as well. In conclusion, the MBR plant designer and/or operator who wishes to use good quality, calibrated models to gain a better understanding of their process, should carefully consider which model type is selected based upon on what their initial modelling objectives are (e.g. using either a physically mechanistic model or an input-output behaviourial model). Each situation usually proves unique. In this regard, this research work creates a "Model Conceptualisation Procedure" for a typical MBR which can be used by future researchers as a theoretical framework which underpins any newly created model type.

There has been insufficient work completed to date on using a times series input-output approach in the model development of a wastewater treatment plant, so only general conclusions can be made from this research work. However, it can be stated that this novel approach seems to be applicable for a membrane filtration model if care it taken to select appropriate input-output model structures, such as those suggested in the "Model Conceptualisation Procedure". In the case of the development of a MBR biological model, it is thought that a conventional Activated Sludge model produced by the IWA could be coupled to a input-output model structure as suggested by this report to give a hybrid model structure that may have the advantages of both model types. Further research work is needed in this area.

Future work that should follow on from this research study should focus on whether these input-output models could be used for predictive control purposes, whether an integrated model could be created, and whether a benchmark could be created for the three main MBR configurations.

Acknowledgements

Firstly I would like to thank my PhD Supervisors for all their support and encouragement in this difficult endeavour. They are Professor Bogumil Ulanicki, Head of Dept. of Engineering and Director of Research at Process Control - Water Software Systems, De Montfort University, and Mr Richard Hill, Director of Whitewater Limited Consulting Engineers, and my PhD Technical Advisor, Dr Alan Merry, Technical Director, ITT Sanitaire.

I am also grateful for support received from the following Industrial collaborators: Mr Steve Goodwin, Managing Director, Aquabio Limited, and Mr Sam Irwin and Mr Steven McColl from Northern Ireland Water.

I would also like to credit considerable assistance I received, particularly in the difficult modelling work, from Research Fellow, Mr Tomasz Janus, former Research Assistant, Mr Hossam Abeldegiud, and former Research Students, Mr Frank Lueder and Mr Christoph Hartung. Without their kind help and support I would not have been able to complete this research work.

Finally I dedicate this thesis work to my recently widowed Mother, Mrs Prem Lata Paul, and my late Father, Mr Sham Lall Paul.

Parneet Paul BSc(Eng) MSc MRes C.WEM CEng CEnv FCIWEM MICE MIChemE
Lecturer in Civil Engineering - Hydraulics/Environmental Fluid Mechanics
Course Director, MSc Water Engineering
Dept. of Civil Engineering
School of Engineering and Design
Brunel University
Uxbridge
Middlesex, UB8 3PH, UK

Contents

List of Figures

List of Tables

Abbreviations and Acronyms

AI artificial intelligence 24

ANN artificial neural network 24

ARIMA autoregressive integrated moving average 45

ARX autoregressive exogenous 28

ARMAX autoregressive moving average exogenous 28

ASI actuator sensor interface 87

ASM1 Activated Sludge Model No.1 22

ASM2 Activated Sludge Model No.2 47

ASM2d Activated Sludge Model No.2d 42

ASM3 Activated Sludge Model No.3 22

AUC area under curve 104

BAP biomass-associated products 42

BSA bovine serum albumen 32

CA cellulose acetate 32

CFD computational fluid dynamics 39

CFV crossflow velocity xxiii

CiP cleaning in place 14

CM capillary membrane 10

CST capillary suction time 32

CUEDSID Cambridge University's Enhanced System Identification Toolbox for Matlab© 67

DAF dissolved air flotation 110

DO dissolved oxygen 22

DOC dissolved organic carbon 30

DSVI diluted sludge volume index 84

DWF dry weather flow 130

F/M food-to-microorganism 22

FNN fuzzy neural networks 46

FP flat plate/sheet 10

GFC glass fibre cloth 77

GUI graphical user interface 27

HF hollow fibre 10

HMI human-machine-interface 81

HPLC high pressure liquid chromatography 104

HRT hydraulic retention time 41

IAE Integral Absolute Error 48

IDE integral-differential equation 36

ISE Integral Square Error 48

IWA International Water Association 6

MBR membrane bioreactor 1

MF microfiltration 8

MIMO multi-input multi-output 28

MISO multi-input single output 28

MP microbial product 44

MPC model predictive control 48

MT multi-tubular 10

MVS multivariate statistical 24

NF nanofiltration 12

PCA principal component analysis 24

p.e. population equivalent 130

PES polyethersulfone 15

PI proportional integral 48

PID piping and instrumentation diagram 82

PLC programmable logic circuit 111

PLS partial least squares 24

PVDF polyvinyldifluoro 15

RO reverse osmosis 93

SBR sequence batch reactor 32

SCADA supervisory control and data acquisition 111

SEC size exclusion chromatography 104

SI scum index 84

SISO single input single output 28

SMP soluble microbial products xxiv

SPES sulfonated polyethersulfone 32

SQP sequential quadratic programming 48

SRF specific resistance to filtration 84

SRT solids retention time 22

SSVI stirred sludge volume index 84

SVI sludge volume index 45

TKN Total Kjeldahl Nitrogen 31

TMP trans-membrane pressure 14

TN Total Nitrogen 31

TP Total Phosphorous 76

TSB Technology Strategy Board 1

TSS Total suspended solids 46

TTF time-to-filter 84

UAP utilisation-associated products 42

UF ultrafiltration 8

UV ultra violet 113

VSS volatile suspended solids 45

WWTP wastewater treatment plant 6

Nomenclature for Chapter 2

General wastewater treatment terms

BOD Biochemical oxygen demand (mg/l)

COD Chemical oxygen demand (mg/l)

COD_{fil} Filtered chemical oxygen demand (mg/l)

$TSS/MLSS$ Total suspended solids/mixed liquor suspended solids (mg/l)

TN Total Nitrogen (made up of organic Nitrogen, Ammonia and Nitrate levels) (mg/l)

TP Total Phosphorous (mg/l)

F/M food-to-microorganism ratio

HRT Hydraulic Retention Time

SRT Solids Retention Time

Membrane fouling terms

Q Volumetric flow rate (m^3/s)

J Filtrate flux (m/s)

$\delta p/TMP$ trans-membrane pressure (Pa)

R_m Resistance of the clean membrane (m^{-1})

R_{total} Total resistance of membrane and deposit combined (m^{-1})

μ Viscosity (kg/m^3)

SMP Soluble microbial products made up of proteins and polysaccharides (mg/l)

EPS Extracellular polymeric substances (mg/l)

Activated Sludge ASM1 / ASM3 component states

S_S/X_S Readily/slowly biodegradable substrate (mg/l)

S_I/X_I Soluble/particulate inert concentration (mg/l)

$X_{BH}(orX_H)$ Heterotrophic biomass concentration (mg/l)

$X_{BA}(orX_A)$ Autotrophic biomass concentration (mg/l)

$S_O(orS_{O2})$ Dissolved oxygen concentration (mg/l)

$S_{NO}(orS_{NOX})$ Nitrate and nitrite nitrogen concentration (mg/l)

$S_{NH}(orS_{NH4})$ Ammonium concentration (mg/l)

S_{ND}/X_{ND} Soluble/particulate organic nitrogen concentration (mg/l)

X_{STO} Cell internal storage product of heterotrophic organisms (mg/l)

S_{ALK} Alkalinity (measures pH level) in soluble $CaCO_3$ concentration (mg/l)

Nomenclature for Chapter 3

Conceptualisation of crossflow MBR model structures

Bioreactor - Inflow input vector

q_{in} Flow rate into plant

COD_{in} COD (Chemical Oxygen Demand) into plant

TKN_{in} Total Kjeldahl Nitrogen into plant (made up of organic nitrogen and ammonia levels)

TP_{in} Total Phosphorous into plant

$S_{PS,in}$ Soluble polysaccharides into plant (responsible for irreversible fouling, part of SMP concentration)

$S_{PP,in}$ Soluble polyproteins into plant (responsible for irreversible fouling, part of SMP concentration)

$X_{TSS,in}$ Total suspended solids into plant (responsible for reversible fouling)

$X_{VSS,in}$ Total volatile suspended solids into plant (responsible for reversible fouling)

$S_{ALK,in}$ Alkalinity into plant (measures pH level)

$S_{O,in}$ Dissolved oxygen concentration into plant

$X_{EPS,in}$ Bound (fixed) extracellular polymeric substances (EPS) into plant

μ_{in} Fluid viscosity into plant

T_{in} Fluid temperature into plant

Bioreactor - Manipulated control vector

q_{air} Air flow rate into bioreactor plant as operator control variable

q_{waste} Wastage flow rate out of bioreactor plant as operator control variable

Bioreactor - Internal state vector

V_T Bioreactor tank volume

COD COD (Chemical Oxygen Demand) in bioreactor

TKN Total Kjeldahl Nitrogen in bioreactor (made up of organic nitrogen and ammonia levels)

TP Total Phosphorous in bioreactor

S_{PS} Soluble polysaccharides in bioreactor (responsible for irreversible fouling, part of SMP concentration)

S_{PP} Soluble polyproteins in bioreactor (responsible for irreversible fouling, part of SMP concentration)

X_{MLSS} Mixed liquor suspended solids in bioreactor (responsible for reversible fouling)

X_{MLVSS} Mixed liquor volatile suspended solids in bioreactor (responsible for reversible fouling)

S_{ALK} Alkalinity in bioreactor (measures pH level)

S_O Dissolved oxygen concentration in bioreactor

X_{EPS} Bound (fixed) extracellular polymeric substances (EPS) in bioreactor

μ Fluid viscosity in bioreactor

T Fluid temperature in bioreactor

Bioreactor - Wastage vector additional state

q_{out} Wastage rate out of bioreactor

Bioreactor - Recirculation flow rate vector

q_{rec} Recirculation flow rate

COD_{rec} COD (Chemical Oxygen Demand) in recirculation flow rate

TKN_{rec} Total Kjeldahl Nitrogen in recirculation flow rate (made up of organic nitrogen and ammonia levels)

TP_{rec} Total Phosphorous in recirculation flow rate

$S_{PS,rec}$ Soluble polysaccharides in recirculation flow rate (responsible for irreversible fouling, part of SMP concentration)

$S_{PP,rec}$ Soluble polyproteins in recirculation flow rate (responsible for irreversible fouling, part of SMP concentration)

$X_{MLSS,rec}$ Mixed liquor suspended solids in recirculation flow rate (responsible for reversible fouling)

$X_{MLVSS,rec}$ Mixed liquor volatile suspended solids in recirculation flow rate (responsible for reversible fouling)

$S_{ALK,rec}$ Alkalinity in recirculation flow rate (measures flow pH level)

$S_{O,rec}$ Dissolved oxygen concentration in recirculation flow rate

$X_{EPS,rec}$ Bound (fixed) extracellular polymeric substances (EPS) in recirculation flow rate

μ_{rec} Fluid viscosity in recirculation flow rate

T_{rec} Fluid temperature in recirculation flow rate

Membrane - Manipulated control vector

ω_{pump} Recirculation pump speed for flow across membrane (higher speed $\Rightarrow$ higher cake removal)

$\nu_{throttle}$ Recirculation throttle valve setting for membrane (valve more closed $\Rightarrow$ higher TMP across membrane $\Rightarrow$ more fouling on membrane)

f_{bwash} Backwash flow intensity and duration ((higher intensity and duration $\Rightarrow$ higher pore constriction and pore blockage removal)

Membrane - Internal state vector

irreversible fouling Internal state variable related to pore constriction. Not specified here since will be specific for each fouling model

reversible fouling Internal state variable related to pore blocking. Not specified here since will be specific for each fouling model

cake Internal state variable related to cake build up. Not specified here since will be specific for each fouling model

Membrane - Permeate flow rate vector

TMP Transmembrane pressure difference across membrane

q_{perm} Permeate flow rate

COD_{perm} COD (Chemical Oxygen Demand) in permeate flow rate

TKN_{perm} Total Kjeldahl Nitrogen in permeate flow rate (made up of organic nitrogen and ammonia levels)

TP_{perm} Total Phosphorous in permeate flow rate

$S_{PS,perm}$ Soluble polysaccharides in permeate flow rate (responsible for irreversible fouling, part of SMP concentration)

$S_{PP,perm}$ Soluble polyproteins in permeate flow rate (responsible for irreversible fouling, part of SMP concentration)

$X_{TSS,perm}$ Total suspended solids in permeate flow rate (responsible for reversible fouling)

$X_{VSS,perm}$ Volatile suspended solids in permeate flow rate (responsible for reversible fouling)

$S_{ALK,perm}$ Alkalinity in permeate flow rate (measures flow pH level)

$S_{O,perm}$ Dissolved oxygen concentration in permeate flow rate

$X_{EPS,perm}$ Bound (fixed) extracellular polymeric substances (EPS) in permeate flow rate

μ_{perm} Fluid viscosity in permeate flow rate

T_{perm} Fluid temperature in permeate flow rate

Nomenclature for Chapter 4

Duclos-Orsello membrane fouling model

A_b Area of membrane blocked by foulant (m^2)

A_u Area of unblocked membrane (m^2)

C_b Bulk concentration (g/l) - equivalent to MLSS

f' Fractional amount of total foulant contributing to deposit growth

J_0 Initial flux rate of clean membrane (m/s)

J_b Filtrate flux within the blocked area (m/s)

J_u Filtrate flux within the unblocked (m/s)

Q Volumetric flow rate (m^3/s)

Q_0 Initial volumetric flow rate (m^3/s)

R_{inb} Resistance of the membrane and the resistance caused by pore constriction (m^{-1})

R_m Resistance of the clean membrane (m^{-1})

R_p Resistance of the deposit (m^{-1})

R_{total} Total resistance of membrane and deposit combined (m^{-1})

R' Specific protein layer resistance (m/kg)

t Filtration time (s)

δp Constant total membrane pressure (Pa)

Greek letters

α Pore blockage parameter (m^2/kg)

β Pore constriction parameter (kg)

μ Viscosity (kg/m^3)

Membrane surface scour terms

$k_p(CFV)$ Membrane surface scour constant term which is a function of crossflow velocity (CFV) and appears in cake resistance differential equation

$k_b(CFV)$ Membrane surface scour constant term which is a function of CFV and appears in unblocked area differential equation

$A_0(after_{backwash})$ Original unblocked area after backwash time

Backwash mode terms

$R_p(after_{backwash})$ Cake resistance after backwash time

$R_p(before_{backwash})$ Cake resistance before backwash time

f_{rp} Cake resistance recovery constant term

$A_0(after_{backwash})$ Original unblocked area after backwash time

$A_u(before_{backwash})$ Unblocked area before backwash time

f_{rAU} Unblocked area recovery constant term

SMP term

S_{SMP} Concentration of soluble microbial products (**SMP**) in the sludge water (g/l)

Variable TMP term

$\frac{dTMP}{dt}$ Rate of change of Δp

Nomenclature for Chapter 5

General terms, and modified ASM1 / ASM3 component states

COD Chemical oxygen demand (mg/l)

COD_{inf} Influent chemical oxygen demand (mg/l)

$TSS/MLSS$ Total suspended solids/mixed liquor suspended solids (mg/l)

S_S/X_S Readily/slowly biodegradable substrate (mg/l)

S_I/X_I Soluble/particulate inert concentration (mg/l)

$X_{BH}(orX_H)$ Heterotrophic biomass concentration (mg/l)

$X_{BA}(orX_A)$ Autotrophic biomass concentration (mg/l)

S_{UAP} Utilization-associated product concentration (mg/l)

S_{BAP} Biomass-associated product concentration (mg/l)

S_{MP} Concentration of microbial products (mg/l)

$S_O(orS_{O2})$ Dissolved oxygen concentration (mg/l)

$S_{NO}(orS_{NOX})$ Nitrate and nitrite nitrogen concentration (mg/l)

$S_{NH}(orS_{NH4})$ Ammonium concentration (mg/l)

S_{ND}/X_{ND} Soluble/particulate organic nitrogen concentration (mg/l)

X_{STO} Cell internal storage product of heterotrophic organisms (mg/l)

$f_B(f_I)$ Inert fraction of biomass leading to soluble products

f_P Fraction of biomass yielding particulate products

f_{SI} Fraction of X_S that hydrolyses to soluble inert products

Oliveira ASM3 model

Stoichiometric parameters

$f_{si} = 0$ Production of S_I in hydrolysis

$f_{xi} = 0.2$ Production of X_I in hydrolysis

$Y_{stoo2} = 0.85$ Aerobic yield of stored product per S_S

$Y_{stono} = 0.80$ Anoxic yield of stored product per S_S

$Y_{ho2} = 0.63$ Aerobic yield of heterotrophic biomass

$Y_{hno} = 0.54$ Anoxic yield of heterotrophic biomass

$Y_a = 0.24$ Yield of autotrophic biomass per $NO_3 - N$

$i_{nsi} = 0.01$ N content of S_I

$i_{nss} = 0.03$ N content of S_S

$i_{nxi} = 0.02$ N content of X_I

$i_{nxs} = 0.04$ N content of X_S

$i_{nbm} = 0.07$ N content of biomass X_{BH} and X_{BA}

$i_{tsxi} = 0.75$ TSS to COD ratio for X_I

$i_{tsbm} = 0.90$ TSS to COD ratio for biomass X_{BH} and X_{BA}

$i_{tssto} = 0.60$ TSS to COD ratio for X_{STO}

$i_{NP} = 0.1$ Fraction of N content in Microbial Product, MP (equivalent to SMP)

Kinetic parameters

$k_h = 3$ Maximum specific hydrolysis rate

$K_x = 1$ Half-saturation constant for hydrolysis of slowly biodegradable substrate

Heterotrophic organisms

$k_{sto} = 5$ Storage rate constant

$n_{no} = 0.6$ Anoxic reduction factor

$K_o = 0.2$ Oxygen half-saturation constant

$K_{no} = 0.5$ Nitrate half-saturation constant

$K_s = 2$ Substrate S_S half-saturation constant

$K_{sto} = 1$ Half-saturation constant for X_{STO}

$\mu_h = 2$ Heterotrophic maximum specific growth rate

$K_{nh} = 0.01$ Half-saturation constant for ammonium

$K_{hco} = 0.1$ Half-saturation constant for bicarbonate

$b_{ho2} = 0.2$ Aerobic endogeneous rate of X_{BH}

$b_{hno} = 0.1$ Anoxic endogeneous rate of X_{BH}

$b_{stoo2} = 0.2$ Aerobic respiration rate of X_{STO}

$b_{stono} = 0.1$ Anoxic respiration rate of X_{STO}

Autotrophic organisms

$\mu_a = 1.0$ Autotrophic maximum specific growth rate

$K_{nha} = 1.0$ Ammonium half-saturation constant for X_{BA}

$K_{oa} = 0.5$ Oxygen half-saturation constant for X_{BA}

$K_{hcoa} = 0.5$ Bicarbonate half-saturation constant for X_{BA}

$b_{ao2} = 0.15$ Aerobic endogeneous respiration rate of X_{BA}

$b_{an} = 0.05$ Anoxic endogeneous respiration rate of X_{BA}

New variables specifically for Oliveira ASM3 Model

$\gamma MP_h = 0.4$ MP formation constant for heterotrophic bacteria

$fB = 0.8$ Fraction of biomass that ends up as MP

$\gamma MP_a = 1.5$ MP formation constant for autotrophic bacteria

Lu ASM1 model

Stoichiometric parameters

$Y_h = 0.666$ Heterotrophic yield

$Y_a = 0.24$ Autotrophic yield

$f_p = 0.08$ Fraction of biomass yielding particulate products

$i_{xb} = 0.086$ Mass N/mass COD in biomass

$i_{xp} = 0.06$ Mass N/mass COD in products from biomass

$i_{xs} = 0.04$ Mass N/mass COD in X_S

Kinetic parameters

$\mu_h = 6$ Heterotrophic maximum specific growth rate

$b_h = 0.62$ Heterotrophic decay rate

$K_s = 20$ Half-saturation coefficient for heterotrophs

$K_{oh} = 0.2$ Oxygen half-saturation constant for heterotrophs

$K_{no} = 0.5$ Nitrate half-saturation constant for denitrifying heterotrophs

$\mu_a = 0.8$ Autotrophic maximum specific growth rate

$b_a = 0.04$ Autotrophic decay rate

$K_{oa} = 0.4$ Oxygen half-saturation constant for autotrophs

$K_{nh} = 1$ Ammonia half-saturation constant for autotrophs

$\eta_g = 0.8$ Correction factor for anoxic growth of heterotrophs

$k_a = 0.08$ Ammonification rate

$k_h = 3$ Maximum specific hydrolysis rate

$K_x = 0.03$ Half-saturation constant for hydrolysis of slowly biodegradable substrate

$\eta_h = 0.8$ Correction factor for anoxic hydrolysis

New variables specifically for Lu ASM1 Model

$fB = 0.1$ Fraction of biomass that ends up as S_I

$Y_{smp} = 0.5$ Heterotrophic yield coefficient from SMP

$\gamma UAP_h = 0.1$ UAP formation constant for heterotrophic bacteria

$\gamma UAP_a = 1.5$ UAP formation constant for autotrophic bacteria

Glossary

A

aerobic Conditions where oxygen is present. *Page 130.*

anoxic Conditions where there is a lack of free oxygen but fixed oxygen is present in inorganic sources, such as in nitrates. *Page 130.*

B

biochemical oxygen demand (BOD5) Amount of dissolved oxygen consumed by microbial activity when a sample is incubated, usually for 5 days at 20řC. *Page 45.*

C

chemical oxygen demand (COD) Amount of oxygen consumed by the chemical oxidation of both organic and inorganic matter present in a sample. *Page 41.*

D

denitrification The breakdown of nitrates present in anoxic wastewater by heterotrophic bacteria, which gain energy from the oxidation of organic compounds whilst allowing the nitrate to act as a terminal electron acceptor. *Page 23.*

E

extra-cellular polymeric substances (EPS) These are substances usually excreted by bacterial microorganisms as part of their metabolic processes. EPS is composed of complex proteins and polysacchrides. Unbound or 'free' EPS detaches from the bacterial biomass and becomes part of the soluble material in the bioreactor. This detached EPS in the sludge water is thought to be the critical fouling agent in MBR systems. *Page 6.*

extracted extra-cellular polymeric substances (eEPS) Bound EPS is proteins and polysacchrides that are attached or entrapped in the bacterial biomass,

and which cannot normally be released during standard metabolism. They are only released during cell breakdown and decay. In terms of fouling of MBR systems they only take part in the normal cake layer build up on the membrane surface which is usually easily removed by physical means. *Page 15.*

G

genetic algorithm The genetic algorithm is a method for solving both constrained and unconstrained optimization problems that is based on natural selection, the process that drives biological evolution. The genetic algorithm repeatedly modifies a population of individual solutions. At each step, the genetic algorithm selects individuals at random from the current population to be parents and uses them to produce the children for the next generation. Over successive generations, the population 'evolves' toward an optimal solution. You can apply the genetic algorithm to solve a variety of optimization problems that are not well suited for standard optimization algorithms, including problems in which the objective function is discontinuous, nondifferentiable, stochastic, or highly nonlinear. *Page 24.*

M

mixed liquor suspended solids (MLSS) The mixture of recycled activated sludge as microbial biomass together with suspended and colloidal solids held in the incoming effluent. *Page xxiii.*

mixed liquor volatile suspended solids (MLVSS) Only the organic fraction of recycled activated sludge as microbial biomass together with the organic suspended and organic colloidal solids held in the incoming effluent. The non-organic, non-volatilisable fraction is not included here. *Page 89.*

N

nitrification The two stage oxidation of ammonia present in wastewater by autotrophic bacteria to nitrate. It requires a large amount of dissolved oxygen in the aeration basin and usually is a much slower reaction in temperate climates then the oxidation of carboneous material, i.e. normal BOD removal. *Page 23.*

P

particulate chemical oxygen demand (XCOD) Amount of oxygen consumed by the chemical oxidation of both organic and inorganic particulate matter present in a sample. *Page 89.*

Chapter 1

Introduction

This Chapter describes the background of the larger project this specific research work is based upon, and the motivations for this specific research. It then outlines the Research Question in detail, and the basic outcomes of this work in terms of personal achievements by the report Author. Finally a brief summary of the contents of follow-on Chapters is provided.

1.1 *Technology Strategy Board project*

As stated this research work forms part of a much larger research Project No.TP/3/DSM/6/I/15123 entitled "*Improving the design and efficiency of membrane bioreactor (MBR) plant by using modelling, simulation and laboratory methods*", which was funded by the Technology Programme of the UK Government's Technology Strategy Board (TSB). This project was formulated by the Author in 2004 in conjunction with three industrial partners, namely Aquabio Ltd, ITT Sanitaire Ltd, and Northern Ireland Water in order to address the critical issue of how to minimise fouling of MBR plant whilst maximising flux throughput and minimising energy usage. These critical issues were addressed by using the Author's expertise in modelling and simulation methods to predict the biological status of the processes in the bioreactor and its affect on overall membrane fouling abased on current research and theory.

1.2 *Motivation for the research*

This research work uses phenomenological models based on both MBR **filtration** processes and MBR **biochemical** processes to measure the effectiveness of alternative time series input-output models based upon system identification methods. Both model types are calibrated and validated using similar plant layouts and data sets derived for this purpose.

The focus of this research is to create practical MBR computer models which can then be applied in MBR design, control and optimisation. Subsequently the subject of this research is to improve upon existing models and apply them to optimise a real treatment plant, and thereby eventually develop a long term energy saving control strategy.

Two aspects of a MBR system are modelled, namely the membrane fouling process and the biological processes in the bioreactor which in themselves are linked and contribute to the fouling/clogging mechanisms. It is thought that an integrated model which considers both these aspects of the MBR system as a continuous process could prove advantageous for improved design, operation and control. This research work contributes to the development of such a model by considering the optimal model type to be used, e.g. phenomenological or input-output behaviourial.

Fig. 1.1 puts the specific PhD work carried out in the context of the larger TSB project work funded by the UK Government. It relates the higher level general project goals to the more specific ones stated relating to this research work.

Fig. 1.2 puts the specific PhD work carried out in the context of the subject areas and topics and sub-topics covered. Therefore the broadest subject areas are shown at the top of the figure and more detailed research areas are depicted at the bottom of the figure. The arrows between different sub-topics show the interlinkage between topics, and any overlap of subject areas.

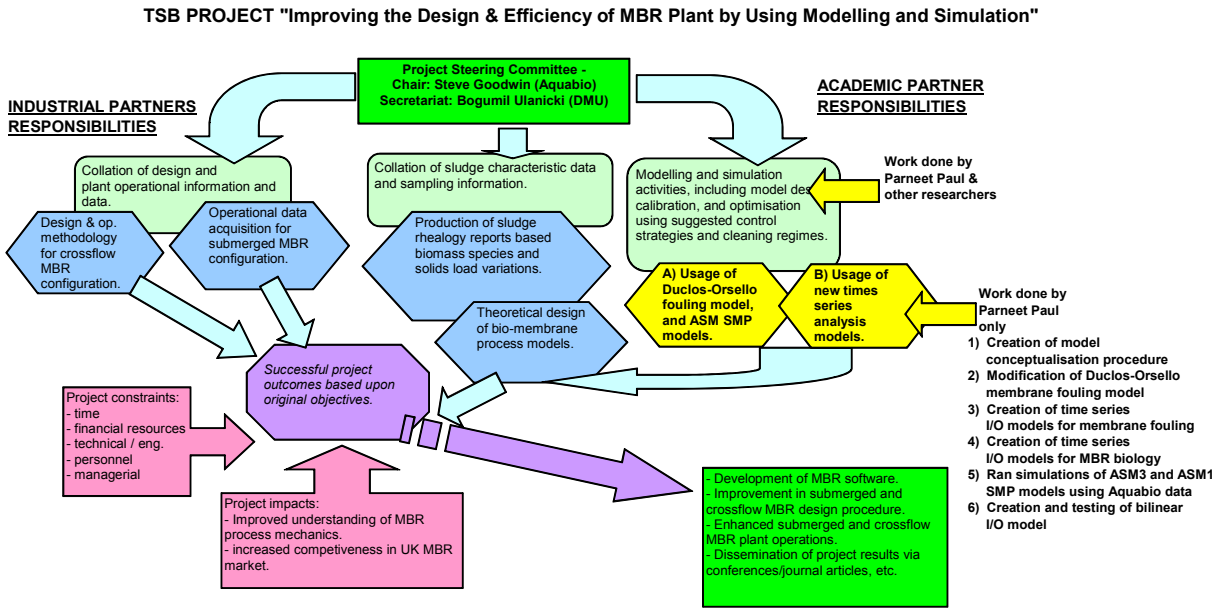

Fig. 1.1: Relation of this specific PhD research to larger TSB Project

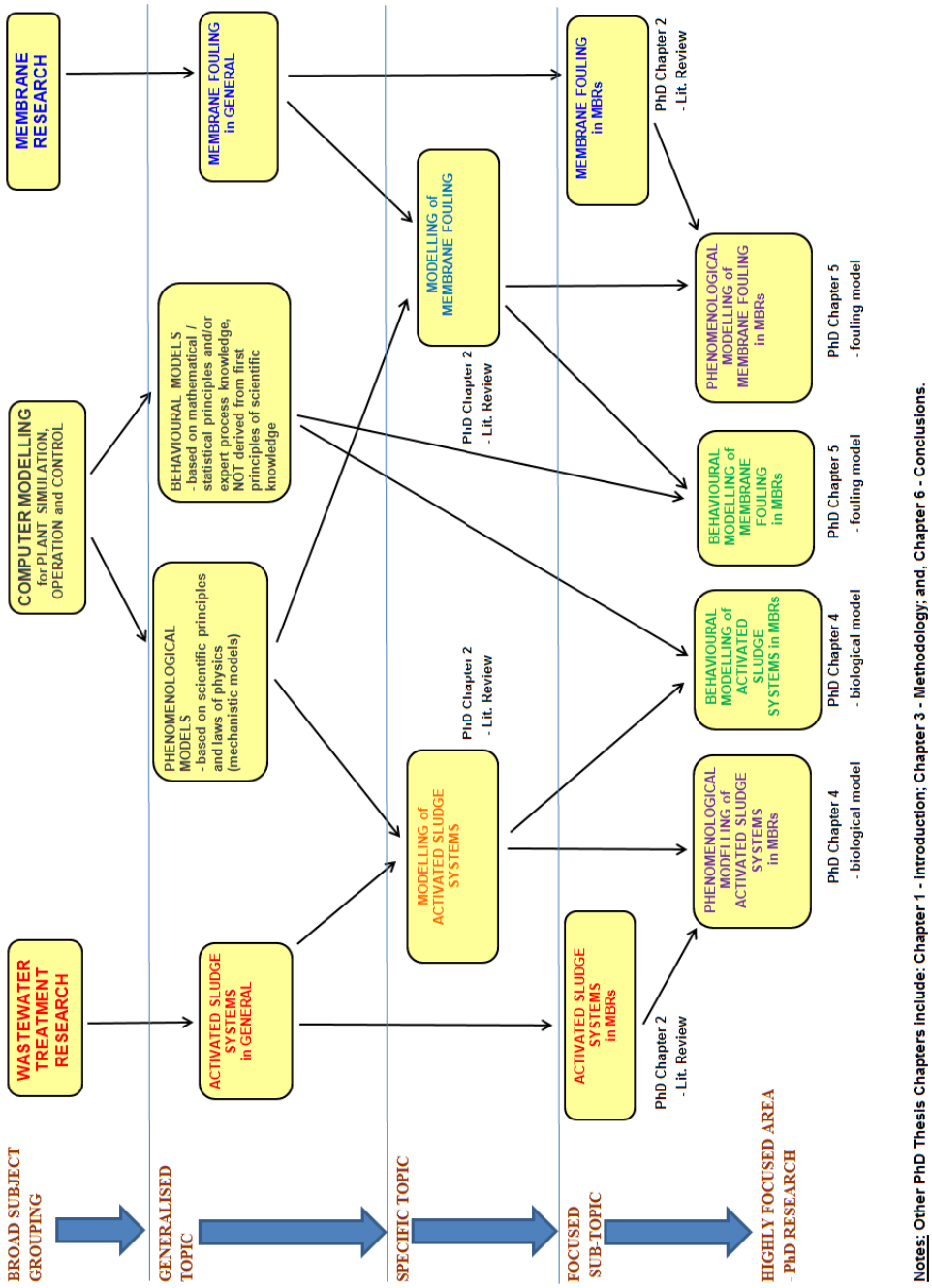

Fig. 1.2: Breakdown of PhD research by topics and subjects covered in specific Chapters

1.3 Research Question - aims and objectives of the research

The aims and objectives of this research can be broken down into answering the following specific research questions:

- How easy is it in practice to calibrate and validate a relatively simple phenomenological **membrane fouling model** for a real life MBR plant which is still rich enough in complexity to express the major membrane fouling mechanisms involved?
- Is a system identification procedure using time series analysis a simpler, quicker behavioural modelling approach to use to determine **membrane fouling** within a real life MBR plant? Can it give the same degree of accuracy as a phenomenological model?
- How easy is it in practice to calibrate and validate a relatively simple phenomenological **biological Activated Sludge model** for a real life MBR plant which is still rich enough in complexity to include the major biological / biochemical agents involved in the fouling of MBRs?
- Is a system identification procedure using time series analysis a simpler, quicker behavioural modelling approach to use to accurately determine the **biological interactions within the bioreactor** of a real life MBR plant? Can it give the same degree of accuracy as a phenomenological model?

1.4 *Summary of personal achievements*

The novel elements of this research are:

- Creation of a thorough "Model Conceptualisation Procedure" for a crossflow MBR plant which outlines how MBR models can be utilised in practical applications (i.e. for operational control). This conceptualisation provides a unique framework that allows the major issues effecting MBRs to be stated in graphical and mathematical form. This can be used by other researchers as a basis for all future MBR model development and MBR benchmark creation.
- Refinement of existing developed phenomenological models for membrane fouling (Duclos-Orsello et al. 2006). Implementation of the model in the Matlab/SIMULINK© software package, and initial calibrations of the model on existing real data sets.
- Using a system identification procedure using time series analysis to produce a membrane fouling and filtration model to be used to effectively design, control and operate a MBR plant.
- Using a system identification procedure using time series analysis to produce a biological activated sludge model to be used to effectively design, control and operate a MBR plant.
- The concept design of a unique pilot MBR plant to be used to collect data in order to validate and calibrate models.
- Formulation of some ideas for the creation of a unique MBR benchmark model and procedure to measure the effectiveness of various control strategies for differing MBR configurations.

1.4.1 Peer Reviewed International Journal Papers

The following journal papers have been published as a direct consequence of this research work:

Paul, P. (2011), "Testing of a MBR membrane fouling model based on input-output system identification procedures", *Desalination and Water Treatment*, Desalination Publications (In press, publication date Nov'2011)

Paul, P. (2011), "Developing alternative non-IWA Activated Sludge models based on input-output system identification procedures for a MBR process", *Desalination and Water Treatment*, Desalination Publications (In press, publication date Nov'2011)

Janus, T., **Paul, P.**, and Ulanicki, B. (2009), "Modelling and simulation of short and long term membrane filtration experiments", *Desalination and Water Treatment*, Vol 8 pages 37 - 47, Desalination Publications

Paul P., and Hartung C., (2008), "Modelling of biological fouling propensity by inference in a side stream membrane bioreactor", *Desalination*, Vol 224 pages 154 - 159, Elsevier press

1.4.2 Peer Reviewed International Conference Papers

The following conference papers have been published as a direct consequence of this research work:

Paul P., and Ulanicki B., (2011), Comparing and contrasting traditional membrane bioreactor models with novel ones based on time series analysis, *11th Computers and Control in the Water Industry Conference*, Centre for Water Systems, University of Exeter Sept'2011

Paul, P., (2010), "Testing of a MBR membrane fouling model based on input-output system identification procedures", *3rd Oxford Membranes and Water Research Event*, Oxford University; Lady Margaret Hall Sept'2010

Paul P., (2010), "Developing alternative non-IWA Activated Sludge models based on input-output system identification procedures for a MBR process", *3rd Oxford Membranes and Water Research Event*, Oxford University; Lady Margaret Hall Sept'2010

Janus T., **Paul P.**, and Ulanicki B., (2008), "Development and validation of a multi-configurable MBR fouling model", *Proceedings of the 2nd European Water and Waste Water Management Conference*, ThinkTank, Birmingham

Paul P., and Janus T., (2008), Validation and calibration of a multi-configurable membrane bioreactor fouling model, *2nd Oxford Membranes and Water Research Event*, Oxford University; St Hilda's College

Paul P., Ulanicki B., and Lueder F., (2007), Development of a microfiltration fouling model to be linked to the biology of an MBR system, *7th Aachen Membranes and Water Conference*, Department's of Chemical Engineering and Environmental Engineering, RWTH Aachen University, Germany

Paul P., Lueder F., and Hartung C., (2007), Development of an integrated activated sludge membrane bioreactor model, *9th Computers and Control in the Water Industry Conference*, School of Engineering & Technology, De Montfort University: Leicester

Lueder F., **Paul P.**, and Ulanicki B., (2007), Modelling the flux decline caused by fouling of microfiltration membranes, *9th Computers and Control in the Water Industry Conference*, School of Engineering & Technology, De Montfort University: Leicester

Paul P., and Hartung C., (2007), Modelling of biological fouling propensity by inference in a side stream membrane bioreactor, 11th Aachen Membrane Colloquium, Department of Chemical Engineering, RWTH Aachen University, Germany

Paul P., (2006), Improving the design and efficiency of MBR plant by using modelling and simulation, *"Bio-fouling in membrane systems" EUROMBRA Project Seminar*, MBR-Network Programme, Norwegian University of Science & Technology

1.5 *Organisation of this thesis*

This thesis is organised into the following Chapters:

Chapter 2 This is split into two sections, with the first giving a basic background theory for the thesis topics covered as a whole, while the remaining section deals with the "state-of-the-art" in these

specific topics. As this thesis covers a range of inter-disciplinary areas such as specialist process engineering, mathematical modelling, biochemistry, control engineering, statistical analysis, etc., it is appropriate that in this Chapter some relatively fundamental theory is provided as the reader maybe unfamiliar with at least some of the subjects and topics covered in this research work.

Chapter 3 In the first half of this Chapter, detailed information is given on the rigourous mathematical formulation and framework that underpins the "Model Conceptualisation Procedure" for a MBR system. In the second half of this Chapter, detail is then given on the various wastewater treatment plant (WWTP) that were used to generate the data required to calibrate and validate the developed models. These include: an Aquabio crossflow full size MBR plant located at Kanes Foods Limited in Evesham, Worcestershire; an unique Aquabio crossflow pilot MBR plant created for this project and also operated at the Kanes Foods site; an ITT Sanitaire submerged pilot MBR plant operated at Coors UK Limited, and an ITT Sanitaire pilot membrane filtration unit operated in dead end mode at Cardiff Wastewater Treatment Works. Some further data was also generated from a fictitious WWTP using a modified version of the standard COST Benchmark simulation model developed by the International Water Association (IWA) (Copp 1999, 2000).

Chapter 4 This inclusive Chapter is split into three main sections. The first deals with the further development and modification of a phenomenological model which describes the fouling of a membrane in a MBR. The second Section outlines the results obtained from running the data obtained from the various plant through this modified and extended model. Finally, the last Section details the results of using this plant data to calibrate and validate the time series input-output version of this fouling model.

Chapter 5 Like the preceding Chapter, this inclusive Chapter is split into three main sections. The first deals with the development of phenomenological models to describe the Activated Sludge biological processes in bioreactor of a MBR especially in relation to extra-cellular polymeric substances (EPS) and **SMP**. The second Section outlines the results obtained from running the plant data through these developed models. Some information is also provided on how other theoretical data was generated to test the time series based models, which themselves require significant data sets that the various plant could not necessarily provide. Finally, the last Section details the results of using both the actual plant data as well as the specially generated data to calibrate and validate the time series input-output version of these Activated Sludge models.

Chapter 6 This final Chapter summarises the conclusions of this research study, and then suggests follow-on work that needs to be carried out in the areas of integrated MBR modelling, MBR control regimes, and the creation of MBR benchmark models to assist in this plant control.

Chapter 2

Theoretical basis of work

2.1 *Introduction*

The purpose of this Chapter is to present basic information about the principles of a MBRs, and all the broader issues and topics related to this specific interdisciplinary research area, together with the latest "state-of-the-art" knowledge in this research area.

The Chapter is split into two main sections, with the first dealing with all background theory while the second deals with a literature review of current research developments. The first Section is further split up as follows into the theory of MBRs, and the theory of wastewater treatment modelling:

Section - Background theory: MBR wastewater treatment processes

Subsection - Membrane filtration processes and mechanisms of fouling related to Activated Sludge

Section - Background theory: Wastewater treatment modelling

Subsection - Membrane filtration modelling

Subsection - Activated Sludge modelling

Subsection - Introduction to modelling typically used in Econometrics

This second Section is split up into latest research into membrane filtration, and also a comprehensive review of the modelling of wastewater treatment processes:

Section - Literature review: Membrane filtration processes and mechanisms of fouling related to Activated Sludge

Section - Literature review: Wastewater treatment modelling

Subsection - Membrane filtration models

Subsection - Activated Sludge models

Subsection - Modelling of wastewater treatment using methods typically used in Econometrics

2.2 *Background theory: MBR wastewater treatment processes*

2.2.1 Membrane filtration processes and mechanisms of fouling related to Activated Sludge

This Section describes the critical aspects of membranes used in microfiltration (MF) and ultrafiltration (UF) whose performance is severely curtailed when filtering Activated Sludge. This reduction in membrane flux is caused by fouling and clogging of the membrane surface and pores by biological agents in the Activated Sludge.

2.2.1.1 Membrane unit processes

The definition of membrane used in the context of this study is the same one according to the nomenclature originally proposed by the European Membrane Society, in which it denotes the third phase which separates two other liquid or gas phases, and further, acts as a passive or active barrier for mass transport between these phases (Gekas 1986). At the turn of the 19th century, most of the physical basis of membrane processes were initially observed, with subsequent advances connected with the production and application of membranes occurring later in the 20th century. A major turning point in the application of membrane processes occurred in the early 1960s when Loeb and Sourirajan (1963) developed a technology for the industrial production of both highly efficient and very selective membranes on a large scale. Further rapid development of membrane techniques progressed once there were significant further advances in materials engineering and polymer chemistry. This meant the variety and applications for available membrane was extended into new areas (Mulder 1996, Peinemann and Nunes 2001). A general classification of membranes according to their material and internal structure is shown in Fig. 2.1.

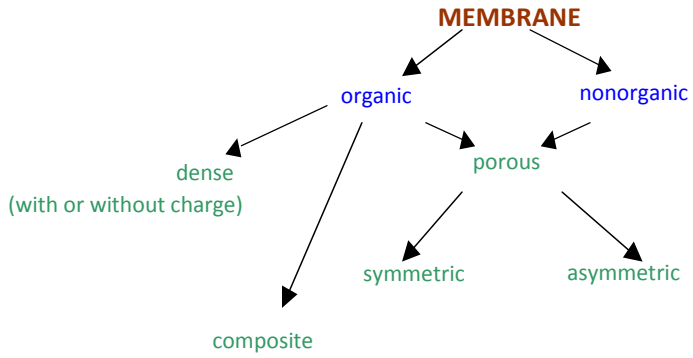

Fig. 2.1: Division of membranes according to material and structure (Paul, 2006)

As can be seen, membranes can be composed of inorganic components, e.g. ceramics, metals, glass and graphite, or organic compounds such as is the case with polymer membranes (Hoffmann 2003, Koch and Habermann 2005, Li 2007). With regard to the membrane structure, a membrane which has significant pores sizes of specified dimensions is called porous, while one with no discernible pores in the macroscopic sense is termed as a nonporous or dense membrane. A membrane with reasonably cylindrical pores where the porosity on both membrane surfaces is identical is termed a symmetrical isotropic membrane, while one with conical pores where the porosity in the surface layer is the lowest and grows perpendicular to the surface, is called a porous asymmetric anisotropic membrane. Asymmetric membranes can also be dense.

A typical asymmetric membrane is composed of a mechanical supporting layer, which has a very porous structure and thickness of approximately 50 to 200 μm, which is attached to or meets with a thin separating layer of thickness 0.1 to 1 μm (Mulder 1996). The basic properties of an asymmetric membrane in terms of species selectivity is solely determined by the thin skin layer. A thin selective membrane layer allows the achievement of high permeation rates and trans-membrane fluxes, while its density ensures good overall

selectivity (Huang 1991, Baker 2004). Typical symmetric membranes are manufactured by either casting in-situ or by using phase inversion techniques. If a membrane consists of two or more layers of different material composition, porosity and function, it is called a composite membrane. A detailed description of preparation procedures and characteristic of composite membranes can be found in Strathmann (1986), Drioli and Giorno (1999). The magnified internal structure of a typical polymeric porous membranes is given in Fig. 2.2.

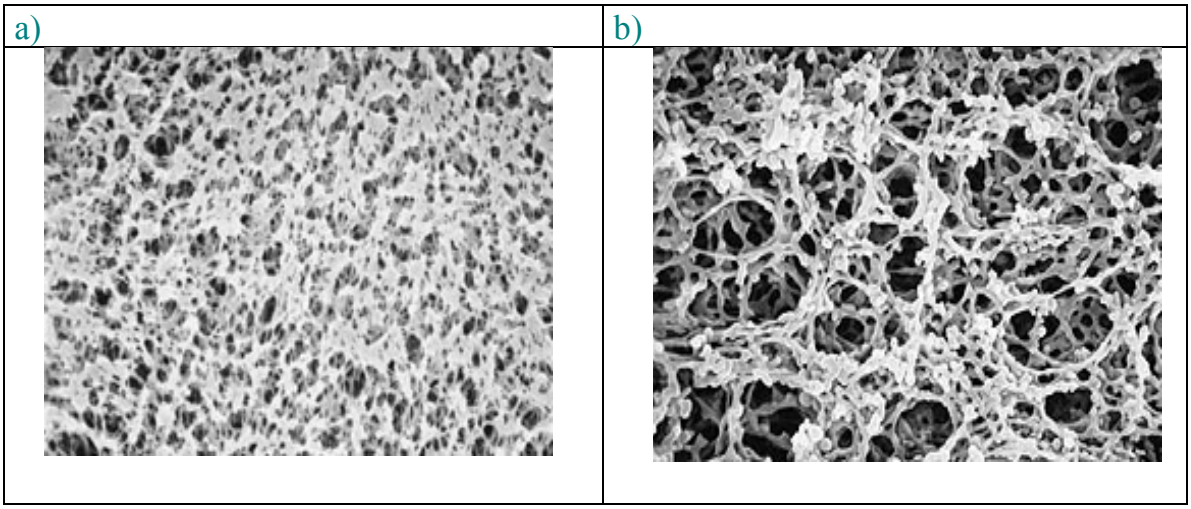

Fig. 2.2: Photographs of polymeric porous membranes made from: (a) polypropylene and (b) cellulose acetate (Judd and Judd, 2006)

Membranes come in various shapes and sizes to suit different industrial applications. Hence, common membrane shapes and forms are spiral wound modules (commonly used for dead filtration of process water), flat plate/sheet (FP) membranes, and cylindrical membranes (Baker 1991, Eykamp 1995). Each membrane shape and configuration has distinct advantages and disadvantages, and come in a range of packing densities. Depending on diameter, the cylindrical membranes are divided into either multi-tubular (MT) membranes with inner diameters of 6 to 24 mm, or less commonly used capillary membrane (CM) with inner diameters of 0.5 to 6 mm, or more commonly used hollow fibre (HF) membranes with the smallest inner diameters of 0.04 to 0.5 mm (Peinemann and Nunes 2001, Baker 2004). Fig. 2.3 details some common membrane shapes and configurations. When considering the membrane packing density, which governs both the module spatial footprint and the membrane area required per unit volume of flux produced (and hence affects the overall capital costs), then generally speaking, the smaller the membrane diameter, the greater is its packing in the specific module. While in the MT module the surface area per specific flux production volume is typically smaller than 300 m^2/m^3, in the HF module it can reach as high as between 10,000 to 30,000 m^2/m^3. In comparison the specific surface area per flux volume for traditional FP membranes is 100 to 400 m^2/m^3, while for spiral wound FP modules it can be higher at 300 to 1000 m^2/m^3 (Drioli and Giorno 1999). All these membranes can also be classified according to the separation mechanism that is employed and the separation level used from very fine to very coarse. Hence the most general classification is based on the type of membrane driving force required to separate a mixture (Mulder 1996, Baker 2004). This separation effect occurs due to a difference in chemical potentials on both sides of the membrane induced by either differences of pressure, concentration, temperature or electric potentials as detailed in Fig. 2.4.

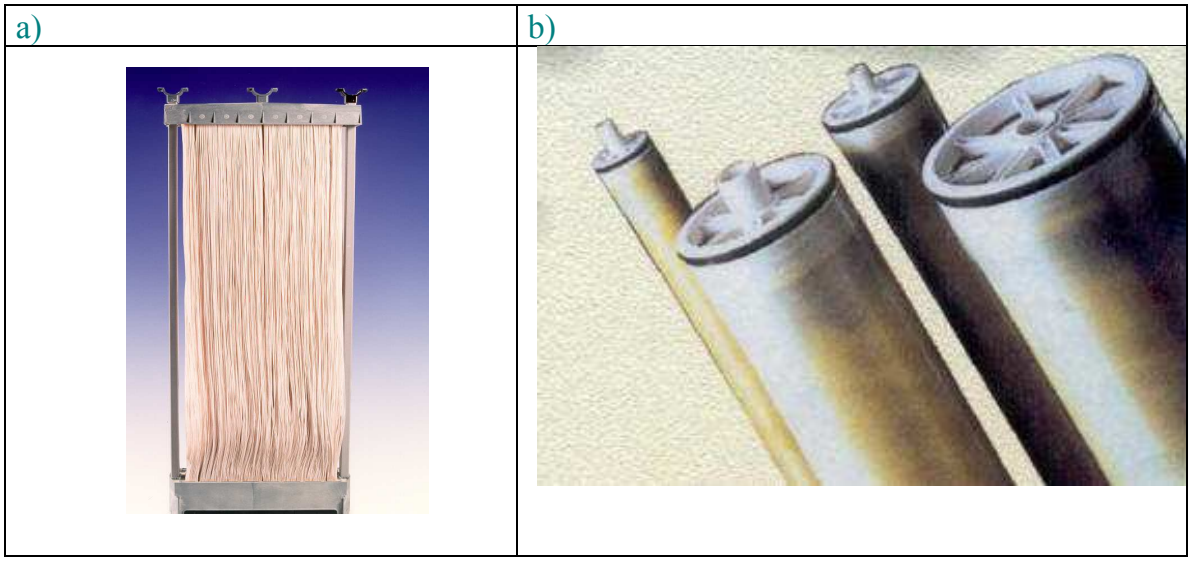

Fig. 2.3: Photographs of (a) ZeeWeed capillary module and (b) Lenntech module with spiral flat membranes (Judd and Judd, 2006)

DRIVING FORCE	KIND OF PROCESS	APPLIED MEMBRANE	SEPARATION MECHANISM
Pressure difference (ΔP)	Microfiltration (MF)	Porous	Pore-flow
	Ultrafiltration (UF)	Porous, asymmetric	Pore-flow
	Nanofiltration (NF)	Porous, asymmetric with ions on surface	Pore flow + Donnan effect
	Reverse osmosis (RO)	Porous, asymmetric	Solution-diffusive (or sorption-capillary solvent flow)
Concentration difference (Δc)	Gas separation (GS)	Asymmetric with nonporous dense skin	Sorption-diffusive
	Pervaporation (PV)	Asymmetric, nonporous	Sorption-diffusive
	Vapour permeation (VP)	Asymmetric, nonporous	Sorption-diffusive
	Dialysis (D)	Polymeric, strong hydrated	Capillary transport
	Membrane extraction (EM)	Porous	Diffusion
	Liquid membranes (LM)	Liquid	Solution-diffusive
Temperature difference (ΔT)	Membrane distillation (MD)	Porous, lyophobic	Diffusion
Electric potential difference (ΔE)	Electrodialysis (ED)	Gel, ionic	Ion migration

Fig. 2.4: Classification of major membrane separation techniques (Narebska, 1996)

2.2.1.2 Pressure-driven processes

In this study, only membrane processes that are driven by pressure differences are considered. These processes are generally used in the separation of different types of compounds from suspensions through to monovalent ions. Fig. 2.5 describes the types of compounds commonly retained by pressure-driven processes of various pore sizes. Incidentally the type of retained compound has in itself an important influence on the process parameters used in the membrane filtration operation as shown in Fig. 2.6. In terms of MBRs, then MF, UF and nanofiltration (NF) are the dominant membrane processes integrated within its bioreactor. The process of MF is used primarily to retain microbial cells on the membrane (Li et al. 1996, Lee et al. 2007), UF to retain proteins and polysacchrides, including enzymatic proteins (Freixo and de Pinho 2002, Knutsen and Davis 2004), while NF is used to retain dissolved reagents (Wintgens et al. 2002, Blocher et al. 2002). Further, the membrane surface in a pressure-driven process can serve as a matrix to immobilize a biocatalyst (Ulbricht and Papra 1997, Yujun et al. 2008).

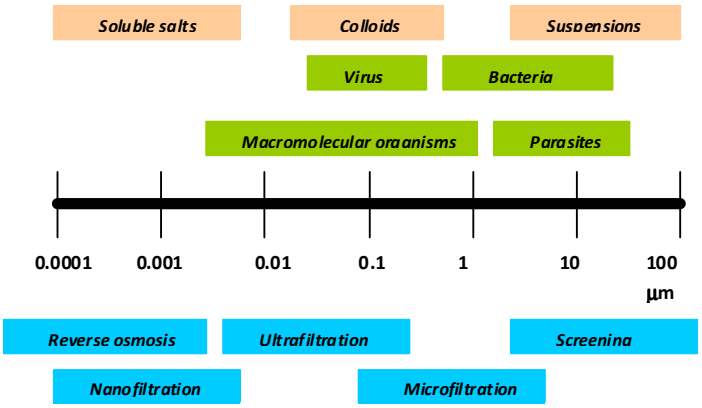

Fig. 2.5: Retention of compounds in pressure-driven processes (Judd and Judd, 2006)

	MF	UF	NF	RO
Driving force	<0.5 MPa	0.1-1 MPa	0.3-3 MPa	1-10 MPa
Membrane parameters: Thickness Pores diameter	 10-150 µm 0.05-10 µm	 150 µm +0.1-1 µm (skin) 0.1-1 µm	 150 µm +0.1-1 µm (skin) 1-5 nm	 150 µm +0.1-1 µm (skin) <2 nm
Membrane material	polymeric, ceramic	polymeric, ceramic	polymeric with charge	hydrophilic polymers
Species passed (in permeate stream)	solvent with dissolved solutes	solvent and low (<1000Da) solutes	solvent and low (<100 kDa) solutes	solvent
Species retained (in retentate stream)	suspended solids, viruses, bacteria	macrosolutes, colloids (proteins also enzymatic)	compound at 100-1000 kDa; multivalent ions	all dissolved and suspended solids

Fig. 2.6: Comparative characteristic of pressure-driven processes (Mulder, 1996; Drioli and Giorno, 1999)

Optimal membrane selection When selecting a membrane type for a specific process application, then the system design engineer needs to assess the variation in individual membrane properties when comparing between different manufacturers. The following membrane characteristics are usually quantified and compared in order to get the best membrane for the job at hand:

1. - Material type.
2. - Porosity.
3. - Membrane pore size distribution.
4. - Hydrophobicity: measured as Contact Angle (e.g. hydrophobic/transphilic/hydrophilic ranges).
5. - Surface roughness: measured with Atomic Force Microscopy.
6. - Surface charge character: measured as Zeta Potential.
7. - Permeability in $(l/m^2/hr)/kPa$ units.
8. - Packing density.
9. - Modular configuration options available.

2.2.1.3 Microfiltration and ultrafiltration

MF and UF belong to the pressure-driven membrane processes. Concerning operating pressure and molecular separation size, they are categorised between NF and sand filtration. The separation mechanisms of the MF and UF membranes are similar and the fields of applications may strongly overlap. According to the principle of a porous filters, all those particles larger than the membrane pores are retained completely. The particles held back can therefore develop a cake layer on the membrane surface. Hence it is assumed that retention of components during MF and UF proceeds according to a simple sieving mechanism. The sieving mechanism is based on the difference of sizes of retained compound in relation to the size of membrane pores (see Fig. 2.7). In reality this can prove complex since the retained compounds have distinct particle size distributions which interact with the membrane's own pore size distribution. In simple terms when a pressure is applied across the membrane to drive the separation process, then compounds, colloids and solvents of diameter smaller than the average pore diameters pass into the filtrate stream which is called the permeate flow, while the components with diameter bigger than average pore diameters are retained by the membrane in what is known as the retentate stream (Blatt, 1976; Eykamp, 1995).

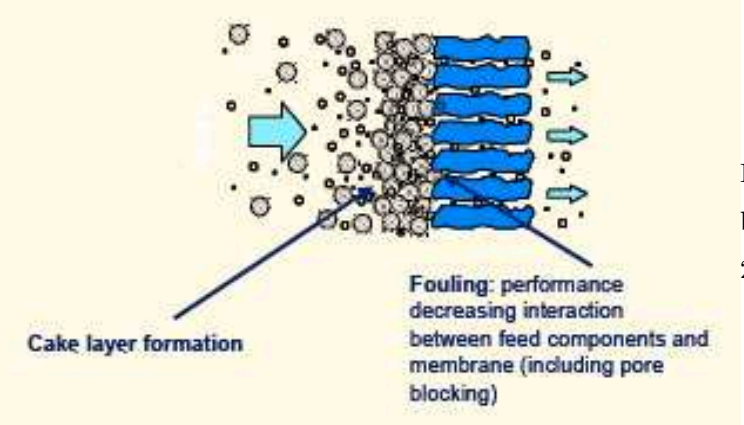

Fig. 2.7: Cake formation on a typical membrane undergoing forward filtration (Paul, 2006)

The exact mechanism responsible for fouling and flux decline across the membrane in a MBR are not very well understood to date, although most researchers now agree that the physicochemical interactions between the membrane and various proteins and polysaccharides present in the supernatant of the Activated Sludge

biomass are largely the cause of biofouling (Rosenberger et al. 2006). It now appears that these dissolved and colloidal species, known as soluble microbial products, precipitate biofouling directly by forming a biofilm on the membrane surface and also by reducing and blocking the pores of the membrane. This process is known as irreversible fouling (Ho et al. 2003). Additionally they indirectly act as attachment agents for suspended solid particulates in the Activated Sludge, although this cake build up of flocs is usually easily removed with standard cleaning protocols dependant on the MBR configuration, e.g. air-sparging, back flushing, high crossflow velocities, operation at low fluxes, membrane relaxation techniques, etc. This type of easily removable fouling is known as reversible fouling (Ho et al. 2003). By the way irreversible fouling often consists of solute ion adsorption on to the membrane even without any suction pressure occurring plus the usual gradual adsorption and pore blocking over the lifetime of the membrane operation (even with proper regular cleaning in place (CiP)). Hence periodic aggressive chemical cleans are needed to recover long term flux decline caused by the irreversible aspect of the biofouling process for plants operated at constant trans-membrane pressure (TMP) regimes (Drews et al. 2008). The rate of increase of this second type of irreversible fouling would increase with poor operation and inadequate cleaning regimes. Hence the older the membrane, the more the intrinsic irreversible fouling. Restricting the categorisation of membrane fouling into reversible and irreversible mechanisms is somewhat simplistic when compared to the reality at the microscopic level, but it is commonly assumed so that any mathematical models that are developed are simple in form.

In truth, the membrane fouling process should be more strictly split into several mechanisms occurring simultaneously as follows. Even these processes, as depicted in Fig. 2.8, are a simplification of reality, but they are more representative of what actually happens during fouling:

1. - Adsorption /scaling of membranes by dissolved solutes coming out of solution. This is usually a small permanent loss of membrane permeability, and occurs in the membrane internal structure itself. Some of it can be recovered sometimes following chemical cleans with anti-scaling / chelating agents.
2. - Pore blocking and plugging, and channel clogging by colloidal matter and small particulates.
3. - Cake build up of large adhesive flocs of biomass composed of organic and inorganic matter.
4. - Formation of gel layers and biofilms by microscopic bacterial growth on the actual membrane surface. In this case the colloidal matter is used as a food source for the adhesive bacteria which can give rise to significant concentration polarisation affects even though the biofilm layer is very thin.

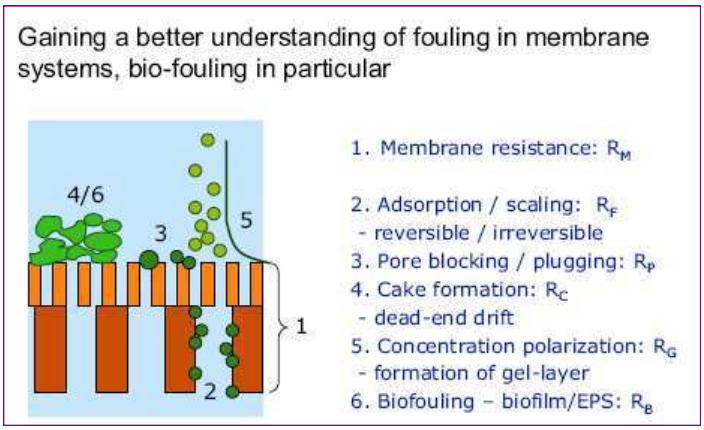

Fig. 2.8: Types of fouling mechanisms for a MBR membrane (Paul, 2006)

Biomass fractionation There have been many studies by membrane researchers based on either the fractionation of biomass by: a) physical particle size; or b) chemical nature of the components. Both approaches present challenges and have largely failed to unambiguously identify primary foulants. Some researchers have found some correlation with particle size and/or chemical nature of fouling agents, but there is also still some disagreement in the academic community at the moment. However, the academic community does now universally agree that the major fouling agents appear to stem from EPS which are formed by microbial conversion. Hence the key foulants arise from biomass and are termed eEPS for the bound/entrapped version, with the unbound fraction being commonly termed **SMP**. These can be further fractionated into chemical types, namely polyproteins and polysaccharides.

This area is the number one topic of research although outcomes to date are difficult to compare since different fractionation methods and measurement protocols are used by differing research groups (Yang et al. 2006, Rosenberger et al. 2006). No agreed standardisation has yet occurred. It has been suggested that chemical spectrometric methods which are cost effective and easy to conduct are used as follows to determine the proteins and polysaccharide fractions respectively (Vocks et al. 2006, EUROMBRA 2007):

- Simple calorimetric methods for protein concentration determination including Lowry-Assay, Phenol-Sulphuric Acid method (also known as Dubois Assay).
- Simple calorimetric methods for polysaccharides concentration determination including Bradford Assay, and Anthron Assay.

Various researchers had identified the colloid fraction of **SMP** as critical in determining fouling rates (Judd and Judd 2006). In fact it is the fraction most identified as responsible for fouling, but not ubiquitously so with generally poor correlation. For example there is poor correlation between the colloidal **SMP** and the **SMP** turbidity, and consequently it is probably unwise to generalise too much regarding foulants. However, it is well known that hydrophilic membranes, like cellulose acetate, cause less fouling whilst hydrophobic membranes like polyethersulfone (PES) and and polyvinyldifluoro (PVDF) can promote it. Fig. 2.9 shows the simplified representation of the complex EPS and **SMP** relationship.

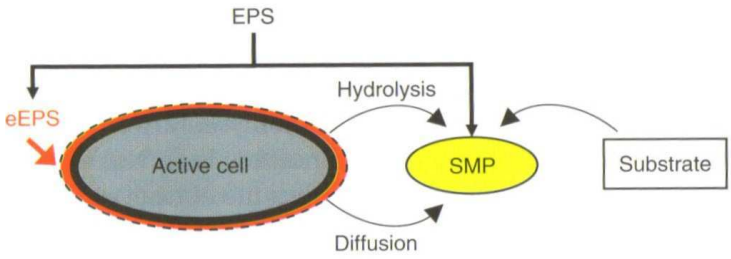

Fig. 2.9: Simplified representation of EPS and SMP relationship (Judd and Judd, 2006)

Flux evolution relationship with fouling It has been found that for a given mixed liquor, membrane type and applied crossflow velocity / TMP regime, there exists a specific flux whose value below which particle deposition on the membrane surface is negligible, and above which it is significant. This specific flux is known as the "critical" flux and is often specified by the membrane manufacturers (Pollice et al. 2005). This critical flux is key in determining whether significant fouling occurs during normal operation of the MBR system, and whether it can be removed by standard cleaning mechanisms. For a typical FP system the critical flux range would be 25 to 30 $l/m^2/hr$, while with a sidestream MT system with high crossflow velocity the critical flux range could be as high as 50 to 60 $l/m^2/hr$.

In reality, the specified critical flux is often exceeded on a localised basis, dependent on how the actual material deposition occurs along, say, a typical tubular membrane in practice. Particles mainly deposit near the membrane inlet because the highest flow/pressure is experienced here. Conversely at the outlet

the flow/pressure is lessened, which can lead to a precipitation of smaller particles due to flux reduction. This is because the solubility limit is exceeded for the concentration at the back end of the membrane, so precipitates form. (Also it is worth noting that the actual pore area of a typical phase inversion membrane only amounts to between 5 to 10 % of the total membrane surface area.) This means in reality, as long as the average net flux is below critical, then major fouling should not occur.

In practice, any measured flux needs to be normalised with respect to the temperature to account for and compensate for mixed liquor viscosity affects which would globally impact on fouling rates. Hence a typical MBR membrane plant is designed for a given flux, pressure and temperature, with usually a doubling of flow equating to a quadrupling in the pressure resistance.

2.3 *Background theory: Wastewater treatment modelling*

Usually a mathematical model is a useful representation or a simplified description of a real-life system, and consequently it never will fully describe and reflect the total complexity of the actual situation. In most instances models only describe the parts of the system that matter to the process engineer, i.e. the bioreactor only, or the membrane only. It is important that the process engineer knows what the model is capable of expressing, the assumptions it is based upon, and its limitations.

This section summarises the background knowledge on the various modelling approaches that can be used for a MBR system. They are as follows:

- Phenomenological / mechanistic models - A phenomenological model is based on the observation of natural phenomena and by applying scientific principles and theories to predict the behaviour of these phenomena. Similarly a mechanistic model obeys the basic laws of physics and can be deduced from scientific principles and theories. This is the traditional approach taken when modelling simple systems.
- Behavioural / input-output / black-box models - Behavioural models focus on the behaviour of the system being studied based on data values only without trying to explain why it occurs (e.g. no prior system knowledge is required). These models are also called black-box models as they only analyse the relationships between different sets of system observations, data values and measurements. No prior scientific knowledge or theory of the system is needed in these models. They simple take input-output data from experimentation and represent it by standard mathematical functions which come in several types and forms. Hence these empirical models are based on convenient mathematical functions that reasonably represent real-life observations and available data from the system.
- Grey-box / hybrid models - This set of models are based upon both the mechanisms of the system and upon empirical functions where the mechanisms are complex or unknown. They try to take the best from the first two approaches, and thus hope to attain a better data fit and improved predictive quality. Thus they can be termed as hybrid model systems.
- Deterministic models have single value fixed inputs and outputs which neglect any uncertainty or randomness in data.
- Uncertainty models have inputs and outputs with some empirical measure of uncertainty included (e.g. interval or fuzzy models with some values which are determined randomly).
- Stochastic models have at least some inputs and outputs described in terms of statistical probability distributions.

There are also discrete models which only output specific values or discrete-time values, while, conversely, continuous models can give any value and can have continuous-time values. A time series model takes continuous values at discrete-time intervals. Therefore the time series itself is a set of data values or measurements usually taken at uniformly spaced time intervals, and time series analysis are methods and techniques developed to analyse this collated data especially for prediction purposes.

Lumped models are ones that simplify or "lump-together" large or complex systems into simpler units or processes, while, conversely, distributed models account for each specific process or individual units of the overall system. A lumped system is one in which the dependent variables of interest are a function of time alone, and generally requires the solution of ordinary differential equations. Conversely, a distributed system is one in which the dependent variables are functions of time and one or more spatial variables, and usually require the solving of partial differential equations.

Finally, macroscopic models only focus on the bigger picture of the processes occurring or use gross assumptions and simplifications on the large scale. Individual small details or nuances are ignored or included as part of the error term. Conversely, microscopic models focus on the smallest level of detail, and account

for all specific nuances and variations.

When deciding on which approach to use, it is important to note that each has distinct advantages and disadvantages, and any approach is only as good as the accuracy of the information provided and data collated for the system. Fig. 2.10 outlines the common basic variables that can be measured for a typical MBR system and on which all the modelling approaches would be based. These variables are the standard ones that are usually collated using inexpensive sampling means.

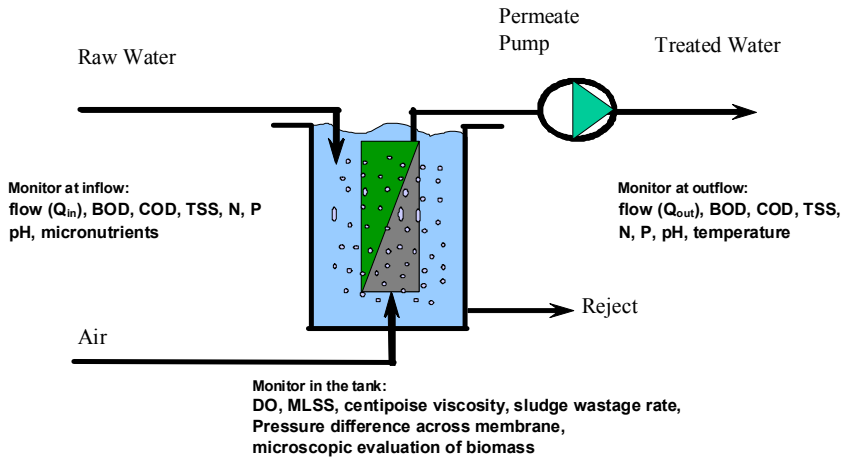

Fig. 2.10: Typical Variables Measured for an MBR (Paul, 2006)

In this study, the modelling work is split into three distinct but overlapping areas for a MBR system:

- Modelling of the membrane fouling process only using a phenomenological mechanistic approach.
- Modelling of the Activated Sludge system only which indirectly impacts on the fouling. Again this is done using a phenomenological mechanistic approach.
- Modelling of both processes already mentioned, again separately, but now using a behavioural input-output approach using time series analysis and system identification procedures. This is done to see if this method proves quicker and easier to complete without a loss in prediction accuracy.

The next Section summarises the background theory regarding these three areas. When the final modelling approach has been decided, and the model structure and form is in place, then a standard iterative procedure is used in order to calibrate and validate this model using real-life plant data. This model verification procedure is summarised in Fig. 2.11.

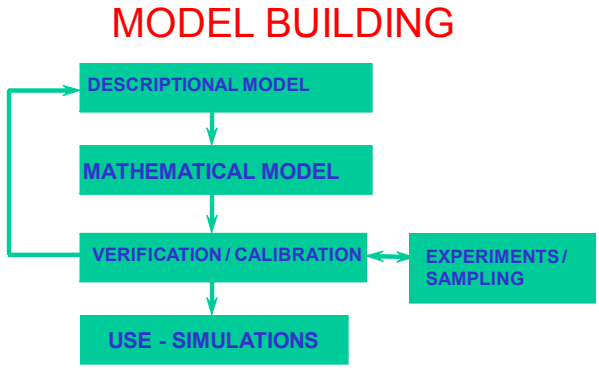

Fig. 2.11: Typical development procedure used to construct calibrated and validated models (Paul, 2006)

2.3.1 Membrane filtration modelling

2.3.1.1 Modelling approaches to fouling

Capturing membrane fouling phenomena in the form of mathematical models has been a task of many different research teams around the globe for the last two decades. There are essentially two approaches that can be used to describe the mass transport of materials in membrane processes (Stephenson et al. 2000).

The first approach, which is also the most common one used, is to simply add the hydraulic resistance of the clean membrane to that offered by the cake and other fouling layers in order to determine the flux through all layers under a given pressure regime. Hence this resistance-in-series modelling approach simply adds all membrane resistance components to give the overall resistance to flow, and therefore relies on a knowledge of these resistance components (e.g. unit resistances such as pore constriction, cake, biofilm, polarisation layer, scaling, etc.). This means the various fouling layer resistances can be measured empirically, and simple physical laws governing flow through porous media can be applied without the need to develop complex theory. Incidentally membrane manufacturer's often provide typical clean membrane resistances for their products. In this approach, the Darcy Law is often used which calculates the TMP for a given flux using a resistance-in-series approach as outlined in Equation 2.1.

$$J = \frac{\Delta p}{\mu \cdot R_{total}} \tag{2.1}$$

where:

J is the filtrate flux (m/s)

Δp is the trans-membrane pressure (Pa)

μ is the viscosity (cP)

R_{total} is the total resistance caused by adding the series resistances: clean membrane, cake build up, pore constriction, and pore blockage by **SMP** deposit (m^{-1})

This total resistance can then be approximated by using the Hagen-Poiseuille Law in Equation 2.2, which assumes the membrane flux can be approximated to laminar flow through cylindrical pores. Other more recent expressions based on classical blocking laws as formulated by Hermia (1982) can also be used to give a fuller more accurate solution. In Section 4.1.1 this specific blocking law approach is delineated further as a preamble to Chapter 4.

$$R_{total} = \frac{K \cdot (1 - \varepsilon_m)^2 \cdot S_m^2 \cdot l_m}{\varepsilon_m^3} \tag{2.2}$$

where:

K is a constant equal to 2 for perfectly cylindrical pores but changes for other geometries

ε is the porosity (or voidage)

S_m is the pore surface area to volume ratio

l_m is the membrane thickness

The other approach that can be used is to develop predictive models for membrane processes from first principles using mathematical descriptions of the specific system hydrodynamics. Most of the models developed in this way, especially for crossflow systems, are based on film theory which is also referred to as concentration polarisation models. Classical film theory assumes that the main mechanism of diffusive transportation across the interfacial region is affected mainly by the amount of concentration polarisation taking place. This build up of concentrated media at the membrane surface can then be calculated by considering the system hydrodynamics. Equation 2.3 gives the basic concentration polarisation expression used as the basis for all film theory models. Table 2.1 displays several common predictive models developed by researchers based on film theory (where γ_0 is the maximum shear rate, r is particle radius, L is the membrane elemental length, and ν_0 is the kinematic viscosity). They include the main mechanisms modelled by film theory, namely by Brownian diffusion transport, shear-induced diffusion transport, and inertial lift transport.

$$J = \frac{D_b}{\delta} \cdot ln \frac{C_m}{C_b} \tag{2.3}$$

where:

D_b is the Brownian diffusion coefficient ($m^2 s^{-1}$)

δ is the thickness of the stagnant region on the membrane surface (m), and varies with hydrodynamic conditions

C_m/C_b are the respective concentrations at the membrane surface and in the bulk solution (kg/m^3), with C_b being analogous to MLSS concentration in wastewater

Model	Equation	Reference
Brownian diffusion	$J = 0.807 \left(\frac{{D_b}^2 \gamma_0}{L}\right)^{1/3} \cdot ln \left(\frac{C_m}{C_b}\right)$	Porter (1972)
Shear-induced diffusion	$J = 0.078 \left(\frac{r^4}{L}\right)^{1/3} \cdot \gamma_0 \cdot ln \left(\frac{C_m}{C_b}\right)$	Zydney and Colton (1987)
Inertial lift	$J = \frac{0.036 r^3 {\gamma_0}^2}{16 \nu_0}$	Drew et al. (1991)

Table 2.1: Steady state expressions for averaged permeate flux based on film theory

2.3.2 Activated sludge modelling

The Activated Sludge process is the most generally applied biological wastewater treatment method in which the bacterial biomass suspension is responsible for the removal of pollutants. Depending on the design and the specific application, an Activated Sludge WWTP can achieve biological Nitrogen removal and biological Phosphorus removal, besides the usual removal of organic carbon substances. Many different Activated Sludge process configurations have evolved during the years for specific waste streams and specific situations. A review on the historical evolution of the Activated Sludge process can be found in Jeppson (1996).

For wastewater treatment modelling, the main biochemical processes occurring in the bioreactor are the ones that matter and the ones that are usually modelled. This is since the modelling procedure is normally used to predict the final effluent quality in terms of meeting environmental consents for the plant in question. Hence, the typical modelling of an Activated Sludge system consists of the modelling of the organic carbon substrate removal and nutrient removal processes, which obviously includes the biomass growth and decay phases, and biomass respiration processes (i.e. oxygen uptake processes). However this type of modelling cannot predict more complex sludge bulking and foaming events.

Activated Sludge processes produce mechanistic deterministic models which are based on first engineering principles. This means that the model equations are developed from general balance equations applied to mass and other conserved quantities. This results in a set of ordinary differential equations that represent the biological and chemical reactions taking place in the Activated Sludge bioreactor. Further sub-models are needed to describe the other aspects of the complete Activated Sludge system. Consequently, a hydraulic model describes the tank volumes, hydraulic tank behaviour (e.g. perfectly mixed versus plug flow behaviour, constant versus variable volume, etc.) and the liquid flow rates in between tanks, such as return sludge flow rate and internal recycle flow rates. The separation process tank also needs to modelled, and dependant on the separation process used leads to models with varying degrees of complexity. For a conventional WWTP this is usually a secondary clarification sedimentation tank, while for a MBR system separation is via a membrane. The most popular models used are simple ideal point settlers with no retention time or a one-dimensional layered settler model such as (Takacs et al. 1991). Fig. 2.12 details the various components of a fully descriptive Activated Sludge model.

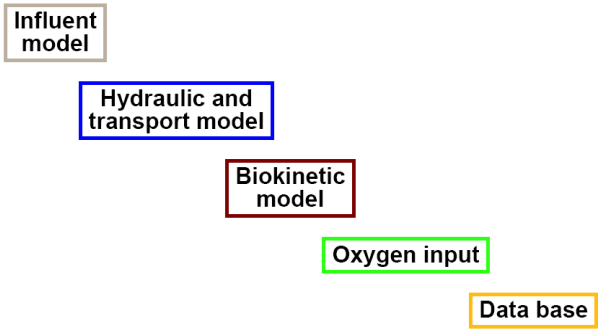

Fig. 2.12: Components of a model (Paul, 2006)

A number of factors have to be considered when Activated Sludge modelling is to be applied in practice. This step-wise approach allows evolution of the model from its initial purpose to the point where the WWTP model is available for simulations. The following main steps form this incremental process in the eventual development of a useful model:

1. Defining the WWTP model purpose or the objectives of the model application (e.g. control, design, simulation, etc.).
2. Model selection: Choice of the models needed to describe the different WWTP units to be considered in the simulation, i.e. selection of the Activated Sludge model (e.g. ASM1, ASM3, etc. mentioned in Section 2.3.2.1), the sedimentation model (e.g. Ideal point settler, Takacs, etc.).

3. Hydraulics of the system, i.e. determination of the hydraulic models for the WWTP or WWTP tanks.
4. Influent wastewater and biomass characterisation, including biomass sedimentation characteristics.
5. Data reconciliation to a steady-state model.
6. Calibration of the Activated Sludge kinetic model parameters using real-life plant data.
7. Dynamic model calibration and validation which determines whether or not the model is sufficiently accurate for its intended purpose.
8. Scenario evaluation for different situations (e.g. low aeration rates, toxic shock loads, etc).

2.3.2.1 General model set-up

The basic balance equations for each process occurring in the reactor form the basis of the model. They describe the change in concentration in a bioreactor in time as the result of biological and chemical conversions and of transport processes. In steady state, this change of concentration over time becomes zero. As explained previously, transport and conversion processes are two different parts of the model of physical and biochemical nature respectively. The biological and chemical conversions are termed micro-kinetics, and are common irrespective of the reactor used (e.g. plug flow or fully mixed, steel or concrete, Activated Sludge or attached growth systems, etc.), so can be considered as global conversion processes.

The basic aspects of the model consists of the following components:

1. General set-up - This includes influent flow details, tanks information and set-ups, plant historical data, plant operational data (e.g. dissolved oxygen (DO) setpoints, etc.), and process information (e.g. solids retention time (SRT), food-to-microorganism (F/M), etc.).
2. Stoichiometry - This refers to the actual conversion processes themselves. For instance for biomass growth, aeration is needed (e.g. as free oxygen or as Nitrates), some level of nutrients is needed (e.g. Nitrogen), and a food source is required (e.g. carbon substrate). The stoichiometry determines how much of each material is needed and used up to allow a specific conversion process to proceed, and also how much new material is generated.
3. Kinetics - Each process has its own reaction rate which determines how fast or slow it occurs dependent on kinetic parameters and also on availability of convertible materials.
4. Transport phenomena - This is the hydraulic model equations that describe flow splitting and combining, recirculation lines, and wastage flows.
5. Matrix notation - In order to simplify the whole process of describing a typical Activated Sludge model in easy to understand terms, a special notation has developed based on the Petersen matrix (Petersen et al. 2001). It summarises very quickly and concisely the salient details of each model, so that complex but repetitive and common equations and processes can be summarised on to one page. This means the modeller can quickly identify the inter-dependent relationships between the model concentration components, and the main differences in any newly developed model description.

A much fuller description of the Activated Sludge models, and more specifically the Activated Sludge Model No.1 (ASM1) and Activated Sludge Model No.3 (ASM3) is provided in Section 5.1.1, so only a cursory summary is provided here.

2.3.2.2 History of the Activated Sludge models

The Activated Sludge models were first developed by specialist working groups of the IWA as an advanced tool for measuring the effectiveness of treatment plant efficacy (Henze et al. 1987). Over the last two decades numerous versions and variations of these models have been developed and tested, but they are all based on the three main models summarised as follows:

- ASM1 - This was the first model developed mainly for research purposes. It considers organic carbon removal, nitrification and denitrification processes. A modified version is used in this study.
- ASM2 - This is the most complex model since not only does it considers the same processes as in ASM1, but also adds biological Phosphorous removal as well. There is a significant increase in the number of process states and process equations as well. It is not considered in this study.
- ASM3 - This model was developed as a more practical model to be used by field practitioners. It considers the same processes as ASM1, but should be easier to calibrate and validate due to its simpler process interactions. A modified version is used in this study.

2.3.3 Introduction to modelling used in Econometrics

The disadvantages of using the traditional ASM1 and ASM3 models are that since they are highly dimensional and contain numerous kinetic and stoichiometric parameters, which need determining by specific plant data and process operation, they are not omnipotent for every situation. Hence, the general application of such complex models, which in themselves require considerable calibration experience to give predictive accuracy, means their take up for process control and the development of operational strategies will always prove limited (Yoo et al. 2003). Other specific disadvantages of Activated Sludge modelling are (Gernaey et al. 2004):

1. For many applications insufficient data is available to allow a full calibration of a typical Activated Sludge model. It may also prove expensive to collect data since some costly respirometric laboratory tests may be needed to accurately determine some kinetic parameters.
2. These models cannot make any allowance for sludge bulking and foaming events in either the bioreactor or separator tanks. They also do not describe the layered Activated Sludge floc structure in which often simultaneous nitrification and denitrification take place.
3. For the municipal sewage treatment plant situation, these models are usually calibrated for dry weather situations resulting in model predictions that might be less accurate when rain events occur in the influent data.

Consequently what is needed is a quick and easy approach to wastewater treatment modelling which can be easily applied, and with very simple calibration procedures so that the model can be constantly "retrained" on newer data sets as and when they become available. Since this "retraining" would be easy, it could be performed as many times as necessary. To make this proposed new approach easy to apply, it should not require an intimate knowledge of the exact processes occurring in the MBR, so it could be applied by a non-specialist who was new to wastewater treatment modelling.

Very few alternative approaches have been used to date when compared to the traditional mechanistic models developed for wastewater treatment plant (Olsson and Newell 1999). This is mainly because wastewater treatment modellers and users come from an engineering background and therefore are unlikely to have an intimate knowledge of non-traditional approaches used in other disciplines such as the economics field. The bulk of the alternative approaches used in wastewater treatment modelling have centred around either multivariate statistical (MVS) methods (such as principal component analysis (PCA) and partial least squares (PLS)), or on an artificial intelligence (AI) methodology, where expert knowledge of the process systems is quantified and the developed system is then "trained" to provide accurate predication. Of these expert knowledge systems, the most commonly investigated are the artificial neural network (ANN) methods (Gernaey et al. 2004). Other AI applications include expert systems (e.g. rule-based systems, knowledge-based systems, ontologies, case-based systems, etc.), fuzzy logic, and genetic algorithm methods.

A lesser known approach is time series modelling using autoregressive models, which is more commonly used in Econometric systems forecasting for the international financial markets. It has only been used in a few limited cases for wastewater treatment modelling, and even then, only for the simple modelling of the effluent coming out of the plant (Dellana and West 2009). It is used here in this study and it is described more fully in the Section below.

2.3.3.1 Using Econometric modelling methods for wastewater treatment

It has been hypothesized that a behavioural model formulation based on simplified input/output times series models, should be developed as an alternate, simpler and faster way of calibrating and verifying MBR wastewater treatment models. This would mean that the exact nature of the biology in the bioreactor and its effects on the membrane fouling process need not be fully understood, as the time series models would be based solely on historical input/output data sets which would be used to predict future output. This procedure which is largely linearised around an operating point or range would be very useful for plant control and operation, and be much quicker than a phenomenological model since an intimate knowledge of the physics and chemistry behind the process would not be required. Additionally, complex theory and mathematics to describe this theory would not be needed thus saving time in model development.

2.3.3.2 What is a time series model?

What is a time series model? It is basically the use of empirical model forms combined with input and output data from a system to predict the future output data values. The times series is the historically known real input and output data points which are used for forecasting. These values are a sequence of observations and/or measurements taken sequential in time, thus producing real data sets. Traditional times series models have been used in the economics field such as to predict share price fluctuations, but theoretically could be used in any field or sector which produces sufficient data sets in time (Box et al. 2008). They are sometimes referred to as input-output models.

What is system identification for a selected data set? It is basically the building of a dynamic systems model based on measured data. The system identification procedure uses empirical model forms to build accurate, simplified models of complex systems from noisy time-series data (Ljung 1999). These methods and model forms have not been used to generate models for wastewater treatment systems, although as these systems are highly complex they should be ideally suited for prediction purposes.

Theoretically speaking there is no reason why a time series input-output model should not produce good results, since the data from a wastewater treatment process has the same sort of variance and unpredictability as data from Econometric sources. However, before any alternative modelling methods can be promoted, it is critical that good practice in the construction, testing and use of these models is codified and maintained. This would then allow independent modellers to fully evaluate any new approach. It is hoped that the alternative approach used in this study will prompt wastewater treatment modellers to fully engage in these alternative methods as quicker modelling procedures without significant loss in predictive accuracy.

The major advantage of an autoregressive modelling approach it that since it is based on the input and output behaviour of the system under investigation, whether the non-linear membrane fouling or bioreactor processes, it does not require any prior scientific knowledge and therefore the parameter estimation procedure can be fully automated. Additionally, if the model is being used only for operational purposes, then a simple linearised structure can be used to estimate state variables around a single operating point or narrow operational range, with linear models being more easier to solve than their non-linear counterparts. If the membrane fouling is being modelled by autoregressive methods, then the backflush process (if it occurs) is seen as a discontinuous process whose initial conditions would need to be reset after each backwash period had elapsed. Conversely, as a biological Activated Sludge model is a continuous process, it would more easily lend itself well to approximation by linear dynamic statistical, time series models at a specific operating point or within a narrow range.

2.3.3.3 Alternative modelling approach using System Identification / ARX models

Data driven modelling procedures refer to the fitting of the models to measured data. In simple terms, this means that the system identification models describe the relationship between one or more measured

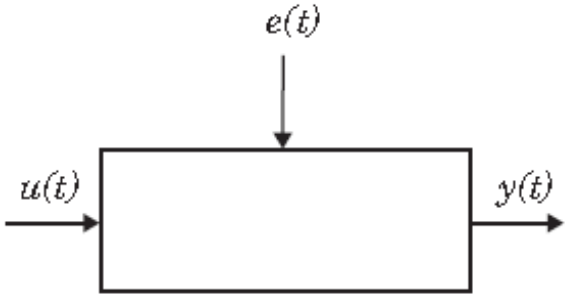

Fig. 2.13: General case for a input / output system (Paul, 2006)

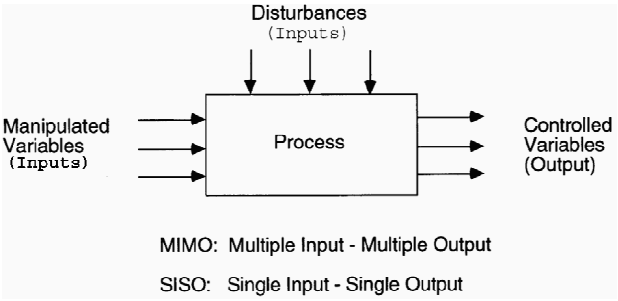

Fig. 2.14: Process control of input-output system (Paul, 2006)

input signals, $u(t)$, and one or more measured output signals, $y(t)$ as shown in Fig. 2.13. Additional inputs that affect the system output but that cannot be measured or controlled are called noise or disturbances, $e(t)$. For example if the system under investigation is an airplane, its inputs might be the positions of various control surfaces, such as elevators and ailerons. The outputs of the system might be the airplane orientation, velocity, and position. The noise might be wind gusts and turbulence that affect the outputs. Therefore system identification methods are used to identify models that are special cases of the general mathematical description of dynamic systems given in Equation 2.4.

$$y(t) = g(u, \theta) + v(t) \tag{2.4}$$

The output $y(t)$ of a system is determined by g, which might be a function of all previous inputs $u(s)(s \leq t)$ and system parameters θ. $v(t)$ is the output noise. For nonlinear models, g can take a variety of forms. For linear models, the general symbolic model description is given by Equation 2.5.

$$y = G \cdot u + H \cdot e \tag{2.5}$$

G is an operator that describes the system dynamics from the input to the output. G is usually called a *transfer function* between u and y. H is an operator that describes the properties of the additive output disturbance and is termed a *disturbance model*, or *noise model*. The actual disturbance contribution to the output, $H \cdot e$, has real importance and contains all the known and unknown influences on the measured y not included in the input u. Hence, if the experiments are repeated with the same input, the $H \cdot e$ vector explains why the output signal would be very slightly different for each case. The source of the noise, e, need not have any physical significance. In the case of the airplane, it is sufficient to estimate the noise in a black-box manner as arising from a white noise source via the transfer function H. Consequently there is no need to know how the turbulence and wind gusts are generated physically and all that matters are the characteristics of $H \cdot e$, such as the frequency content of the spectrum of $H \cdot e$. If the measured data includes noise, a model structure can be chosen that computes H to produce a more accurate dynamic model.

2.3.3.4 Autoregressive Exogenous Models - ARX and ARMAX

The autoregressive exogenous model is one of a group of linear prediction formulas based upon the general linear case described in Equation 2.5. This model type attempts to predict an output $y[n]$ of a system based on the previous outputs $(y[n-1], y[n-2]...)$ and inputs $(x[n], x[n-1], x[n-2]...)$. Deriving the linear prediction model for the estimated output, $y_e[n]$, involves determining the coefficients $a1, a2, ..$ and $b0, b1, b2, ...$ in Equation 2.6 (Box et al. 2008).

$$y_e[n] = a1 \cdot y[n-1] + a2 \cdot y[n-2]... + b0 \cdot x[n] + b1 \cdot x[n-1] + ... \tag{2.6}$$

There is is a remarkable similarity between the prediction formula and the difference equation used to describe discrete linear time invariant systems. Calculating a set of coefficients that give a good prediciton for $y_e[n]$ is tantamount to determining what the system is within the constraints of the order chosen.

A model which depends only on the previous outputs of the system is called an **A**uto**R**egressive e**X**ogenous(ARX) model, while a model which depends only on the inputs to the system is called a **M**oving **A**verage model (MA), and of course a model based on both inputs and outputs is an **A**uto**R**egressive **M**oving **A**verage e**X**ogenous (ARMAX) model.

2.3.3.5 Matlab's System Identification Toolbox© and GUI - Black Box modelling

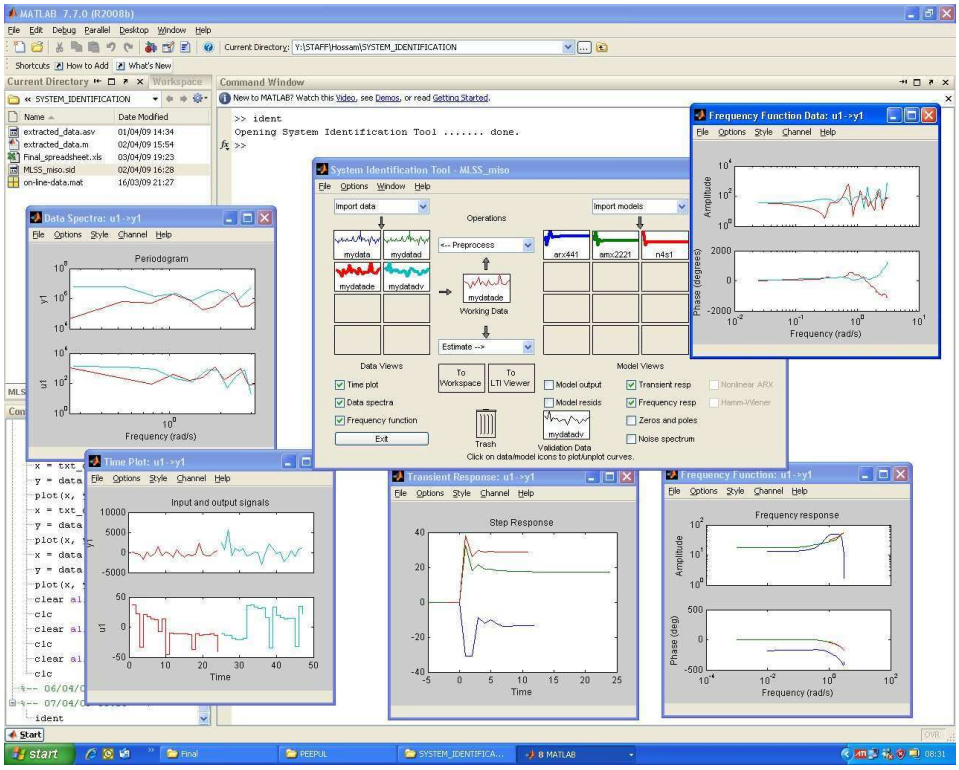

Fig. 2.15: Using Matlab's System Identification Toolbox and GUI

Matlab's System Identification Toolbox© and graphical user interface (GUI) was used later on in this research study to test the collated data from various MBR WWTP against several system identification models. Fig. 2.15 shows the typical GUI for this software package, which allows various input and

output systems to be modelled from single input single output (SISO), through to multi-input single output (MISO), and more complex multi-input multi-output (MIMO) systems. In this research study most systems being considered are of the MIMO variety.

To give a simple example of the types of data that can be modelled, some real life data from a working MBR was taken and modelled using three standard system identification models. These were autoregressive exogenous (ARX), autoregressive moving average exogenous (ARMAX), and state space models, the last of which is a special case of models utilising intermediate state vectors in the calculation procedure. Each model type has its own advantages and disadvantages. The input and output data used was as follows:

Inputs - Incoming COD (COD_{in}), incoming Ammonia (NH_{3in}), incoming Nitrate (NO_{3in}), incoming organic Nitrogen ($OrgN_{in}$), incoming total Phosphorus (TP_{in}).

Output - Bioreactor tank mixed liquor concentration ($MLSS_{bio}$).

Fig. 2.16 is a specific plot for a MISO system. In this plot all three models are compared against the actual measured values for the output, $MLSS_{bio}$), to ascertain the best fit. In this simple case the ARX model type gave the optimal fit for output data.

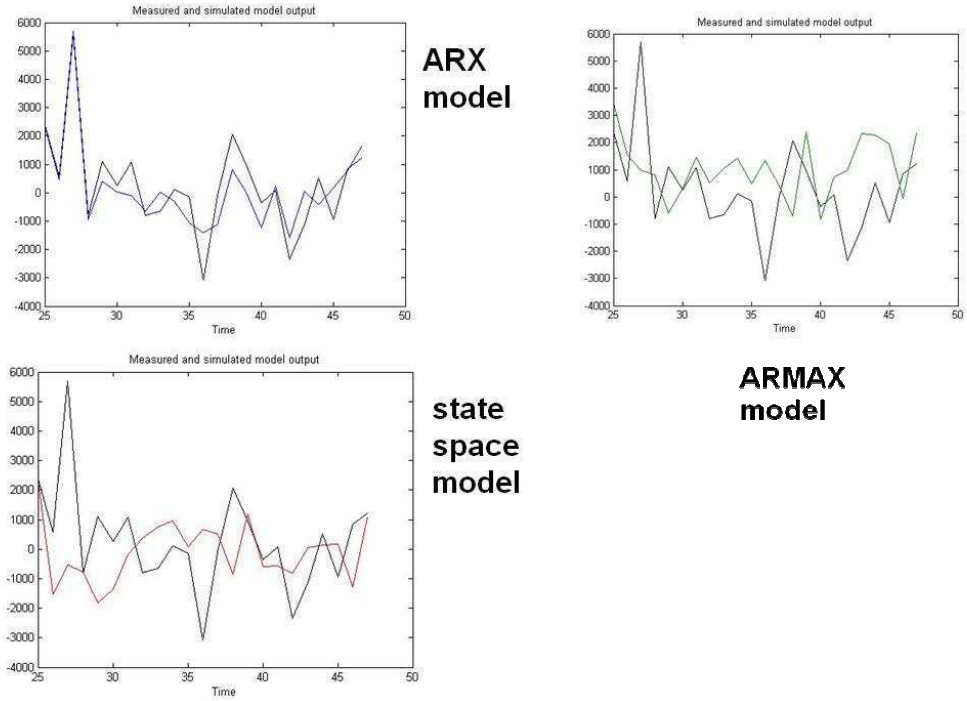

Fig. 2.16: Comparison of simulated output and modelled output for various model types available in the GUI

2.4 *Literature review: Membrane filtration processes and mechanisms of fouling related to Activated Sludge*

2.4.1 Main factor assumed to cause fouling

At present the concentration of EPS in either bound or soluble/colloidal form is considered by many researchers as the major cause of membrane fouling in a MBR system. As explained previously, EPS in its soluble/colloidal form found in the sludge supernatant is usually termed **SMP** and thought to play a more critical role in fouling than its bonded counterpart. The concentration of **SMP** in the supernatant can be highly variable, and depends on numerous factors such as the influent characteristics, solids loading rate, aeration system employed, SRT, MLSS concentration, shear stresses on the biomass flocs due to the hydrodynamic regime being employed, etc. Other factors that seem to promote **SMP** formation conditions are unsteady or intermittent plant operation, intermittent loading, hydraulic shock loads, biochemical toxic shock loads, irregular sludge wastage, variations in DO concentrations, and highly saline/acidic conditions (Barker and Stuckey 1999). All these factors contribute to the stressing of the microbes in the biomass which in turn leads them to produce cell encapsulation, i.e. produce EPS as a protective coating, with some of it subsequently being released and thereby dissolving into the supernatant as **SMP**.

Thus for a fixed membrane type with known operating conditions, the fouling is then mainly a function of unbound EPS and **SMP** concentration, and particle floc size distribution, and the various interactions between the floc size distribution and pore size distribution of the membrane. However the exact relationships between these factors and the degree of fouling are still unknown. Since the floc size distribution of a polydispersed Activated Sludge is hard to evaluate in practice, most research to date has concentrated on establishing correlations between fouling and EPS and **SMP** concentration in the sludge supernatant. Nielsen and Jahn (1999) reported that the bound EPS in flocs is composed of sheaths, condensed gel, capsular polymers, loosely bound polymers and attached organics, whilst free soluble, unbound EPS also termed **SMP** is composed of soluble macromolecules, colloids and slimes (Nuengjamnong et al. 2005). Soluble **SMP** is biodegradable and can be produced by the dissolution of bound EPS (Hsieh et al. 1994, Nielsen et al. 1997).

It is generally accepted that **SMP** contributes to irreversible fouling such as pore constriction mechanisms, while MLSS and EPS cause reversible fouling such as cake formation mechanisms (Drews et al. 2008). Some properties of the Activated Sludge flocs themselves are changed by the EPS levels, and is reported to increase the cake resistance (Nuengjamnong et al. 2005, Broeckmann et al. 2006). It has been reported by Grelier et al. (2006) that not only are the relative concentrations of EPS and **SMP** important on the fouling rate but also the composition of the EPS and **SMP** themselves as polysaccharides and protein content. The **SMP** is composed of polysaccharide and proteins of various sizes and types. Further, **SMP** has been found to contribute not only to irreversible fouling but reversible fouling as well (Grelier et al. 2006, Hoa et al. 2003). Rosenberger and Kraume (2002) cited in their study that the polysaccharide fraction is the major culprit component of the **SMP** that is responsible for the increase in significant fouling potential in a MBR. Lesjean et al. (2004) backed these findings by ascertaining a linear correlation between the polysaccharide concentration and fouling rate. Therefore some researchers insist that **SMP** is the main fouling agent, whilst others feel further research is needed in this area, and that **SMP** may only be important under specific conditions such as low SRTs and large pore sizes of the membrane under use (Drews et al. 2008).

Despite the large number of investigations and publications, no universal correlation or agreement has been found between the **SMP** concentration and the membrane fouling rate apart from very generalised ones. In fact in some research findings the relationship between fouling factors and fouling rate is often even contradictory (Drews et al. 2008). This can partly be attributed to the huge variation in the plant used in studies, with each having a variety of influent wastewater loadings, configurations, operating conditions, membrane materials, types and membrane operation (e.g. flux produced, backwash interval employed, etc.). Another problem in evaluating and comparing results from different research teams is the difference in sample preparation and analytical methods as well as in the way fouling itself is characterised (EUROMBRA 2007, Judd and Judd 2006).

Due to the current inconsistency in results from different research studies and due to the disagreement between researcher's on membrane fouling mechanisms, it was decided that for the sake of clarity the best approach to adopt in this study would be to assume that the **SMP** concentration can be largely correlated to the membrane fouling rate as this is what most researchers have found. This is as suggested by Drews et al. (2008) in her paper although the relative error in using this approach cannot be exactly quantified. Thus all other modelling results produced would be based on this basic assumption holding true.

2.4.2 Other important fouling factors

In reality fouling in MBRs is an extremely complex process as it is induced by various types of foulants in the Activated Sludge from solids, colloidal matter, and soluble substances. It is also caused by the interaction of different mechanisms in and on the membrane from the build up of cake material, the accumulation of soluble material in the pores, the formation of biofilms on the surface, and the adsorption of scalant material into the actual membrane structure. In recent research studies it has been determined that fouling is influenced by the following main factors:

1. Characteristics of the membrane itself - pore size distribution, membrane material, membrane type, membrane hydrophobicity (Choi et al. 2005a).
2. Characteristics of the biomass sludge - floc structure (Meng and Yang 2007) and floc size distribution (Wisniewski and Grasmick 1998), EPS type and concentration, **SMP** formation conditions.
3. Configuration of plant and operating conditions, especially permeability recovery mechanism (Meng and Yang 2007) - flux regime (e.g. constant flux / constant TMP, periodical air or permeate backwash sequencing (Psoch and Schiewer 2006, Mugnier et al. 2000), and/or periodical relaxation, and/or intermittent suction operation, and/or air sparging intensity (Psoch and Schiewer 2006), and/or CFV (Choi et al. 2005a, Tardieu et al. 1998), process operation conditions (e.g. SRT, MLSS, liquor viscosity, etc.).

Off course the influent characteristics are also important in determining the fouling potential on the membrane, although usually in an indirect way, unless the influent stream induces an extreme rapid toxic shock loading into the bioreactor. For example in a recent study by Arabi and Nakhla (2008), he investigated the fouling in submerged MBR systems under two different Calcium levels of 280 and 830 mg/l respectively. These dissolved Calcium cations contribute to the system alkalinity and thus affect the biological reactions. Two MBRs were operated on a synthetic wastewater stream at a SRT of 15 days using a control influent Calcium level of 35 mg/l and a test reactor at two influent Calcium concentrations of 280 and 830 mg/l. Whilst in operation, various measurements were taken at regular intervals including permeability, eEPS concentration, Calcium ion concentration, and particle size distribution. Arabi and Nakhla (2008) found that the test reactor showed a 35% higher permeability level than the control when at a Calcium concentration of 280 mg/l. Conversely for a feed concentration of 830 mg/l of Calcium ions, the permeability in the test reactor was 50% lower than the control. He hypothesised that this lower membrane fouling rate for the MBR system fed at an influent Calcium concentration of 280 mg/l was due to cationic bridges being formed with the eEPS within the floc thus preventing its release. Further, he hypothesised the reduction in permeability at the higher concentration could be attributed to the increased inorganic scalant fouling potential of the sludge.

More common operating conditions, such as SRTs, are known to considerably affect the fouling potential of the mixed liquor. In the study by Nuengjamnong et al. (2005), the affects of both eEPS and the supernatant of the sludge flocs was investigated on the membrane fouling in submerged MBRs for various SRTs. Three laboratory scale MBRs were operated at a sub-critical constant permeate flux of 12.5 $l/m^2/hr$ using FP MF membranes at different SRTs times of 8, 20 and 80 days respectively. The membranes were hydrophilic polyolefin material with average pore size of 0.25 μm. The concentrations of eEPS, which was extracted by the cation-exchange resin method, and the dissolved organic carbon (DOC) in the supernatant were compared while at steady state operation. The results obtained indicated that as the SRT increased, the

organic carbon content in the eEPS decreased, whereas the DOC in the supernatant tended to be independent of the SRT. Further batch filtration tests were carried out to evaluate the specific cake resistance of the fouling layer using both the raw sludge and twice washed sludge with buffer solution. It was found that for these additional tests, the supernatant contributed 50% of the total specific cake resistance. In conclusion, Nuengjamnong et al. (2005) found that the organic carbon and protein content in the eEPS decreased with increasing SRT, and the protein content in the supernatant also exhibited this same tendency. This is as expected as higher SRTs would normally produce a better conditioned sludge with balanced species diversity and "non-stressed" bacterial biomass.

The breakdown of organic carbon substrate by bacterial biomass, which is the natural wastewater treatment process, does contribute to **SMP** levels and thus fouling. Additionally, higher **SMP** levels can be experienced due to nutrient imbalances, especially in Nitrogen levels, which would then impact on both substrate removal and the nitrification and denitrification rates. These in turn could cause potential upset to the bacterial biomass thus provoking a reaction by increased eEPS production and subsequent increased **SMP** levels, all of which promote membrane fouling. Thus it is essential that a properly configured and run MBR is operated at optimal nitrification and denitrification rates based upon on incoming influent Total Nitrogen (TN) level and the DO setpoint level. Sarioglu et al. (2009) in his study investigated this potential route to increased fouling by evaluating the optimal simultaneous nitrification and denitrification processes in a MBR operated with no separate anoxic volume. His MBR was fed with strong domestic sewage and operated at a SRT of 36 days under steady state conditions with a corresponding MLSS range of 17,500 to 21,000 mg/l and average wastewater temperature range of 20 to 25 $^{\circ}C$. The DO level was kept at approximately 1.8 mgO_2/l in the bioreactor, while simultaneous nitrification/denitrification was maintained due to the limited diffusion of oxygen into large flocs. It was found that nitrification was only partial since the Ammoniacal Nitrogen profile always remained high at above 50 mg/l and essentially followed the fluctuating trend of the influent Total Kjeldahl Nitrogen (TKN) level. Conversely it was found that the available Nitrate was fully depleted with complete denitrification occurring. This enabled an average of 57 mgN/l of the influent TN to be removed in the MBR without the need for a separate anoxic volume. In a bid to improve the nitrification and denitrification rates, modelling simulation studies were carried out to by using an Activated Sludge model with experimental data. The model's kinetic parameters were optimised to account for the floc diffusion limitation and the resulting simultaneous nitrification/denitrification in terms of the high half saturation constants. This yielded subsequent half saturation constants of K_{OH} 1.75 mgO_2/l for heterotrophic bacteria and K_{OA} 2.0 mgO_2/l for autotrophic bacteria. The calibrated model was then used to optimize the MBR operation for Nitrogen removal. This study identified a MLSS threshold level of about 16,000 mg/l below which Nitrogen removal was essentially controlled by the denitrification process, and above which the rate limiting mechanism shifted to the nitrification process. The study also concluded that a conservative DO level of about 1.5 mg/l enabled Nitrogen removal efficiencies in the range of 85-95% for a typical domestic sewage.

As mentioned in the previous study, DO control is essential in maintaining a healthy biomass with reduced fouling potential. Air sparging which indirectly adds to the DO level is also used to control fouling on the membrane but obviously has an operational cost implication. Therefore there is also a need to optimise this air usage to prevent excess aeration for controlling membrane fouling in a submerged system. In this regard, Kim et al. (2008) proposed an alternative strategy for membrane fouling control by reconfiguring the membrane module's vertical location. Hence to reduce the biomass concentration on the membrane surface, the membrane position was elevated from the bottom to the top of the bioreactor. This essentially divided the bioreactor into two different zones termed upper and lower. Sparging air was not supplied at the lower zone whereas aeration was given to the upper zone where membrane filtration was carried out. The MLSS concentration, and subsequent membrane fouling, was accordingly reduced in the upper zone because the mixed liquor settled down to the lower zone. In this study it was found that when the membrane was moved vertically higher up in the bioreactor, less fouling was observed. This could potentially assist in fouling control while reducing air sparging needs. Additionally, Kim et al. (2008) stated in his study that the reduced DO levels in the returned sludge to an anoxic tank would increase denitrification efficiency if this configuration was directly applied for biological nutrient removal.

In a similar study by Choi et al. (2002), the Activated Sludge biomass was cultivated under three conditions in a MBR. These were: 1) normal with high DO levels; 2) bulking sludge; and, 3) normal conditions with low DO levels. Membrane filtration tests were performed using three different membrane materials. These

were cellulose acetate (CA), sulfonated polyethersulfone (SPES) and PES membranes respectively. It was found that, as anticipated, the relatively hydrophobic PES membrane fouled more seriously than the hydrophilic CA membranes. This phenomena was especially pronounced under bulking conditions. However, the ultimate flux was almost equal for all three membrane types as the PES and SPES started with higher initial fluxes. In terms of effluent quality, this was not affected by the membrane fouling or flux rates but did deteriorate at low DOs. This study again backs up the conclusion of using several different factors to mitigate against membrane fouling. In this case the factors would be by using well conditioned sludge with reasonable DO levels and hydrophillic membranes to keep overall fouling low.

Currently some researchers are developing additives which could in future be used to control membrane fouling rates without greatly affecting the sensitive bacterial biomass. Wang et al. (2009) reported that he could achieve the same filterability behaviour of an EPS solution taken from Activated Sludge produced by a WWTP with that of a synthetic EPS solution with five times the protein concentration. In his study he prepared a series of model EPS solutions by using sodium alginate, humic acid and some proteins on the basis of the components of actual EPS extracted from sludge for a laboratory scale sequence batch reactor (SBR) by using the Formaldehyde/Sodium Hydroxide method. He then dead-end filtered these model solutions through a 0.1 μm PVDF MF membrane under a TMP of 0.1 MPa. The experimental results showed that the filterability behaviors of bovine serum albumen (BSA), β-lactoglobulin and lysozyme model solutions with five times the protein concentration in the actual EPS were similar with that of the actual EPS solution. Also the addition of humic acid and sodium alginate enhanced the rejection of proteins. This means possible mechanisms could be developed in future to reduce EPS fouling potential by the judicious use of additives.

Of course some factors that routinely contribute to membrane fouling cannot be environmentally controlled such as the impact of air temperature. In a very recent study, Guglielmi et al. (2010) measured the physical properties of sludge from a pilot MBR plant over a two year period. It was found that the air temperature significantly impacted on the capillary suction time (CST) and hence the sludge filterability due to the increase of organic matter in the liquid phase. It was further found that although MLSS levels are the most important component affecting sludge filterability, the impact of colloids and solutes (i.e. **SMP** and EPS) increased when the temperature decreased, thus confirming the generally worse sludge conditioning at reduced temperatures.

2.5 *Literature review: Wastewater treatment modelling*

At the moment the practical application of models developed by the research community to predict the performance of MBR processes is very limited. Several factors are thought responsible for this perceived gap between research and practice. Firstly a solid understanding of the various fouling mechanisms has not been achieved to date and research is still on-going. Secondly, the current knowledge of existing process models has not been consolidated into a single set of design guidelines for use by the practising engineer. Finally practical examples of the successful use of models in plant design, operation and control is still lacking.

In terms of this specific research work, it does not definitively clarify the exact fouling mechanisms responsible for fouling of the membrane, although it does come up with a single set of framework guidelines to be used when setting up all future MBR models of all types.

Modelling simulation studies using rigorous process models can prove to be a powerful tool used to increase the understanding of the process and its decisive characteristics in order to design optimal processes and efficient operational strategies. As such Ng and Kim (2007) carried out a comprehensive mini-review of MBR modelling studies for municipal wastewater treatment in which three categories of models were reviewed, evaluated and discussed, namely, membrane fouling models, biomass kinetic models (such as the IWAs Activated Sludge variety models), and integrated models with light couplings to describe the full MBR process. Although this was an interesting review from a layman's point of view, it provided little or no additional insight than was already known by researchers in this complex field.

2.5.1 Membrane filtration models

2.5.1.1 Proposed fouling mechanism

In Le-Clech et al. (2006), it is suggested that a "Three-Stage-Fouling" model should be considered for the whole membrane fouling and clogging process for the entire flux range from sub-critical up to supra-critical fluxes. Fig. 2.17 summarises this model. It was developed to explain the experimental results commonly found when measuring fouling across the entire flux range. These results expressed by this "Three-Stage-Fouling" model have been replicated by many researchers (Barker and Stuckey 1999, Ye et al. 2005b,a) both by using pilot membrane plant being fed either actual wastewater or synthetic solutions. Hence Le-Clech et al. (2006) hypothesises that for constant flux operation, this fouling process consists of the following distinctive stages in this model formulation:

1. Passive conditioning - this is adsorption of protein macromolecules and refractory organics onto the virgin membrane without a flux being induced. At this stage the fouling is independent and unaffected by the flux/shear developed.
2. Slow/steady fouling - this is a pseudo-steady state operation in which operation occurs at sub-critical flux. The fouling gradually increases between cleaning periods usually quasi-linearly with TMP. This is the normal or best operating window for a MBR.
3. Rapid TMP jump - at this final stage there is a catastrophic decrease in permeability caused when sub-critical flux is exceeded. This is when more aggressive membrane cleaning is required as it is outside the usual operating window. Significant irreversible fouling may also occur during this stage which cannot be removed with later chemical cleans. This is also when the membrane could receive some permanent damage to it.

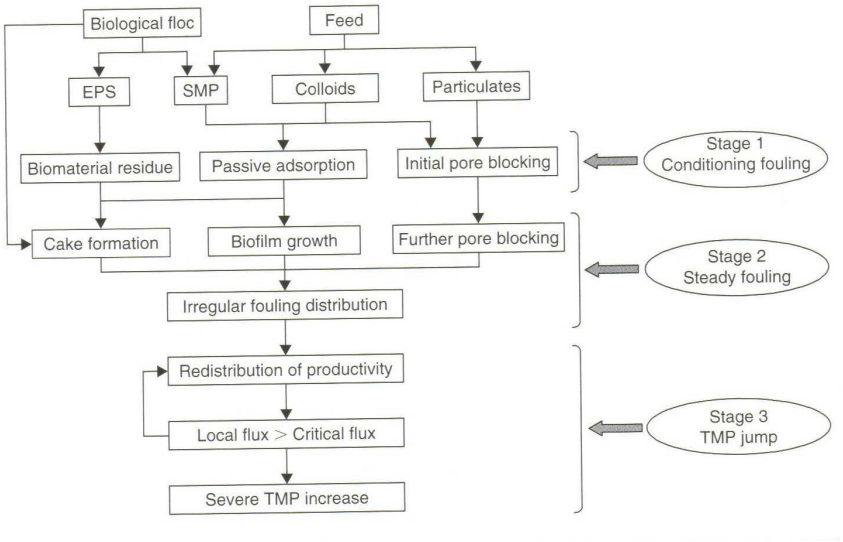

Fig. 2.17: Fouling mechanisms for a MBR operated at constant flux using TMP Jump Theory (Judd and Judd, 2006)

2.5.1.2 TMP Jump

Fig. 2.18 shows typical experimental plots of this sudden and catastrophic increase in fouling for a MBR operated under constant conditions for a long period of time (Ognier et al. 2004). This happens irrespective of plant configuration or membrane type used. All they determine is how quickly this jump in TMP occurs at constant operation. Fig. 2.19 details the relationship between flux and TMP for a standard MBR, in which the relationship is fairly linear at sub-critical fluxes and then, as expected, becomes almost exponential at supra-critical fluxes (Ognier et al. 2004). Another way of showing this relationship is outlined in Fig. 2.20 in which at fluxes well above critical, the TMP jump occurs almost immediately while at fluxes well below critical this TMP takes along time to occur and even when it does it is less detrimental (Ye et al. 2005a).

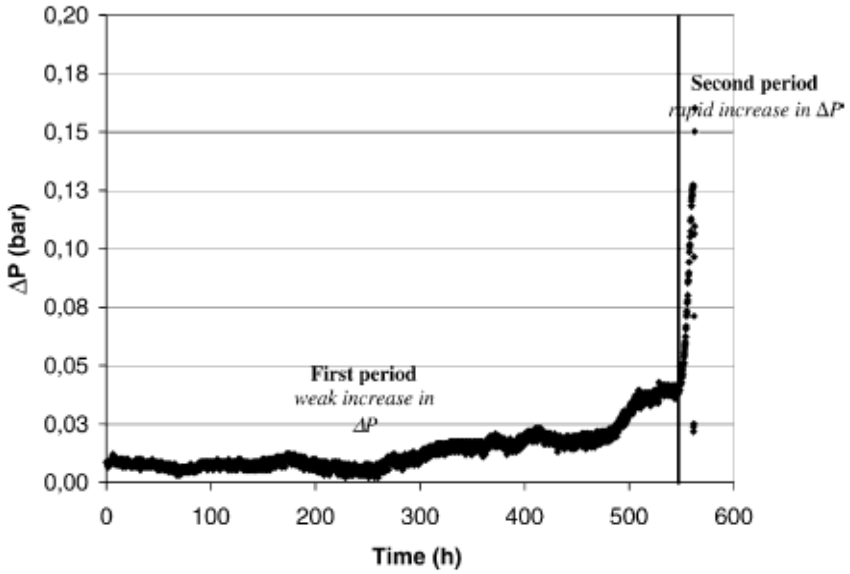

Fig. 2.18: TMP changes during long term constant flux operation of a MBR under stabilised biological conditions (Judd and Judd, 2006)

Various models have been developed to explain this sudden and often deleterious exponential increase in fouling. They can be summarised as follows:

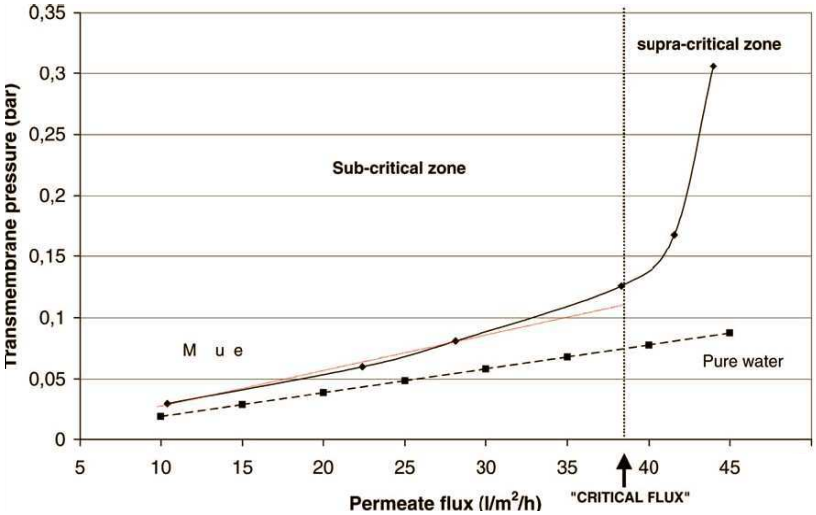

Fig. 2.19: Plot of TMP versus Flux for a typical MBR (Judd and Judd, 2006)

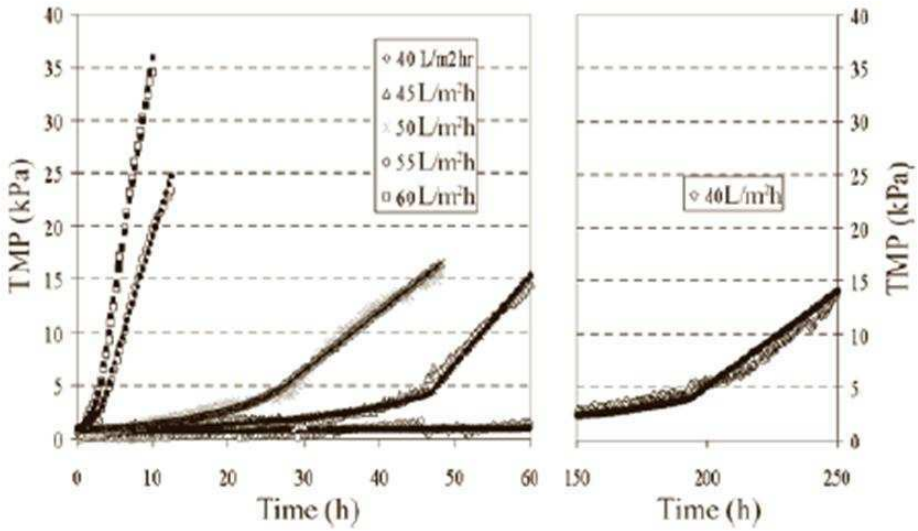

Fig. 2.20: TMP Jump versus Flux relationship (Judd and Judd, 2006)

- Non-uniform distribution of foulants - Area Loss model (Cho and Fane 2002), Pore Loss Model (Ye et al. 2005a). In these models the sub-critical flux is exceeded at a local or regional level for certain portions of the membrane. These localised supra-critical fluxes then further reduce the area/pores contributing to sub-critical fluxes, and when they reach a critical tipping point, the dramatic TMP increase occurs.
- Critical Suction Pressure Model (Chang et al. 2005) - This model describes the sudden collapse of the cake layer under a critical TMP. This cake material can be highly compressible depending on the hydrodynamic regime employed and the cake composition (i.e. floc size and structure). This sudden cake compression causes a rapid build up in resistance in a very short space of time.
- Percolation Theory (Hermanowicz 2004) - This model uses the critical loss of diffusivity of the cake layer since more particles aggregate in the cake layer pore spaces. This means that the cake layer is taken as being highly porous with smaller particles, aggregates and colloidal material travelling towards the concentration polarisation zone by natural convective transport, and taking up the void spaces in the cake layer which is currently taken up by fluid. When this mechanism reaches a critical point, the cake resistance increases dramatically, causing the apparent TMP jump.

2.5.1.3 Fouling models operating at normal operational conditions

The above models are useful for experimental and laboratory tests, however, are of lesser significance for plant design, operation and control, when the normal plant operating conditions do not usually or intentionally exceed the membrane manufacturer's range of design fluxes/TMPs which are always well below critical. Therefore capturing these membrane fouling phenomena in the form of a useful mathematical model for plant design, operation and control has been a task of many different research groups around the world for more than a decade (Ng and Kim 2007). Over that time many approaches of various complexities and usefulness have been adopted (Kim and DiGiano 2009), with the major ones being described below.

2.5.1.4 Comprehensive models

Several comprehensive mechanistic models which include all possible process interactions and mechanisms have been developed. Their advantage is that they can fully model the system under investigation, but their main disadvantage is that they contain many unverified parameters needing estimation (i.e. they are over parameterised). They can also prove to be too complex for general use and may be better suited as pure research tools.

In this regard, a theoretical model of dead-end MF of dilute suspensions was proposed by Kosvintsev et al. (2003). This model was based on a MF sieve mechanism and accounts for the probability of membrane pore blocking during filtration of dilute colloidal suspensions. Kosvintsev et al. (2003) produced an integral-differential equation (IDE) that included both the membrane pore size and the particle size distributions. This model includes only one fitting parameter which accounts for the full range of hydrodynamic influences on a single pore. Therefore for a narrow pore size distribution in which one pore diameter predominates, such as for track-etched membranes, the IDE was solved analytically and the derived equation gave good agreement with measurements taken from different track-etched membranes. A simple approximate solution of the IDE was also derived and was used on the output from a Teflon MF membrane, again giving good results. In his paper, Kosvintsev et al. (2003) further develops his model theory to account for the presence of multiple pores (e.g. double, triple and so on pores) on a track-etched membrane surface. He observed three stages of filtration with the initial stage being well described by the proposed pore blocking model. The second stage corresponded to the transition from the blocking mechanism to the third stage, which was cake filtration. Consequently, this model bridges the gap between the "Three-Stage-Fouling" model described earlier and a more practically useful model with a simple parameter set.

Broeckmann et al. (2006) later developed a fouling model for a MBR system that also considered pore size and floc size distributions which are an important aspect in contributing to overall fouling potential. In his

model the irreversible fouling was modelled as pore blocking with the porosity of the membrane decreasing over time. Hence this pore blocking resistance was represented with the Karman-Kozeny equation, which is usually used for flow modelling in porous media. Conversely, the cake formation which was the reversible fouling was calculated using the mechanistic equation for forces acting on a spherical particle in contact with a flat membrane. Thus the cake resistance was calculated using the Blake-Kozeny equation. Broeckmann et al. (2006) states that both phenomena are essential characteristics which need to be considered for a reliable prediction of process behavior. The model was successfully tested by using simulation studies and the output was compared to experimental data from a pilot submerged MBR plant with HF membranes.

Busch et al. (2007) developed a fully comprehensive model which consisted of several sub-models that modelled different aspects of the MBR process. These models could then account, for example, with membrane configuration and geometry (e.g. HF, FP, MT, etc.), the hydrodynamics of the feed flow, the hydrodynamics of the permeate flow, the cleaning mechanisms employed (e.g. backflushing, air sparging, relaxation, etc.), and the various filtration resistance components. This filtration resistance was broken down into component parts using a high level of detail. It consisted of clean membrane resistance, pore blocking resistance, cake layer formation resistance, polydispersed particle resistance, biofilm formation resistance, and concentration polarisation effects. The cake layer formation was considered as polydispersible flocs, and irreversible fouling was based on the Karman-Kozeny equation. This model was fully analysed in simulation and sensitivity studies, and the influence of important operational parameters of the biological system and the membrane cleaning mechanisms on the filtration performance was also investigated. Busch et al. (2007) stated that his model provided a major insight into the MF and UF processes in MBRs and the interplay of the related physical, chemical, and biological phenomena.

Gehlert et al. (2005) created a rigorous mathematical model of an open channel cassette module for use in a MBR. The idea behind the model was to apply the resistance-in-series approach to both forward filtration and the backflushing procedure. Also the geometry of the cassette module was modelled using an one-dimensional approach to gain more detailed information regarding the permeate flux, the cake layer and the TMP as a function of the module length. Gehlert et al. (2005) stated that this full modelling approach produced good agreement with experimental results for various different operating points. It also allowed the backflushing pressure to be optimised, as well as allowing the investigation of the cake layer formation as a function of the module length.

In contrast, Zarragoitia-González et al. (2008) created a mathematical model to simulate the filtration process and aeration influence on a submerged MBR operated under aerobic conditions. The model included the biochemical kinetics and the dynamic effect of the sludge attachment and detachment from the membrane, in relation to both the filtration and a strong intermittent aeration process. It also contained the formation and degradation of **SMP**, and the fouling components responsible for pore clogging, sludge cake growth, and temporal sludge film coverage. This comprehensive model included the influence of **SMP**, TMP, and MLSS on the specific filtration resistance of the sludge cake. The model was also developed to evaluate the influence of an intermittent aeration rate on the sludge cake removal rate.

2.5.1.5 Simple models

Simple models based on many assumptions and simplifications of the real processes have the advantage of reduced parameter sets. The main disadvantage is that either the model behaviour is too simplistic thus making them not very useful or the model's degrees of freedom are severely limited. For instance Lee et al. (2002) developed a very simple cake build up model which just considered the MLSS in very simple terms. Similarly Wintgens et al. (2003) produced a easy-to-use cake build up and pore blocking model based upon a simple resistance-in-series expression, which however didn't reflect reality that well as it depicted total membrane resistance as reaching a saturation value at supra-critical fluxes when in actual fact it should be an exponential increase.

This does not mean to say that a simple but relevant model can never be developed, since Ognier et al. (2004) did just this by introducing the concept of local critical flux to explain the TMP jump conditions

experienced at long filtration periods when no CiP procedures are applied. In this simple model, which does consider pore size and particle sizes, albeit in a limited way, and which was developed under constant flux operation, the membrane pores are depicted as round openings of identical diameter that are gradually closed due to the deposition of **SMP**. This model version only has one single global parameter requiring calibration whose value can be derived from monitoring the changes in TMP. Ognier et al. (2004) has a clever but simple switching mechanism to reflect reality when pore blocking ceases and cake build up predominates. Ognier et al. (2004) states that this model accurately depicts the TMP jump process even when the plant is operated for long periods at constant flux, since it considers local flux conditions becoming critical even when the notional overall net flux is well below critical. It works on the hypothesis that the open surface is reduced locally due to a successive blocking of membrane pores, thereby creating localised critical flux conditions.

Ye et al. (2006) developed a very similar but slightly more complex model for predicting TMP evolution under long term sub-critical filtration of synthetic EPS solutions. In this model, she uses a combined standard pore blocking expression (i.e. gradual pore closure) and complete pore blocking expression (i.e. particles block individual pores) which is coupled to a cake filtration model, with the notional diameter of single protein aggregate acting as the switching function between pore closure and cake build up. Ye et al. (2006) states that this model is capable of predicting a sudden transition between a slow rate of TMP increase to a rapid rise of in the resistance, with the lower the sub-critical flux applied, the longer the first fouling stage lasting. This model accounts for the pore size distribution of the membrane, which other models do not consider, and models the membrane pores as capillary pipes to which is then applied the Hagen-Poiseuille Law for the calculation of pressure losses during filtration. Hence, the pore sizes gradually reduce as **SMP** is deposited inside the membrane, and when the pore sizes reach a critical value in the distribution (i.e. becomes greater than the single aggregated protein particle size), the fouling mechanism changes from pore constriction to cake build-up and a sudden increase in TMP occurs. Consequently, the pore blocking depends purely on the pore size distribution, and switching mechanism between pore blocking and cake build up depends solely on the protein particle size, with cake build up linearly increasing with **SMP** concentration.

In an alternative vein, Psoch and Schiewer (2006) constructed a model based on pore constriction resistance, cake resistance and clean membrane resistance with air sparging and backflushing mechanisms also included. It was calibrated and validated using a synthetic wastewater fed to a submerged MBR system with average MLSS of 12 to 18 g/l. Experimental results indicated that the highest permeate yield occurred with simultaneous air sparging and backflushing occurring, and this also led to reduced measured cake layer thickness. In a similar fashion, Choi et al. (2005b) investigated the influence of crossflow velocity on the formation of the fouling layer during filtration of biomass with MLSS concentration of 5 g/l. He formulated a resistance-in-series model, which was verified using experimentally determined total filtration resistances caused by adsorption, concentration polarization, and reversible and irreversible fouling. Choi et al. (2005b) found that permeate flux increased linearly with increasing CFV and a high CFV was more effective at reducing fouling of MF membranes than that of UF membranes. In fact the formation of a reversible fouling layer was actually prevented by a CFV of 3 m/s for MF membrane and 2 m/s for UF membrane. Additionally, he found that along with its mass and thickness, the density of the fouling layer was another important factor affecting overall filtration resistance and DOC rejection rate.

2.5.1.6 Classical blocking law models

This set of models use the classical blocking laws developed by Hermia (1982) as the start point for developing a model description. Ho and Zydney (2000) developed the first real combined fouling model which accounted for the classical complete pore blockage equation, intermediate pore blockage equation and cake filtration mechanisms. The model was validated and was in good agreement with flux decline data obtained from BSA filtration experiments. This model was further extended by the extensive and comprehensive work of Duclos-Orsello et al. (2006) in which an internal pore constriction mechanism was modelled as a reduction of pore diameters by the Hagen-Poiseuille Law.

Vela et al. (2006) created and applied a dynamic model that combined pore blocking and cake formation in crossflow UF membranes, again using Hagen-Poiseuille Law and the Karman-Kozeny equation for water flow in porous media. Conversely, Hermanowicz (2004) proposed a unified model based on a percolation theory which accounted for the full flux range and also which catered for the dramatic decrease of permeability at long operational times that is encountered in practice.

2.5.1.7 Non-classical modelling approaches

Other modelling methods which do not rely either on standard mechanistic equations taken from first principles or on classical theory have been developed by some researchers as an alternative. Seminario et al. (2002) evolved a stochastic approach to the modelling of fouling in MF membranes, in which the membrane pore spaces were represented by a bundle of non-intersecting tubes. The permeability reduction over time during the crossflow filtration of a well characterised synthetic particle suspension was determined using this model which was based on a Monte-Carlo technique. Seminario et al. (2002) found in his model that the dominant mechanisms of membrane fouling were found to be particle capture and size exclusion at pore segments.

Meng and Yang (2007) developed a permeation model based on Fractal theory and Darcy's law to evaluate the permeability of cake formed in membrane filtration of Activated Sludge. He hypothesised that as the microstructure of a cake layer is very disordered and complex and is difficult to describe by conventional geometry, then Fractal theory can be effectively applied to characterise the irregular objects in terms of its average and similar properties. Consequently, this Fractal permeation model provided a method for determining the resistance of the cake build up on a membrane surface. However, Meng and Yang (2007) stated that more validation studies were needed in order to determine it's applicability in real life situations.

All of the fouling models discussed so far can be loosely termed as "lumped models" since they do not represent spatial variability of fouling and filtration conditions on the membrane. For more accurate modelling of fouling where spatial differences and geometry is fully accounted for, a "distributed model" is required such as those developed by using computational fluid dynamics (CFD) methods. However, as things stand these models would usually prove impractical in real situations and prohibitively expensive to develop as they would be very site specific. They are mentioned here for the sake of completeness even though they are more research tools at the present moment.

A selection of these "lumped" fouling models were assessed for suitability to be utilised in this study as a starting point for developing an improved membrane fouling model which could be used for practical purposes whilst still being rigorous enough mechanistically speaking. Table 2.2 compares the selected models and rates them numerically in terms of usefulness to this study. As can be seen the Duclos-Orsello et al. (2006) is rated as the most useful, and so was used as a start point in Chapter 4.

Model author	Usefulness (0-10)	Comments
Ye et al. (2005b)	2	Sequence model.
Ognier et al. (2004)	7	Simple model formulation.
Ho and Zydney (2000)	6	Steady state simulations only conducted.
Kosvintsev et al. (2002)	3	Dead end model only.
Psoch and Schiewer (2006)	2	Mathematical description is poor.
Vela et al. (2006)	2	Time dependant model.
Busch et al. (2007)	8	Full model developed with add ons.
Gehlert et al. (2005)	5	Good model formulation.
Broeckmann et al. (2006)	7	Good model formulation.
Lee et al. (2002)	1	Too simplistic model.
Kosvintsev et al. (2003)	3	Dead end model only.
Liang et al. (2006)	5	Reversible and irreversible resistances.
Choi et al. (2005b)	2	No full model but good experimental results.
Wintgens et al. (2003)	7	Has connections to biological models.
Duclos-Orsello et al. (2006)	9	Contains all three major blocking mechanisms.

Table 2.2: Comparison of several fouling models for MBRs

2.5.2 Activated Sludge models

2.5.2.1 Appropriateness of using unmodified ASM models for MBRs

Before considering whether an Activated Sludge model should be used to express an MBR system, it is important to consider whether a MBR was a process in its own right or was simply a typical Activated Sludge process which has been combined with a typical membrane filtration process at the MF and UF ranges. If the latter was the case then standard Activated Sludge models like ASM1 could be utilised without major changes in stoichiometric structure and kinetic parameters. Some researchers feel that it should be treated as a unique process in its own rights (Stephenson et al. 2000, Fenu et al. 2010), for two main reasons:

- The membrane selectivity pressure means that specific biomass characteristic and floc morphology is apparent, i.e. pin flocs.
- The process intensification means that operation is at high mixed liquors and SRTs, so that further selectivity occurs. This situation is further pronounced as the membrane totally divorces the hydraulic retention time (HRT) and SRT from each other unlike all other main types of wastewater treatment technologies.

In a very recent extensive study by Fenu et al. (2010), he noted that all the main types of Activated Sludge models such as the ASM1 have been simply applied to a MBR without any significant modifications. However he also notes that recent studies in MBR processes all report several crucial similarities between MBR plant, namely, high SRTs, high MLSS, the accumulation of **SMP** rejected by the membranes, good nitrification performance, and constant membrane CiP requirements.

In a very early study by Chaize and Huyard (1991) when a conventional ASM1 model was used in an unmodified way to try to describe experimental results from a MBR, it was found that the model predicted lower MLSS concentrations than observed, and this prediction improved at higher HRTs. This discrepancy was probably due to the very high SRT of 100 days which a ASM1 type model is not strictly designed to cater for. Overall Chaize and Huyard (1991) found that the ASM1 gave reasonable estimates for effluent COD and TKN, but shows its limitations at low HRTs and high SRTs. This illustrates the need to apply great care when selecting and applying an Activated Sludge type model, especially when carrying significant modifications to the basic model by adding new processes, state components and kinetic/stoichiometric parameters. Hence, the Activated Sludge type biological models selected for later use in Chapter 5 of this study, are thoroughly evaluated by applying extensive sensitivity analysis protocols, to ensure their predictive capabilities are not compromised in any way. They were also carefully selected by referring to the results of other researchers (Ng and Kim 2007), so that they included light or strong couplings to allow their integration to the membrane fouling model which is assessed earlier on in Chapter 4.

In a very recent study by Jimenez et al. (2010), he tries to calibrate his version of the ASM1 under a broad range of operating conditions, such as from SRTs of 40 days down to 15 days, in order to validate and identify these model's limits. He also wishes to investigate the impact of a pre-treatment by primary sedimentation on sludge production, sludge characteristics and permeate quality. He does this by operating two MBR pilots side-by-side under the same operating conditions, one fed by 1 mm screened raw municipal wastewater and the other by primary settled raw municipal wastewater. This series operation allows a true comparison of the performances and model calibration. It was observed that screened water contained 30% more solids than settled water. He found that with a SRT of 15 days, sludge production was less of a concern in the pilot fed by settled water because it could be more easily degraded by having less slowly biodegradable components. Also in comparison with the ASM1 default parameter values, calibrated parameters proved quite different in magnitude for nitrification and denitrification processes, probably due to improved oxygen transfer induced by lower floc size distribution.

2.5.2.2 Main ASM models with SMP inclusion

Several Activated Sludge type models have already been proposed and tested by researchers over recent years to describe a typical MBR system. These models usually include the production and decay of **SMP** and/or EPS state variable components which can then be linked to an appropriate membrane fouling model. Some of these modified models are quite simple in structure so often prove easy to calibrate and validate, but cannot express fully the range of specificities of a MBR system (Oliveira-Esquerre et al. 2005). Others are very complex and comprehensive with numerous process couplings and additional component states, but prove difficult to calibrate and even often hard to interpret (Lu et al. 2001). Finally, others models like Laspidou and Rittmann (2002) although comprehensive in design and probably quite useful are not part of or originally based upon the IWA group of recognised models, such as ASM1, so do not have the historical pedigree to draw upon in terms of verifiability. So they are less likely to be taken up by the general research and practising engineering community.

Quite of few of the complex model formulations that extend the basic Activated Sludge models to include the fouling dynamics of a MBR system, further break the **SMP** (or EPS) into several components such as utilisation-associated products (UAP) and biomass-associated products (BAP). For example, Jiang et al. (2008) took this idea and applied it to the complex Activated Sludge Model No.2d (ASM2d), by introducing UAP and BAP and four additional **SMP** related parameters. However he noted that this model was unduly complex, difficult to handle, and over-parameterised resulting in inadequate or absent parameter estimation and validation. By calibrating this model on several batch experimental results from a laboratory situation, he concluded that the SRT was the crucial parameter controlling the **SMP** concentration. Thus a lower SRT increased the UAP concentration whilst simultaneously lowering the BAP concentration, and vice versa. He further concluded that a moderate SRT is sufficient if biological nutrient removal is needed.

Saroj et al. (2008) in his study which utilised a modified version of the Sin et al. (2005) ASM3 model which included EPS mechanisms, concluded that an integrated model of the biological processes and the filtration processes for MBRs was possible. He also notes that due to the fundamental differences between conventional wastewater treatment processes and MBRs, the distinct biological dynamics of a MBR system mean that the Activated Sludge models in their original form are not expected to be workable and need to include extra components to describe the dynamic MBR sludge matrix fully.

2.5.2.3 Investigating SMP production with non-ASM model structures

Several researchers have decided to take a slightly different approach in this field by constructing non-specific models for MBR **SMP** processes that are not based on the IWA group of models first mentioned in Henze et al. (1987). They have done this for a variety of reasons, the main ones usually being that only the specific biological processes thought contributory to the fouling mechanisms are considered, while others are entirely ignored. This simplifies the situation for some engineers who are not interested in the finer points of Activated Sludge modelling, influent and sludge characterisation, and parameter estimation.

In this regard Jang et al. (2006a) produced a model to predict the membrane bio-fouling potential for a MBR that included the production and degradation of EPS and **SMP**. In order to measure the foulability of different sludge mixes, he created a modified fouling index that was used for the prediction of bio-fouling potentials. His investigations revealed that, as expected, the SRT had a greater impact on the bio-fouling potential than the HRT. The simulation results also showed that an increased SRT decreased microbial activity in the MBR. In conclusion, he suggests that changes to the model parameters caused by the properties of the biological flocs, the influent characteristics, the membrane type, and the microorganism community structure and diversity would need further research to get a better understanding of the bio-fouling potentials in a MBR.

Janga et al. (2007) found in his follow-up study that most protein as **SMP** in the MBR bioreactor existed at a molecular weight of above 10 kDa, while over 86% of the polysaccharide **SMP** contained in the permeate had a molecular weight below 1 kDa. Additionally both the protein and polysaccharide **SMP** in the

permeate account for 83 to 91% of the overall effluent COD. The relative hydrophobicity of the protein and polysaccharide **SMP** was strongly affected by the characteristics of the influent with the hydrophobicity decreasing after membrane filtration. He further found that the total EPS concentrations increased with increases in the F/M ratio.

Jeong et al. (2007) employed a submerged MBR to research the behaviour of various **SMP** components, especially the UAP which is thought to be the predominating culprit for initiating membrane fouling (Jiang et al. 2008). He found in his experiments that the rate of accumulation of **SMP** relates directly to the biodegradability of the UAP which itself is linked to the influent loading rate. He concludes that the volumetric loading rate affects **SMP** production, which not only impacts on membrane bio-fouling but also on the microbial activity in the bioreactor.

As can be seen, this approach of only considering the important aspects of the biochemical processes that are intimately related to the membrane bio-fouling process can deliver promising results without the need for expert knowledge of Activated Sludge process models. Recently Ni et al. (2009) attempted to kinetically model and characterise the eEPS by its molecular weight distribution and its chemical natures which were identified by gel-permeating chromatography and three dimensional excitation-emission matrix fluorescence spectroscopy. His results showed chromatograms of eEPS exhibit seven peaks out of which proteins have four peaks and polysaccharides have three peaks. He found that the proteins and fulvic-acid-like substances in the EPS increase in the substrate utilization phase but decrease in the endogenous respiration phase of the Activated Sludge. These new techniques for the complex measurement of bio-fouling substances, such as eEPS, and their subsequent modelling could prove the way ahead for addressing the complex membrane fouling process.

2.5.2.4 Attempts at integrated MBR models

Off course the primary goal of current researchers in this field is the ambitious one of creating a suitably detailed unified integrated model that adequately describes the entire MBR processes. This idea of creating an integrated MBR model specifically for plant operation and control was first mentioned and promoted internationally by Paul (2006) in which he stated that it was essential that the biological portion of the model contained **SMP** / EPS mechanisms to make it comprehensive enough. He also stated that the fouling model needed to include the major blocking mechanisms which were universally accepted by researchers in that field.

Early work in this area created unified models, but as the understanding of MBR fouling was poorly understood at that time, they did not cater for **SMP** components, or used very basic fouling models. For instance Lee et al. (2002) used a modified ASM1 version model for a submerged MBR and then combined it with a simple membrane fouling model. This fouling model was of limited use being too simplistic in addressing the various types of foulant mechanisms encountered in practice. The ASM1 was modified to take account of the biological characteristics of a typical MBR process, and the resistance-in-series membrane fouling model was integrated into the modified ASM1 to describe the whole MBR system. Four additional 1st order linear differential equations were incorporated into the Petersen Matrix to describe the creation and degradation of **SMP** and its effects on membrane fouling. Lee et al. (2002) found that his model could easily predict not only effluent quality but also membrane fouling behavior. He concluded that F/M ratio and SRT were key factors in controlling **SMP** production in the bioreactor. It also appeared to play a vital role in membrane fouling and effluent quality as well.

More recently Di Bella et al. (2008) developed an integrated model which was composed of two sub-models, the first being an Activated Sludge biological one and the second one modelling the physical filtration process. Unlike Lee et al. (2002), the filtration processes were modelled in a complex manner by considering the deep-bed theory which accounts not only for physical membrane filtration but also the cake layer effect. The model was tested on a pilot submerged HF MBR fed by raw wastewater collected from the Palermo WWTP. It was in operation for a total period of 130 days at constant MLSS which was maintained consistently by periodic sludge withdrawal. This meant the role of the cake layer on organic removal could be

measured. Di Bella et al. (2008) result's confirm the importance of cake deposition in the filtration process. He concludes that his formulated model can be employed for the optimisation of the operational conditions as well for plant design.

2.5.2.5 Selected modified ASM models under this study

As Chapter 5 of this report will show, two modified Activated Sludge models that represent the two ends of the spectrum of model complexity were selected to be further investigated. Both these versions of modified Activated Sludge models take into account the production of EPS as **SMP**. The first version of the modified model used the ASM1 (Henze et al. 1987) combined with a **SMP** model and is based on the work carried out by Lu et al. (2001). The second version of the modified model used the ASM3 (Gujer et al. 1999) combined with a microbial product (MP) model based on the work carried out by Oliveira-Esquerre et al. (2005). This investigation was carried out in order to see which version better predicted substrate removal efficiency and by inference the production of EPS which would directly impinge upon membrane fouling rates by subsequent pore blocking. Additionally the modelling exercise would give a better understanding of whether EPS production could be modelled for a full scale plant using the usual type of cost effective sampling methods for measuring biological and nutrient loads.

2.5.3 Using Econometric modelling methods for wastewater treatment

2.5.3.1 Early work using a times series approach

Historically speaking the first real instance of using a times series approach to analyse wastewater treatment data was carried out by Berthouex et al. (1978). In this study, he analysed the relationship between influent BOD5 and effluent BOD5 in an Activated Sludge process at a Wisconsin sewage treatment plant. This analysis was carried out by using data collected hourly over a two week period, and then by developing a dynamic model for the system using a Box-Jenkins approach. Incidentally, the Box-Jenkins time series approach sometimes known as an autoregressive integrated moving average (ARIMA) system is a generalisation of the ARMAX model case, and takes into account any data seasonality and deals with any stationarity issues as well. Thus it contains autoregressive, integrated, and moving average components. With this approach, he combined the stochastic and transfer function components into a first-order model to obtain a good fit. In this empirical model, which did not need flow as a predictor variable, the stochastic component proved more critical than the transfer function component.

Soon after this, Debelak and Sims (1981) created a Box-Jenkins time series transfer function model of the effluent COD by using the influent COD from a sewage treatment process. The data was taken from an industrial waste treatment plant encompassing a fourteen month period. He found that as expected the influent COD had an insignificant effect on the effluent COD, and that good prediction of effluent COD could be obtained by using ARIMA difference models.

2.5.3.2 Follow-on work

In 1991, Tan et al. (1991) successfully modelled the time-varying dynamics of dry and wet weather sewer flow using the MISO ARMAX model for a sewered catchment in Melbourne, Australia, which had a sewer system separate from the stormwater system. The model parameters were recursively estimated at each time step by the method of extended least squares. By using this method to represent the rainfall disturbances, reliable predictions up to two hours ahead for wet weather sewer flow could be made. Hence the accurate forecasting of wastewater flow rates, which themselves exhibit a diurnal flow pattern (with large variations dependent on rainfall and groundwater infiltration), could then help to reduce overflows and the operational costs of wastewater pumping stations and treatment plants. This predictive model used the measured sewer flow, the pre-filtered area-averaged rainfall intensities and/or the dimensionless flow pattern.

In 1993, Christodoulatos and Vaccari (1993) extended a method based on multiple linear regression with autocorrelated errors to developed a model which correlated Activated Sludge response variables, such as sludge volume index (SVI), effluent volatile suspended solids (VSS) or effluent BOD5, with state variables such as F/M ratio, influent BOD5, dynamic SRT, etc. The method was applied to three different data sets from two full scale Activated Sludge plants with one being a regional municipal plant while the other one was an industrial facility. By using this method, statistically significant models were developed that could explain 65-82% of the variability in effluent total oxygen demand, 22-60% in effluent VSS and 48-88% in SVI. It was only necessary to model up to second order lag terms. The models were tested for bias using different data sets and produced accuracy levels of up to 96% between predicted and observed values. Christodoulatos and Vaccari (1993) concluded that these results proved useful predictive relationships could be developed for full scale Activated Sludge processes using autoregression techniques, with the follow-on being that these methods could then be used to develop a range of automatic process control schemes.

A slightly different formulation by Berthouex and Box (1996) which used exponentially weighted moving average terms for the Box-Jenkins time series modelling procedure, was able to predict up to five days ahead process upsets at a wastewater treatment plant. This proved useful for calculating predictions within confidence intervals for effluent quality, which themselves could be used to serve as an early warning system to flag up potential process upsets that would sometimes enable an operator to take preventive action.

Following these initial studies into using autoregressive time series methods for analysing wastewater treatment processes, they did seem to lose their appeal in the late 1990's and other AI methodologies became in vogue instead. This loss of appeal was probably less to do with their predictive capacity and more to do with the increasing popularity and familiarity with AI methodologies by researchers over a wide range of differing academic disciplines.

2.5.3.3 ANN and FNN approaches as an alternative

Of the AI methodologies, the two most studied for wastewater treatment have been ANN and fuzzy neural networks (FNN) to date. In fact they have rapidly progressed to being capable of producing reliable models for any WWTP. Their main disadvantages are they need highly proficient operators to "train" the system properly before it can be used, and they can prove very complex with very high processing times for large neural networks.

In terms of ANN systems, Mjalli et al. (2007) took data from the Doha West WWTP and developed an accurate trained ANN model to predict accurate effluent stream outputs for BOD5, COD and Total suspended solids (TSS) when using the same as inputs in the crude supply stream. He justified using an ANN approach instead of an Activated Sludge model as he felt this plant process was complex and attained a high degree of nonlinearity due to the presence of bio-organic constituents that were difficult to model using mechanistic approaches. This study concludes that ANNs are capable of capturing the plant operation characteristics with a good degree of accuracy.

In the same year, Raťduly et al. (2007) developed an ANN system that dramatically reduced the model simulation time when using extremely long data sets accumulated over long time periods of over twenty years for a WWTP. This was carried out by combining an influent disturbance generator with a mechanistic WWTP model for generating a limited sequence of training data of four months of dynamic data. The component inputs included effluent Ammonium, BOD5 and TSS. This training data was then used to simulate the remainder of the influent time series of twenty years of dynamic data generated with the influent disturbance generator. He calculated that this enhanced procedure reduced computational and simulation time by a factor of 36 even when including the time needed for the generation of training data and for ANN training. He calculated that for repeated integrated urban wastewater system simulations that do not require repeated training of the ANN, the ANN reduces simulation time by a factor of 1300 compared to the mechanistic model with only a small loss in accuracy of 10%.

In 2003, Yoo et al. (2003) used a new approach to nonlinear modelling by using FNN linked to a PCA to produce a model which was applied to a real WWTP. He termed this new combined approach as fuzzy principal component regression. In this method, the PCA is used to reduce the dimensionality of data and to remove collinearity, while the adaptive fuzzy method is used to appropriately monitor diverse operating conditions based on the PCA score values. The combined approach then employs a Takagi-Sugeno-Kang fuzzy model to model the relation between the PCA score values and the target output to avoid over-fitting the problem with original variables. The rule bases, the centers and the widths of the fuzzy model are found by heuristic methods. The proposed combined method was found to be able to accurately predict the reduction of COD in the full scale WWTP. The result showed that this combined approach had the ability to model the nonlinear process and multiple operating conditions.

In another more recent similar study, Qiaoa and Wang (2008) used an adapted FNN procedure to solve the problem of conventional input-output space partitioning. This new learning algorithm for creating self-organizing FNNs simultaneously automated the structure and parameter identification based on input-target samples. Two specific implementations of the algorithm, including function approximation and forecast modelling of the WWTP were developed. These were compared with other approaches, and apparently comprehensively demonstrated that the presented algorithm was superior in terms of compact structure and learning efficiency.

Finally, Huang et al. (2010) recently successfully created a software sensor based on the FNN approach for

the real-time estimation of nutrient concentrations in bioreactors. This sensor used a split network structure for anaerobic and aerobic conditions coupled with dynamic ARX modelling methods for inputs and multi-way PCA. The proposed integrated methodology was successfully applied to a bench-scale anoxic/oxic process for biological Nitrogen removal, with the simulation results indicating that the learning ability and generalization of the model performed well.

2.5.3.4 Other approaches

Other newer and more exotic methods for model prediction are coming on-line all the time. For instance Honga and Bhamidimarri (2003) used genetic programming as a self-organising modelling tool to model the dynamic performance of municipal Activated Sludge WWTP. This method works by evolving several process models automatically based on methods of natural selection, such as "survival of the fittest". These models can then predict the dynamics of MLSS and TSS in the effluent. The predictive accuracy of this genetic programming approach was compared with a nonlinear state space model with ANNs and the well-known Activated Sludge Model No.2 (ASM2) mechanistic model. Honga and Bhamidimarri (2003) found that the genetic programming system evolved some models that were an improvement over the ANNs and ASM2, and showed that the transparency of the model evolved could allow inferences about the underlying processes to be made. The output from this study could prove useful for a typical MBR situation where membrane fouling quantification is difficult to ascertain. He concluded that genetic programming can work as a cost-effective intelligent modelling tool enabling creation of quick inexpensive prototype process models instead of requiring an experienced engineer in having to develop a complex mechanistic process model, or having to "train" an ANNs model.

2.5.3.5 Comparison of times series methods with other approaches

Often ARIMA models prove more effective at prediction than the more commonly used ANN models, even though the latter have been used more extensively to date. In fact in a study by Dellana and West (2009), he compared the multi-period predictive ability of linear ARIMA models to nonlinear time delay ANN models for wastewater treatment, and found the former proved more accurate for nonlinear data sets. These data sets were artificially generated data sets that simulated the characteristics of wastewater process variables and watershed variables. In fact in some cases of the artificial nonlinear data, where multi-period predictions were made, the linear ARIMA model proved more accurate than the time delay ANN model. His study suggests that practitioners should carefully consider the nature and intended use of water quality data if choosing between ANNs and other statistical methods for wastewater process control or watershed environmental quality management.

Time series data from water resources often contains both linear and nonlinear patterns, and hence Ömer Faruk (2010) recently suggested that neither a strictly ARMAX nor a ANN can be adequate in modelling and predicting time series data. In his study he stated that the ARMAX model cannot deal with non-linear relationships while the ANN model alone is not able to handle both linear and nonlinear patterns equally well. Consequently he developed a hybrid ARMAX and ANN network model which was capable of exploiting the strengths of the traditional time series approaches and ANNs. This approach consists of an ARMAX methodology and feed-forward, backpropagation ANN network structure with an optimized conjugated training algorithm. He tested this proposed model using 108 months worth of observations of water quality data, including water temperature, boron and DO during 1996 to 2004 at Büyük Menderes River in Turkey. He found better accuracy of this hybrid system when compared to using either of the two methods on its own. He suggests this improvement in accuracy is due to the hybrid system having a robust modeling framework which was more capable of recognizing complex time series patterns and nonlinear characteristics for water quality predictions.

All of these studies basically prove that using an ARMAX or similar approach to modelling of MBR processes, whether fouling or biological, for wastewater treatment is a perfectly valid and bona fide approach

to take.

2.5.3.6 Model predictive control

Once good models with excellent predictive capability have been developed, whether mechanistic or times series, then they could also be used for model predictive control (MPC) for improved process control and optimisation. For instance (Stare et al. 2006) developed two separate Ammonia models that could be used for MPC of nitrification processes in a WWTP. The first was based on a reduced order non-linear model whose expression for nitrification reaction rate was the one used in the ASM1 with attached biomass processes. The second was a unspecified linear black box model. Both models were properly validated using data collected during several weeks of experiments on a real plant. During the validation stage both models showed relatively large errors when compared to the real plant data. Hence a closed loop simulation study was performed to specifically determine the differences between the performance of each MPC using previously estimated non-linear and linear models and a standard proportional integral (PI) controller. From the simulation study results it was found that both MPC algorithms gave better results in terms of Ammonia removal compared to the PI controller, while the non-linear model MPC gave additional improvement over the linear model MPC.

In a similar vein, Munoz et al. (2009) proposed and tested a MPC based on optimisation of the pH and DO set points for a SISO controller which then maintained the process at stable partial nitrification. The controller implemented a Takagi-Sugeno-Kang fuzzy model to estimate the Ammonium degradation and Nitrite accumulation from on-line DO and pH values and updated off-line measurements. An Activated Sludge reactor was successfully operated for over three months by this MPC, achieving Ammonium degradation and Nitrite accumulation values higher than 95% and 80%, respectively. The on-line estimates of this FNN model showed a prediction error of less than 7% at steady state operation.

In a much more complex real-time control study by Novotny and Capodaglio (1992), he used stochastic real-time MPC of a wastewater treatment and disposal facility operating under dynamic wet weather and dry weather conditions. The stochastic transfer functions used for prediction of the inputs and response of the system belonged to the class of ARMAX models. He demonstrated that a ARMAX model could be used in real-time as an automated expert system to assist the operators of WWTP.

Finally, Akyurek et al. (2009) carried out a fully comprehensive study of MPC where he evaluated six alternate control strategies for an Activated Sludge WWTP. The strategies evaluated were all measured against a traditional PI controller output. They were as follows: 1) a MPC with a linear model; 2) a MPC with a non-linear model; 3) a non-linear ARMAX MPC; 4) a ANN MPC; and, 5) a optimal controller with sequential quadratic programming (SQP) algorithm based on the simulation of a ASM1 treatment process. All controller's performance was assessed on rise time, overshoot, Integral Absolute Error (IAE) and Integral Square Error (ISE) performance criteria. Since the DO level in the aerated bioreactor played an important role in obtaining the effluent quality and in operational cost terms, it was chosen as the controlled variable. It was emphatically concluded that the ARMAX MPC and the optimal control with SQP out performed all the others in achieving the specified study objectives.

2.6 *Chapter Summary*

MBRs are a recent innovation that combines a membrane filtration unit with a biological process technology in order to treat a wastewater. The down side of MBRs are that membrane fouling occurring on the membrane surface and within the pores reduces the long term stability of the flux performance. Understanding by researchers of the nature of and the factors contributing to this fouling process is still currently limited.

Various model types have been used to describe both the biology in a MBR and the fouling of the membrane by biological agents. Most are of the phenomenological type that describe the processes using the laws of physics and scientific theory. They are good model types and give reasonable results, although they often prove difficult to calibrate requiring expert process knowledge. Other model types have been tried with limited degrees of success. Each of these other model types have advantages and disadvantages. One of these other types, which has only been used in a limited manner in this area, is times series input-output models traditionally used in the econometric field.

Chapter 3

Methodology: experimental procedure, data collection, model conceptualisation

3.1 *Introduction*

This Chapter describes the basic methods used to address the research questions posed in Chapter 1. This methodology consists of two types. The first is the creation of a modelling framework that will allow all the models developed later on, whether phenomenological or behavioral in nature, to be tied to reality. This framework is needed as none such currently exists for MBR systems. The second methodology is more standard as it consists of a description of the wastewater treatment plants utilised and the data collected from them that is used in the models described in later chapters.

Hence this Chapter is split into two main sections. The first Section of this Chapter focuses on the development of a thorough MBR "Model Conceptual Procedure" with supporting framework to be specifically used on sidestream crossflow plant. This extensive formulation can be used by other researchers as a basis for all future MBR model development and MBR benchmark creation. This initial Section is also used as the basis of the models formulated later in Chapters 4 and 5.

The second longer Section deals with actual plants both MBR and membrane filtration ones which were used to generate data which is later used to validate and calibrate both the phenomenological and behavioral time series input-output models. Hence the purpose of this Section is to first describe the plant themselves, and then how data was collected and generated for the models that were later tested (See Section 3.4.2.4). This data was collated by carrying out biochemical sampling programmes, both on-line and off-line, on real life MBR WWTP which were operated by the industrial collaborators involved in the wider project. Some of this data and results is then presented in graphical form to give an indication of the type of data used to test the models formulated later in Chapters 4 and 5.

One plant was an existing full scale MBR plant installed by Aquabio Limited and owned and operated by Kanes Foods Limited in Evesham, Worcestershire. The other Aquabio plant, which provided a considerable amount of the information to calibrate the MBR models, was a purpose built small pilot MBR plant which was operated at the same site. Some data was also collected and used to calibrate the fouling model used in Chapter 4 from a pilot membrane filtration plant operated by ITT Sanitaire at Cardiff wastewater treatment works. This took treated effluent from the main wastewater treatment plant SBRs, and fed it into this pilot membrane filtration unit. Other data came from an ITT Sanitaire submerged pilot MBR plant operated at Coors UK Limited.

After various data sets were collated from all these plant, it was found that they still proved insufficient

to verify the input-output biological models developed later on as part of Chapter 5. This was because a considerable amount of biological data is needed to produce even a basic first order autoregressive model structure. Consequently, a fictitious WWTP had to be used to generate sufficient data sets to allow this calibration and validation to proceed. This fictitious WWTP is described in the final Section of this Chapter, and is based around a modified version of the IWA COST Benchmark simulation model which itself is based around the ASM1 model (Copp 1999, 2000).

3.2 *Conceptualisation of crossflow MBR model structures*

For a conventional Activated Sludge system which uses settlement processes in the secondary clarifier, a biochemical Activated Sludge model is needed which describes final effluent quality based upon the efficiency of the microbial biomass in removing organic carbon and nutrients. Its main limitation is its inability to predict sludge bulking and foaming events. Activated Sludge models of this type perform reasonably well in most situations when used for plant design and rudimentary plant control and operation to achieve best effluent quality.

Conversely for a MBR system, the effluent quality is never an issue, so the focus of any model should be on improving the performance of the membrane, and how the biological process can be optimised to achieve this higher level goal. Hence any detailed MBR model should ideally consist of two parts. The first part would consist of a biochemical Activated Sludge model which had been altered to include elements and variables which current research work indicate are the main agents responsible for increased membrane fouling (e.g. EPS and **SMP**). The second part would model the effect of these agents and other elements and processes on the membrane performance, overall resistance and flux production rates. Consequently the collective models would describe the MBR system as a whole, whose main limitation is the propensity for membrane fouling, which the models would ideally predict.

3.2.1 Generalised MBR Model formulation

A model of a process is typically represented by an ordinary differential equation of the general form:

$$\dot{x}(t) = f(x(t), m(t), z(t), u(t)) \tag{3.1}$$

where:
$\dot{x}(t)$ is the state of the system
$m(t)$ are the manipulated (control) variables
$z(t)$ are input variables from the external environment
$u(t)$ are input variable connections from other subsystems

This generalised form of a process is the starting point for developing any generalised MBR model. Basically any MBR model based on a real life plant can be divided into two distinctive composite parts or processes: a "bioreactor" and a "membrane" joined together. These can then be separately and easily modelled with their own inputs and outputs for each; which for the "bioreactor" focus on the biochemical processes occurring in the reactor, whilst for the "membrane" they relate to the membrane fouling processes. Hence in this model structure, both parts have distinctive input variables, and control variables which can be manipulated by the operator, and internal state variables which are taken for simplicity sake as the same as the output variables (e.g. for complete mix reactors). All variables can be measured either directly or indirectly using either on-line sensors or composite / grab sampling methods.

A structure of a typical crossflow MBR system is presented in Fig. 3.1. Incidentally it is worth noting that the whole "Model Conceptualisation Procedure" described in this Section can be easily altered to reflect a submerged / immersed MBR system instead.

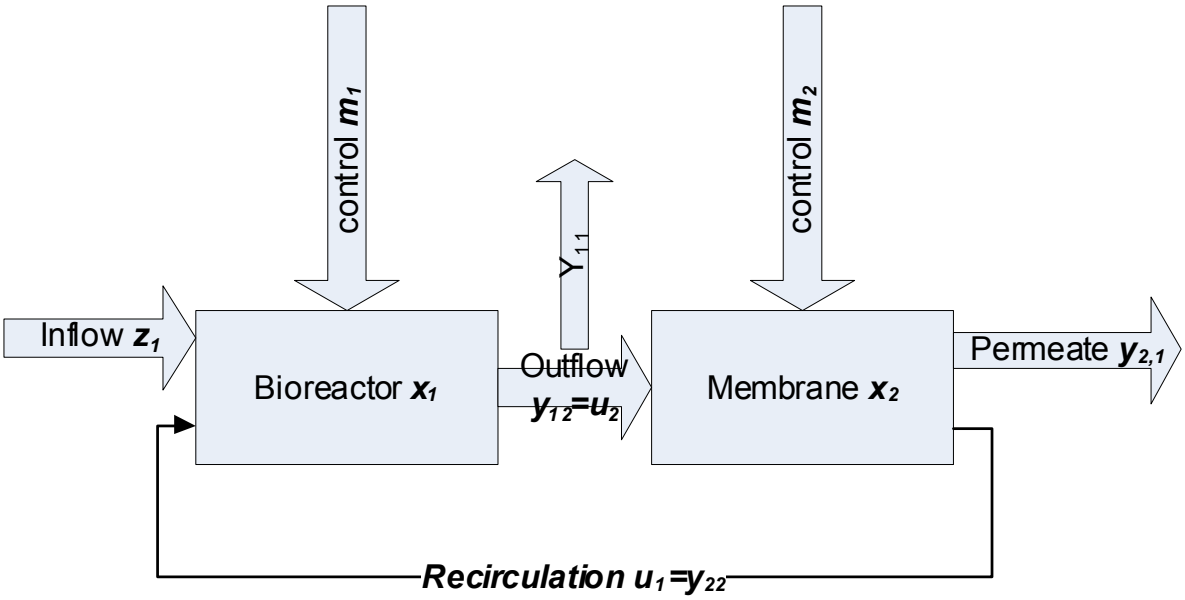

Fig. 3.1: Structure of a MBR plant

3.2.1.1 Bioreactor variables

In Fig. 3.1, the various variables and states can be grouped into vector matrix form. These same variables would then appear in any final model formulation. The variables used in this formulation which are defined in the Nomenclature Section of this report are the standard ones used in conventional Activated Sludge modelling together with some additional ones which have been found to be largely responsible for membrane fouling. The variable listing provided here is not an exhaustive one, but could be easily added to or have some less relevant variables removed from it based upon the model complexity used.

Considering the "bioreactor" system only then:

- Vector z_1 is the input variables found in the wastewater inflow.
- Vector m_1 is the manipulated operator variables, such as wastage rate, for the reactor.
- Vector x_1 is the internal states in the reactor.
- Vector y_{11} is the output wastage variables coming from the reactor.
- Vector y_{12} (also known as u_2) is the output of the "bioreactor" system which then becomes the input to the "membrane" system.
- Vector y_{22} (also known as u_1) is the recirculation of the crossflow system which then joins with the inflow vector to become the total input into the "bioreactor" system.

$$\mathbf{z_1} = \begin{bmatrix} q_{in} \\ COD_{in} \\ TKN_{in} \\ TP_{in} \\ S_{PS,in} \\ S_{PP,in} \\ X_{TSS,in} \\ X_{VSS,in} \\ S_{ALK,in} \\ S_{O,in} \\ X_{EPS,in} \\ \mu_{in} \\ T_{in} \end{bmatrix} ; \mathbf{m_1} = \begin{bmatrix} q_{air} \\ q_{waste} \end{bmatrix} ; \mathbf{x_1} = \begin{bmatrix} V_T \\ COD \\ TKN \\ TP \\ S_{PS} \\ S_{PP} \\ X_{MLSS} \\ X_{MLVSS} \\ S_{ALK} \\ S_O \\ X_{EPS} \\ \mu \\ T \end{bmatrix} ; \mathbf{y_{11}} = \begin{bmatrix} q_{out} \\ COD \\ TKN \\ TP \\ S_{PS} \\ S_{PP} \\ X_{MLSS} \\ X_{MLVSS} \\ S_{ALK} \\ S_O \\ X_{EPS} \\ \mu \\ T \end{bmatrix}$$

$$\mathbf{y_{12}} = \mathbf{u_2} = \begin{bmatrix} q_{out} \\ S_{PS} \\ S_{PP} \\ X_{MLSS} \\ X_{EPS} \\ \mu \\ T \end{bmatrix}; \mathbf{u_1} = \mathbf{y_{22}} = \begin{bmatrix} q_{rec} \\ COD_{rec} \\ TKN_{rec} \\ TP_{rec} \\ S_{PS,rec} \\ S_{PP,rec} \\ X_{MLSS,rec} \\ X_{MLVSS,rec} \\ S_{ALK,rec} \\ S_{O,rec} \\ X_{EPS,rec} \\ \mu_{rec} \\ T_{rec} \end{bmatrix} \tag{3.2}$$

3.2.1.2 Membrane variables

Next considering the "membrane" system only then:

- Vector y_{12} is the input to the "membrane" system which relates to the fouling process.
- Vector m_2 is the manipulated operator variables, such as pump speed, for the "membrane" system.
- Vector x_2 is the internal states in and on the membrane directly related to the fouling process.
- Vector y_{21} is the output of the "membrane" system which is the related to the permeate flow.
- Vector y_{22} is the recirculation of the retentate flow out of the "membrane" system.

$$\mathbf{y_{12}} = \mathbf{u_2} = \begin{bmatrix} q_{out} \\ S_{PS} \\ S_{PP} \\ X_{MLSS} \\ X_{EPS} \\ \mu \\ T \end{bmatrix}; \mathbf{m_2} = \begin{bmatrix} \omega_{pump} \\ \nu_{throttle} \\ f_{bwash} \end{bmatrix}; \mathbf{x_2} = \begin{bmatrix} irreversible\ fouling \\ reversible\ fouling \\ cake \end{bmatrix}; \mathbf{y_{21}} = \begin{bmatrix} TMP \\ q_{perm} \\ COD_{perm} \\ TKN_{perm} \\ TP_{perm} \\ S_{PS,perm} \\ S_{PP,perm} \\ X_{TSS,perm} \\ X_{VSS,perm} \\ S_{ALK,perm} \\ S_{O,perm} \\ X_{EPS,perm} \\ \mu_{perm} \\ T_{perm} \end{bmatrix};$$

$$\mathbf{y_{22}} = \begin{bmatrix} q_{rec} \\ COD_{rec} \\ TKN_{rec} \\ TP_{rec} \\ S_{PS,rec} \\ S_{PP,rec} \\ X_{MLSS,rec} \\ X_{MLVSS,rec} \\ S_{ALK,rec} \\ S_{O,rec} \\ X_{EPS,rec} \\ \mu_{rec} \\ T_{rec} \end{bmatrix} \tag{3.3}$$

3.2.1.3 Recirculation variables

The total flow out of the whole "membrane" system is the combined permeate and recirculation flows as follows:

$$q_{out} = q_{perm} + q_{rec}$$

In this case q_{out} refers to the input flow into the "membrane" system which is the output flow from the "bioreactor" system.

It is easy to measure the state variable concentrations of the various components in the input flow into the "membrane" system, and for the permeate flow. However it is not easy to measure the state variable concentrations of the various components in the recirculation flow. This can be deduced by carrying out a mass balance of the system as outlined below.

Concentration, C, of any substance in the recirculation flow can be calculated from a mass balance equation of a particular substance, A, as follows:

$$q_{out} \cdot C_A = q_{perm} \cdot C_{A,perm} + q_{rec} \cdot C_{A,rec}$$

and subsequently the recirculation can be calculated from the following expression:

$$C_{A,rec} = \frac{q_{out} \cdot C_A - q_{perm} \cdot C_{A,perm}}{q_{rec}} = \frac{q_{out}}{q_{rec}} \cdot C_A - \frac{q_{perm}}{q_{rec}} \cdot C_{A,perm} \tag{3.4}$$

3.2.2 Decomposed MBR model

Since a crossflow MBR system can be considered to be composed of two distinct but inter-dependant elements, namely the "bioreactor" and the "membrane", the overall modelling work can be split into these two elements, with each being modelled separately to give a decomposed MBR system. There would obviously be common linkages between the elements, namely the output state variables from the "bioreactor" feeding in as input states to the "membrane", thus giving an overall integrated system.

3.2.2.1 Bioreactor model

In the decomposed MBR system, the "bioreactor" is isolated from the "membrane" system as shown in Fig. 3.2.

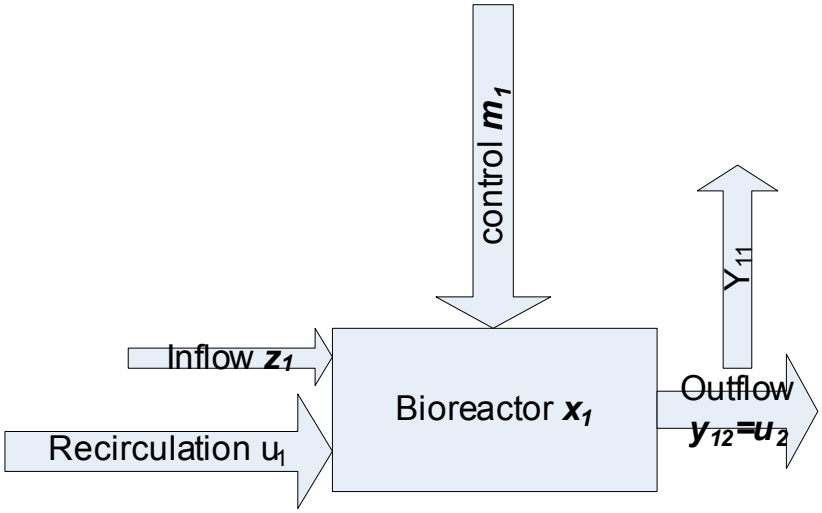

Fig. 3.2: Bioreactor isolated from the MBR

The causal model of a "bioreactor" can be calculated as relationships between input and output variables as follows:

$$\{z_1, u_1, m_1\} \Rightarrow x_1 \qquad or \qquad \{z_1, u_1, m_1\} \Rightarrow y_1 = \begin{bmatrix} y_{11} \\ y_{12} \end{bmatrix}$$

The variables z_1, m_1, x_1, and y_1 are measured directly whereas the variable u_1 can be calculated indirectly from the measured values of x_1 and y_{21}.

3.2.2.2 Membrane model

In the decomposed MBR system, the "membrane" is isolated from the "bioreactor" system as shown in Fig. 3.3.

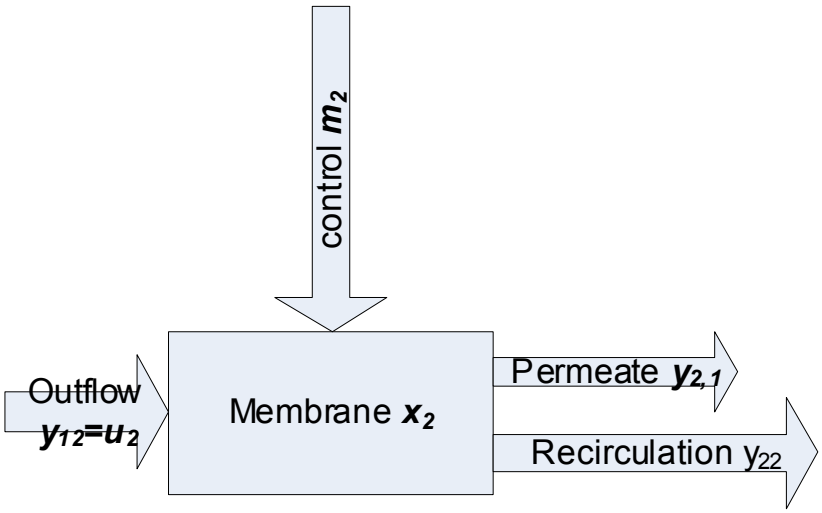

Fig. 3.3: Membrane isolated from the MBR

The causal model of the "membrane" is $u_2 \Rightarrow y_{21}$ (from u_2 to y_{21}). The recirculation output, y_{22}, can be calculated from the mass balance equation unless it is assumed that the membrane accumulates a significant mass of material, and then the model needs to be identified as:

$$u_2 \Rightarrow \begin{bmatrix} y_{21} \\ y_{22} \end{bmatrix}$$

3.2.3 Model of the MBR as a whole

Once the decomposed systems for the "bioreactor" and "membrane" are solved individually, then the results are for an integrated MBR system which for all intents and purposes can be considered as one unit blackbox process as presented in Fig. 3.4 and Fig. 3.5.

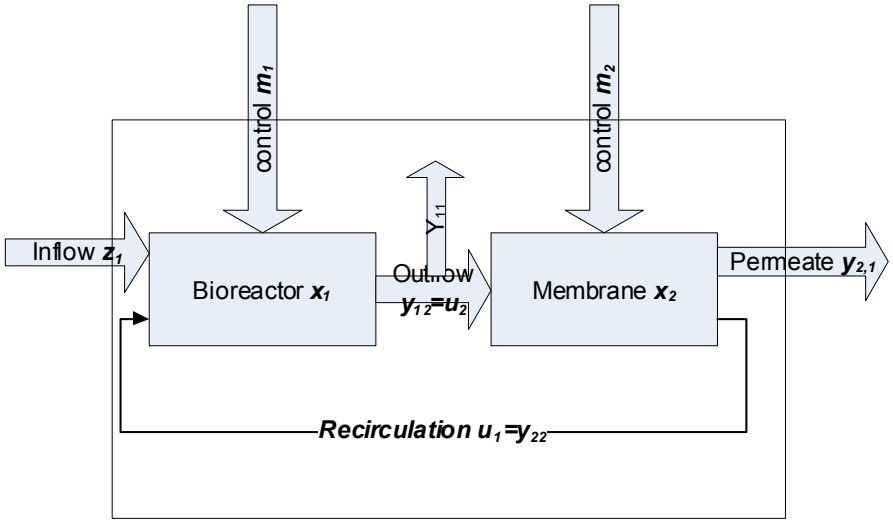

Fig. 3.4: A MBR considered as one whole unit process

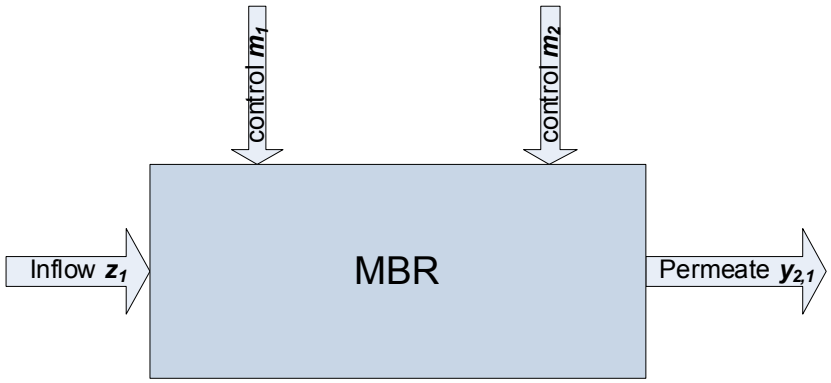

Fig. 3.5: A MBR considered as one whole unit blackbox process (i.e. masked)

If the MBR system is considered simply as a complete unknown black box process, such as in a behavioural time series model, where only historical data sets of input and output variable values are needed, and the exact nature of the mechanisms of the physical and biochemical processes occurring within the MBR is not needed, then the system portrayed in Fig. 3.5 can be used. In this formulation the system is treated as a whole with the input z_1, the control variables, m_1 and m_2, and the output y_{21}. This is an attractive possibility since as all measurements are directly available then the model identification procedure should be a straightforward task to perform providing there are more than sufficient data points for the model calibration and validation steps.

3.2.4 Approximate decomposed MBR model

The decomposed formulation can be simplified further into an approximate system as outlined in Fig. 3.6. Although this formulation is a simplification of reality in terms of mass balancing of flows and state variable concentrations, it should not incur too many errors due these assumptions, and should be acceptable in most circumstances as a reasonable accurate reflection of the actual situation within acceptable error tolerance limits.

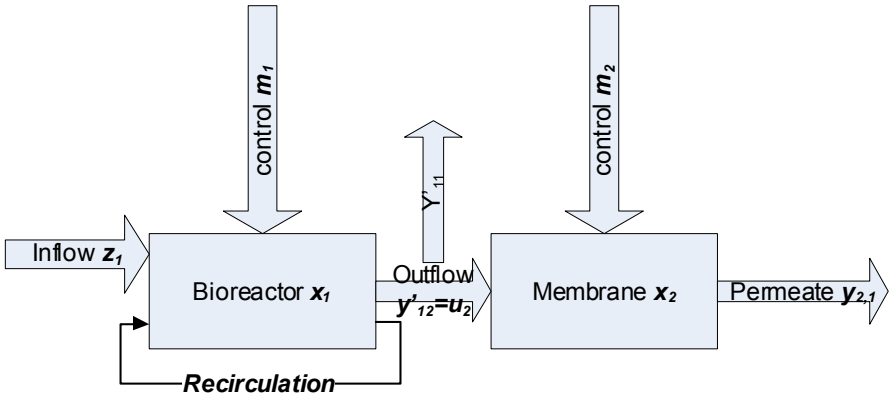

Fig. 3.6: An approximate MBR model

In this simplified, approximate model composition, it is assumed that the the recirculation flow is exactly the same as the output flow, and the flow connecting the "bioreactor" and the "membrane" is equal to q_{perm}. This approach yields the approximate model decompositions as described below in Sections 3.2.5.1 and 3.2.4.2.

3.2.4.1 Approximate bioreactor model

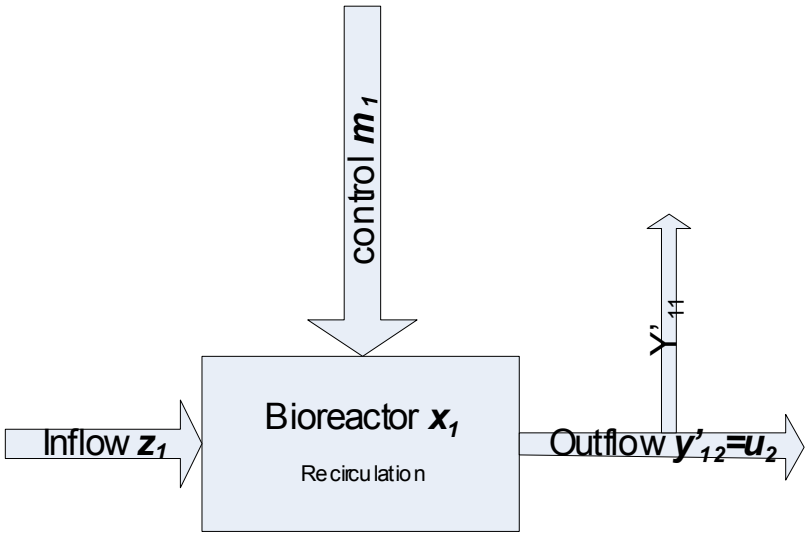

Fig. 3.7: An approximate bioreactor only model

In this approximate decomposed "bioreactor" system, the modified output, y'_{12}, includes the flow, q_{perm}, instead of q_{out}, as follows:

$$\mathbf{y'_{12}} = \mathbf{u_2} = \begin{bmatrix} q_{perm} \\ S_{PS} \\ S_{PP} \\ X_{MLSS} \\ X_{EPS} \\ \mu \\ T \end{bmatrix}$$

3.2.4.2 Approximate membrane model

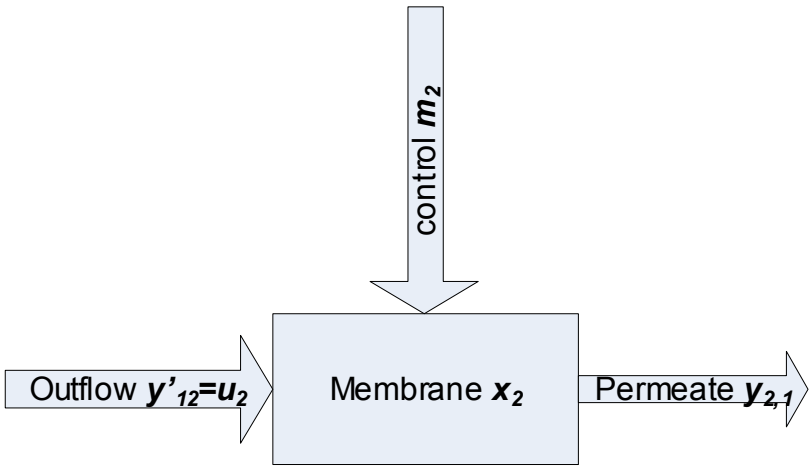

Fig. 3.8: An approximate membrane only model

Again in this approximate decomposed "membrane" system, q_{out} is replaced by q_{perm} in $y_{12}^{'}$.

3.2.5 Fast and slow dynamics

An important issue to consider when decomposing or decoupling the system into different approximated element systems, is that the dynamics of individual physical and biochemical processes occurring for the separate systems have to match up to give an accurate integrated system with integrated results. This is crucial since most of the "bioreactor" system processes have much slower time constants (e.g. hours, days, weeks) then the "membrane" system ones (e.g. seconds, minutes and hours). Even within the "bioreactor" system itself the dynamics of specific processes vary considerably. For instance the aeration dynamics are fast (e.g. minutes and hours), while the growth of autotrophic microorganisms is very slow (e.g. days and weeks).

3.2.5.1 Approximate modified bioreactor model

The aeration dynamics is much faster than biological processes as illustrated in Fig. 3.9 which shows the DO setpoint control used to vary the airflow rate. If the aeration control loop is implemented and works correctly, it can be assumed that the dissolved oxygen in the reactor is equal to the DO setpoint without much loss of accuracy in the model formulation. Consequently, due to the fast aeration dynamics, it can be assumed for the slower "bioreactor" system processes, that the S_0 concentration can be equated to the measured DO level in the tank, and the state equations corresponding to S_0 variable can be removed from the model formulation. This means that this approximate but modified model is greatly simplified.

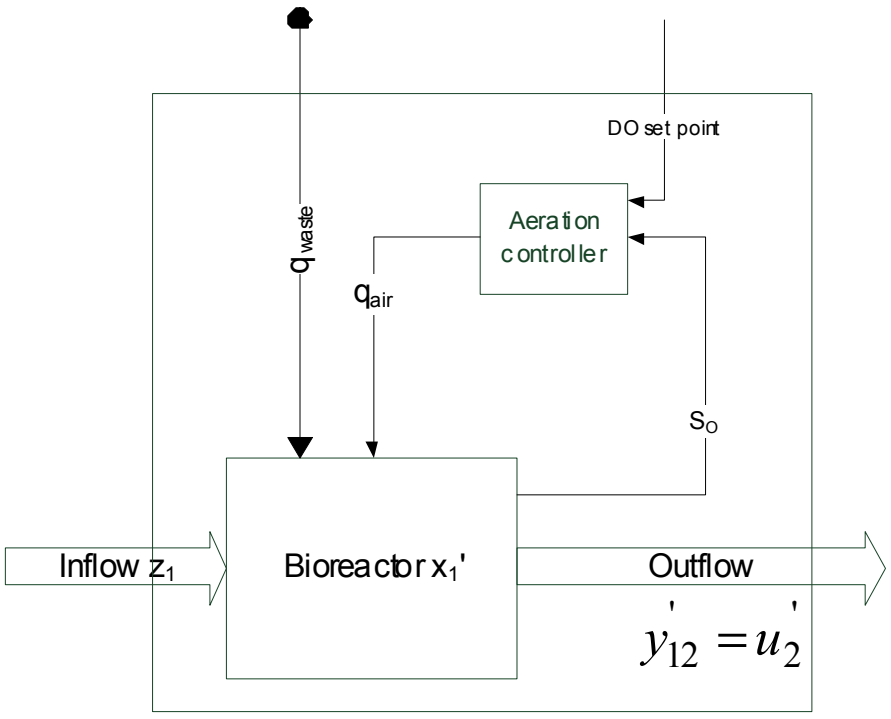

Fig. 3.9: DO setpoint control in an approximate modified bioreactor model

Therefore the causal model of the complete mix reactor can then be redrawn as in Fig. 3.10. In this revised model formulation, the following changes occur to variables:

Input variables -

S_O and μ_{in} have been removed from the input vector, since they are negligible in size, and there consequent

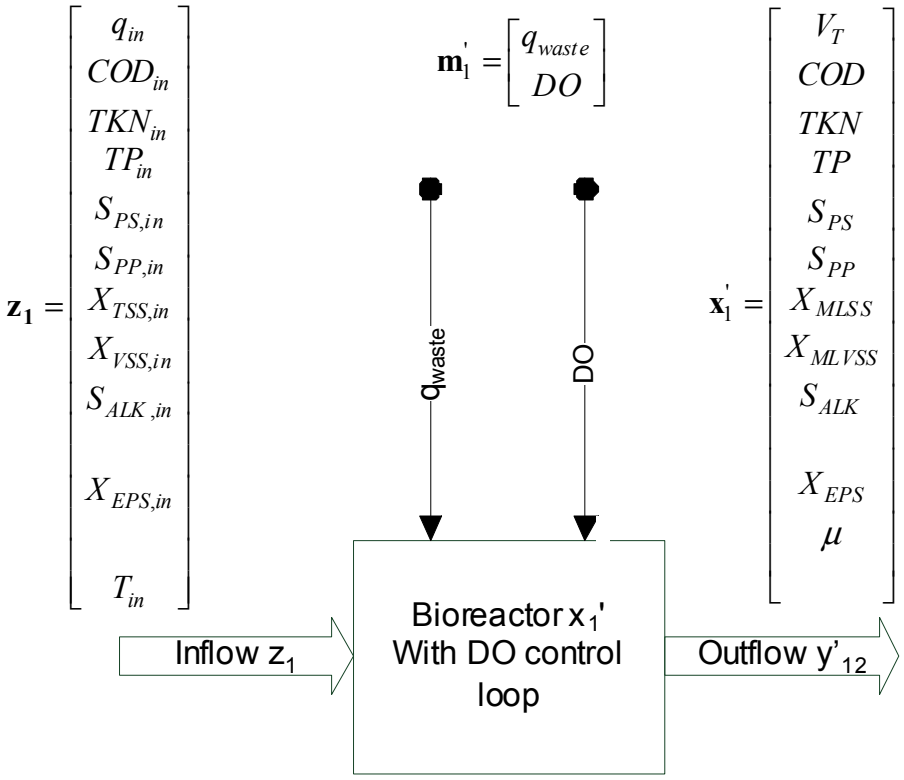

Fig. 3.10: An approximate modified bioreactor model

impact is negligible. It also reduces the input vector size so less computation is needed.

Output variables -

S_O is not considered a state variable any longer, and there is no state equation corresponding to this variable. In the other equations it is replaced by the DO variable, and is then assumed to be an input variable. The temperature is not considered a state variable, and is removed from the state (output) vector.

All these model revisions greatly simplify the approximate decomposed model formulation for the "bioreactor" system. Hence the corresponding variables as vectors are as follows for the final system:

$$\mathbf{z_1} = \begin{bmatrix} q_{in} \\ COD_{in} \\ TKN_{in} \\ TP_{in} \\ S_{PS,in} \\ S_{PP,in} \\ X_{TSS,in} \\ X_{VSS,in} \\ S_{ALK,in} \\ X_{EPS,in} \\ T_{in} \end{bmatrix}; \qquad \mathbf{m_1} = \begin{bmatrix} q_{waste} \\ DO \end{bmatrix}; \qquad \mathbf{x_1}' = \begin{bmatrix} V_T \\ COD \\ TKN \\ TP \\ S_{PS} \\ S_{PP} \\ X_{MLSS} \\ X_{MLVSS} \\ S_{ALK} \\ X_{EPS} \\ \mu \end{bmatrix}$$

3.2.5.2 Approximate modified membrane model

The process dynamics for the "membrane" are much quicker in response then for the "bioreactor", especially the operator control variables, with the input biochemical variables having slower response times on the fouling processes. The final approximate decomposed model formulation for the "membrane" system is shown in Fig. 3.11:

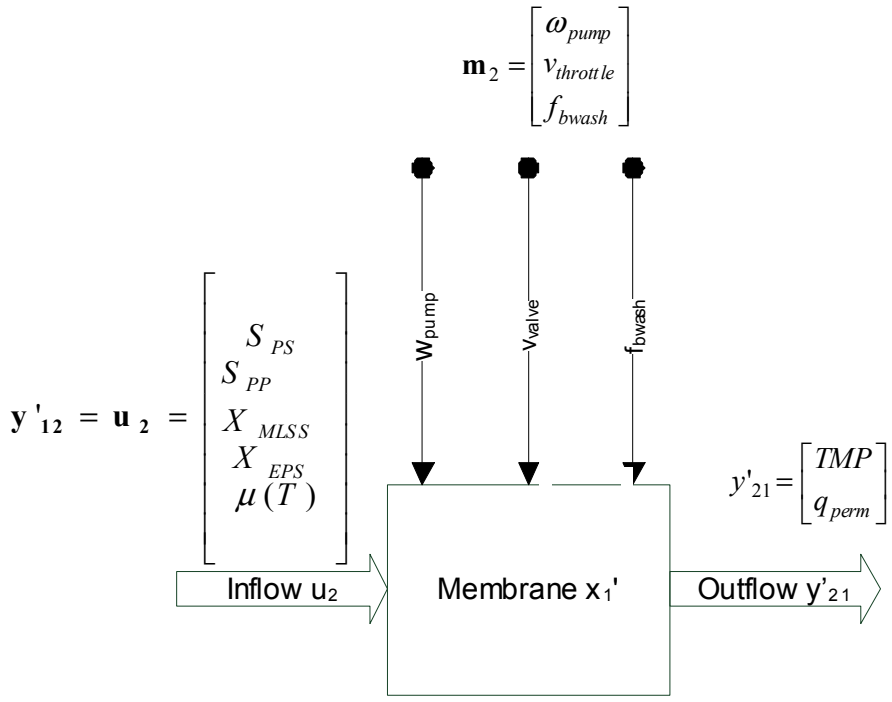

Fig. 3.11: An approximate modified membrane model

In this formulation, again q_{out} is replaced by q_{perm} in y'_{12}. This means that this approximate but modified model is greatly simplified. This yields the following system vectors, with the state variable being 'discovered' during the identification procedure:

Input variables - *Output variables -*

$$\mathbf{y'_{12}} = \mathbf{u_2} = \begin{bmatrix} S_{PS} \\ S_{PP} \\ X_{MLSS} \\ X_{EPS} \\ \mu(T) \end{bmatrix}; \mathbf{m_2} = \begin{bmatrix} \omega_{pump} \\ \nu_{throttle} \\ f_{bwash} \end{bmatrix}; \mathbf{x_2} = \begin{bmatrix} irreversible\ fouling \\ reversible\ fouling \\ cake \end{bmatrix}; \mathbf{y'_{21}} = \begin{bmatrix} TMP \\ q_{perm} \end{bmatrix}$$

Even though environmental temperature changes considerably affect the biochemical processes occurring in the "bioreactor" system, it is worth noting that the temperature also affects the "membrane" system, although in a less pronounced manner, by altering the filterability and fouling process via the viscosity, $\mu(T)$, of the mixed liquor.

3.3 *Matlab System Identification Toolbox© and the CUEDSID software*

This section deals with how the variables from the *approximate modified bioreactor model* (described in Section 3.2.5.1) and the *approximate modified membrane model* (described in Section 3.2.5.2) are prepared in the correct format for the software tools that are used to run the model simulations and that produce the output results detailed in Chapters 4 and 5. The specific software that is used is Matlab/SIMULINK© for the phenomenological model versions, and Matlab's System Identification Toolbox© and Cambridge University's Enhanced System Identification Toolbox for Matlab© (CUEDSID) (which itself is formulated to run in the Matlab© workspace) for the behavioural input-output model versions.

3.3.1 Preparing the bioreactor model in the format required

The software does not distinguish between the input variables and the control variables and for the identification procedure these two types needs to be merged together into a single input vector. Since the temperature in the bioreactor affects the reaction rates, it is treated as a global input (measured) variable. Therefore the model structure is simplified into the one shown in Fig. 3.12.

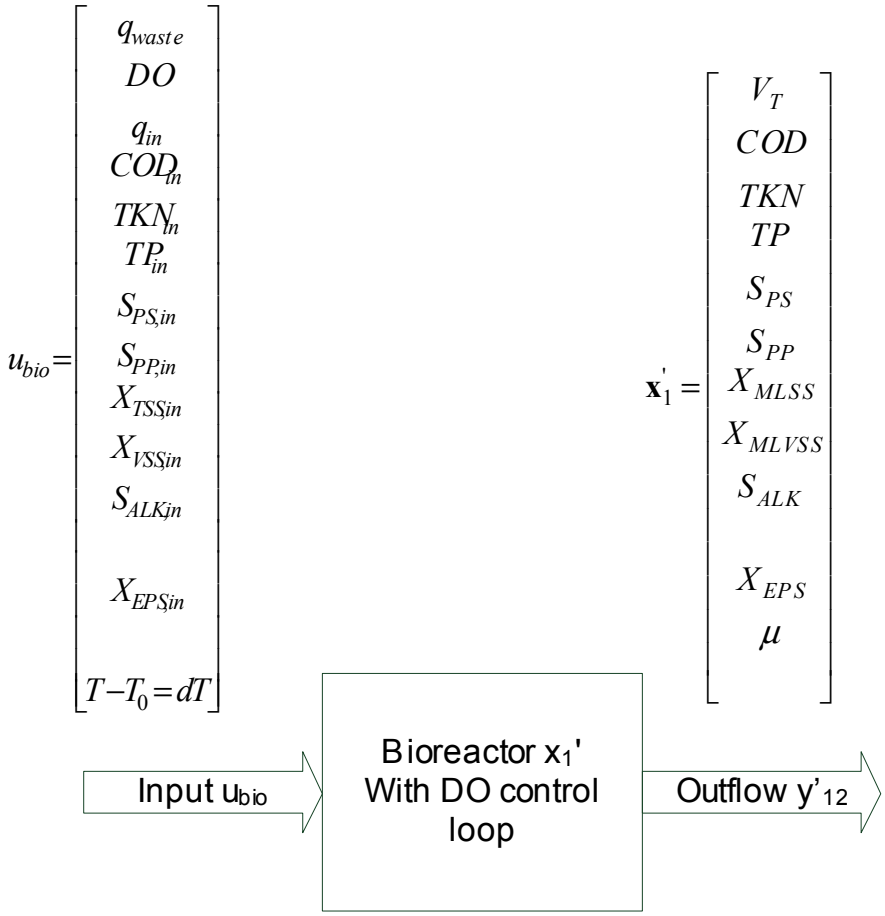

Fig. 3.12: The bioreactor model formulation ready to be used in Matlab / CUEDSID

When using the fluid temperature data sets, they can be interpreted for the different cases as follows:

1. **Data generated from the various models** - After the model has been calibrated and validated accurately it can used to generate further data for simulation purposes, and to see how the plant would react under varied operational conditions. When the model is being used for this purpose, the temperature in the reactor can be assumed to be constant and thus can be removed from the input vector. This simplifies the situation by normalising the generated data with respect to the temperature so that the focus can be on the generation of the fouling components in the biochemical conversion processes.
2. **Data obtained from plant measurements** - When the actual plant measurement data is being used, then in this case the temperature in the reactor is treated as an input variable. It is assumed again for simplification purposes that the inflow fluid temperature can be ignored from the model formulation. It is convenient to consider the deviation, $dT(= T - T_0)$, from the nominal temperature, T_0, rather than the actual temperature, T, so that again temperature affects can be measured from a notional temperature.

3.3.2 Preparing the membrane model in the format required

Again as the software doesn't distinguish between the input variables and the control variables, then for the identification procedure these two types are merged together into a single input vector as shown in Fig. 3.13. The temperature dependency in this case is the mixed liquor viscosity.

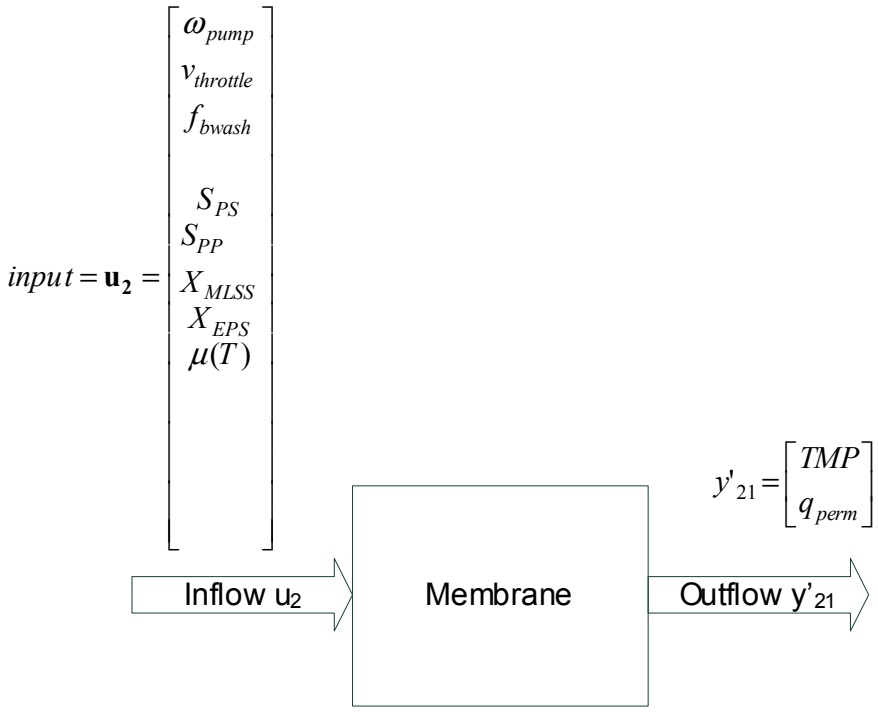

Fig. 3.13: The membrane model formulation ready to be used in Matlab / CUEDSID

Hence the above two model formulations for the general crossflow MBR scenario were used directly in the Matlab's System Identification Toolbox© and CUEDSID software to develop the input-output time series models described in Chapters 4 and 5.

3.3.3 System identification methods: General and specific cases

As stated earlier system identification is an iterative process, where models are identified with different structures from data and the model performance compared. The normal start point for this system identification procedure is by estimating the parameters of simple model structures. If the model performance is poor, then the model structure is gradually increased in complexity. Ultimately the simplest of all the model structures that are applied is eventually selected that best describes the dynamics of the system under scrutiny, which in this case could be either the "bioreactor" system or "membrane" system.

In this iterative process, the system identification procedure commences by initially using linear continuous input-output polynomial model structures, such as ARX and ARMAX ones, and later on linear continuous input-output state space model structures to calibrate and validate all the developed behavioural models using the supplied times series data. The best fit structure is then chosen as the optimal model formulation. If the data fit is still poor then other more complex formulations can be tested such as non-linear model structures. However it has been found that this step is not needed in the type of data being used in this research study.

Matlab's System Identification Toolbox© is a proprietary software package that has been specially developed for running many model formulations of which the ARX, ARMAX and state space ones are particularly utilised in this study. Although the ARX model does not allow modelling of the noise and process dynamics independently, it is a good start point for estimating and gives a simple model at good signal-to-noise ratios. The ARMAX model extends the structure by providing more flexibility for modeling noise by using a moving average of white noise. This ARMAX model is best used when the dominating disturbances enter at the input which is the case in terms of wastewater treatment plant data sets. State space models are models that use state variables to describe a system by a set of first-order differential or difference equations, rather than by one or more n^{th}-order differential or difference equations. State variables can be reconstructed from the measured input-output data but are not themselves measured during an experiment. The state space model structure is a good choice for quick estimation because it requires only two parameters, namely the model order and one or more input delays.

All these model formulations are solved using iterative optimisation techniques and algorithms like the least squares method. However, this requires a lot of computing power and they are prone to inaccuracies. A much more attractive model formulation is the subspace one which does not need to be solved using iterative optimisation techniques and algorithms, but by only using algebraic calculations (Chen and Maciejowski 1999). This means the subspace model formulation is a very powerful one that uses only a single-shot solving procedure with improved accuracy. Matlab's System Identification Toolbox© does have a very poorly constructed subspace formulation which is prone to inaccuracies and often fails to deliver a solution since it uses a very crude four block solving algorithm. Hence, the CUEDSID software was specifically developed in Matlab© workspace to address this oversight by supplying the user with a much more refined and sophisticated four block solving algorithm which always provides a good solution. CUEDSID has its own specially developed Matlab© functions which run the subspace formulation as well as a bilinear state subspace model formulation.

In terms of a MBR wastewater treatment plant, a bilinear state subspace model formulation is also very useful since both the data from "bioreactor" system or "membrane" system are temperature dependant. This means a model structure which takes into account the time and temperature as global operators is suitable in this "Model Conceptualisation Procedure". Bilinear systems are attractive models for many dynamical processes since they allow a larger class of behaviours than linear systems even though they based on simpler linear system theory as opposed to the more complex class of non-linear systems. They exhibit phenomena encountered in many engineering situations such as amplitude-dependent time constants. Many practical system models are bilinear and more general non-linear systems can often be reasonably well approximated by bilinear models which are a special class of non-linear systems. All these aspects of the system identification procedure which the CUEDSID software is capable of undertaking mean that it is an attractive package to be used in this study to develop time series wastewater treatment system models. For the following formulations detailed below, the data sets are again prepared in the correct format to be used in the CUEDSID software format.

3.3.3.1 Subspace formulation for a MBR

Hence the general subspace formulation for a typical state space system is:

$$x(t+T_S) = A.x(t) + B.u(t) + K.e(t); \qquad x(0) = x0$$
$$y(t) = C.x(t) + D.u(t) + e(t)$$

where:
$u(t)$ is input vector of the system
$y(t)$ is the output vector of the system
$e(t)$ is the disturbance (control) vector of the system
$x(t)$ is the (unobserved) state vector of the system
A, B, K, C and D are the (initially unknown) coefficients of the individual vectors respectively

In this MBR case, it is assumed that a complete mixed reactor is used so the output is exactly equal to the state of the reactor, hence the input vector $u(t)$ can be omitted from the expression for determining the output vector $y(t)$, thus giving the formulation to be used in the CUEDSID software for a subspace system:

$$x(t+T_S) = A.x(t) + B.u(t) + K.e(t); \qquad x(0) = x0$$
$$y(t) = x(t) + e(t)$$

3.3.4 Temperature dependent model of a MBR

3.3.4.1 General form of a bilinear model

The general form of a bilinear model is as follows:

$$x(t+T_S) = A.x(t) + N(u(t) \otimes x(t)) + B.u(t) + w(t); \qquad x(0) = x0$$
$$y(t) = C.x(t) + D.u(t) + v(t) \tag{3.5}$$

where:
$u(t)$ is input vector of the system
$y(t)$ is the output vector of the system
$w(t), v(t)$ are unobserved random process vectors of the system
$x(t)$ is the (unobserved) state vector of the system
A, B, N, C and D are the (initially unknown) coefficients of the individual vectors respectively
$N(u(t) \otimes x(t))$ This term is bilinear where $\otimes$ is the Kronecker product operator. If this term is absent the model then becomes linear.

3.3.4.2 How to represent temperature effects by a bilinear model

The temperature dependent "bioreactor" system formulation can be represented by a bilinear model as outlined in Section 3.3.4.1. This is also the case for the "membrane" system formulation, however for the sake of brevity only the "bioreactor" system will be considered.

The starting point is to assume that the model of the "bioreactor" system can be represented by a state space linear model in which the state vector's parameters, A, are depend on the temperature. It is also assumed that parameters vector B which represents the effects of the control variables on the process does not depend on temperature which maybe a simplification of reality.

The constant vector A is now replaced by a temperature dependent matrix, giving the following changed formulation for the specific MBR "bioreactor" situation:

$$A = A_O + A_1.dT$$

so:

$$\begin{aligned} x(t+T_S) &= (A_O + A_1.dT).x + B.u(t) + K.e(t) \\ x(t+T_S) &= A_O.x + A_1.dT.x + B.u(t) + K.e(t) \end{aligned} \tag{3.6}$$

where:

$$x = \begin{bmatrix} V_T \\ COD \\ TKN \\ TP \\ S_{PS} \\ S_{PP} \\ X_{MLSS} \\ X_{MLVSS} \\ S_{ALK} \\ X_{EPS} \\ \mu \end{bmatrix} = \begin{bmatrix} x_1 \\ x_2 \\ x_3 \\ x_4 \\ x_5 \\ x_6 \\ x_7 \\ x_8 \\ x_9 \\ x_{10} \\ x_{11} \end{bmatrix} ; and, u = \begin{bmatrix} q_{waste} \\ DO \\ q_{in} \\ COD_{in} \\ TKN_{in} \\ TP_{in} \\ S_{PS,in} \\ S_{PP,in} \\ X_{TSS,in} \\ X_{VSS,in} \\ S_{ALK,in} \\ X_{EPS,in} \\ T - T_0 = dT \end{bmatrix} = \begin{bmatrix} u_1 \\ u_2 \\ u_3 \\ u_4 \\ u_5 \\ u_6 \\ u_7 \\ u_8 \\ u_9 \\ u_{10} \\ u_{11} \\ u_{12} \\ u_{13} \end{bmatrix}$$

Since the $A_1.dT.x$ expression occurs in the state equation, it is part of the Kronecker product and thus the "bioreactor" system model now falls into this category of bilinear models.

Using general denotations for

$$u = \begin{bmatrix} u_1 \\ \vdots \\ u_m \end{bmatrix}$$

$$u \otimes x = \begin{bmatrix} u_1.x \\ \vdots \\ u_m.x \end{bmatrix}$$

This specific case is much simpler because only one control variable, dT, is multiplied by the state vector x.

The identification procedure applied to a bilinear model will result in calculation of the N matrix, so we are facing the task of understanding the structure of this matrix and how to go back from matrix N to matrix A_1 which is present in our original model as stated in Equation 3.6.

The term $A_1.dT.x$ corresponds to the generic term $N.(u \otimes x)$ in Equation 3.5, hence giving:

$$A_1.dT.x = A_1.u_{13}.x = A_1 \begin{bmatrix} 0_{11\text{x}11} & \dots & 0_{11\text{x}11} & I_{11\text{x}11} \end{bmatrix} \begin{bmatrix} u_1.x \\ \dots \\ u_{13}.x \end{bmatrix} = N.(u \otimes x)$$

where:

$$u_{13}.x = dT$$

and

$$N = A_1 \begin{bmatrix} 0_{11\text{x}11} & \dots & 0_{11\text{x}11} & I_{11\text{x}11} \end{bmatrix}$$

and

$$x(t + T_S) = A_O.x + N.(u \otimes x) + B.u(t) + K.e(t)$$

which is the same as the general form given in Fig. 3.14. (Incidentally, when determining matrix N, it should have a block structure with 13 of 11x11 blocks, with the first 12 blocks being equal to $0_{11\text{x}11}$, and the last N_{13} block being $N_{13} = A_1$, i.e. A_1 is equal to the last nonzero 11 by 11 block in the matrix N.)

The input and output data is prepared in the same format as for the linear model but this time the CUED-SID software will calculate the following matrices: A_O, N, B and K.

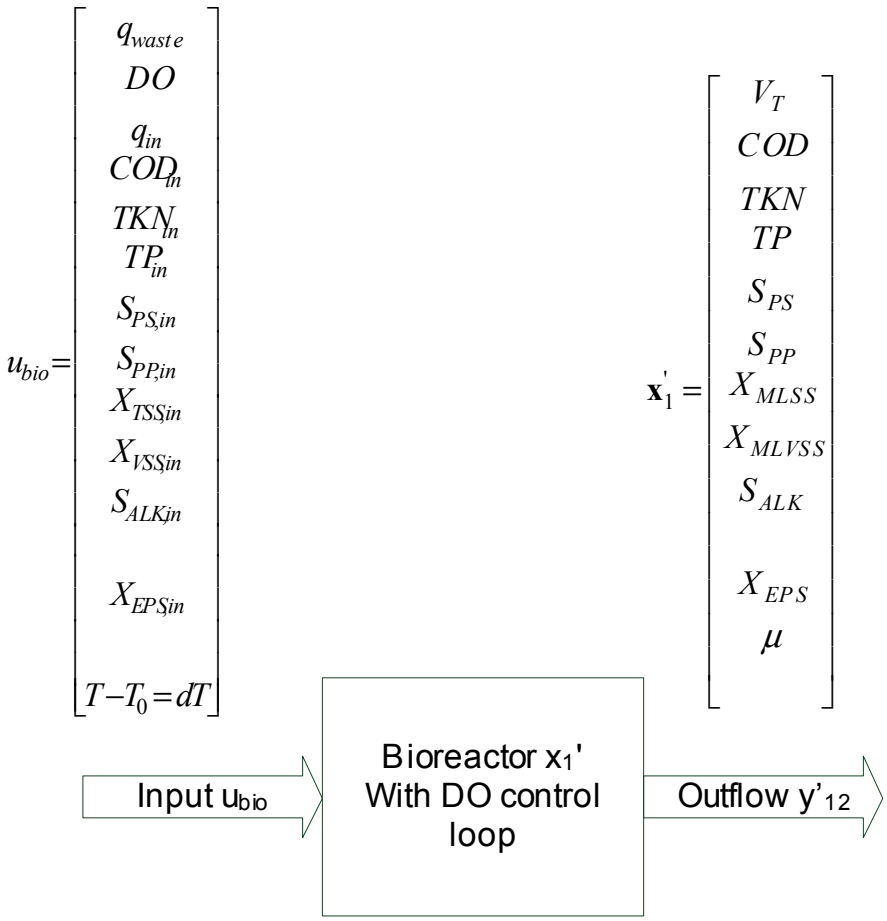

Fig. 3.14: Bilinear bioreactor model formulation including for temperature dependancy

3.4 *Plant descriptions and data collation issues*

The general "Model Conceptualisation Procedure" described earlier has been used to develop models for a MBR which relate specifically to two key areas: (a) The membrane fouling process; and, (b) The Activated Sludge system which affects the membrane performance. Two types of models were developed for these systems under investigation, namely phenomenological ones and behavioural input-output ones. These models were tested and validated using real life wastewater treatment plant data, collected in some cases specifically to allow this to happen. Based on the results from these simulation studies, conclusions can be made on the effectiveness and usefulness of the two model types used for the two key areas under investigation.

The following data was collected and processed from various plant which relates to the membrane fouling model covered in Chapter 4. This data refers mainly to specific flux stepping experiments and membrane tests:

- Aquabio pilot crossflow MBR plant at Kanes Foods - flux stepping and membrane tests July/Dec 2008.
- ITT pilot membrane unit at Cardiff WWTP - flux stepping tests July 2007.
- ITT pilot submerged MBR plant at Coors UK - long term flux and TMP measurements August 2004/February 2005.

The following data was collected and processed from various plant which relates to the Activated Sludge model covered in Chapter 5. This data refers mainly to specific biochemical tests and assays:

- Aquabio main crossflow MBR plant at Kanes Foods - sampling programme and regime Nov/Dec 2006.
- Aquabio pilot crossflow MBR plant at Kanes Foods - sampling programme and regime July/Dec 2008.

All the four plant and units mentioned are described in greater detail in the following sections, with key information provided on the plant layouts, tests carried out, sampling programmes run, etc. Some output data from the plant is also shown to give an indication of the type of data typical collected and processed under this research study.

Later in the forthcoming Chapter 5, it is found that the data collated from the four plant and units used in this study was not sufficient to fully test a MBR Activated Sludge type biological model based on an input-output system identification procedure. In order to allow this testing to go ahead as planned, sufficient data (i.e. nearly 20,000 values) was generated by using a special modified fictitious WWTP based on the commonly used COST Benchmark simulation model as described in Copp (1999, 2000). This fictitious plant was made more realistic by modifying it to include for temperature effects. This would mean a full testing procedure could then be carried out of the developed biological input-output model structure. Hence the last Section of this Chapter describes this fictitious plant layout, its modifications, and plots of the generated data sets.

3.4.1 Data requirements for MBR wastewater treatment modelling

Before descriptions of individual plant layouts are provided together with sampling programmes run and measurements taken, this Section outlines the type of information and data needed to verify and test the models formulated in Chapters 4 and 5. Consequently the specific data collation needs are as follows:

Physical Data:

- Tank sizes and number of tanks.
- Aeration tank volumes, if applicable.
- Membrane unit dimensions, effective surface areas and depths.
- Similar volume data for all other unit processes.
- Connectivity between tanks - pipe diameters and pipe lengths.
- Aeration system data.
- Type of aerators (e.g. mechanical, diffused, jet aeration, etc.).
- Details on aeration grid and diffuser heads (e.g. transfer efficiency) for diffused air systems.

Operational Data:

- Trans-membrane pressure across membrane units.
- Waste sludge flow (i.e. sludge pump operation).
- Waste sludge concentration.
- Time series of waste sludge flow rates and waste pipe location/s.
- Recirculation flow rates (i.e. recirculation pump capacity).
- Control strategies.
- Air flow rates and air flow distribution for diffused aeration systems.

Compositional Data:

Influent

- Raw wastewater.
- Flow (diurnal preferably).
- Total COD, filtered COD, BOD5, TSS, VSS, TN, Total Phosphorous (TP), TKN.
- Ammonia, soluble TKN.
- Soluble phosphorus (i.e. ortho-phosphate).
- Wastewater temperature, pH, conductivity.

MBR Tank Unit Process Data

- All Processes (in and out of each process).
- TSS, VSS.
- Total COD, filtered COD, BOD5, TN, TP, TKN (both total and soluble).
- Ammonia, soluble Phosphorus.
- Aeration Basin (within the aeration basin and in addition to the above data).
- Spot DO measurement.
- Mixed liquor Viscosity (measured in centipoise, cP).
- DO profiles.
- pH, conductivity.
- MLSS profiles.
- Ammonia profiles.
- Nitrate profile/s.
- Soluble COD profiles.

Final Effluent

- Final Effluent.
- Total COD, filtered COD, BOD5, filtered BOD5, TSS, VSS, TN, TKN.
- Ammonia, soluble TKN.
- Soluble phosphorus, pH, conductivity.

Note: Filtered COD or BOD5 is determined by filtering the sample through at least a 0.45 μm glass fibre cloth (GFC) filter paper, and this is the minimum pore size thought to remove all solids and colloids in suspension.

3.4.2 Aquabio pilot MBR plant design and operation

Fig. 3.15: Pictures of (a) Author standing next to pilot plant; (b) Berghof vertical membrane modules

For the sake of brevity and in order to stop repetition and duplication of information, only full detail is given for this particular plant. This details include information on its design, operation, layout, biochemical sampling programmes carried out both on-line and off-line, and flux stepping experiments carried out as well. For the other three plant, only summarised details are given.

3.4.2.1 Design of Aquabio's New "Vertical Air-Lift" Pilot Plant

Under the TSB Project No. 15123, "Improving the Design and Efficiency of MBR Plant by using Modelling, Simulation and Laboratory Analysis Methods" a specialist, one-off pilot plant was designed so that both the Activated Sludge models and membrane fouling models could be calibrated and validated.

Originally, the technical staff of Aquabio Limited (which is the main industrial collaborator in this TSB project), only wanted the layout of the new pilot plant to consist of a simple membrane filtration module. This would be hooked up to the bioreactor of an existing wastewater treatment plant. Hence this would be a very cost effective way of measuring the membrane's performance as it could be easily moved from site to site and therefore be used to test mixed liquors from different treatment plant. It would also be a very portable pilot plant with only limited ancillary mechanical and electrical control equipment. Aquabio also wished to test a new MBR technology known as "Vertical Air-Lift" which apparently has many advantages over traditional sidestream configurations (Futselaar et al. 2007). Since this new technology would not interfere with the usual model calibration and validation procedure, it was agreed that the new pilot plant would incorporate it so that Aquabio's portfolio of MBR technologies offered to Client's could be potentially increased. Consequently this pilot plant could serve a simultaneous dual purpose.

3.4.2.2 Negotiations with Aquabio regarding the final pilot plant configuration

The Author insisted that in terms of meeting the TSB project's deliverables, he needed a comprehensive plant configuration which incorporated a separate bioreactor (see Fig. 3.16). This would mean that the biology within the reactor could be experimentally varied to promote extreme EPS fouling conditions which in turn would impact on membrane fouling rates. For example very low DO levels could be maintained in the pilot plant bioreactor for extended periods to purposely "stress" the microbial biomass and thereby potential produce increased EPS levels. Thus this broad variation in biochemical readings taken during the sampling programme period would give sufficient information to allow a thorough model calibration and validation exercise to be conducted. Conversely this experimental operation of a bioreactor could never be done on any fully operational large scale wastewater treatment plant as it would impact greatly on flux rates, and any Client operator would never allow this as it would have significant financial implications.

Additionally the Author stated that he needed a pilot plant which was totally flexible in its membrane operation unlike the basic filtration plant initally suggested by Aquabio's technical staff which has limited flexibility and limited use. This would mean the pilot plant would have a membrane system that was capable of being operated under multiple operational regimes. For instance it should be capable of being forward fed with biomass via a variable speed recirculation pump which would allow different cross flow velocities to be developed across the membrane which in turn would induce varying permeate flows. This permeate flow could also be enhanced by incorporating a smaller variable speed suction pump on the permeate side, which could also operate as a backflush pump to clean the membrane with a reverse flow. Obviously these crucial additions which the Author required had major cost implications in terms of additional piping, automatic control valves, control equipment, sensors, variable speed pumps, etc. However the Author managed to convince Aquabio that in the long run this proposed configuration would give them much more flexibility, thereby allowing a better understanding of their process, and hence more useful output, which they could apply to their full scale version for their Clientele.

Based upon the successful outcome of these negotiations, the Author designed with help of the project design team an entirely novel one-off pilot plant which is flexible enough to meet all project objectives and industrial partner objectives. From Aquabio's point of view, part of the pilot testing procedure would be to optimise the flux production for both minimal energy usage with minimal fouling accumulation.

This pilot plant was designed and constructed over a one year period, and eventually installed in late June 2008 at Kanes Foods site, and was operated for just under six months. The construction of the plant was carried out by a specialist sub-contractor hired by Aquabio to carry out this task. Soon after it was commissioned using potable water, it became fully operational and was fed wastewater from the Kanes Foods' commercial salad washing operation. This is the same wastewater that is treated and then success-

fully recycled via the large full scale MBR plant that Aquabio installed and commissioned several years earlier. This means the performance of the membranes from both the pilot plant and main plant can be directly compared against each other for the same influent stream albeit with different bioreactor biologies and plant configurations. Fig. 3.15 shows the installed pilot plant, and crosssection of typical Berghof© vertical membranes like the ones used in this plant.

The pilot was run off and on until late December 2008. During this period a prolonged daily off-line sampling programme was initiated which measured various biochemical concentrations of standard and non-standard variables in the influent stream, in the bioreactor, and in the outlet permeate flow. This sampling programme included simple filtering, simple protein/polysaccharide measurements, and flux-stepping operations which are described in the next sections. A comprehensive list of in-situ membrane resistance tests are also given.

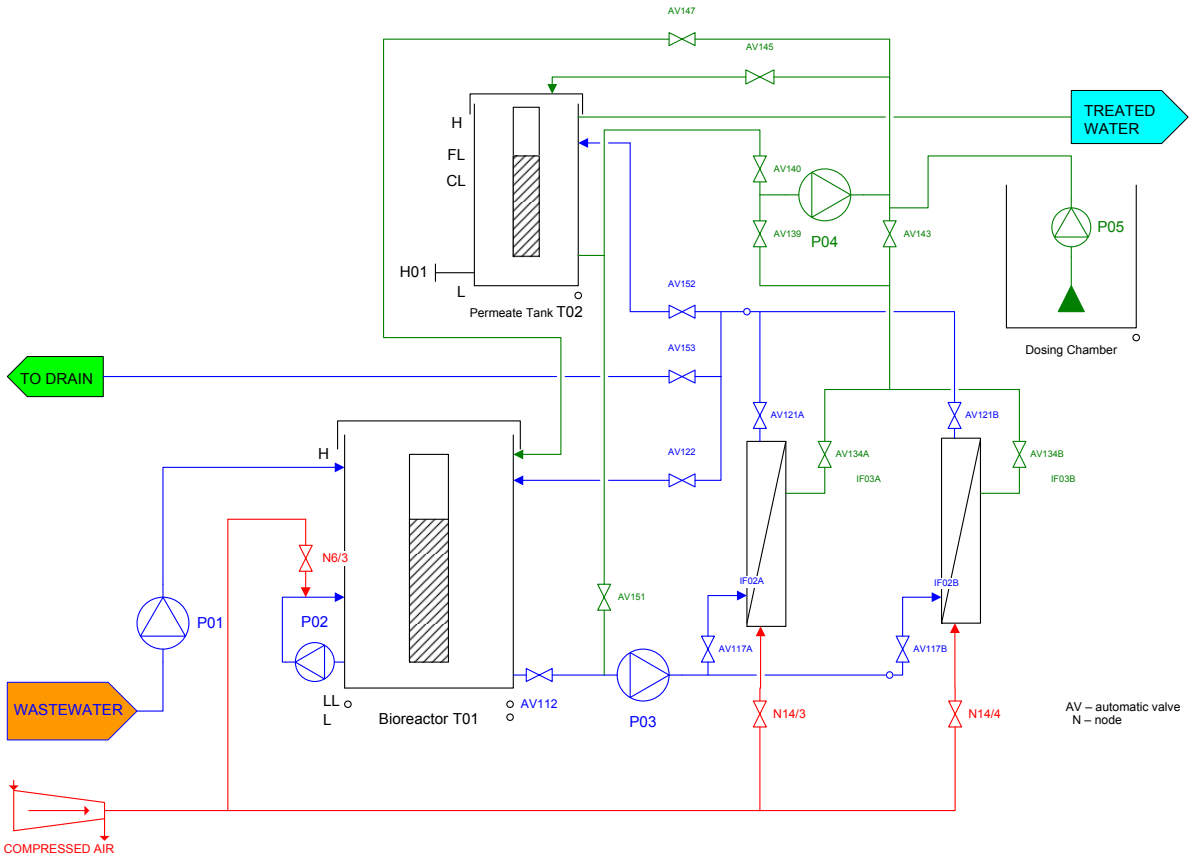

Fig. 3.16: Detailed Schematic of Aquabio's New "Vertical Air-Lift" Pilot MBR Plant

3.4.2.3 Aspects of pilot plant configuration

Various aspects of this new pilot plant's technical configuration are listed below:

i) – The plant has jet aeration in the bioreactor tank with a DO controller so that the optimal DO setpoint is achieved. A combined DO probe, pH and temperature sensor are also mounted in the tank.

ii) – A 5 m^3 bioreactor tank connects to two sets of 3 m long Berghof© potted tubular membrane units of 3 inch diameter. They are operated vertically mounted and in parallel, so that any local difference in performance can be ascertained. Each of the tubes in the potted housing are 8 mm in diameter.

iii) – A variable speed recirculation pump of maximum rating of 40 m^3/hr is used to pump the liquor through the membranes. With this type of centrifugal pump the CFV can be varied and optimised for maximal shearing effect and thus reduced cake build up.

iv) – Each membrane tube can be sparged continuously or by intermittent pulsation on a timer by coarse bubble aeration if operated in vertical air-lift mode. It is suggested that an intermittent sparging mode maybe more beneficial since no dead zones are introduced into individual tubes and also there is a saving in energy. A sparging controller with actuator valves allows different intermittent regimes such as 10 seconds on with 10 second off to maximise the sequential pulsation effect stimulated between the two membrane tubes. The sparging aeration rate itself can be varied and optimised to allow maximum shear.

v) – A back pressure butterfly valves has been added to the return leg of the recirculation pipework after the membranes so that the shear effects due to the CFV can be isolated from the shear effects due to the sparging alone. This would potentially allow optimisation of these two hydrodynamic conditions. This variable "throttle" valve also allows the back pressure across the membrane to be varied manually for specific TMP regimes. The normal TMP would be up to 2 bar as opposed to a typical backwash pressure of up to 0.3 bar.

vi) – A variable speed forward suction pump is connected on the permeate line to allow both constant flux and constant TMP operation. It is connected to an automatic controller which takes readings from a flow meter in the permeate line to allow constant flux operation, or it take readings from a differential pressure transducer located over the membranes themselves which allows constant TMP operation. (This pump can be switched off periodically to allow a relaxation step to be introduced during the forward flux and back flush steps, to assist the flux recovery regime whilst simultaneously reducing energy consumption.)

vii) – This suction pump also acts as a back flush pump with a valve assembly arrangement of automated actuators. This allows the permeate water from the permeate tank to be flushed backwards through the membranes at a rate of up to 2 m^3/hr for between 30 seconds to two minutes at a low pressure. This backwash operation allows membrane cake build up and pore blockage to be physically removed so that during the next forward flux operation, permeate flux production is recovered to previous levels. In back flush mode the pump speed is limited so only a maximum of 1 bar in pressure is generated in order to prevent the membrane tubes from imploding at higher back pressures.

viii) – A data logging system with sensors is incorporated so that the flux and TMP is measured and logged automatically on a preset measurement interval of every couple of minutes. A memory stick can be connected to this data logging system so that the historical evolution of flux/TMP can be either downloaded, or seen on-line on the control panel's human-machine-interface (HMI).

ix) – For the sake of simplicity in the pilot plant set-up, a single air compressor is used to deliver all the plant's air requirements. Thus this compressor supplies air to the bioreactor jet aeration system, and air to turn all the valve actuators on and off, and finally supplies air to the coarse bubble aeration system as well. In a full scale system this would obviously not be practicable, and would need to supplied by separate air compressor and/or blower systems.

x) – A cleaning tank is incorporated into the plant so that a weekly maintenance clean of the membranes can be carried out by forward flushing the membranes with permeate water. This coupled with a complex set of pipework and valve arrangement also allows permeate water to fill the membrane tubes when the plant is non-operational, as any extended contact with anaerobic biodegrading mixed liquor would permanently damage the membranes.

xi) – A dosing chamber with a peristaltic pump has been incorporated into the design, so that automated dosing of chemicals can be done when an intensive chemical clean is needed to recover long term irreversible fouling. This chemical clean can be programmed at the HMI as either a backflush operation, or as a forward flush operation, or combination of both sequentially. It is recommended that a weekly chemical clean using very dilute concentrations of hypochlorite and caustic chemicals is used to retain forward flux levels. A citric acid chemical clean is recommended at least every 1 to 2 months to remove accumulation of inorganic scalants.

The pilot plant can be operated in three different modes as follows, with the valves operated automatically from the HMI panel according to the selected mode:

i) – Normal high velocity crossflow mode (e.g. 2.5 m/s) with no backwash cycling and no coarse bubble aeration. (An automated backwash can be programmed in if required but probably the additional energy needed will lead to very little gains in membrane permeability, and a drop in net flux produced.) In this mode the permeate suction pump is usually kept off with only the forward mixed liquor recirculation pump in continuous operation at high speed. This mode is the standard one offered by Aquabio, and Kanes Foods full scale plant operates in this same way. Although this mode is a very simple one, operationally speaking, it consumes a significant energy for every m^3 of permeate produced when compared to all submerged configurations. When the pilot plant was first commissioned, this mode was used to test the membrane performance for the first few days.

ii) – An experimental low velocity crossflow mode (e.g. 1 m/s) with automated backwash but no coarse bubble aeration. The permeate suction pump can be used to assist the recirculation pump during forward flux production by an automatic controller (e.g. if the forward permeate flux falls below 50 $l/m^2/hr$ it will come on to suck further permeate through). The backwash cycle is definitely needed of sufficient intensity and duration and at least every 30 minutes to keep the membrane regularly clean as the flux drops dramatically between backwash cycles since the CFV is very low. For most of the sampling programme period, this was the selected mode for continuous operation of the new pilot plant.

iii) – An experimental vertical air-lift mode with coarse bubble aeration and low inertial lift velocity due to a limited forward feed pump speed (e.g. 1 m/s). This mode would use probably both a backwash cycle and relaxation cycle and theoretically produce a flux range of 20 to 50 $l/m^2/hr$. The energy usage under this mode is projected as 0.25 kWh/m^3. This is very low when compared to the standard range for a high pressure sidestream system which is usually in the 3-8 kWh/m^3 range (typically 5-7 kWh/m^3) (Futselaar et al. 2007, Chang and Judd 2002). In comparison Aquabio's current system has an energy usage of approximately 1.6 kWh/m^3. As mentioned already, due to time constraints of experiments and to keep the hydrodynamic modelling work as simple as possible, this third mode was never used during the sampling programme period.

Again for the sake of brevity, the following further information on this plant which is available was not provided in this thesis:

- piping and instrumentation diagram (PID) with equipment list and specification (e.g. membrane information, pump information, valve arrangements, pipe sizes, tank sizes, etc.).
- Operational strategy - backflush, cleaning regime, constant TMP/flux:
    1. - Physical: layout, pump characteristic.
    2. - Operational regime: constant flux or constant TMP or constant pump speed (constant CFV).
    3. - CFV (if applicable).
    4. - Backflush schedule (if applicable) and/or aeration rate-type.
- Controller arrangements - aeration, pumps, alarms.
- Operational personnel and period.

3.4.2.4 Aspects of pilot plant testing procedure

List of on-line sensor measurements The plant is fully equipped with sensors and analysers to automatically measure and log various process and operational variables under consideration. The following instrument list with tag numbers gives a summary of the critical sensors used:

$IL01LEVEL$ - Bioreactor Tank Level Transmitter, m

$IL02LEVEL$ - Permeate/Cleaning Tank Level Transmitter, m

$IF01FLOW$ - Bioreactor Feed Flowmeter, $litres/hr$

$IF02AFLOW$ - Vertical Membrane A Feed Flowmeter, m^3/hr

$IF03AFLOW$ - Vertical Membrane A Permeate Flowmeter, $litres/hr$

$IF04FLOW$ - Jet Aeration System Air Flowmeter, Nm^3/hr

$TOTALPERMEATEFLOW$ - Daily Volume Totaliser of Permeate Produced, m^3

$IP01PRESSURE$ - Membrane Inlet Pressure Transmitter, bar

$IP02PRESSURE$ - Membrane Outlet Pressure Transmitter, bar

$IP03PRESSURE$ - Membrane Permeate Pressure Transmitter, bar

$P03ACTSPEED$ - Recirculation Pump Speed Setting with 100% being 40 $m^3/hour$

$P04ACTSPEED$ - Permeate Suction/Backflush Pump Speed Setting with 100% being $m^3/hour$

$IQ01DO$ - Bioreactor Tank DO Probe Transmitter, mg/l

$IQ02QpH$ - Bioreactor Tank pH Probe Transmitter, pH

$IT01TEMP$ - Permeate/Cleaning Tank Temperature Transmitter, $°C$

$IQ02TTEMP$ - Bioreactor Tank Temperature Transmitter, $°C$

$OPERATIONTREND$ - Number system from 0 to 6 [e.g. 0 - not in operation; 1 - normal mode; 4 - backflush mode]

Composite sampling A refrigerated composite sampler (with air pressure driven guillotine head) was specifically purchased for the inlet flow so that flow-composite samples could be automatically collected from the inlet line and properly stored. This would mean that as the inlet flow and load could vary considerably during the day, grab sampling at a single point in time would give large inaccuracies in the results. Consequently a twenty four hour flow-composite sample would give a much more accurate reflection of the actual flow and load into the plant. Samples taken from the bioreactor and the permeate tank were relatively representative even though they were simply grab samples as it was assumed the tanks were complete mix ones and large enough to attenuate incoming flow and load conditions. An attempt was made to ensure samples were collected at the same time daily to further reduce error in the sampling protocol.

Comprehensive sampling programme design A comprehensive "extended" sampling programme was designed with biochemical protocols. This included initial one-off tests for the membrane resistance when the membrane module was virginal. This newly designed sampling programme enhanced the existing daily sampling regime already carried out by Kanes Foods laboratory staff (e.g. COD, TN, TP, conductivity, etc.) in which they use test kits to speed up the results procedure. These additional tests included simple filtered COD, BOD5, simple protein/polysaccharide measurement with some being carried out by De Montfort University's laboratory staff.

Sludge properties measurements The properties of the mixed liquor can be quantified by adding additional tests to the grab samples taken. They can range from very simple filter tests to see any variation in sludge properties to more complex protocols for sludge settleability. Researchers have found that good filterability and settleability properties of a mixed liquor improve the performance of the MBR membrane.

Filterability - This can be measured using either the CST method, the time-to-filter (TTF) method, or by the specific resistance to filtration (SRF) method. These methods measure how filterable the sludge is under a standard filter protocol measured either by length of time taken to pass the mixed liquor through a standard filter at known conditions, or by how much of a certain volume of liquid is passed under standardised conditions. These tend to be dead end pressure tests, and give a rough indication of sludge compressibility and hence cake filtration build up.

Settleability - This can be measured by carrying out a SVI test where a value of 50 to 100 ml/g indicates good settleability, with a high value over 150 ml/g indicating low filterability. In this test the volume of sludge settled in 30 minutes is divided by the MLSS concentration to give the SVI value. There are various variations on this test to include the stirred sludge volume index (SSVI), or the diluted sludge volume index (DSVI). Researchers have found that good settleability indicates a well conditioned sludge in which filamentous flocs do not predominate which in themselves cause sludge bulking. A well conditioned sludge also is less likely to experience the build up of Nocardia bacteria which cause foaming events. Another method which measures the foaming ability of the mixed liquor is the scum index (SI) test which is the mass of biomass in foam divided by total mass of biomass. Bad foaming usually gives poor settleability and filterability.

Normalising measured permeability of membrane When using the collated data to determine the membrane resistance/permeability, it is important that any data is normalised. This normalisation of the actual membrane permeability is to remove the affects of three associated factors, namely the wastewater temperature, the MLSS concentrations, and short extreme gross flux conditions which exceed critical flux even though daily net flux is below critical. Once the data is fully normalised by making allowances for these factors, then the real permeability trend of the membrane can be deduced. Normalising of the data is crucial for the following reasons:

- It has been found in recent research that temperature can cause a 100% decrease in permeability whilst MLSS concentrations and gross flux events can have similar decreases of 40% and 16% respectively (Melin et al. 2006). Therefore these three factors, which are described further below, need to be included in the data normalisation procedure.
- Temperature has a very strong effect on membrane permeability by changing the water viscosity leading to a 2 to 3% change in permeability per $^{\circ}C$ compounded. In fact a 5 $^{\circ}C$ change in temperature leads to an exponential 1.02 x 10^5 increase in permeability. This can be accounted for by using an Arrenhius expression.
- MLSS increases both impact on overall liquor viscosity and the amount of cake build up, and the reduced shearing effect on the membrane interface.
- Extreme gross flux events are the actual flux at an instant in time and will exceed critical flux. Its associated head losses due to flow through pipes and fittings will be much greater but this is not taken into account when calculating the net averaged daily flux. The net flux is calculated as follows: Net flux = volume of permeate produced per day / (24 hours x membrane area). So when normalising, this is done either up or down to a standardised operating condition and point of, say, 15 $^{\circ}C$ at MLSS of 12,000 mg/l and a net daily flux of 50 $l/m^2/hr$.

Pilot plant start-up procedure and follow-on operations The following plant start-up procedure was designed in order to determine the various membrane resistance components.

1. R_m, Clean membrane resistance - 1 hour test at constant TMP with measured flux drop (if any). Repeat several times ideally.
2. $R_{porePERM}$, **SMP** permeate resistance - Similar to test conditions for Test 1. Not a critical test.
3. R_{absorp}, Short irreversible fouling resistance (due to adsorption only) - Leave in tank for up to 6 hours minimum. Very low crossflow or vertical air-lift with no suction pressure.
4. R_{pore}, **SMP** mixed liquor sludge water fouling resistance - Use a sack screen of millimetres screen size to remove particulates from sludge water.
5. R_{cake}, particulate only mixed liquor fouling resistance - This is calculated by running with unfiltered mixed liquor, and then taking this value away from the filtered value to give the R_{cake}.

This procedure then is followed by a recommended operations procedure to test the plant fully. This consists of running at steady state TMP which is below critical (with periodic backflushing) for all three modes of operation that are possible with this plant in order to determine the affect on the bioreactor biology. Steady state operation for each mode would occur for as long as necessary, especially to allow the newly seeded sludge time to adapt to the new environmental conditions. This acclimatisation may take days or weeks.

- Seed plant with sludge by taking liquor from main WWTP tanks.
- *Mode 1* - Start pilot at same conditions as main plant i.e. high crossflow operational mode with no sparging above critical flux.
- *Mode 2* - Eventually switch to low crossflow operation with/without sparging.
- *Mode 3* - Time permitting, then switch mode to vertical air-lift mode with coarse bubble aeration sparging.

After this steady state operational period, the plant would be ready to experience the more extreme gross fluxes generated during a flux stepping procedure and testing regime. This would be done in *Mode 1* operation.

1. Keep TMP constant via a fixed mixed liquor CFV with no permeate suction flow and measure flux drop. Vary the throttle valve setting for the next flux step up. Do the tests for several flux steps up and then down, with consistent backflush cleans between steps. This would involve starting at 100% pump recirculation speed then stepping up from throttle valve notches 2 through to 6, and then down again with step durations of 30 minutes to one hour to allow flux stabilisation between steps.
2. Time permitting, keep TMP constant via a fixed mixed liquor CFV with a fixed permeate suction pressure for each step. Repeat as Step 1.
3. Time permitting, repeat as Step 1 but now with air-sparging added, initially at a constant intensity rate, followed by tests with intermittent air-sparging operation and with fixed duration and intensity.

Again time permitting, other variations of the standard cleaning procedure used to recover the flux after each stepping cycle is completed could be tried as follows:

1. Introduce, with the consistent backflush regime, relaxation periods between flux steps of various durations.
2. Introduce varying backwash periods between flux steps of various intensity and duration.

3. Introduce a fixed chemical cleaning regime between steps using sodium hypochlorite of fixed concentration and dose.
4. Try different chemical cleaning liquids such as liquid acids and/or alkali with fixed concentration and dose.

Final tests that could be tried would be to operate the plant at steady state conditions but then vary the biological and process parameters instead. This would mean a consistent operational mode, CFV, sparging if used, backflushing procedure, relaxation if used, and cleaning regime if used. The process parameters and biological changes that then could be introduced at this constant steady state operation could include:

1. Vary jet aeration intensity by increasing and decreasing the air compressor rate.
2. Vary the DO setpoint for the DO probe.
3. Vary SRT and/or F/M by adding carbon substrate of known quantity and concentration into the bioreactor.
4. Vary pH by adding buffering solution.
5. Vary C/N/P ratios by adding various nutrient solutions of known dosing and concentration such as liquid fertiliser.
6. Vary salinity and thereby conductivity by adding salt solutions of known dosing and concentration.

These final tests would change the biology in the bioreactor and hopefully promote **SMP** production by "stressing" the bacterial biomass. Any changes would then be measured by microscopic analysis. A day book should be kept for the plant which records and logs all events such as periodic manual wastage, and any unusual events like bulking, foaming, breakdowns, etc.

Actual pilot plant operational information Below is a summary of the actual operational information obtained from commissioning the plant:

- Operated for first few weeks at high crossflow mode with no backflush, then switched to the low energy low crossflow mode with backflush every half an hour. It must be noted that chemical cleans were only every done manually and periodically, even though the plant could do it automatically and very frequently. This was to prevent membrane damage.
- For a 210 l/hr feed rate and a 205 l/hr permeate suction flow, a flux of 50 $l/m^2/hr$ is generated for a 4 m^2 area of a single tube.
- The DO setpoint is taken as 1.25. A measured DO value of 6 is too high while 0.1 is too low. The DO is controlled by a simple ON/OFF controller.
- The bioreactor tank level maximum height is 1.7 m, with low level being 1.3 m. The tank volume is 3 m^3, with a normal operating level of about 1.5 m.
- The design pH range is 5.5 to 9.0 to stop the membrane from being damaged. However the wastewater actually used has a less extreme range of 6.5 to 8.0 so that the bacterial biomass is not greatly affected by it.
- The normal temperature range is 10 to 50 $°C$. Rapid temperature increase can become an issue when carrying out very rapid recirculation of the liquid in system. It can raise by 10 $°C$ in one hour.
- In high crossflow mode the velocity is 3.8 to 4 m/s with no backflush and no permeate suction. In this mode only an automated forward flush is available followed by automated forward CiP regime.
- In low energy low crossflow mode the velocity is 1.5 to 2.5 m/s with no coarse bubble aeration. A backflush is possible (and recommended) as well as permeate suction. Relaxation is also possible.

- Vertical air-lift mode has coarse bubble aeration, continuous or intermittent or even simply off.
- The HMI interface introduces time lags between automated events to prevent clashes between prior programmed automated sequences and events such as coarse bubble aeration introduction, backflush regimes, backflush regimes with cleans, relaxation steps, and forward flush procedures to protect the membranes during automated shutdowns.
- The permeate flow can be recycled if the inlet flow is not sufficient to maintain bioreactor tank levels. The permeate tank volume is 330 to 400 *litres* depending on the level sensor settings.
- The flow meter locations are at: a) inlet; b) Tube 1 on both biomass and permeate lines; and, c) Tube 2 on both biomass and permeate lines.
- The pressure sensor locations are at: a) $P1$ into both tubes; b) $P2$ out of both tubes; and, c) $P3$ on the combined permeate line. So, the calculated TMP $= \frac{P1+P2)}{2} - P3$.
- The actuator sensor interface (ASI) system is similar to the standard Profibus system and is used to send analogue and digital signals from the sensors and valve actuators back to the HMI system which then processes the information and then operates the various plant machinery such as pumps.
- The single air compressor supplies pressurised air to operate the following:
    1. Jet aeration system which can be throttled by hand.
    2. Tube 1 and Tube 2 air-sparging system which can be throttled by hand.
    3. All valve actuators with the valves being of the butterfly type.
    4. The diaphragm pump at inlet to pump fresh influent into the bioreactor.
    5. The composite sampler's guillotine head which automatically sucks a flow-proportional influent amount from the inlet line.
- The permeate pump which can operate in either forward suction mode or as a backwash pump is controlled by a step controller system (i.e. the step controller increments/decrements in several successive steps with the step size set in the controller arrangement).
- The biomass recirculation pump can pump to one or both tubes and has a maximum rating of 40 m^3/hr. In high crossflow mode with both tubes operating, a much larger recirculation pump of rating 80 m^3/hr is ideally needed to simultaneously supply adequate air to each tube. However this system limitation can be overcome by operating in an alternating high crossflow mode for each tube. This means the system automatically switchs between each tube after a set period while still using the current 40 m^3/hr pump. This pump is also used for flushing the system and for running the membrane forward cleaning regime where recirculation of clean mix is carried out. This variable speed pump works on setpoint speeds to determine the high and low level alarm points, with the variable speed being set manually on the HMI.
- In high crossflow mode, the forward flush procedure can be initiated to entirely remove the biomass from the membrane tubes before a chemical cleaning regime is initiated, either as a forward flow or as backflush. The CiP procedure consists of recirculating the chemically dosed permeate liquid for 20 minute periods. This is repeated several times.
- The dosing line is incorporated into the backflush line so that a pulsed dosing can be introduced.
- The membrane has 55 tubes each of 8 mm diameter with 55 air-sparging tubes in the coarse bubble aeration housing, so that each tubes gets its own air-sparging. The membrane material, pore size and manufacturer is PVDF 0.03 μm Berghoff©.

3.4.2.5 Results - Data collected under sampling programme

Fig. 3.17 shows the start and stopping periods of running the pilot plant, and when the sampling programme switched to the main plant instead. In terms of quality control, it also compares the results obtained for the inlet COD from the two different laboratories involved in the sampling programme. These were De Montfort Universty's laboratory which carried out specific measurements for the sampling programme using full biochemical assays, and the Kanes Foods laboratory which continued its standard measurements for the main plant during the duration of the sampling programme using rapid biochemical test kits. Since each of the two plant's inlet COD values were measured at different laboratories and using different means (i.e. either standard test kits or full biochemical assays), that is the reason why there is a large variation in the values between them as depicted in Fig. 3.17.

During the pilot plant operation, regular calculation were completed to determine the F/M ratio for the plant based upon the measured MLSS concentration and the inlet COD load (see Figs. 3.18 and 3.19). This F/M ratio is one of ways of controlling the bioreactor biology, the other being the determination of the SRT which is sometimes known as the sludge age. Both methods of process control work in a similar way and are virtually interchangeable. The F/M ratio is the ratio of COD loading (i.e. food) to the specific concentration of biomass (i.e. microorganisms), so strongly determines the microbial growth rate. For instance an underloaded system with low respective F/M ratio, would create starvation conditions in the biomass and prohibit further growth, and thus eventually affect substrate removal and overall treatment efficiency. In the pilot plant's case, an optimal F/M ratio range to be met was 0.05 to 0.15 which would give the best performance for this system. If the F/M ratio was lower than this range, then the amount of sludge to be manually wasted from the system could be determined and then removed. If the F/M ratio was higher than this range, then the incoming flow rate could be reduced, so that more influent was held up in the header balance tank, allowing sufficient time for the microbial biomass to grow. Alternatively, for very high F/M ratios being experienced, the bioreactor tank could be reseeded with fresh sludge from the sludge wastage/dewatering tank.

Issues with the sampling data During the sampling programme, the following data inconsistencies were found:

Inlet values

1. Higher than expected Nitrate concentrations in the influent which maybe just a factor of this specific industrial wastewater stream. It could be due to soil fertiliser washing off from the salad washing procedure.
2. Proportional speaking, low Phosphorous concentrations when compared to Ammonia and organic Nitrogen concentrations. Such low Phosphorous values would cause nutrient deficiency issues in the biomass.
3. Although the conductivity is not used in the modelling procedure, these figures seemed a factor or so higher than they should be, which was later found to be due to the calculation procedure employed.

Bioreactor values

1. There were substantial differences between the MLVSS and MLSS values (Janus and Paul 2009). Some results did not make sense as usually the ratio of MLVSS to MLSS should usually be in the range of 0.6 to 0.9, but in this case it was sometimes above 1.0 which patently is incorrect. Those MLVSS values that gave a ratio greater than 1.0 had therefore to be ignored as there was obviously something wrong with that measurement procedure (i.e. the laws of conservation of matter are not being obeyed). This meant there were less decent MLVSS values to use in any modelling procedure.
2. If the bioreactor's combined polysaccharide and protein values are thought to be representative, then the capture ratio of **SMP** by the membranes appears to be quite high at over 90% (Janus and Paul 2009). It would usually be expected to be in the 60 to 80% range, although these membrane's pore size is in the smaller UF range so they would have better selectivity.
3. The ammoniacal Nitrogen and organic Nitrogen concentrations in the bioreactor were higher than in the influent stream when they should have reduced due to effective treatment. This is clearly due to degradation of samples during the storage and preservation step. Hence these results were ignored.
4. When mass balancing, the Phosphorus concentrations in the bioreactor was found to be low but generally higher than in the influent. This was clearly incorrect so again these values were ignored.
5. The ratio of XCOD to MLVSS should be near 1.42 or thereabouts, but this ratio is too high at the beginning of the sampling period (Janus and Paul 2009). It settles down later on so those values were taken as correct.
6. A considerable variation in viscosity also occurs for the sampling period (Janus and Paul 2009). This was later found to be due to the test procedure itself which could easily be upset by unexpected floc clumps occurring.

Outlet values

1. The Nitrogen fractions did not balance properly. This is due to the incorrect bioreactor results due to improper storage and testing of samples by the De Montfort University laboratory staff.
2. There were lower than expected ammoniacal Nitrogen, organic Nitrogen and Phosphorous removal efficiencies. Again, this is due to the incorrect bioreactor results due to improper storage and testing of samples by the De Montfort University laboratory staff.
3. The outlet Nitrate concentrations were low which would usually indicate denitrification occurred in the bioreactor. Again, this is due to the incorrect bioreactor results, caused by degradation of samples during the storage phase, meaning that any Nitrates are used up.

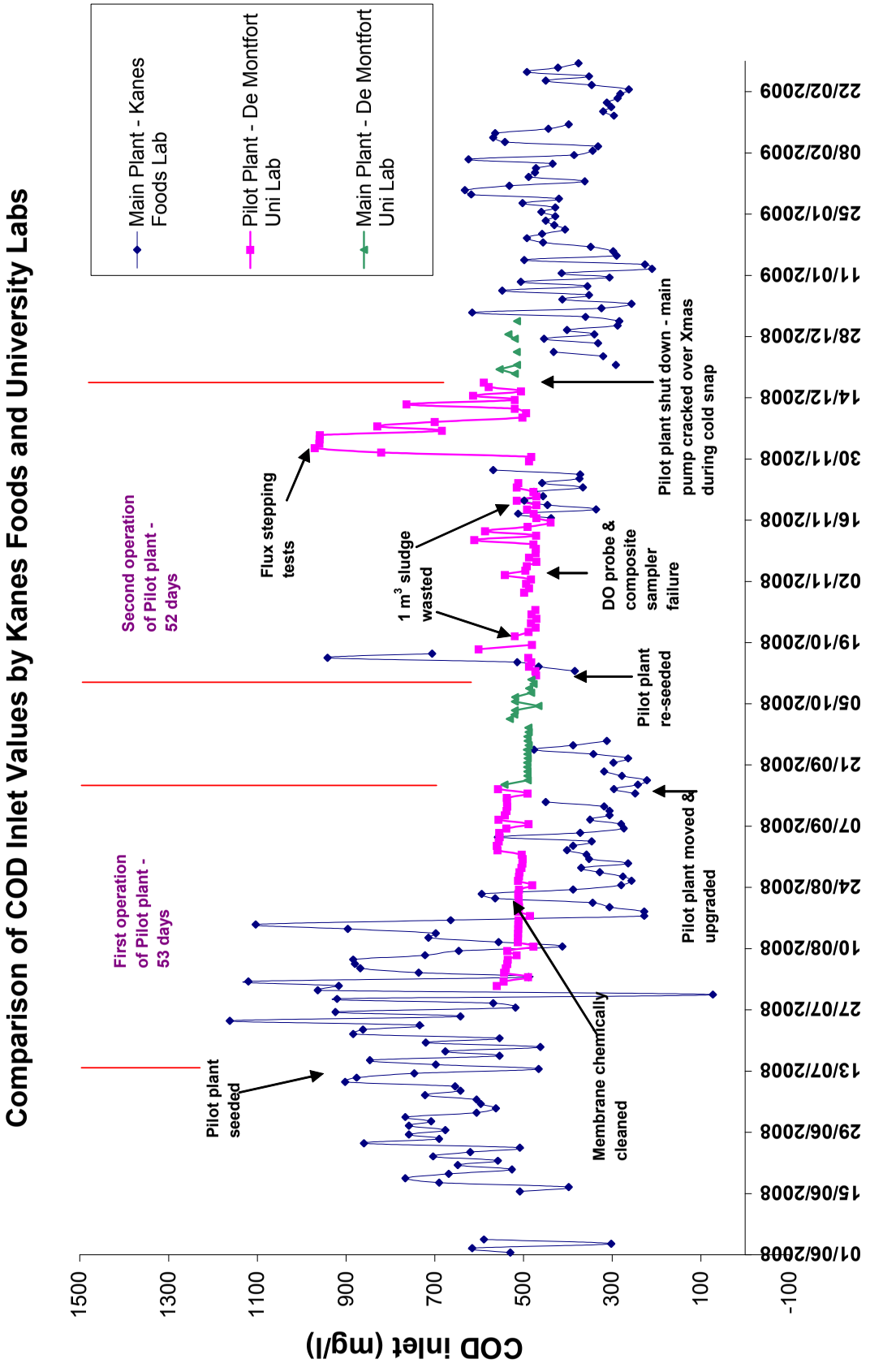

Fig. 3.17: Aquabio pilot plant at Kanes Foods - Comparison of sampling results for COD at inlet

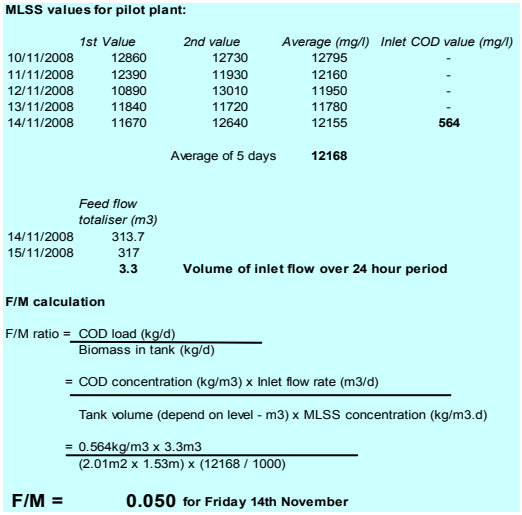

MLSS values for pilot plant:

	1st Value	2nd value	Average (mg/l)	Inlet COD value (mg/l)
10/11/2008	12860	12730	12795	-
11/11/2008	12390	11930	12160	-
12/11/2008	10890	13010	11950	-
13/11/2008	11840	11720	11780	-
14/11/2008	11670	12640	12155	**564**

Average of 5 days **12168**

	Feed flow totaliser (m3)
14/11/2008	313.7
15/11/2008	317
	3.3

Volume of inlet flow over 24 hour period

F/M calculation

F/M ratio = COD load (kg/d) / Biomass in tank (kg/d)

= COD concentration (kg/m3) x Inlet flow rate (m3/d) / Tank volume (depend on level - m3) x MLSS concentration (kg/m3.d)

= 0.564kg/m3 x 3.3m3 / (2.01m2 x 1.53m) x (12168 / 1000)

F/M = 0.050 for Friday 14th November

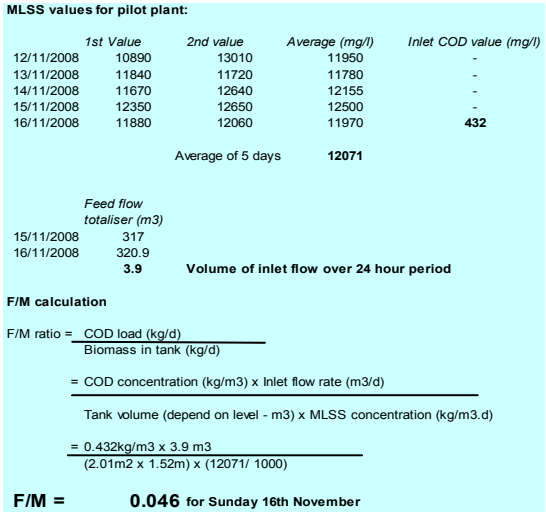

MLSS values for pilot plant:

	1st Value	2nd value	Average (mg/l)	Inlet COD value (mg/l)
12/11/2008	10890	13010	11950	-
13/11/2008	11840	11720	11780	-
14/11/2008	11670	12640	12155	-
15/11/2008	12350	12650	12500	-
16/11/2008	11880	12060	11970	**432**

Average of 5 days **12071**

	Feed flow totaliser (m3)
15/11/2008	317
16/11/2008	320.9
	3.9

Volume of inlet flow over 24 hour period

F/M calculation

F/M ratio = COD load (kg/d) / Biomass in tank (kg/d)

= COD concentration (kg/m3) x Inlet flow rate (m3/d) / Tank volume (depend on level - m3) x MLSS concentration (kg/m3.d)

= 0.432kg/m3 x 3.9 m3 / (2.01m2 x 1.52m) x (12071/ 1000)

F/M = 0.046 for Sunday 16th November

Fig. 3.18: Aquabio pilot plant at Kanes Foods - 1) F/M ratio calculations

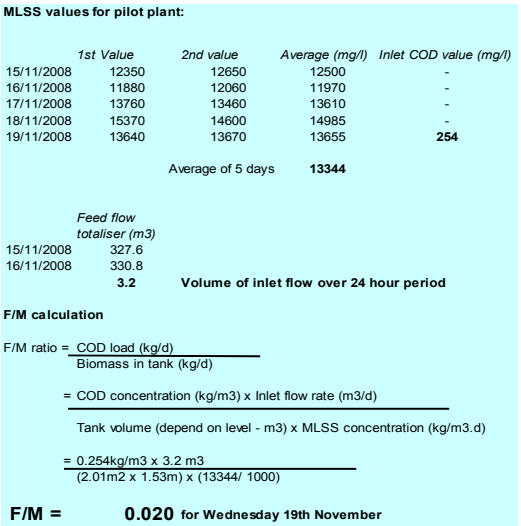

MLSS values for pilot plant:

	1st Value	2nd value	Average (mg/l)	Inlet COD value (mg/l)
15/11/2008	12350	12650	12500	-
16/11/2008	11880	12060	11970	-
17/11/2008	13760	13460	13610	-
18/11/2008	15370	14600	14985	-
19/11/2008	13640	13670	13655	**254**

Average of 5 days **13344**

	Feed flow totaliser (m3)
15/11/2008	327.6
16/11/2008	330.8
	3.2

Volume of inlet flow over 24 hour period

F/M calculation

F/M ratio = COD load (kg/d) / Biomass in tank (kg/d)

= COD concentration (kg/m3) x Inlet flow rate (m3/d) / Tank volume (depend on level - m3) x MLSS concentration (kg/m3.d)

= 0.254kg/m3 x 3.2 m3 / (2.01m2 x 1.53m) x (13344/ 1000)

F/M = 0.020 for Wednesday 19th November

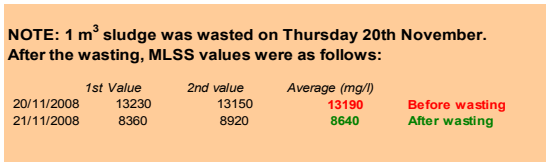

NOTE: 1 m^3 sludge was wasted on Thursday 20th November. After the wasting, MLSS values were as follows:

	1st Value	2nd value	Average (mg/l)	
20/11/2008	13230	13150	**13190**	**Before wasting**
21/11/2008	8360	8920	**8640**	**After wasting**

Fig. 3.19: Aquabio pilot plant at Kanes Foods - 2) F/M ratio calculation

The inconsistencies were higher in the bioreactor values and less apparent in the inflow and outlet values, so most of the bioreactor values were not used in the modelling procedure. This could be done because in modelling terms the filtered sample values from a complete mix bioreactor should equate to the outlet values for all fractions particularly for the Nitrogen and Phosphorous fractions. This means that when modelling, only the inflow and outlet COD and Nitrogen fractions are needed together with the MLSS values in the bioreactor. This greatly simplifies the situation.

3.4.2.6 Results - Membrane resistance tests

On pilot plant startup, the in-situ membrane resistance tests outlined in Section 3.4.2.4 were conducted. Incidentally, the specific test using the coarsely screened mixed liquor was dropped due to time constraints. The following protocol was designed to measure the various types of fouling resistance on the membrane which cause a gradual drop in flux (or increase in TMP). These membrane resistance tests were constructed to be carried out on a virginal membrane module before it has been conditioned by running with mixed liquor. These various resistances can be calculated from the simple Darcy's Law. Equation 3.7 shows the Darcy's Law and its relation to the general resistance-in-series model of membrane resistance.

$$J = \frac{\Delta p}{\mu \cdot (R_m + R_r + R_i)} \tag{3.7}$$

where: $R_t = R_m + R_r + R_i$

where: J is permeate flux, Δp is TMP, μ is permeate viscosity, and R_t is total membrane resistance made up of clean (R_m), reversible (R_r) and irreversible (R_i) components.

Therefore the membrane resistance can be simply determined by measuring the change in TMP for an applied flux; or by measuring the eventual drop in flux for a specific TMP difference. Either way, as long as we have sufficient information gathered from a data logger for a sufficient period, and as long as the operational conditions of the pilot plant are known, (e.g. high crossflow operation, etc), then the resistance can be calculated.

For Aquabio's normal mode of high crossflow velocity operation, then this total membrane resistance is split into three components as follows:

1. R_m - The membrane's intrinsic resistance, known as clean water resistance. This is measured simply by running the pilot plant on distilled (reverse osmosis (RO)) water.
2. R_r - The reversible fouling resistance. For simplicity's sake it will be considered that R_r is largely made up of cake resistance, R_{cake}, due to suspended solids in the mixed liquor sticking to the membrane surface. This would be usually washed off by the high crossflow velocity operational conditions. [Note: The definition of reversible resistance, as opposed to irreversible resistance, is any resistance that can be recovered by standard operation by either high crossflows, air-sparging, relaxation, etc, without the need to resort to a full chemical clean.]
3. R_i - The irreversible fouling resistance by definition can only be removed by chemical cleaning. It is made up of: short term fouling resistance, R_{absorp}, due to the absorption of ions, scalants and other soluble matter into the membrane structure; plus longer term pore constriction resistance, R_{pore}, which is due to protein/polysaccharide macromolecules in the mixed liquor supernatant (known as **SMP** or EPS) blocking the membrane pores and/or forming a biofilm. For simplicity's sake it shall be assumed that R_{absorp} can never be removed, even with a chemical clean, (i.e. it is permanent loss in membrane permeability when the virgin membrane is dipped into mixed liquor even without an applied TMP), and that R_{pore} can be completely recovered with a chemical clean.

For most of these resistance components, they could only be measured once using the virgin membrane. Therefore it was recommended that all tests on the new pilot plant be carried out using Aquabio's standard high crossflow operational regime, which they are very familiar with, and not by using the new vertical air-lift system or any other new operational regime. This was so that unknown factors such as coarse bubble air-sparging, backflushing, relaxation, etc, are not introduced into the membrane resistance testing protocol, which would complicate the eventual results. Hence the following suggested protocol allowed the determination of the basic membrane fouling resistances, namely R_m, R_{cake}, R_{absorp} and R_{pore}:

a) Determine R_m using RO water from Kanes Foods full scale main WWTP. Run under usual Aquabio's high crossflow operational regime for, say, 1 hour (e.g. 4 m/s). Log the flux and TMP data. The permeate viscosity would be 1 cP for a standard temperature 20 $°C$. In actuality this test was not done.

b) Determine $R_{porePERM}$ due to permeate **SMP** only. This is the same test as above except instead of using RO water, the permeate water from the full scale main WWTP is used (before it goes into the RO unit). This test should give an indication of the drop in flux due purely to soluble permeate **SMP**. After the test a chemical clean should be carried out using sodium hypochlorite solution, and another RO water test performed, to measure the extent of the membrane permeability recovery (if any).

c) Determine R_{absorp} due to the first contact off the virgin membrane with mixed liquor but without any applied flux/TMP across the membranes. Ideally this test would involve simply dipping the membranes in mixed liquor from the full scale plant for, say, a six hour period and then removing them. However as this cannot be done due to the plant configuration, then it is suggested that the mixed liquor is passed over the membranes at a very low crossflow velocity so that little (ideally none) flux is produced. The danger here is that the tubes could block up so that the test time would probably need to be short of one hour. Alternatively, the tubes could be filled with mixed liquor and the crossflow switched off for some time. This test should confirm what short term irreversible fouling is occurring (if any). After this test a chemical clean should be carried out, and another RO water test performed, to measure the extent of the membrane permeability recovery.

d) Determine R_{pore} due to mixed liquor supernatant **SMP** only by filtering out the particles from the liquor from the full scale plant bioreactor. A 0.5 mm diameter filter cartridge could be used on the influent line to remove all large particles that cause cake build up from entering the pilot plant bioreactor. This would mean only soluble liquid would hit the membranes and thus allow the measurement of the true R_{pore} value. After the test a chemical clean should be carried out, and another RO water test performed, to measure the extent of the membrane permeability recovery.

e) Determine R_{pore} plus R_{cake} due to normal mixed liquor from the full scale plant. This would meaning filling up the pilot plant bioreactor with the usual mixed liquor and carrying out the usual test. Using the results from the other tests, the resistance due only to R_{cake} can be determined.

f) After each specific test, the membranes would be chemically cleaned and retested using RO water. This would mean flushing out the pilot plant bioreactor each time. It was expected that all these tests would take between 1 to 2 working days to complete.

From the outcome of these tests it is useful to see the size and extent of R_{absorp}, what the intrinsic R_m value is, and how much of the recoverable membrane permeability is dependant on the mixed liquor particles only (i.e R_{cake}) and on the mixed liquor itself (i.e. R_{pore}). It would also allow comparison of these results with those found by other researchers.

Figs. 3.20 to 3.25 are operational plots of each test conducted. They are plots of the permeability ($l/m^2/hr$ *per bar*), temperature ($°C$) and CFV (m/s). From these plots, the various membrane resistance components can be computed as detailed in Table 3.1 and in Equation 3.8. These values are of the right order for a membrane of this type. It is worth noting that when first running with mixed liquor, there is a permanent loss of permeability amounting to 25% which can never be recovered. This dramatic permanent loss is as expected for any virgin membrane that has never been exposed to a wastewater stream since it is due to permanent adsorption of macromolecules into the actual membrane structure. After this initial permanent loss, all other fouling due to adsorption of macromolecules is usually recoverable by cleaning.

$$R_{TOTAL} = R_m + R_{absorp} + R_{MLSS} = 1.4 \text{ x } 10^{12} m^{-1} \tag{3.8}$$

where: $R_m = 7.4 \text{ x } 10^{11}$ $R_{absorp} = 2.5 \text{ x } 10^{11}$

Resistance due to mixed liquor normal operation is $R_{MLSS} = R_{pore} + R_{cake} = 3 \text{ x } 10^{11}$

Resistance test carried out	Calculated membrane resistance (m^{-1})
RO TEST No.1	7.8228 x 10^{11}
RO TEST No.2 before cleaning and flushing,R_m	7.35877 x 10^{11}
RO TEST No.2 after cleaning and flushing	6.30666 x 10^{11}
UF TEST	6.20971 x 10^{11}
RO RETEST	6.55176 x 10^{11}
Change in resistance, $R_{porePERM}$	3.42 x 10^{10}
RO before BIOMASS Contact Test	7.39369 x 10^{11}
RO after BIOMASS Contact Test	9.9 x 10^{11}
Increase in resistance, R_{absorp}	2.51 x 10^{11}
NORMAL BIOMASS RUN Test of 2 hours	1.40077 x 10^{12}
RO after NORMAL BIOMASS RUN Test followed by clean and flush	1.09623 x 10^{12}
Decrease in resistance due to cleaning, R_{MLSS}	3.05 x 10^{11}

Table 3.1: Membrane resistance tests - Calculated resistances after each test

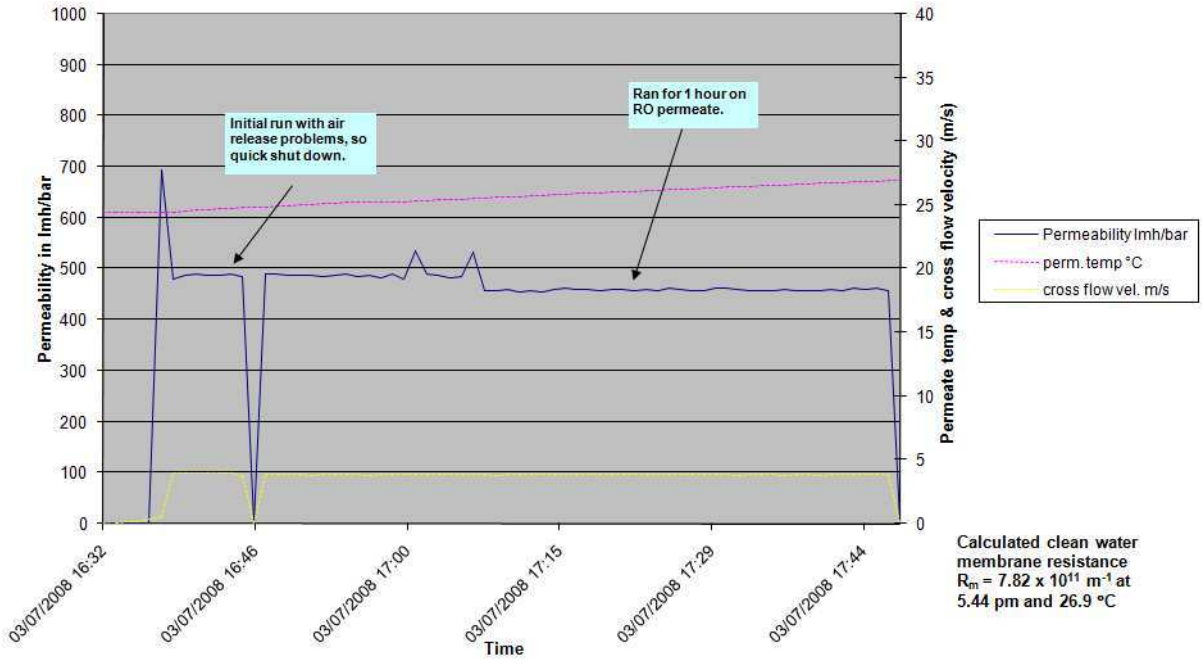

Fig. 3.20: Aquabio pilot plant at Kanes Foods - RO permeate Test No.1

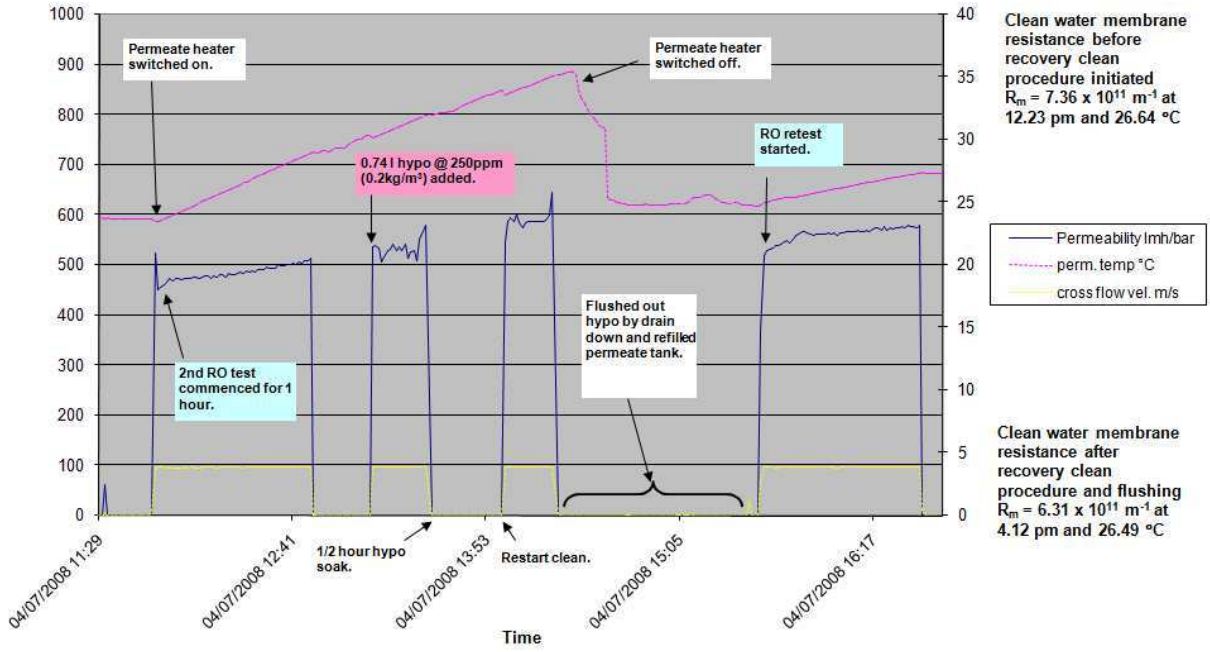

Fig. 3.21: Aquabio pilot plant at Kanes Foods - RO permeate Test No.2

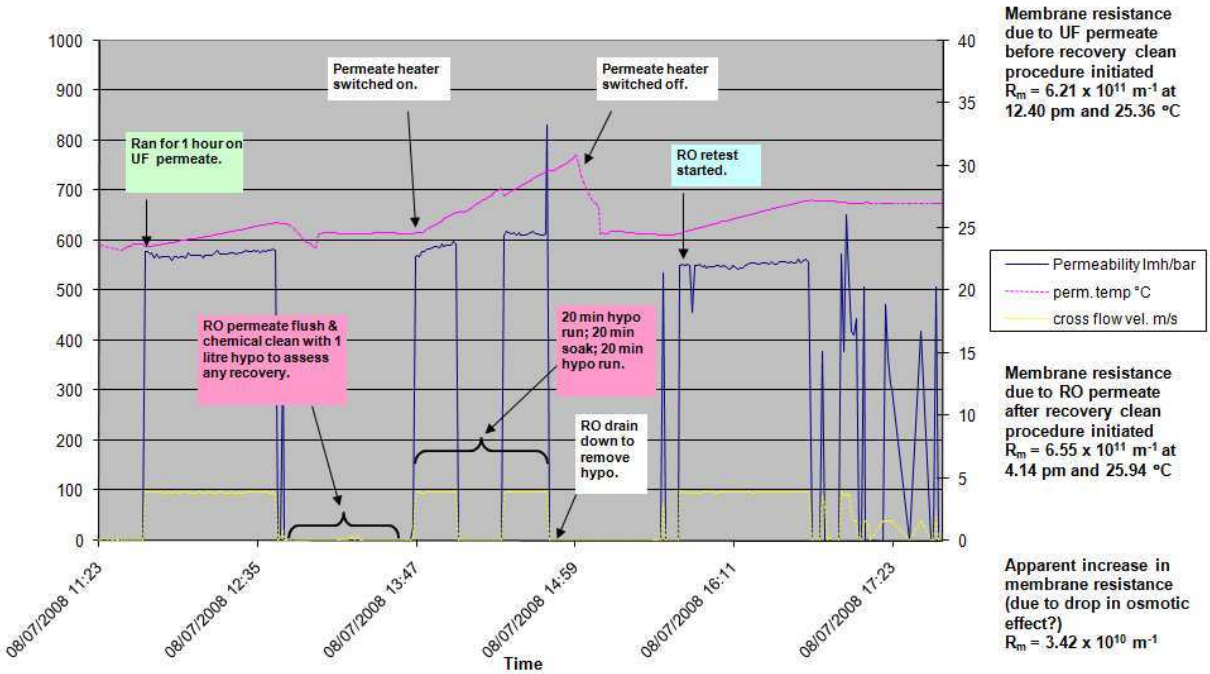

Fig. 3.22: Aquabio pilot plant at Kanes Foods - UF permeate Test

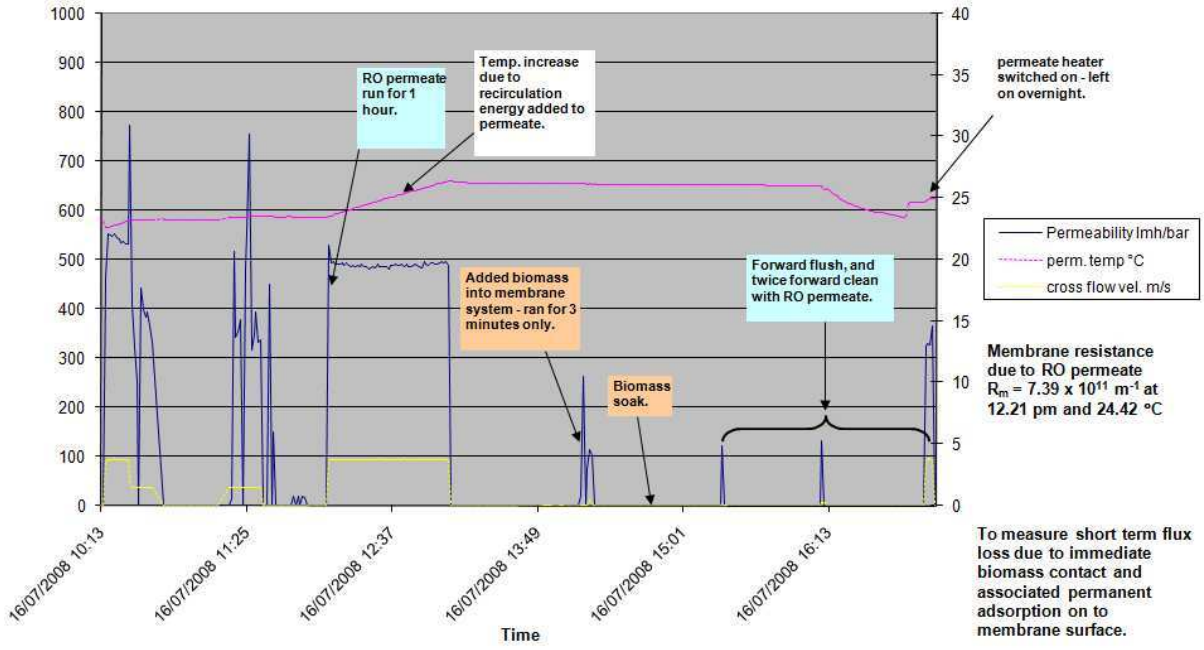

Fig. 3.23: Aquabio pilot plant at Kanes Foods - Biomass soak Test

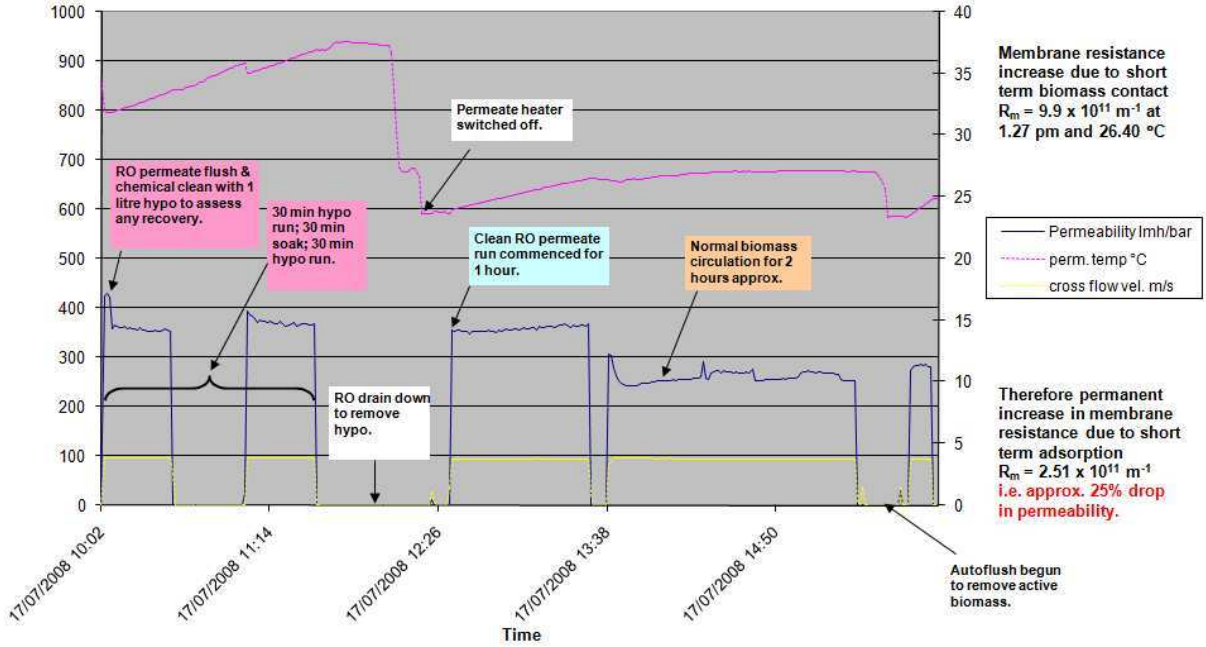

Fig. 3.24: Aquabio pilot plant at Kanes Foods - Biomass pressurised run Test

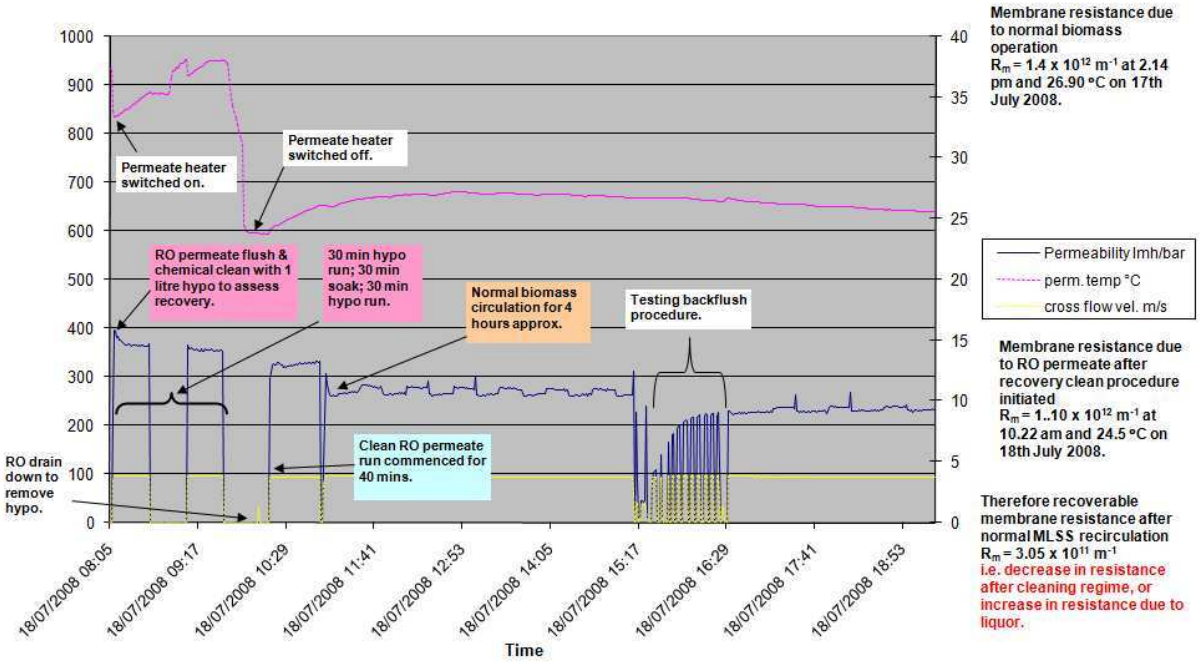

Fig. 3.25: Aquabio pilot plant at Kanes Foods - RO clean followed by normal biomass run

Plots of plant operation for different operational regimes and modes Figs. 3.26 to 3.28 indicate the permeability changes under the two operational regimes, namely standard high crossflow operation with no backflush, and low energy low crossflow mode with regular automated backflushes. In fact the permeability decreases significantly when in the second mode, although intuitively this would at first appear to not make much sense. However, the permeability is a measure of the flux produced per bar of TMP, so at very low fluxes due to low crossflows, the permeability is proportionally smaller even though the applied TMP is less as well.

Since the pilot plant was not operated long enough in standard high crossflow mode to obtain any useful data, Fig. 3.29 shows instead the main Kanes Foods WWTP operating in this mode, while Fig. 3.30 shows this pilot plant operating in the low energy low crossflow mode. When comparing the two modes of operation, an attempt is made in the plots to ascertain any correlation of the MLSS and viscosity to the temperature. This data, before use, was normalised to remove any affects due to temperature variations. There does not appear to be any strong correlation either way for either plant or mode.

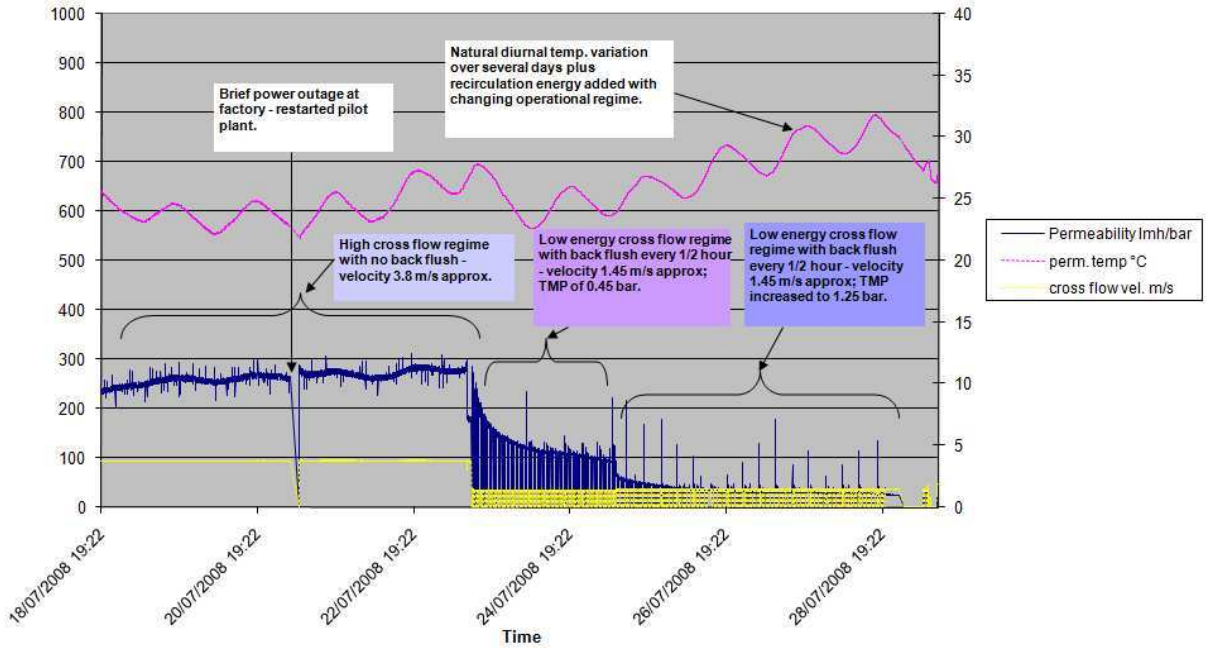

Fig. 3.26: Aquabio pilot plant at Kanes Foods - 10 days operation under different regimes

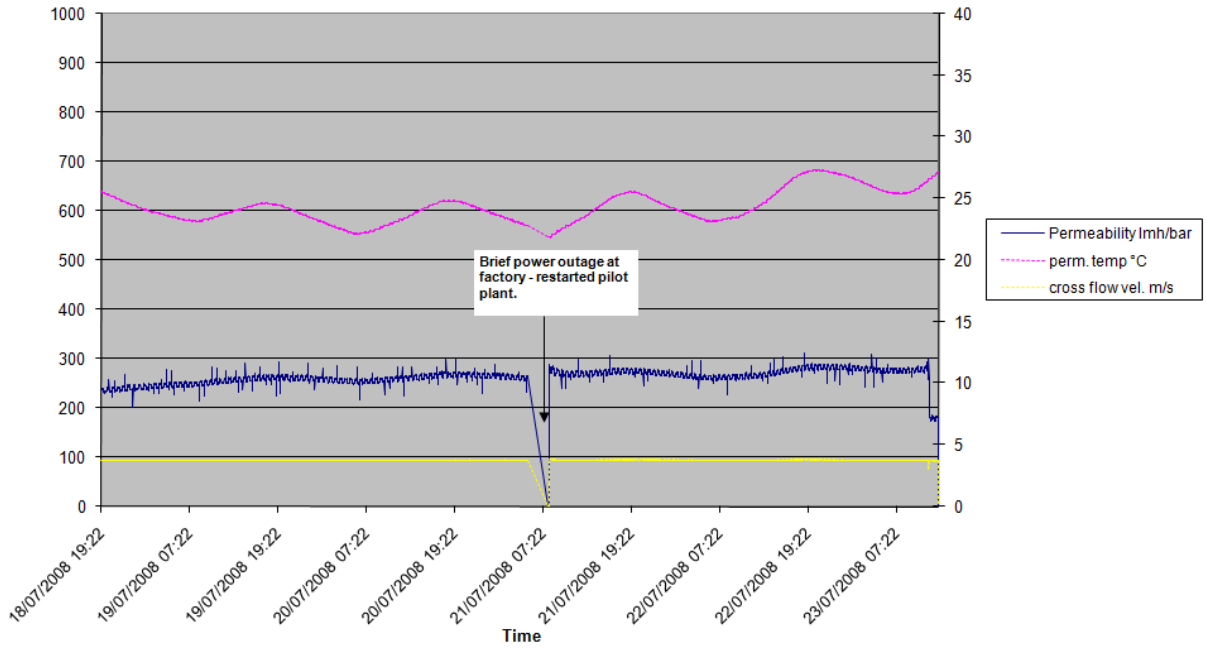

Fig. 3.27: Aquabio pilot plant at Kanes Foods - High crossflow regime only

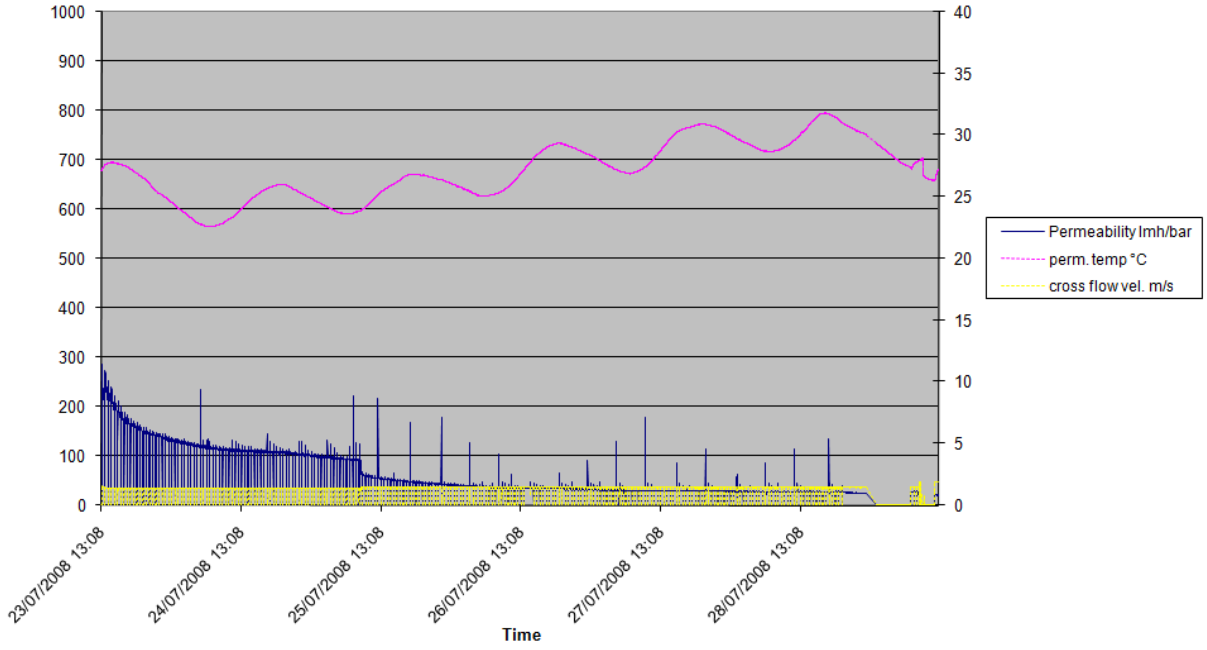

Fig. 3.28: Aquabio pilot plant at Kanes Foods - Low energy with backflush only

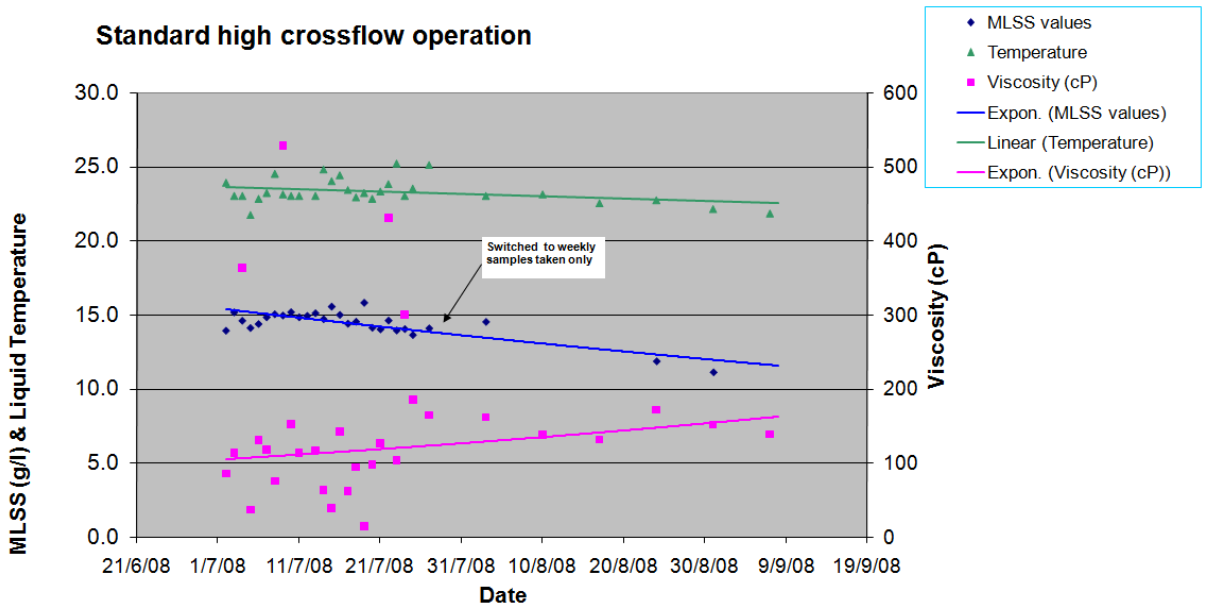

Fig. 3.29: Aquabio main plant at Kanes Foods - high crossflow operation: MLSS, temp. and viscosity

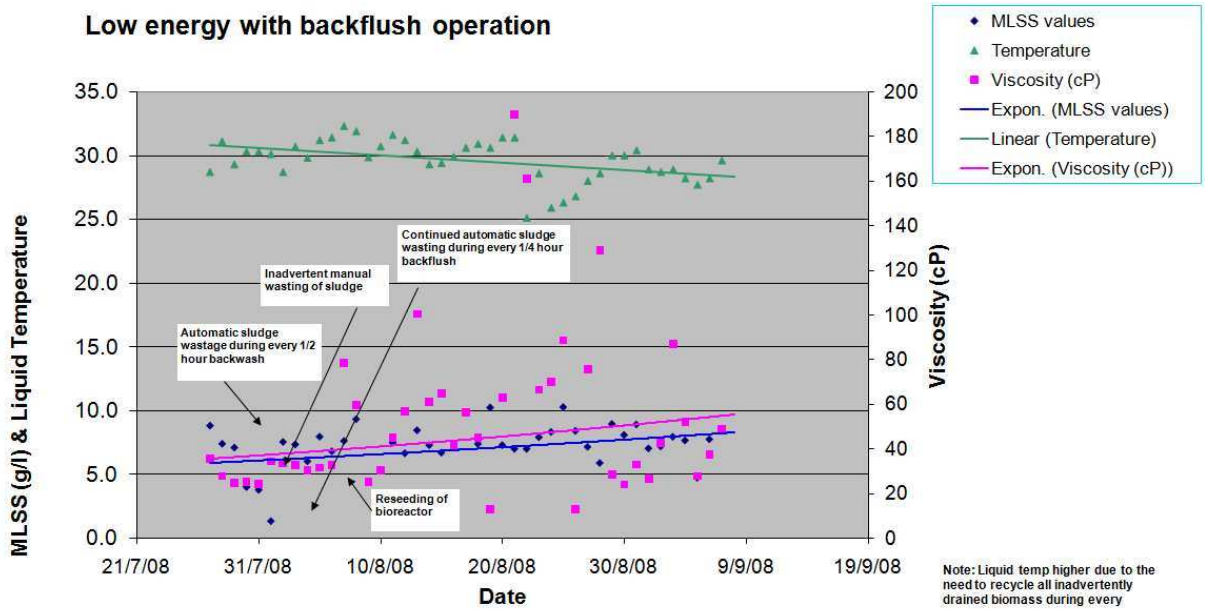

Fig. 3.30: Aquabio pilot plant at Kanes Foods - low energy with BF operation: MLSS, temp. and viscosity

3.4.2.7 Results - Flux stepping experiments

This new pilot plant with sidestream membrane arrangement operates at constant TMP but with reducing flux. In the standard Aquabio high crossflow mode, the permeate flow depends solely on the CFV developed across the membrane which itself is dependant on the recirculation pump speed setting and the throttle valve setting on the recirculation pipework. By holding the pump speed at a particular optimal setting, the developed flux can then be then changed by gradual throttling of the valve until cake build up/pore blockage is minimised.

Flux stepping experiments with a constant CFV during each flux step were carried out over a two day period. The flux stepping was conducted by hold the recirculation pump speed constant whilst manually changing the throttle valve settings on the membrane outlet. The valve has six intermediate settings for use from 2 to 6. Setting 1 is not useful with the valve being fully open, so was not employed. Settings 7 and 8 are not useful being either almost closed or fully closed, so again were not employed. A backwash regime was instigated between each flux step either up or down to allow the membrane to recover its permeability.

On 3rd December 2008, the tests commenced with a gradual stepping up at 100% pump speed for 1 hour flux step durations. At the end of each flux step, two 120 second backflushes followed before the next step was initiated (see Fig. 3.31). On 5th December 2008, the same procedure as before was employed but this time in reverse order with a stepping down at 100% pump speed for 1 hour flux step duration followed by two 120 second backflush intervals before the next step (see Fig. 3.32). After this test, new tests were conducted by this time stepping up at 75% pump speed for 30 minute flux step durations followed by a single 240 second backflush interval before the next step. Finally, with these new pump settings, a stepping down was carried out at 75% pump speed for 30 minutes flux step durations followed by a single 240 second backflush interval before next step. It was hoped that this would provide sufficient data to allow the fouling model developed later in this study to be tested.

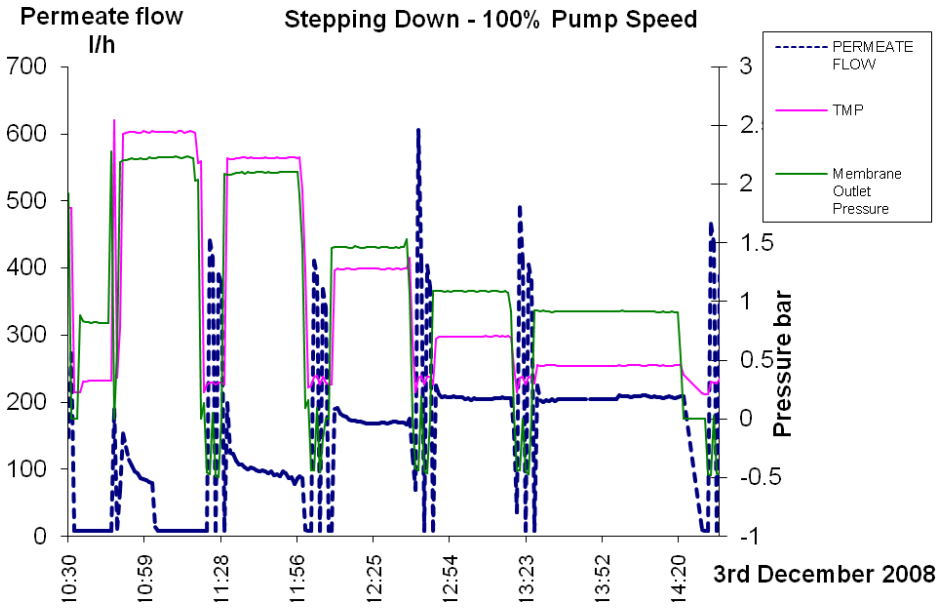

Fig. 3.31: Flux stepping tests on 3rd December 2008 - Full pump speed

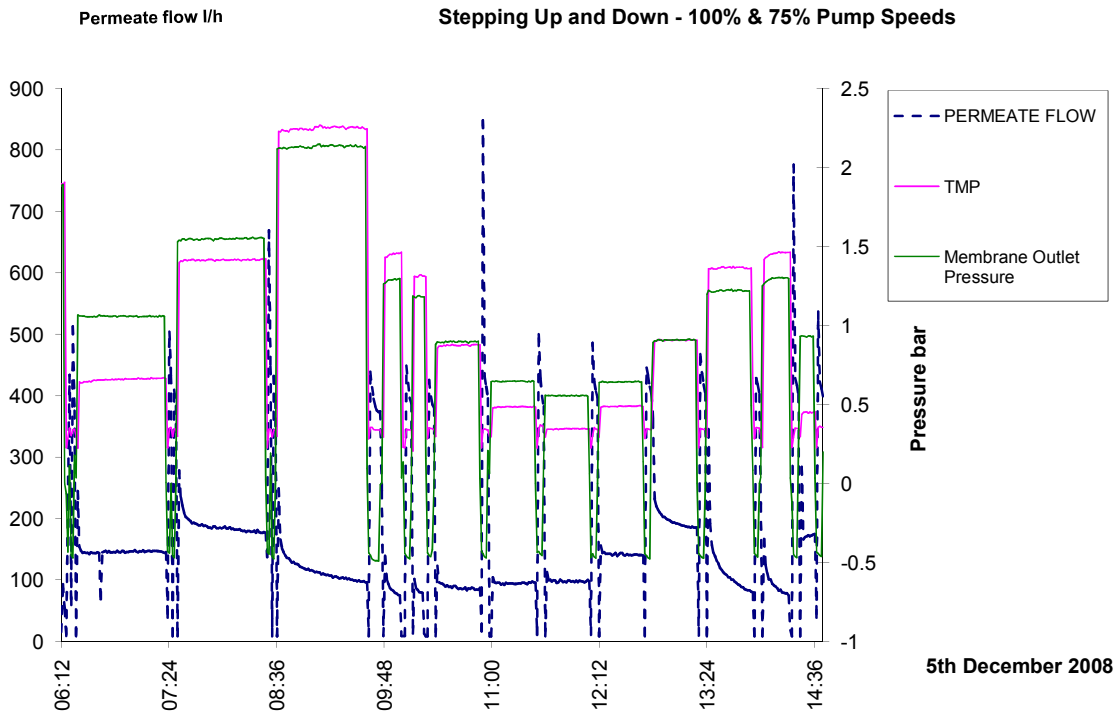

Fig. 3.32: Flux stepping tests on 5th December 2008 - Full and 3/4th pump speed

3.4.2.8 Results - Microbiological analysis and HPLC measurements

SEC protein measurement involving HPLC with DOC detection The membrane fouling and Activated Sludge models used in later chapters incorporate **SMP** concentration of the sludge water in the model formulations as these are thought to be the main agents responsible in fouling process. They are measured using standard biochemical assays to measure polyprotein and polysaccharide levels, such as the Lowry and Dubois (Phenol/Sulphuric acid) methods. The combined polyprotein and polysaccharide levels give the sludge supernatant's **SMP** concentration.

As an alternative method to determine specifically protein levels, size exclusion chromatography (SEC) was used to compare against the levels found using the standard biochemical assays such as the Lowry method. This SEC with DOC detection involves a high pressure liquid chromatography (HPLC) procedure. The output from the SEC procedure is in the form of a spectral plot of the molecular weights of materials detected against their detection signal strength. This plot is known as a chromatogram, with the area under curve (AUC) for the plot being directly related to the concentration of material detected. Fig. 3.33 shows a typical sludge supernatant and permeate chromatogram from a real life MBR based on work carried out by Rosenberger et al. (2006). As can be seen in this plot, the distinctive first peak at low molecular weights of combined polysaccharide and proteins is the one that is responsible for fouling on and within the membrane structure. In fact this first peak size and the AUC are directly correlated to the fouling propensity of the sludge liquor. The second peak of humic substances and low molecular weight acids can be ignored as it does not impact on the fouling process.

Since SEC is a expensive and lengthy procedure requiring considerable expertise and specialist equipment, only an occasional measurement was taken in both the Aquabio pilot and main plant being operated at Kanes Foods site. The main plant protein value was measured for comparative purposes because its sludge was fully acclimatised and so should give fully representative spectral peaks.

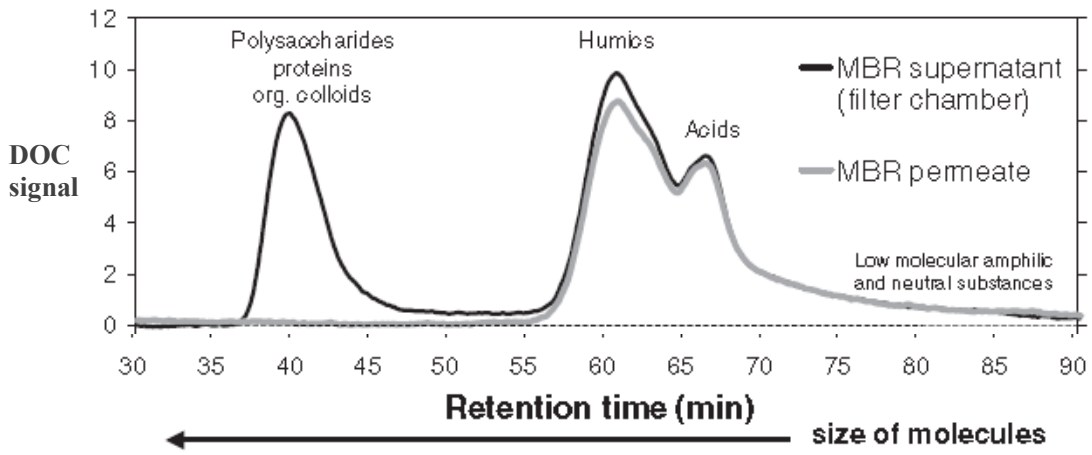

Fig. 3.33: Example of sludge supernatant and permeate chromatograms (Rosenberger, et. al., 2006)

When using the SEC with HPLC method to analyse single proteins, as is the case with these sludge liquid measurements, then a BSA curve is needed for calibration purposes so that accurate protein levels are given. Fig. 3.34 shows the results from running a pure sample of BSA at 5 mg/ml concentration especially purchased from a wholesale chemical supplier to allow initial calibration of the chromatograph machine.

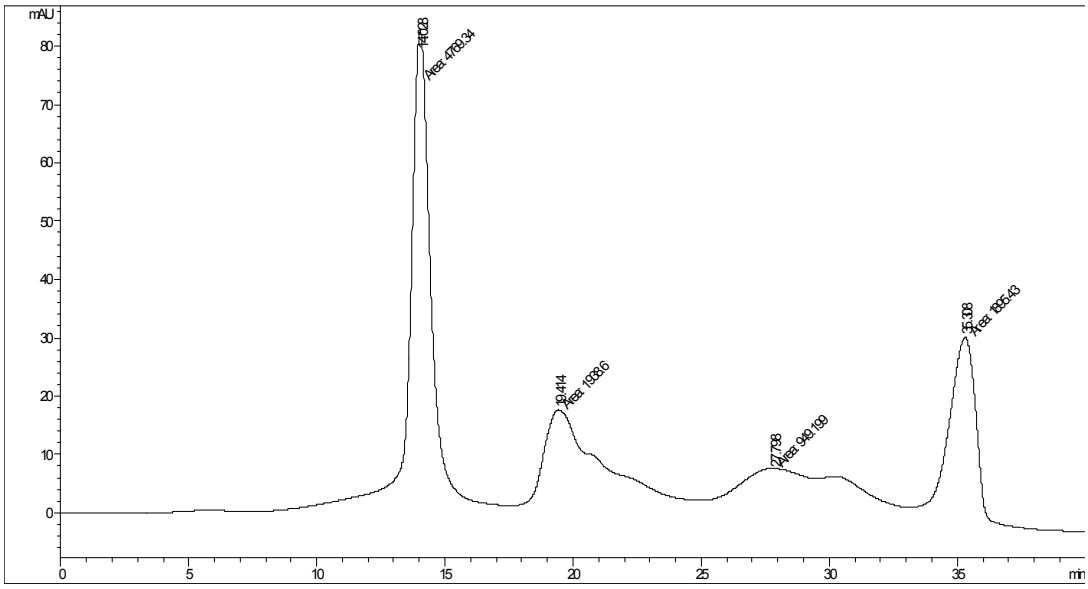

Fig. 3.34: HPLC calibration curve results for 5 mg/ml of pure BSA solution

When comparing the SEC results from the Aquabio pilot and main plant in Fig. 3.35, it is apparent that the pilot plant results in October for the bioreactor has a double peak, while both outlet results for the same day look very similar. The reasons why the October pilot plant spectral plot in the bioreactor sample looks initially different from the main plant one is that the pilot had only been up and running for a very short period of time so that the sludge had not acclimatised sufficiently. This "stressed" sludge was therefore producing proportionally greater **SMP** levels, so that membrane removal levels were low as well as shown in Table 3.2. However a month later when the November pilot plant spectral plot in the bioreactor sample are compared with the main plant one, the shapes of the AUCs prove similar. This means that the sludge microbiology has now settled down and stabilised somewhat, so that the **SMP** retention efficiency of the membrane has considerably improved as shown in Table 3.2. In fact when the spectral protein plots for the stabilised sludge in Fig. 3.36 are compared with the typical composite **SMP** sludge plot in the work by Rosenberger et al. (2006), they seem very similar, thus proving the accuracy of this method.

Incidentally, the membrane retention rate is simply calculated by taking the difference in the bioreactor AUC and outlet AUC for protein which then gives the retention of **SMP** protein material as detailed in Table 3.2.

Plant and SEC test date	Bioreactor - Total AUC	Outlet - Total AUC	% Protein passing thro' membrane
Main - on 11th Oct'08	402,928	265,024	66%
Pilot - on 11th Oct'08	367,734	252,832	69%
Pilot - on 10th Nov'08	317,625	124,205	39%

Table 3.2: Aquabio SEC test results - Areas Under Curve values for bioreactor and outlet

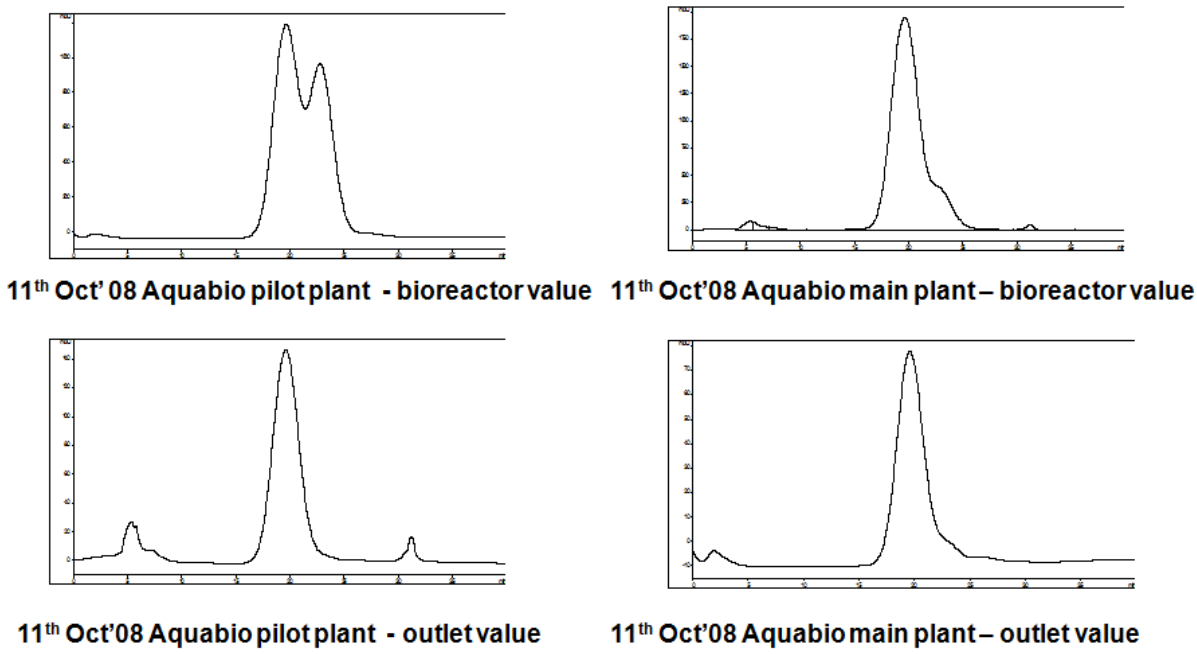

Fig. 3.35: Both Aquabio plant at Kanes Foods - 1) Comparison of HPLC results for protein at bioreactor and outlet

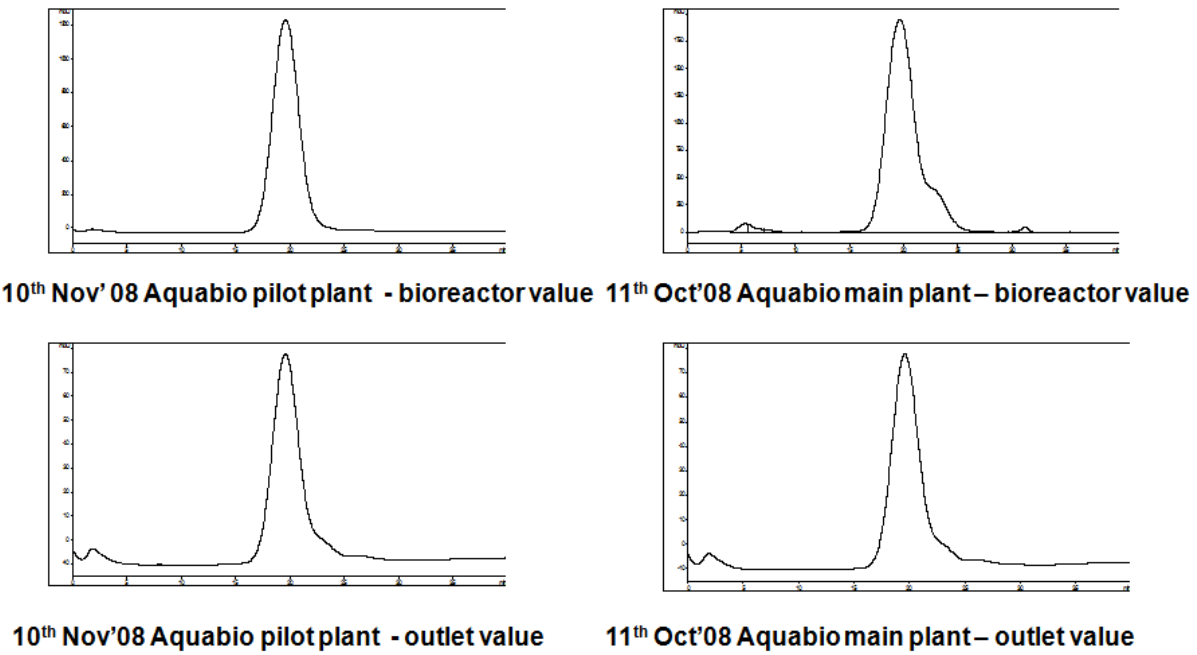

Fig. 3.36: Both Aquabio plant at Kanes Foods - 2) Comparison of HPLC results for protein at bioreactor and outlet

Microbiological analysis A regular microbiological analysis of the sludges from both Aquabio's pilot and main plant were performed so that the microbiological morphology, floc size and species diversity could be evaluated. Fig. 3.37 shows the magnified differences in the mixed liquor and sludge for December 2008 which proves significant. The main difference in the sludges is that the pilot one is less healthy with pin flocs predominating and less species diversity due to poor ecological conditioning of the mix. As expected the main plant's liquor is more consistent since it experiences less shear stresses due to the much greater recirculation pipe lengths which attenuate the turbulent shearing affects from the CFV.

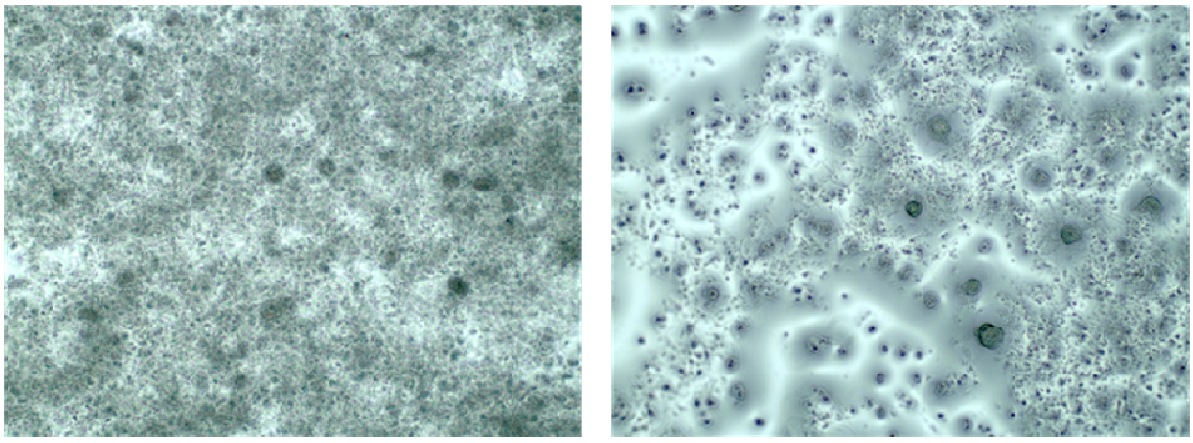

Slide of Main Plant – December 2008

Slide of Pilot Plant – December 2008

Fig. 3.37: Both Aquabio plant at Kanes Foods - Microbiological analysis of bioreactor mixed liquor

3.4.3 Aquabio main crossflow MBR plant operated at Kanes Foods, Evesham, Worcestershire

3.4.3.1 Plant layout and operational details

Fig. 3.38: Aquabio main plant at Kanes Foods - Pictures of the four membrane modules

Fig. 3.39: Aquabio main plant at Kanes Foods - Pictures of Author next to permeate tanks

Fig. 3.40: Aquabio main plant at Kanes Foods - Picture of external bioreactor tank

Fig. 3.41: Aquabio main plant at Kanes Foods - Picture of jet aeration and pump recirculation system

Plant description Figs. 3.38 to 3.41 are some pictures taken of the main permanent plant at Kanes Foods site. These include pictures of the membrane modules and permeate tanks inside their covered building, and the external bioreactor seen from high level and the jet aeration and pump recirculation system. Incidentally, Aquabio's proprietary jet aeration system is known as JETOX©. This permanent WWTP designed and installed by Aquabio is part of Kane Foods large industrial complex located in Middle Littleton near Evesham, Worcestershire. This industrial complex produces pre-packed salads and coleslaw, with most of the wastewater being generated largely from washing of vegetables and from the daily cleaning of equipment and machinery. Products are made on an order-by-order and seasonal basis so daily and monthly wastewater characteristics including plant load and flow are apt to large variations and unpredictability. This is offset by having a very large header tank before the WWTP which can contain up to two days incoming flow.

Unusually this WWTP was designed primarily as a water recovery facility. Since the nearby mains sewers are very small and as the daily discharge from the Kanes Foods complex is large, it was estimated by the local council that it would cost over £ 2.5 million to upgrade the sewer network to cope with any future increased load. Hence Kanes Foods management decided that if they could carry out maximum water recovery, then their daily discharge would remain low, meaning existing sewer capacity would be adequate. They could also make significant savings on water usage costs, i.e. a reduction in annual water charges. Since the plant came on-line, it produces a high proportion of water recovery of up to 80% for reuse. Hence no discharge consent was needed from the environmental regulator apart from that any recovery water meets national water quality reuse guidelines. The plant was designed for COD removal only and not for any nutrient removal.

The design summer temperature is 20 $^{\circ}C$ while in winter it is 15 $^{\circ}C$. The sludge yield is 0.2, i.e. 200 kg/day dry weight of sludge. Consequently the average design load and the maximum design load are the same at 1000 m^3/day. This entire load is industrial in composition with no domestic component. The plant has been in operation for over 9 years. The plant configuration and forward process train consists of the following units:

1. Preliminary treatment - filter screens for solids removal.
2. A 1200 m^3 balance tank.
3. A pH adjustment/coagulation/polymerisation and flocculation units (if needed).
4. A dissolved air flotation (DAF) unit.
5. A buffer tank with nutrient addition (if needed).
6. Two 300 m^3 bioreactors using jet aeration systems connected to a sidestream bank of four 10 mm diameter tubular membrane units.
7. Sludge holding/dewatering tanks.

Plant operational data Since the Kanes Foods industrial complex produces food products on a on-demand basis, COD values can vary between extremes of 8,000 to 20,000 mg/l. A typical TSS level is 800 mg/l. Since the incoming influent tends to be fairly neutral, i.e. pH 7, buffering is not normally carried out so that biological activity in the bioreactor is not usually inhibited. Although MLSS levels in the bioreactor have reached 32,000 mg/l during extreme conditions, they are normally kept between 14 to 16,000 mg/l by varying the recirculation flows. Membrane permeate flow usually has a 98% solids removal level when compared to the retentate flow. Typically 2 bar back pressures are developed during the membrane operation. Nutrient addition has been carried out in the past on occasion when flux rates have dropped dramatically. This is order to keep the C:N:P ratios in line with design values. The plant is constantly manned 24 hours a day and on a seven days a week basis.

Current process control methods The plant is fully automated and operated using a programmable logic circuit (PLC) and supervisory control and data acquisition (SCADA) based system which is connected to the treatment plant monitoring and control equipment by a joint Ethernet/Profibus network system. The aeration is controlled and supplied to the bioreactor using a normal DO PI setpoint control method with the DO setpoint being usually 1.5 mg/l. Actual aeration is provided by a bank of three automated air compressors which come on and turn off as required. During the sidestream filtration operation, normally only three banks of membranes out of four are used at any time whilst the other is either being flushed and cleaned or on standby. Membrane switch over usually occurs every four weeks.

3.4.3.2 Results - Data collated under sampling programme

Fig. 3.42: Aquabio main plant at Kanes Foods - 1) Pictures of sampling programme carried out in 2006

The Author designed an individual sampling programme and measurement campaign specifically for this plant which went ahead in November/December 2006. Before the sampling commenced the following issues

Fig. 3.43: Aquabio main plant at Kanes Foods - 2) Pictures of sampling programme carried out in 2006

were clarified, resolved, noted or initiated:

- Collated a list of photometric test kits which Kanes Foods laboratory staff use in their spectrophotometer. They included kits for TN and TP measurement.
- Checked the pore diameter for glass fibre filter paper to be used to calculate the filtered COD. It is produced by Whatman Schleicher & Schuell. On checking it was found that GFC grade C 90mm has a pore size of 1.2 μm. The ideal filter paper pore size should be 0.45 μm, but the lowest grade that is produced by this manufacturer is of pore diameter 0.7 μm, and is called GFC grade F 90mm.
- Noted that the dynamic viscosity was measured using an Anton Paar© DV-2P machine. It appears to be a rotational viscometer with two concentric cylinders which rotate relative to each other around a concentric axis. Viscosity was measured for mayonnaise production as standard but during the sampling programme it was also measured for the mixed liquors in the bioreactor tanks.
- Controlled the MBR plant operation based on F/M loading rates. Calculated the F/M ratio for both bioreactors. This ratio is then used as a control check to ensure the plant is operating within its correct operational range/window. 0.05 to 0.2 is the typical range used by Aquabio for design and operation.
- Compared the laboratory's current measurement methods for all biochemical tests it conducts on the WWTP, and determined what additional data could be collected in an efficient and cost effective manner which would make any computer models developed easier to calibrate and verify. Consequently the Author went through the current list of variables that are measured, and introduced the new ones that were needed under any future sampling scheme. This data would then be used in the wastewater characterisation method, i.e. to fractionate the influent into the various state variables in the model.
- During this programme period, sampled twice per day (for the main variables like COD, TP and TSS). The Author explained to the lab staff the exact nature of the measurement campaign, including a "walk-through" procedure which highlighted the exact measuring protocol for this specific plant. This included the exact testing procedure to be employed for each variable, the exact sampling extraction points to be used, and the data logging procedure.

- Designed and devised the data acquisition spreadsheets for this measurement campaign be based on the existing Aquabio sheets.
- Sampling points were located as follows: after the DAF unit and filter screens but before the bioreactors. There was a point located just indoors of the membrane banks. This would make modelling easier as only the MBR portion of the treatment works would then need to be modelled, and not the pre-treatment and post-treatment stages, i.e. the balance tank, DAF unit, screening arrangements, RO unit, ultra violet (UV) step, and chlorine dosing and pre-mix steps.
- There was also a sludge measurement point just after the sludge pump. This would mean the concentration of the wastage flow could be determined as a confirmatory step when the SRT is calculated indirectly using a Phosphorus mass balance. It was also decided to measured on the return recycle points from the membrane banks.
- It was decided that November would be a good time to commence the sampling since fluxes usually drop due to cold weather operation, meaning that all four banks of membrane are typically in use.
- It was noted that the plant operation is not a simple parallel operation as shown in the original PID. It is a quasi-series step-feed operation with 70% of the initial load being fed in *Bioreactor A* and the remaining being fed into *Bioreactor B*. The load from *Bioreactor A* would then after passing through its membrane banks would then pass into *Bioreactor B*.

This intensive sampling programme that then ensued involved the following sub-tasks:

i) – Site visits to Kanes Foods plant and laboratory, to carry out a basic "walk through" of the intended sampling regime and negotiations with Kanes Foods Management regarding the enhancement of their current sampling regime, i.e. to include filtered COD, mixed liquor viscosity, TN, TP, etc.

ii) – Designed sampling regime, i.e. sampling points; data collection sheets; liaised with Kanes Foods personnel in laboratory and with plant operators.

iii) – Intensive three week programme carried out commencing in mid November 2006.

iv) – Requested standard data one month before event, during event, and one week after to ensure no major fluctuations in data set during sampling period.

v) – Sufficient data collated to allow initial model preparation to commence (i.e. unknown parameters / variables to be estimated using this data).

vi) – Measured: COD; COD filtered (0.45 μm GFC; TSS; VSS; TN; Ammonia; Nitrates; TP; Phosphates. Single biological/nutrient measurements in feed, bioreactor, permeate and waste stream.

Using the information gained from this sampling programme the following steps were carried out to be used later on during the model testing stage:

- An influent and sludge characterisation so that the state variables for an Activated Sludge model can be evaluated.
- A detailed evaluation of the plant flow scheme (e.g. design documents, existing process scheme and current operation modes) so that a hydraulic and hydrodynamic model can be formulated.
- A static data mass balancing (i.e. steady-state) of COD fractions, Nitrogen fractions and Phosphorous fractions, so that the Activated Sludge model is fully balanced and obeys the laws of physics.
- An adjustment of kinetic parameters, if necessary, used in the Activated Sludge model to take into account local biological effects. This is mainly done if the nitrification rate is greater or less than normal.
- Current historical biological data for this plant was collated and complete, i.e. it allowed an accurate influent characterisation and SRT determination. A 97% accuracy is needed in the SRT evaluation in order to get a realistic influent characterisation into its constituent parts.

3.4.3.3 Results - Plots of collated data and initial analysis

Since the sampling programme was only for a three week period, some older data was used that was collated over a longer period to see any initial trends occurring in the plant over the long term. This data was from 2005 onwards until 2006. The following can be deduced from these plots:

- For Fig. 3.44, it is apparent that there can be large differences in flux production rates which are independent of temperature and which are very variable for individual modules. In this case the temperature remains relatively uniform but the flux fluctuates greatly. The reason for the difference in flux rates between membrane modules is that the two banks of membranes are not fed in parallel operation but rather in a semi-series fashion that is unique to this plant. This means modules fed first are prone to greater fouling and reduced fluxes. Also localised clogging of individual membrane tubes exacerbates this situation.
- The results from Fig. 3.45 indicate that flux can vary considerably between each membrane module due to localised affects and fouling. It is also clear when manual chemical cleans have been carried out for individual membranes as the flux recovers significantly after the event.
- Figs. 3.46 and 3.47 confirm the high removal rates in a MBR system for COD and TSS.
- Fig. 3.48 indicates that the F/M ratio varies from 0.05 up to 0.15, and initially is not kept consistent but later on better wastage control is achieved.
- Fig. 3.49 shows that the MLSS varies greatly from 4,000 up to 20,000 mg/l, with both bioreactors being fed consistently.

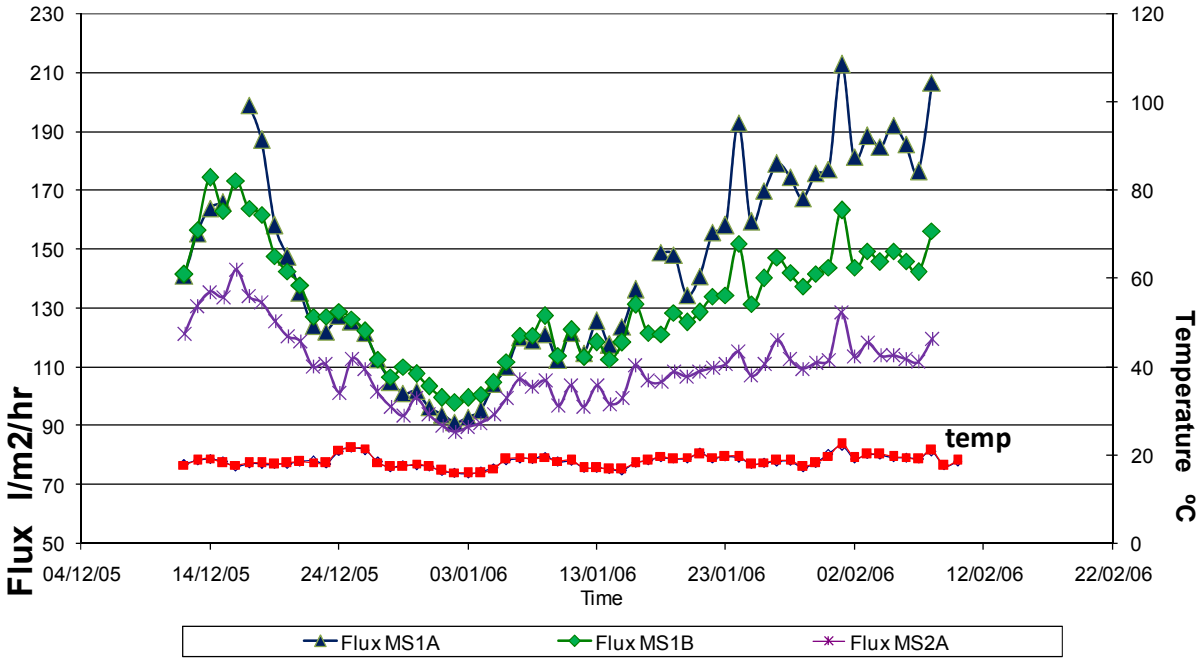

Fig. 3.44: Aquabio main plant at Kanes Foods - flux rates and temperature for 3 membrane modules

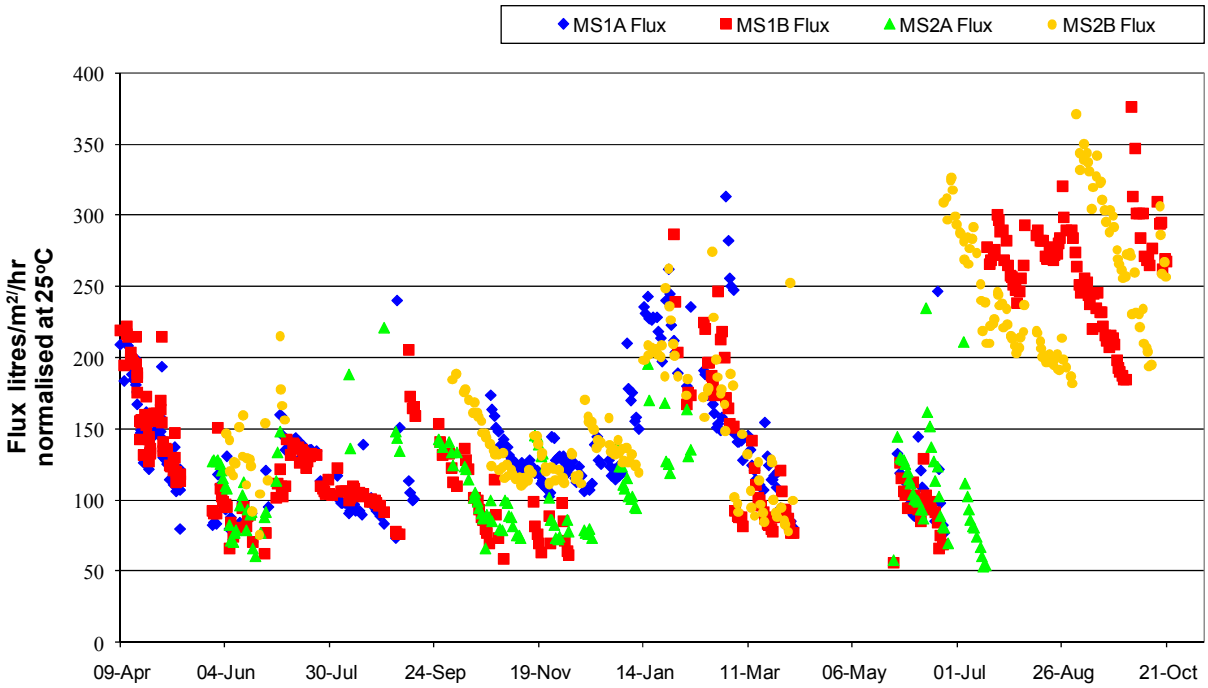

Fig. 3.45: Aquabio main plant at Kanes Foods - flux rates for all 4 membrane modules

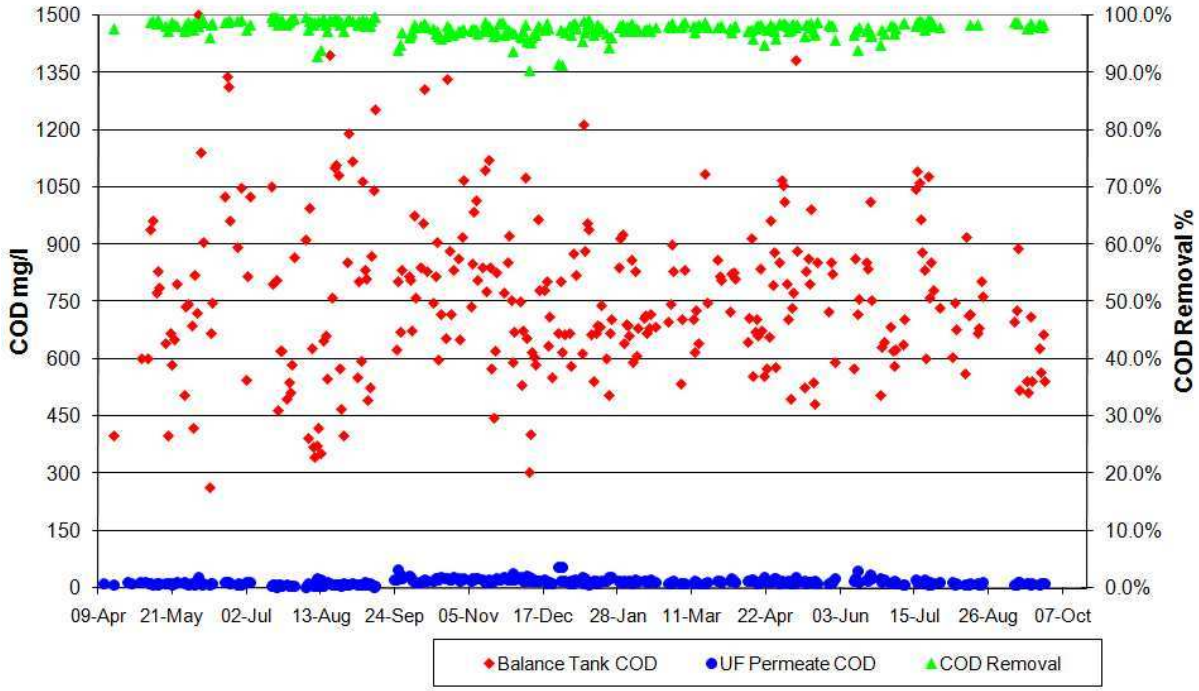

Fig. 3.46: Aquabio main plant at Kanes Foods - COD removal rates

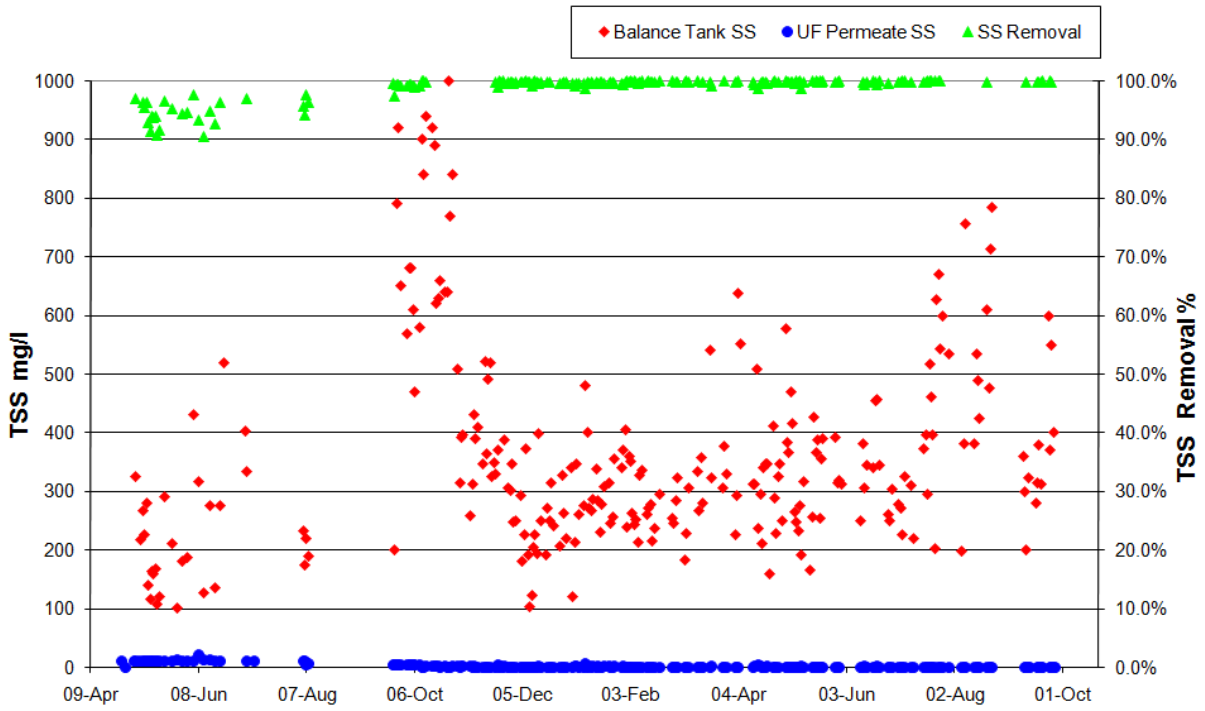

Fig. 3.47: Aquabio main plant at Kanes Foods - TSS removal rates

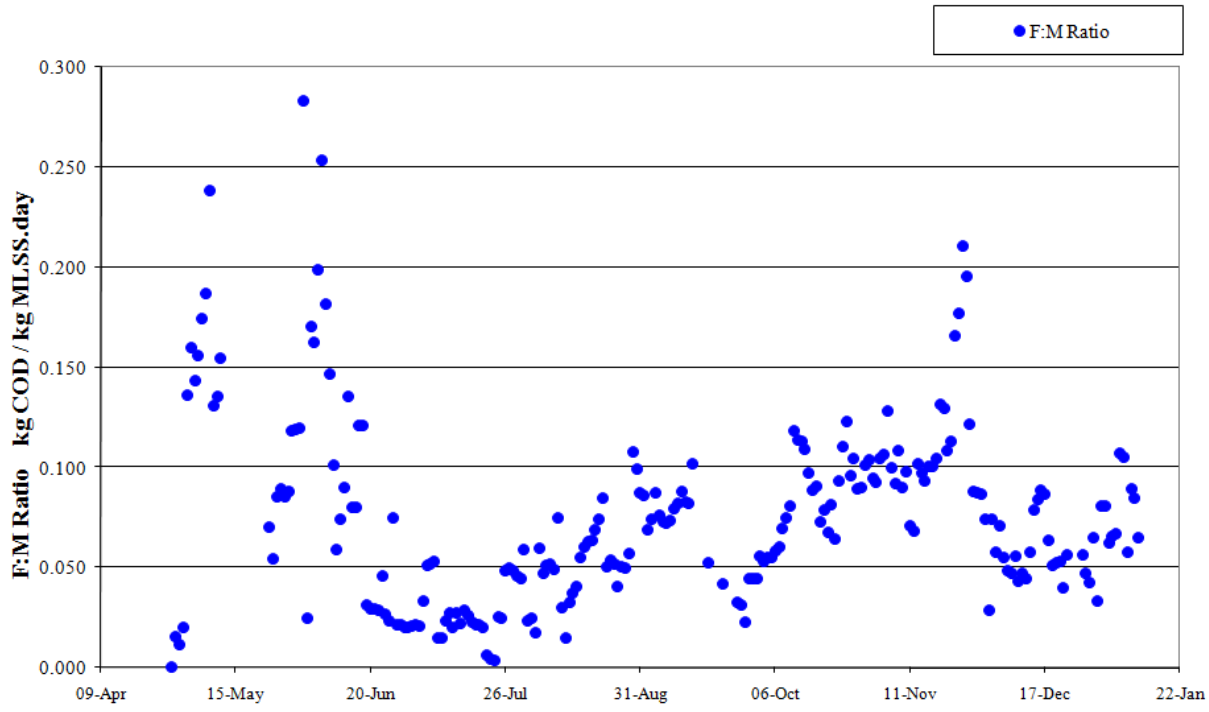

Fig. 3.48: Aquabio main plant at Kanes Foods - Bioreactor food-to-microorganism ratio

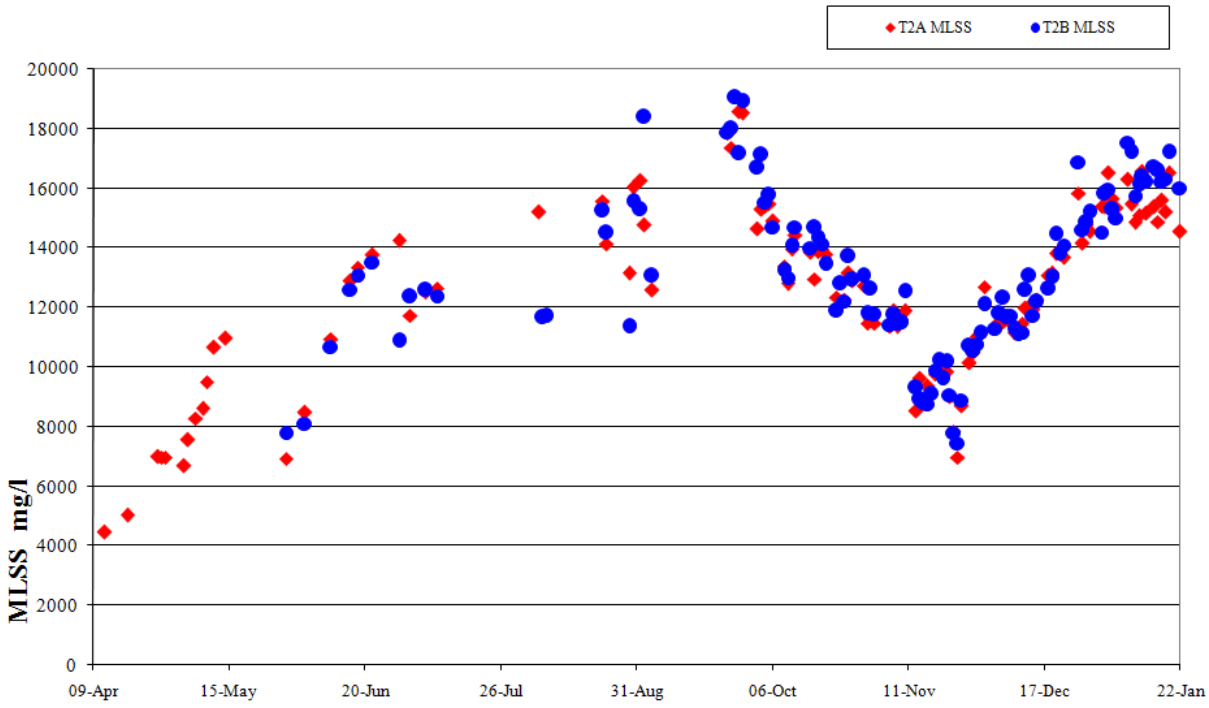

Fig. 3.49: Aquabio main plant at Kanes Foods - Bioreactor MLSS concentration

3.4.4 ITT Sanitaire pilot membrane filtration unit operated at Cardiff WWTP

3.4.4.1 Plant layout and operational details

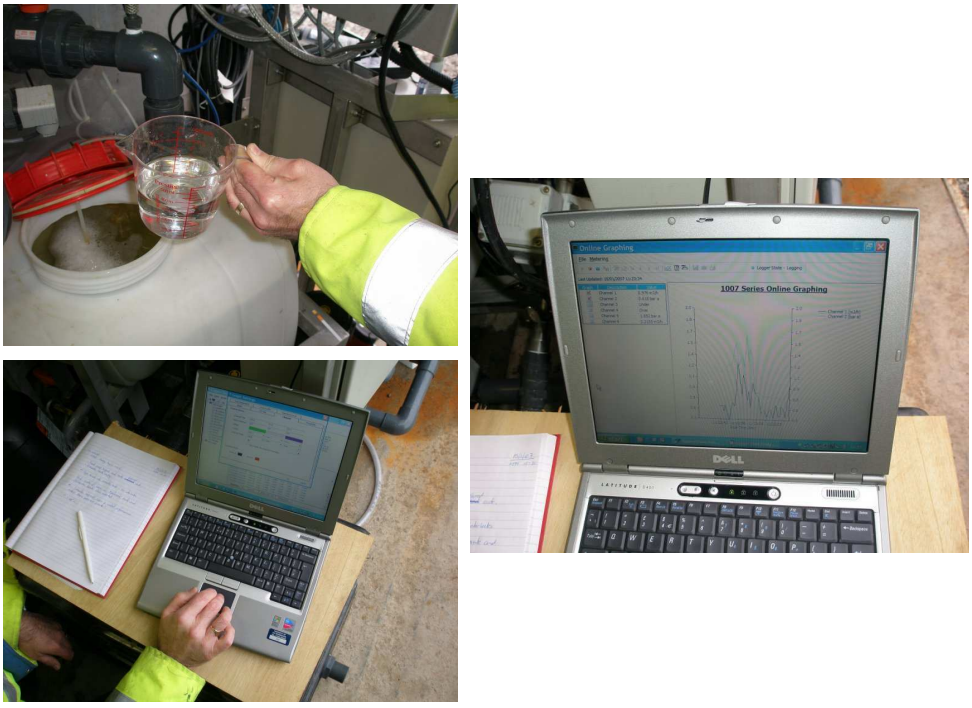

Fig. 3.50: ITT pilot membrane unit at Cardiff WWTP - Pictures of effluent quality produced and data logger system

As part of the TSB project, ITT Sanitaire allowed access to their pilot plant and units to be used to provide further data to allow calibration of the models that appear in later chapters. In this regard, in June 2007 the Author visited ITT Sanitaire's pilot membrane filtration unit which polishes effluent from the SBRs of Cardiff's WWTP. This was to collate design and operational information as necessary to allow accurate plant layout modelling and control simulation. Following the visit a sampling programme and flux stepping procedure was designed to suit to include simple filtering, simple protein/polysaccharide measurement, and flux stepping operations. The actual testing then occurred in July 2007. Fig. 3.50 are pictures of the pilot unit (in the container) and its data logger.

As mentioned this pilot plant is fed by effluent from the main municipal works in Cardiff city and hence it effectively carries out tertiary level treatment of said effluent. The Author carried out a sampling programme to include free EPS and **SMP** concentration measurements (e.g. combined proteins and polysaccharides). These results then could be used to test the validity of the membrane fouling model developed in Chapter 4. Table 3.3 summarises the unit's main operational information.

3.4.4.2 Results - Data collated off-line

The following issues relate to the flux stepping operation and sampling regime:

- For the unit, the new horizontal membranes were fitted in late June and run at a steady 25 $l/m^2/hr$ with negligible TMP increase.

Membrane Filtration Unit (without bioreactor)	Operational details
Operating since 01/11/06	Treats effluent from SBR sump of Cardiff WWTP
Membrane type and area	Horizontal "Kolon" fibres; PVDF 0.1 μm pore size; A = 20 m^2
Feed flow; permeate flow; backwash	1 to 2.4 m^3/hr; 0.6 to 1 m^3/hr; 1.2 to 1.8 m^3/hr
Backwash interval and duration	Every 4 minutes with 30 seconds ON
TMP range	300 to 500 $mbar$ (3 to 5 m head)
Aeration rate and type	11 m^3/hr from coarse bubble tube diffuser
Cleaning regime	hypochlorite dosed 4 times daily into permeate tank
Biological feed data	COD $\approx$ 50 mgO_2/l; TSS $\approx$ 25 mg/l
Volumetric Concentration Factor	= 2.5 i.e. 10 mg/l TSS influent leads to 25 mg/l MLSS
SMP feed data	Glucose $\approx$ 5 mg/l; Proteins $\approx$ 100 mg/l
Data logger	Logs feed flow, permeate & backwash flow, permeate & backwash pressure
Other information	No DO probe; Effluent in SBR sump should contain SMP but no biomass

Table 3.3: ITT Sanitaire pilot membrane filtration unit operational data

- Flux stepping tests were then carried out a month later. Membranes were not cleaned before stepping tests.
- Three sets of samples were taken. Each sample set consisted of samples taken from the membrane tank and the permeate tank.
- With the exception of protein and polysaccharide analysis which were completed in-house, analysis were carried out by Southern Water laboratory (now part of Eurofin).
- Temperature throughout the test was 17 $^\circ C$, and air flow rate was 13 Nm^3/hr.
- Each flux was run through 3 filtration/backwash cycles. Flux was stepped up and then down again.

The following technical issues and recommendations relate to the unit's operation during the flux stepping tests:

i) – Data logger was separate to the PLC.

ii) – Measured: COD; COD filtered using 0.45 μm GFC; TSS; VSS; TN; Ammonia. Additionally measured single biological/nutrient measurements in the feed and permeate flows.

iii) – Assumptions: Full saturated feed tank (i.e. DO 8 mg/l or above); pH 7.0; Viscosity 1 to 2 cP.

iv) – Flux step experiments: 1 hour between ramp up period; step size 5 $l/m^2/hr$; 4 steps at least; stepping increases free EPS and **SMP** concentration at membrane surface.

v) – At least one free EPS and **SMP** concentration measured (as combined protein/polysaccharides) at beginning and end of day. Ideally after each ramp up.

vi) – Shorten data logging cycle from 2 minutes to 30 seconds when carrying out flux stepping.

vii) – Protein/polysaccharide concentration measurement: Simple methods for proteins include Lowry Assay, Dubois Assay (also known as Phenol/$H_2SO_4^-$ method); For polysaccharide includes Bradford Assay, Anthron Assay (which needs a cooking step).

Table 3.4 details all the off-line biochemical data collated during the flux stepping operation.

Sample type	18 Jul'07 12:00 Feed	18 Jul'07 12:00 Permeate	18 Jul'07 14:14 Feed	18 Jul'07 15:00 Feed	18 Jul'07 15:00 Permeate	19 Jul'07 13:50 Feed	19 Jul'07 13:50 Permeate
E-coli (presumptive) number/100ml	950	110		5200	100	46000	3200
Suspended solids mg/l	28.6	4.08		18.4	0	5.1	1.02
Ammonia mg/l as N	0.7	1		2.28	2.15	2.29	2.23
COD mg/l	51.9	19.2		50.8	19.1	38.2	17.8
COD filtered mg/l	30	19.1		34.3	17.8	35.3	16.9
Solids (suspended at $105°C$) mg/l	28	4		18	<1	5	1
Solids (suspended at $500°C$) mg/l	6	<1		3	<1	<1	<1
pH	6.69	7.25		7.14	7.5	7.3	7.68
Turbidity FTU	6.53	0.8		4.48	0.4	3.38	0.41
TOC mg/l	6.02	4.34		7.59	5.1	6.7	4.49
Glucose mg/l	4.44		6.06	7.83			
Protein mg/l	112.6		106.6	105.4			

Table 3.4: ITT Sanitaire pilot membrane filtration unit - flux stepping biological data

3.4.4.3 Results - Plots of collated data and initial analysis

The finalised multi-configurable fouling model used in Chapter 4 has been calibrated on data obtained from flux stepping tests performed on this ITT Sanitaire pilot PVDF membrane filtration unit. This unit was simply a filtration cell fed with treated effluent with very low TSS and very low COD levels which is mostly composed of **SMP**. Low suspended solids levels means that multiple flux steps can be carried out in the unit in a single day, which speeds up the experimental procedure, without repeated clogging or even permanent membrane damage occurring. The concentration of TSS was however large enough to create cake build up on the membrane surface during the filtration cycles. In this flux stepping experiment the membrane was subjected to a range of fluxes from 30 $l/m^2/h$ to 55 $l/m^2/h$ in increments of 5 $l/m^2/h$. This allowed for testing the irreversible and reversible fouling under different operating conditions both below and above the critical flux. Figs. 3.51 and 3.52 are plots of the increasing TMP with each constant flux step upwards, followed by a few steps downwards when the TMP naturally reduces. As can be seen even the so-called constant flux itself has some "noise" within it due to the suction pump creating negative pressure affects. For the TMP, it becomes more scattered data with larger applied fluxes, and also the third cycle of the three flux steps tends to show the greatest inconsistencies and instabilities particularly at larger fluxes. For the low value flux steps below critical, then recovery between backflushes is good, but this becomes less so with increased fluxes with some permanent irreversible fouling occurring.

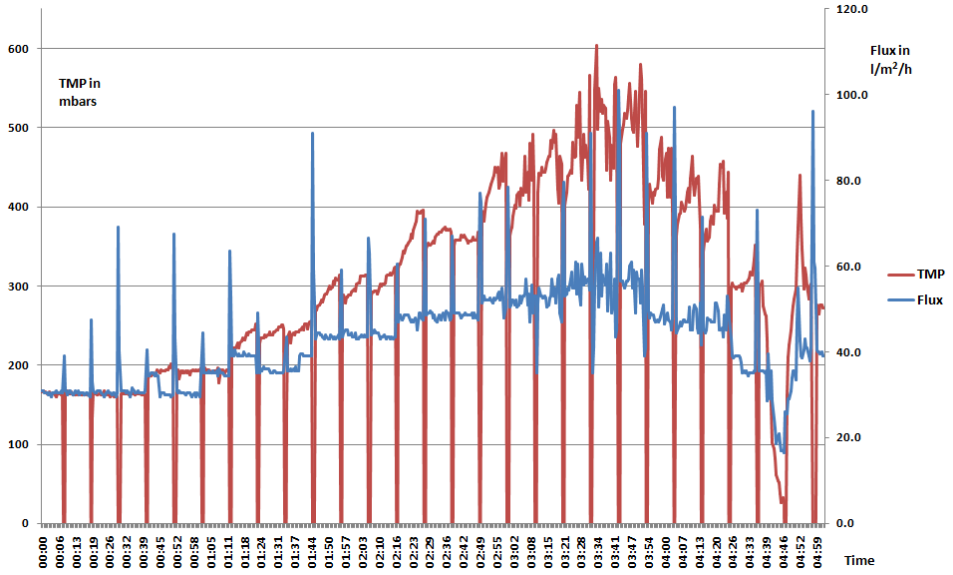

Fig. 3.51: Measured varying TMP steps for ITT membrane filtration unit based at Cardiff

After the flux stepping exercise, the data collected was analysed to ascertain any trends or technical conclusions that could be made or inferred. In this regard each flux step of three cycles was critically examined with those below 35 $l/m^2/h$ being rejected as not showing sufficient trend, and all steps down being rejected altogether as they were carried out with much too large flux jumps down and also showed too much scatter with "white noise" predominating. An attempt was made to manually correlate in a linear fashion the relationship of the gradually rising TMP over time during each flux step period which was composed of three cycles. Hence the gradient of the manually fitted linear line was calculated as shown in Figs. 3.53 to 3.55. It can be deduced from these manual plots and associated gradients, that the linear fit is very good at fluxes below critical, and becomes extremely poor at fluxes above critical particularly for the second and third cycles of the specific flux step. It should be noted that the gradient of the TMP is the rate of change of trans-membrane pressure. It is tabulated in Table 3.5.

The calculated gradients, $\frac{dTMP}{dt}$, were plotted against their respective fluxes for all three step cycles to ascertain any trends, correlations or deduced relationships between the rate of change of trans-membrane pressure and flux (see Fig. 3.56). An attempt was made to fit these points using both exponential and

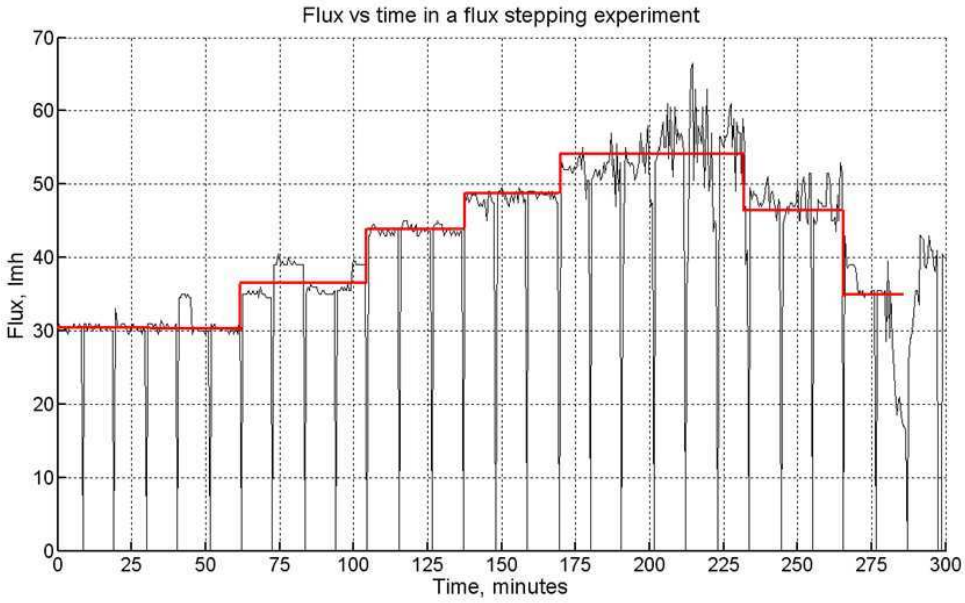

Fig. 3.52: Measured constant flux steps for ITT membrane filtration unit based at Cardiff

power curve equations (Janus and Paul 2009). As can be seen in this plot, the third cycle points have a much greater scatter at the higher fluxes, so the respective correlation between $\frac{dTMP}{dt}$ and flux is poor.

	dTMP/dt			
Flux $l/m^2/h$	1st cycle	2nd cycle	3rd cycle	Average
35	3.31	2.36	2.57	2.75
40	4.97	4.67	4.08	4.57
45	8.89	3.23	1.00	4.37
50	12.00	15.56	11.71	13.09
55	25.50	8.42	20.00	17.97

Table 3.5: ITT Sanitaire pilot membrane filtration unit - TMP gradients

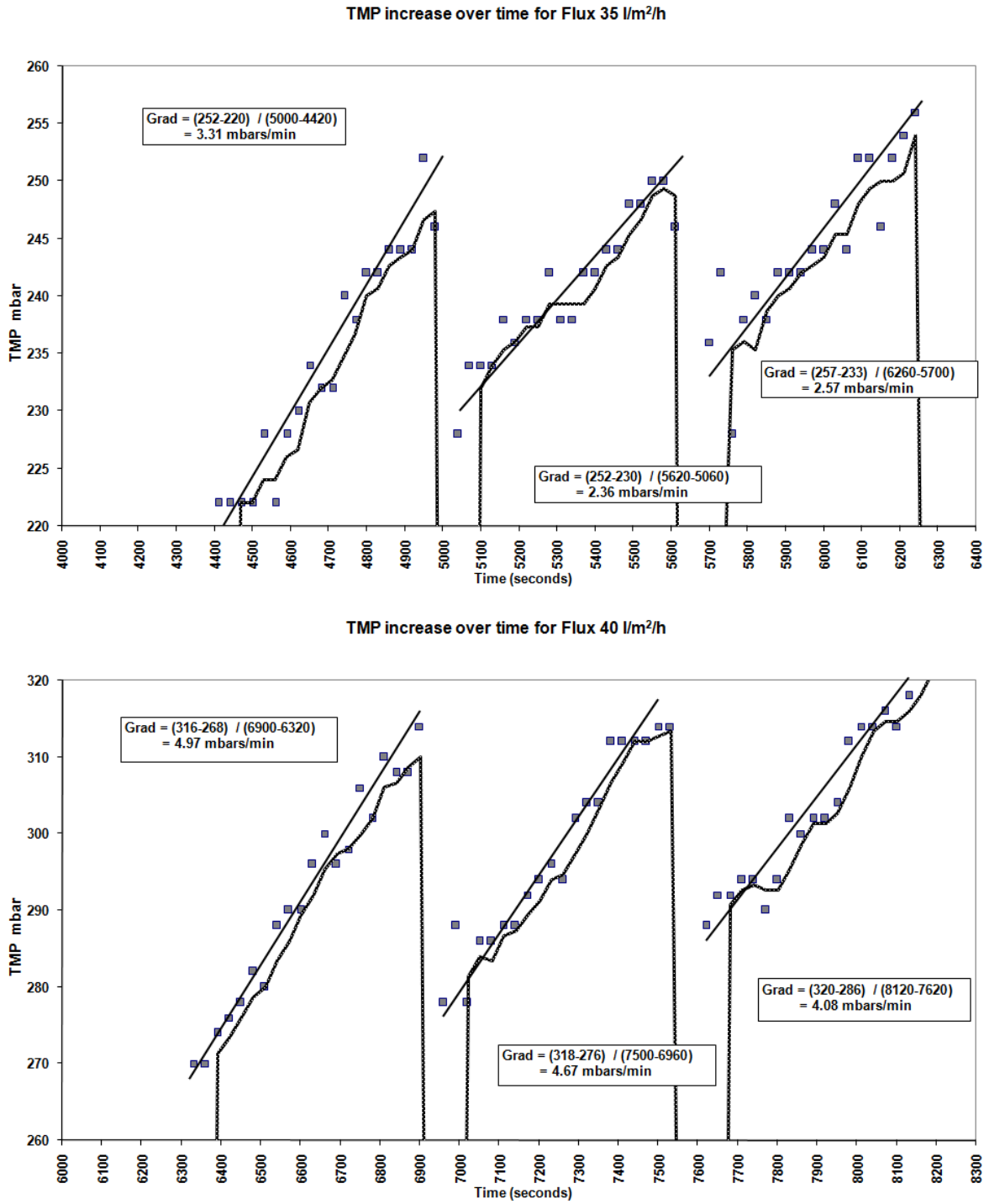

Fig. 3.53: ITT pilot membrane unit at Cardiff WWTP - 1) TMP Gradients for flux steps 35 and 40 lmh

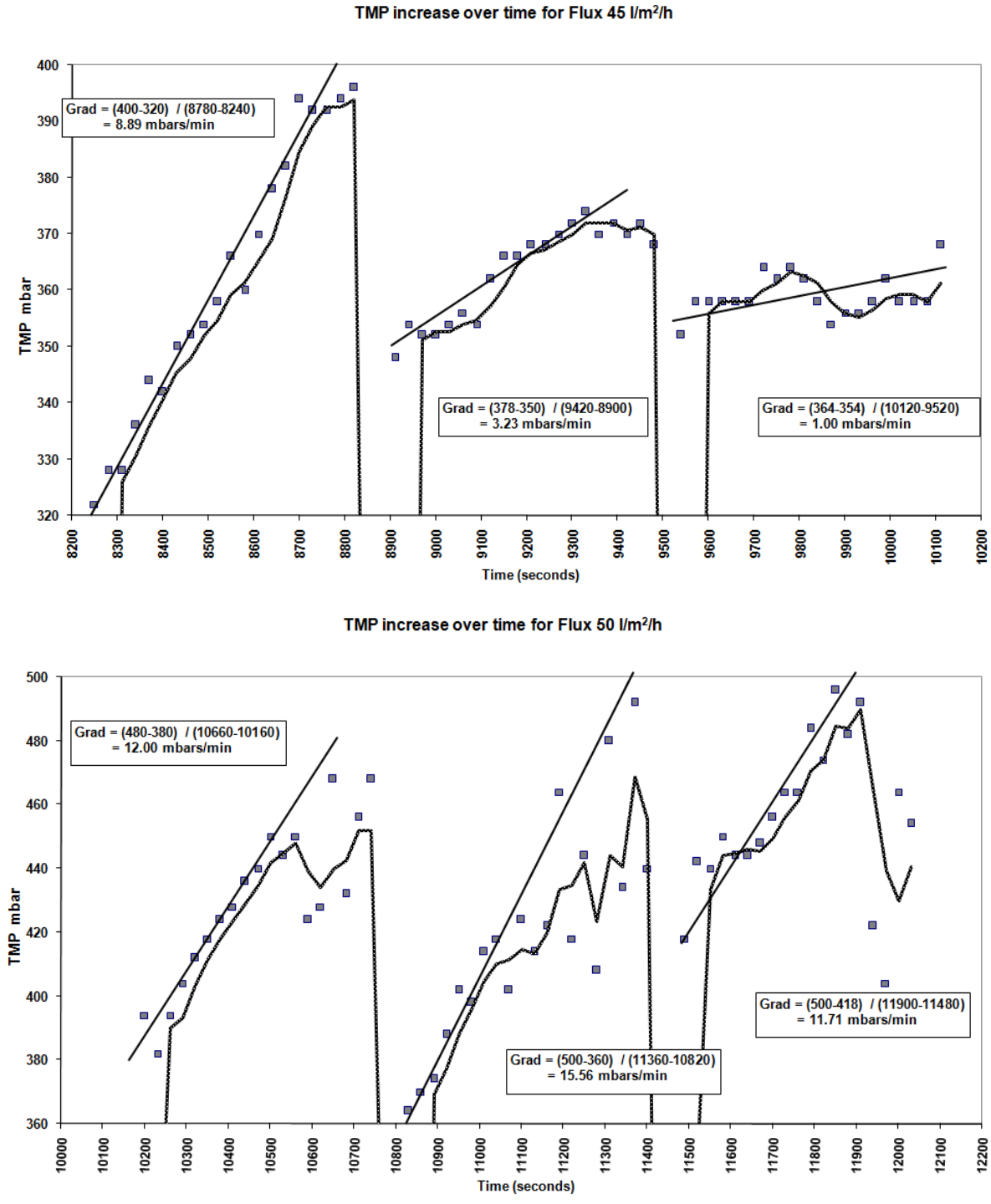

Fig. 3.54: ITT pilot membrane unit at Cardiff WWTP - 2) TMP Gradients for flux steps 45 and 50 lmh

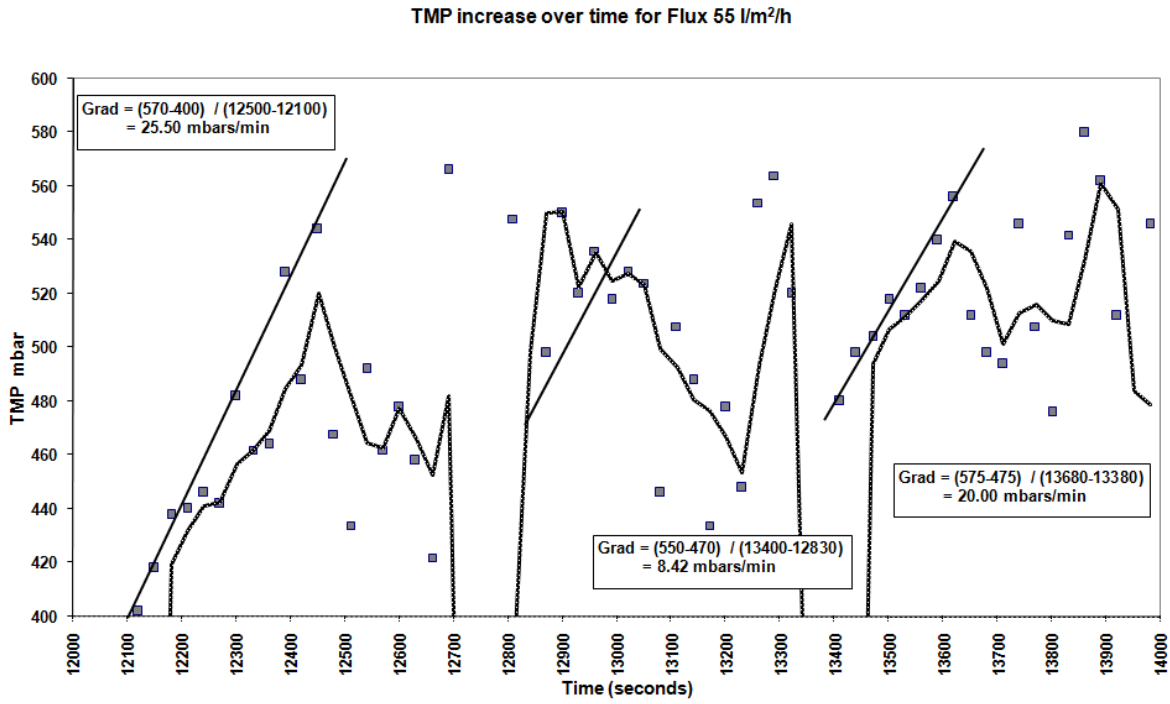

Fig. 3.55: ITT pilot membrane unit at Cardiff WWTP - 3) TMP Gradients for flux step 55 lmh

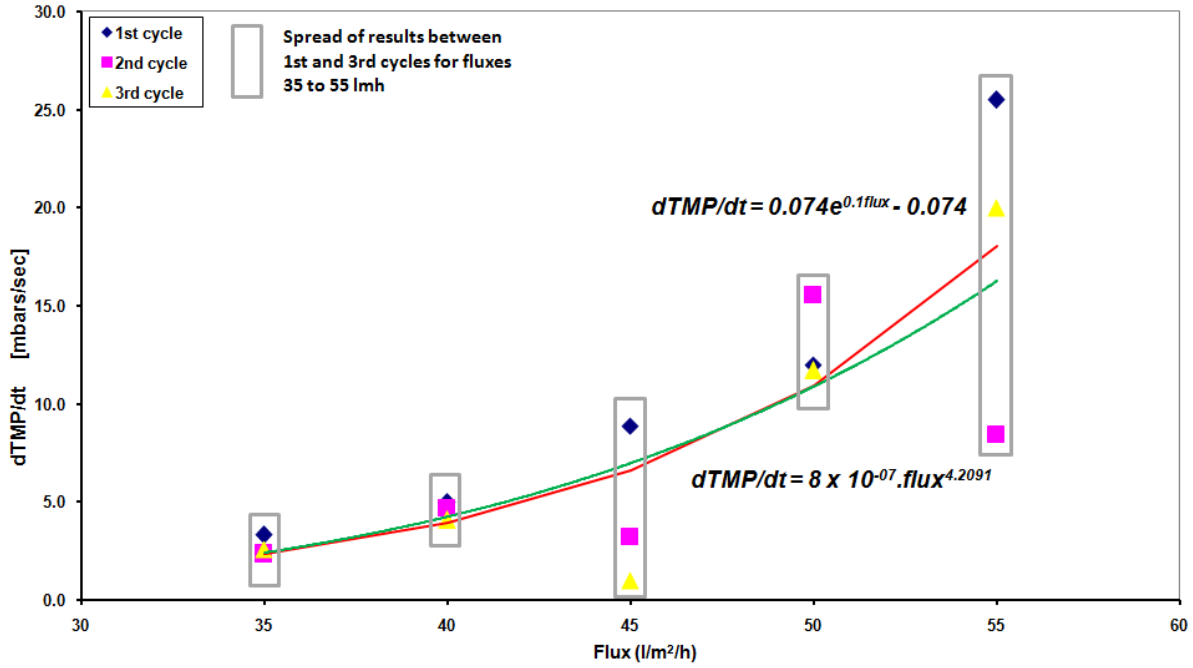

Fig. 3.56: ITT pilot membrane unit at Cardiff WWTP - Plot of Rate of Change of TMP versus Flux for all three stepping cycles

3.4.5 ITT Sanitaire submerged pilot MBR plant operated at Coors UK Limited

3.4.5.1 Plant layout and operational details

Fig. 3.57: ITT pilot MBR plant at Coors UK - Picture of Author switching on pilot plant

Fig. 3.58: ITT pilot MBR plant at Coors UK - Picture of permeate tank with suction pump

This ITT Sanitaire pilot submerged MBR plant was based at the Coors Shobnall Maltings site in the Midlands. This portable plant consists of a simple submerged layout typical for a constant flux variable TMP pilot. Thus there is an inlet pump leading to a small anoxic tank zone, from which the liquid is pumped into an aerobic bioreactor tank section with overflow weir. When the weir level is overtopped, the mixed liquor falls under gravity into the adjacent membrane module which is connected to a permeate suction pump. The module is equipped with vertical hollow fibre PES membranes. There is a small recirculation

Fig. 3.59: ITT pilot MBR plant at Coors UK - Picture of liquor recirculation pump and aeration system

pump system which can be used, if needed, to recirculate the mixed liquor from the membrane module back into the anoxic zone. The forward permeate suction pump system is automated to periodically operate in reverse mode as a backflush pump, with the option to allow a periodic chemical clean with sodium hypochlorite if necessary. It is a variable speed pump allowing differing constant fluxes to be developed.

In order to keep the membranes constantly "wet", then the permeate flow can also be recycled back to the anoxic zone if the inlet line stops functioning. There is also a small dosing tank connected to the system which allows additional carbon substrate or liquid nutrient solution to be dosed into the anoxic tank. A HMI with PLC system allows full automation of the plant operation by automatic valve actuators. Aeration to operate all systems is provided by a small compressor (e.g. tube diffusers, membrane sparger, actuators, etc.). The plant sensors consist of flow meters, pressures transducers, tank level sensors, a combined pH and DO probe, temperature probes, and a MLSS analyser and sensor. All sensor information is automatically transmitted to a data logger. Table 3.6 summarises the operational information for this plant.

3.4.5.2 Results - Data collated off-line

On first start up the plant was operated with water to test the system for leaks. After this it was seeded with sludge from a nearby Severn Trent Water municipal treatment works, after which it was fed the brewery wastewater for a six month operational period from late 2004 until early 2005. Initially the F/M ratio was quite high at 0.5 d^{-1} which created a higher oxygen demand for the blower. This led to too much air in the tank thus causing foaming events. On lowering of the F/M ratio down to 0.1 to 0.25 d^{-1}, which led to higher MLSS concentrations of over 10,000 mg/l, the foaming disappeared. Eventually a spray ball was fitted at the end of the permeate recirculation line, so that recirculated permeate could be sprayed on top of the mixed liquor in the aeration tank. This would help to reduce the amount of foam produced. The plant shutdown automatically several times over the entire operation period due to numerous reasons such as: valve actuator motors burning out; plant stoppage due to lack of influent to the plant; software problems in HMI; feed pump cutout due to the low level sensor triggering in the aerobic tank; and, permeate tank level sensor breakdown. This meant that some of the plots that appear later on in Section 3.4.6.2 shows gaps in the data. Every few days samples were taken at the feed and permeate points, as well as in the bioreactor, so that a comprehensive listing of biochemical values could be determined.

Submerged MBR Plant (with bioreactor)	Operational details
Operated at Coors UK	Treats effluent from brewery process
Membrane type and area	Vertical "Puron" fibres; PES 0.04 μm pore size; A = 20 m^2
Permeate flow; backwash flow	0.6 m^3/hr; 1.1 m^3/hr
Permeate recirculation flow	0.27 m^3/hr
Backwash interval and duration	Every 6 minutes with 45 seconds ON
TMP range	300 to 500 $mbar$ (3 to 5 m head)
Aeration type	Coarse bubble tube diffuser
Bioreactor DO operating range	2 - 4 mg/l
Full air scour flow	27 Nm^3/hr for 15 seconds every 60 seconds
Low air scour flow	$\approx$ 2 Nm^3/hr for 45 seconds every 60 seconds
Biological feed data	MLSS $\approx$ 7,500 mg/l
Bioreactor tank data	Volume 1 m^3; operating level of weir 1.9 - 2.0 m
Data logger	Logs feed flow, permeate & backwash flow, permeate & backwash pressure

Table 3.6: ITT Sanitaire pilot MBR plant operational data

3.4.5.3 Results - Plots of collated data and initial analysis

This particular plant supplied a very extensive on-line data set as the sensors took readings automatically every few seconds or minutes depending on which process variable they were measuring. This vast data set was collected over an extensive eight month period (when the plant was operating and not down). Some interesting plots of this data are discussed in this Section but for the sake of brevity are not provided. The main data sets that were used later on in this research work were as follows:

- Influent flow rate results - Inflow variations into the plant, with actual values plotted as well as moving average values. The moving average value is one that simply gives the net inflow values as opposed to actual gross ones which have considerable variance as they include all values.
- Automated MLSS analyser results - This is a very useful data plot as it shows the output from the automated MLSS sensor. These sensors work either directly or indirectly. A direct sensor uses a dense membrane probe that measures concentrations on-line but which is also prone to frequent fouling by biofilm growth and internal contamination by mixed liquor. Conversely, indirect systems measure MLSS concentration by inference by shining light of fixed intensity and wavelength through the liquor, with the reflection and refraction caused by liquors giving an indirect way of measuring MLSS concentration. The analyser in this case was of the indirect variety. The plot shows that on plant startup, it indicates a seeded concentration of 1,000 mg/l which gradually builds up by biomass growth to nearly 14,000 mg/l.
- Total calculated membrane resistance results - Since both the flux flow rate and TMP were both measured, and as the liquor viscosity was determined periodically during the sampling analysis, the total membrane resistance could be evaluated. This calculated total membrane resistance increases dramatically near the end of the plant operation period due to extreme TMP levels experienced then.
- Filtered flux and TMP results - These values are for the whole timescale of plant operation including down periods. They can also be plotted as moving average filtered Flux and TMP with a connected timescale so that all down periods of the plant are removed. These plots are of filtered data that has been deliberately removed of the regular backflush events that occur which otherwise would simply confuse the plots thereby making it difficult to discern the overall trend. In the first plot for the entire operational period, which includes downtime periods, the constant flux was gradually ramped up to ascertain its affects on the generated TMP. In the next plot, the whole timescale is not shown as the downtime periods of the plant have been removed as well instances when key sensors were not

operable. This filtered flux and TMP plotted with a connected timescale then gives a continuous plot which is much easier to read and which clearly displays the TMP evolution over time. The last plot is the moving average form of the filtered flux and TMP with a connected timescale which also allows the removal of any peak events. This one is the easiest to examine for any long term trends. Incidentally, this long term filtration data set which includes the most extensive set of biochemical MLSS values under this TSB project is used later on in Chapter 4 to validate the finalised multi-configurable fouling model.

3.4.6 Fictitious WWTP based on IWA's modified COST Benchmark simulation model

3.4.6.1 Plant layout and operational details

As mentioned already the four plants just described did not produce enough data points to allow the full testing of a system identification input-output biological model as is outlined in Chapter 5. This is due to the fact that if there are up to thirteen component input and outputs states, then to test a fully MIMO model will require at least several hundred if not several thousand data points to allow an adequate calibration and validation procedure to proceed.

In order to address this crucial problem, the standard IWA COST Benchmark simulation model was utilised (Copp 1999, 2000) which can be used for the dynamic simulation of a given complex plant layout. This Benchmark is a fictitious Activated Sludge WWTP with an approximate population equivalent (p.e.) capacity of 10,000 m^3/day which was developed so that reported improvements in plant control by researchers and operators could be measured and verified independently, since most improvements tend to turn out to be very site specific so have no global applicability. The Benchmark, which has been used by numerous researchers over the years and which is fully documented at the Nancy (2010) website, consists of five bioreactor tanks: two anoxic denitrification tanks of volume 1,000 m^3; two fully aerobic tanks of volume 1,333 m^3; and, one aerobic tank for nitrification of volume 1,333 m^3 where the oxygen supply is controlled by a DO setpoint of 2 mg/l. Fig. 3.60 details this plant layout. The plant inflow has a average flow rate of 18,446 m^3/day and the internal return flow is set up to a constant value of 55,338 m^3/day which is three times the considered inflow average. A secondary clarifier tank recycles part of the sludge with a fixed rate of 18,446 m^3/day to the first denitrification tank. The remaining part of the settled sludge is removed from the system at a rate of 385 m^3/day to maintain a suitable SRT.

Since the creation of this Benchmark is based on real life plant data values and on the practical operational experience of numerous global researchers, it results can be thought of as extremely realistic for a plant layout of this type. The Benchmark was developed primarily to test municipal WWTP and therefore comes with three different influent files, namely: a dry weather flow (DWF) file which is the basic data set; a wet weather file which includes for a long rainfall period; and, a wet weather file which includes for a short, intense storm event. In this case only the DWF influent file was used, as the finer points regarding the operation of a municipal treatment works are not under consideration here. The influent files are for a full fourteen day period with measurements provided at every 15 minute intervals, and thus for a particular state this means 1344 values. The Benchmark was developed to be tested using the IWA's ASM1 model and thus the influent files also contain initial state values in each of the tanks for the thirteen components, and also the influent data is provided directly as the thirteen component state values. This means that a complex trail-and-error influent characterisation procedure is not required, and that the data is already in a state that can be easily adapted for a MIMO model simulation.

The COST Benchmark's layout includes a ten layer settler model for the secondary clarifier as developed by Takacs et al. (1991) in which the upward flux rate is crucial in determining the settling velocity of the biomass flocs. However, as this study only is considering MBRs, this part of the COST Benchmark was replaced by a simple ideal settler model which basically replicates the membrane filtration and separation process. This means settling velocities of biomass flocs are not required in the COST Benchmark simulation. The ideal settler acts as a membrane by simply removing all solid components, and allowing through all soluble components. Incidentally this simplification greatly reduces the COST Benchmark simulation time.

The other change made to the COST Benchmark simulation model was to include temperature variations so that it more closely replicated a real life situation (Paul et al. 2005), since the standard Benchmark is for a fixed temperature for the whole simulation period. This was done in Paul et al. (2005) by modifying the Benchmark's standard dry weather influent data file by combining it with temperature data from an appropriate source (Agrimet 2004) with the same 15 minute time intervals.

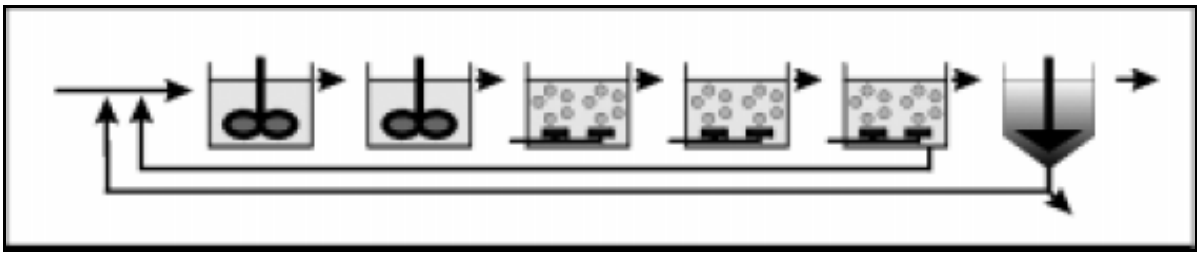

Fig. 3.60: COST Benchmark simulation model plant layout

Obviously, this modified COST Benchmark simulation model can only be used to test an input-output biological model structure which contains no **SMP** or EPS in its state variables. Therefore any developed model could not be linked to a membrane filtration model as these **SMP** and/or EPS connections would not exist. However, it is simply being used here to prove the principle of using input-output model structures for biological Activated Sludge systems.

Temperature dependent kinetic parameters Values of all kinetic and stochastic parameters in a typical constant temperature COST Benchmark simulation model are usually defined for a temperature of either 15 or 20 $°C$. However, some of the kinetic parameters can be varied using a temperature dependent Arrhenius type relationship as described in Eqn. 3.9 (van Veldhuizen et al. 1999).

$$r_T = r_{293} \cdot e^{\theta(T-293)} \tag{3.9}$$

where:
r_T is the varying temperature dependent kinetic parameter value.
r_{293} is the reference temperature dependent kinetic parameter.
θ is a temperature coefficient.
T is temperature in Kelvin.

Fig. 3.61 lists data extracted from several sources which summarise the various kinetic parameters in the ASM1 that are sensitive to temperature changes along with their various coefficients and range of limits (Jeppson 1996, Dixon et al. 1999, Abusam 2001, Smets et al. 2003, Reichl 2004).

The actual kinetic parameter data used in this modified COST Benchmark simulation model are those found in Reichl (2004). The other parameter that is strongly temperature dependent is the oxygen saturation concentration, $S_{O.SAT(WW)}$, for wastewater which varies inversely with salinity, wastewater temperature and atmospheric hydrostatic pressure. Its usual range varies between 6 to 14 mg/l. Eqn. 3.10 below gives the temperature dependent clean water oxygen saturation concentration,$S_{O.SAT(CW)}$, where T is the temperature and Chl is the chlorinity in kg/m^3 (Makinia and Well 2000).

$$S_{O.SAT(CW)} = e^{[(-139.344+\frac{-1.575701\text{x}10^5}{T}-\frac{6.642308\text{x}10^7}{T^2}+\frac{1.2438\text{x}10^{10}}{T^3}-\frac{8.621949\text{x}10^{11}}{T^4})-Chl\cdot(3.1929\text{x}10^{-2}-\frac{19.428}{\text{T}}+\frac{3.1929\text{x}10^3}{\text{T}^2})]} \tag{3.10}$$

To account for changes in wastewater characteristics, the β factor is introduced in Eqn. 3.11, where $S_{O.SAT(CW)}$ is converted into an actual $S_{O.SAT(WW)}$. β is usually taken as 0.95.

$$S_{O.SAT(WW)} = \beta \cdot S_{O.SAT(CW)} \tag{3.11}$$

Source	Jeppsson 1996			Dixon 1999		Abusam 2001		Smets 2003		Reichl 2004	
Temp. or Temp. Range or Temp. Coefficient θ	20° C	10° C	Range	Temp not specified	Range	Temp not specified	Range	20° C	θ	15° C	θ
Kinetic parameters heterotrophs											
μ_H maximum specific growth rate (1/day)	6.0	3.0	0.6 - 13.2	2.7	1.0 - 8.0	4.59	3.0 - 13.2	6.0	1.072	4.0	0.069
b_H specific decay rate (1/day)	0.62	0.20	0.05 - 1.6	1.0	0.2 - 1.0	0.64	0.05 - 1.6	0.62	1.072	0.28	0.069
Kinetic parameters autotrophs											
μ_A maximum specific growth rate (1/day)	0.8	0.3	0.2 - 1.0	-	-	0.66	0.2 - 1.2	0.80	1.103	0.5	0.098
b_A specific decay rate (1/day)	0.20	0.10	0.05 - 0.2	-	-	0.10	0.05 - 0.15	0.10	1.120	0.10	0.080
Hydrolysis parameters											
k_h maximum specific hydrolysis (1/day)	3.0	1.0	-	1.0	1.0 - 25.0	1.72	1.0 - 4.0	3.0	1.116	1.75	0.11
K_X half-saturation coeff. for hydrolysis of slowly biodegradable substrate (g COD(g cell COD.day)$^{-1}$)	0.03	0.01	-	0.5	0.01 - 0.5	0.02	0.01 0.15	0.03	1.116	0.0175	0.11
Ammonification											
k_a Ammoniification rate constant (m^3 /(g cell CODday))	0.08	0.04	-	-	-	0.09	0.016 - 0.8	0.08	1.072	0.06	0.069
Arrhenius relationship form	$r_T = r_{20} . \theta^{T-20}$									$r_T = r_{15} . e^{\theta(T-15)}$	

Fig. 3.61: Summary of Temperature Dependent Kinetic Parameter Data for ASM1

In this modified COST Benchmark simulation model the simple $S_{O.SAT(WW)}$ equation produced in Reichl (2004) was used since it does not include an additional salinity term.

3.4.6.2 Results - Plots of generated data sets and initial analysis

Relationship between DWF influent file data and temperature file data As only indicative temperature data was needed that showed a marked diurnal variation, then ambient air temperature data was retrieved from an Agrimet weather station located at Eureka Town in Nevada, USA that is at an altitude of over 2000 m and experiences a dry, desert type climatology (Agrimet 2004). Hence these specific environmental and site conditions meant that there was a very significant temperature change within a single day which could be matched to the existing influent data file. Data retrieval times commence from midnight on 2nd May 2004 until midnight on 17th May 2004. Since the simulation model was considered to be a benchmark plant in a totally fictitious locale it was assumed that these air temperature figures were actual wastewater ones. Fig. 3.62 shows a 4 day plot of the original influent DWF data file that comes with the COST Benchmark simulation model and the assumed wastewater temperatures that are now linked to it. In order to make this link in flow and temperature data as realistic as possible, Fig. 3.62 shows a strong correlation in peak flows during the morning period that corresponds with the initial rise in temperatures due to increased solar radiation. Conversely the temperature drops dramatically during the night period whilst the diurnal flow data quite closely follows this shift to lower wastewater production during these night time hours.

Simulation runs for modified ASM1 - constant versus varying temperatures Several simulations were run using this modified COST Benchmark simulation model with altered influent data file using the gPROMS© software package. Incidentally gPROMS© stands for *g*eneral *P*rocess *M*odelling *S*ystem and is a specialist optimisation software package used in process engineering applications (PSE 2004). The process variables calculated were compared with the original values given in the unaltered COST Benchmark simulation model. Fig. 3.63 is a plot comparing the original constant temperature COD effluent quality out of the plant against the new varying temperature COD effluent quality. As can be seen there is really not much difference as one would expect since the kinetic parameters associated with substrate utilisation and uptake are not very temperature dependent. The very slight difference between values can probably be attributed solely to the the secondary clarifier model being a ideal point settler

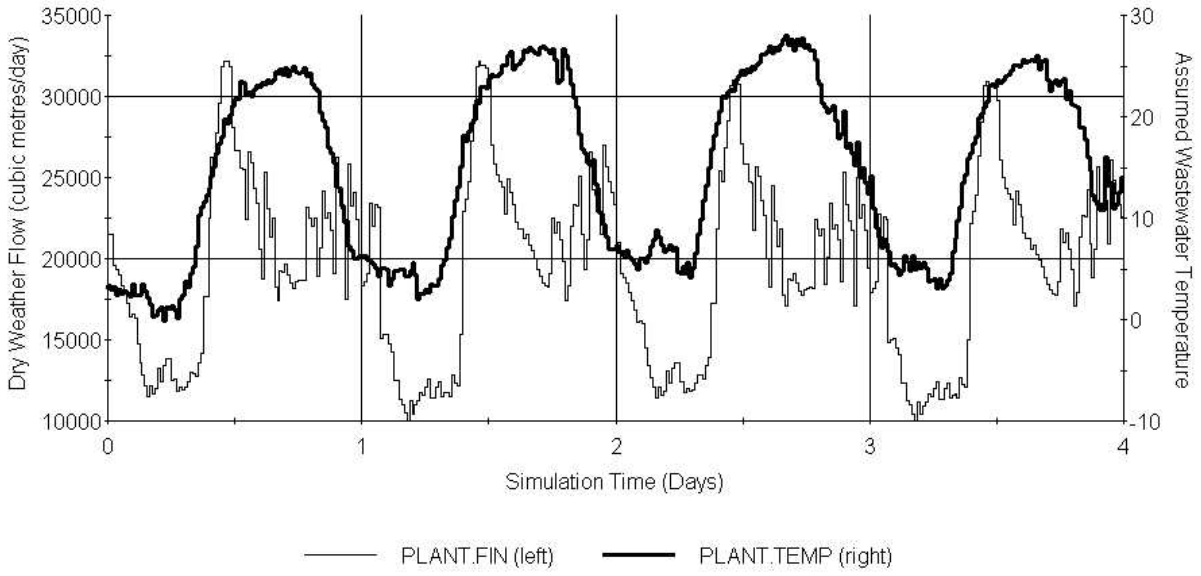

Fig. 3.62: Modified COST Benchmark simulation model - Original DWF flow data and new matching liquid temperatures

instead of the ten layer settler model advocated by Takacs et al. (1991).

Fig. 3.64 is a plot comparing the original constant temperature TN and Ammonia levels out of the plant against the new varying temperature ones. It can be clearly seen that there is a significant difference in simulation values for the constant and varying temperature scenarios since as one would expect the nitrification and denitrification rates and their subsequent kinetic parameters are extremely temperature sensitive. Thus a fairly realistic set of data for a typical ASM1 model has now been developed for a fictitious plant layout that can be used for simulation purposes. Since the secondary clarifier model used in this set up was a simple ideal point settler, as opposed to the ten layer settler used in the original COST Benchmark simulation model, this modified COST Benchmark setup can easily be adapted to study a MBR system.

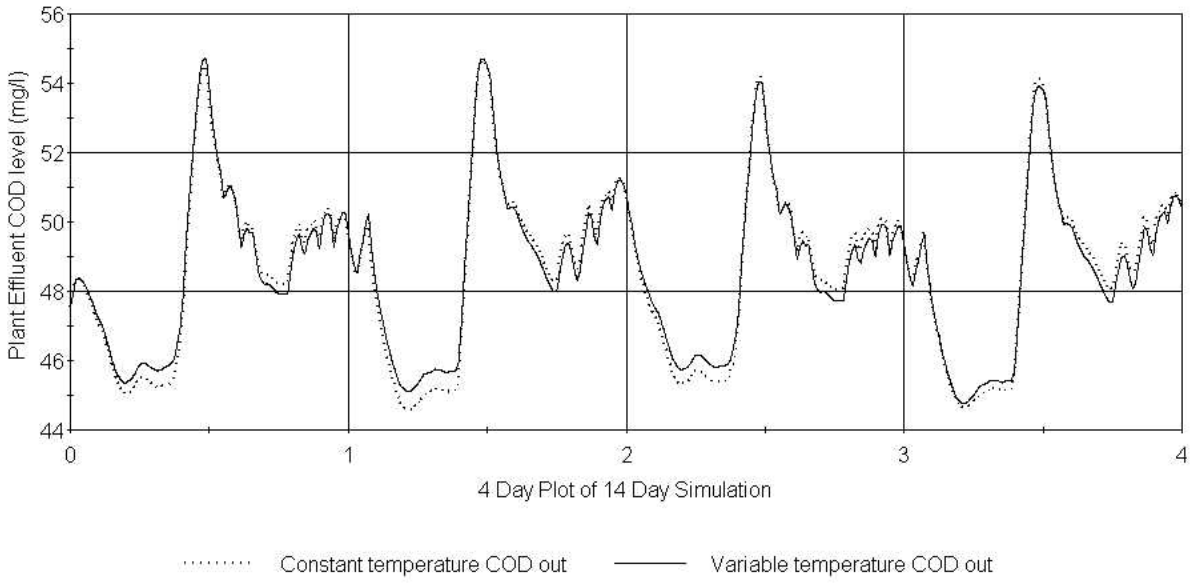

Fig. 3.63: Modified COST Benchmark simulation model - Original constant temperature CODout versus varying temperature CODout

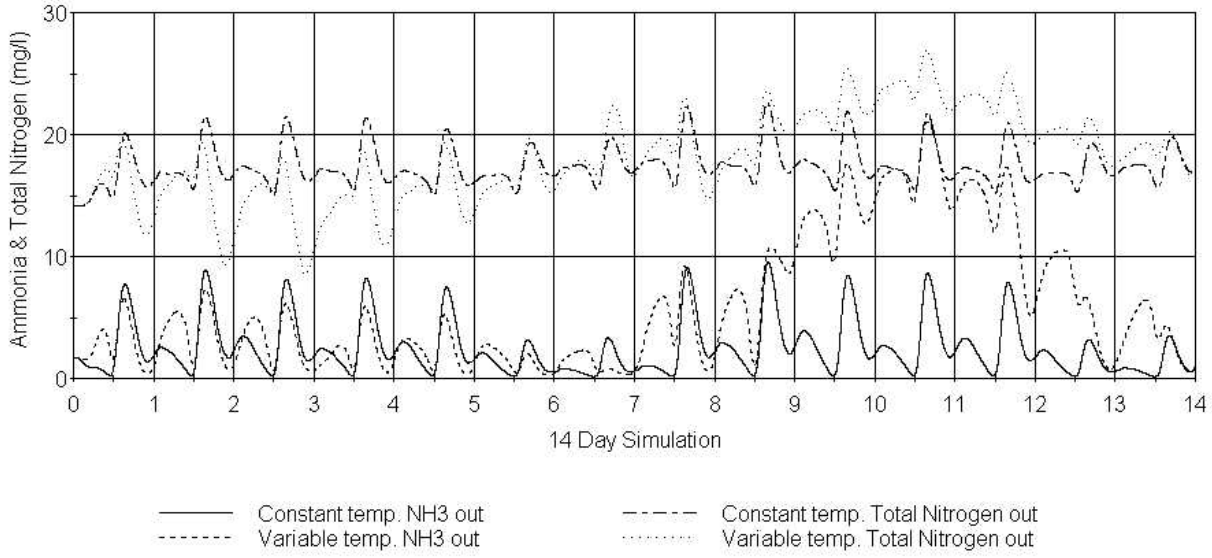

Fig. 3.64: Modified COST Benchmark simulation model - Original constant temperature NH3out and TNout versus varying temperature NH3out and TNout

3.5 *Chapter Summary*

A "Model Conceptualisation Procedure" was developed in this Chapter to help in the formulation of various input-output model structures used in later Chapters by ensuring that they conform to the basic biochemical and hydrodynamic process knowledge of MBR systems. This means that models developed, whether phenomenological or input-output data based, remain consistent to theory, and thus the results obtained from running their simulation models when using the same sets of data can be, by and large, compared against each other.

The remainder of this Chapter then described the various plants used to test the models which are developed and used in the later Chapters. They were as follows:

- A full scale MBR plant installed by Aquabio Limited and owned and operated by Kanes Foods Limited in Evesham, Worcestershire.
- A purpose built small pilot MBR plant which was operated at Kanes Foods Limited in Evesham, Worcestershire.
- A pilot membrane filtration plant operated by ITT Sanitaire at Cardiff wastewater treatment works.
- An ITT Sanitaire submerged pilot MBR plant operated at Coors UK Limited.
- A fictitious WWTP had to be used, based on the IWA COST Benchmark simulation model which itself is based around the ASM1 model, to generate additional data sets to allow the calibration and validation of the input-output biological models developed later on as part of Chapter 5.

Chapter 4

MBR model development work: membrane fouling

4.1 *Phenomenological membrane fouling model - Duclos-Orsello model*

This Chapter describes in detail the redevelopment and modification of a phenomenological model which describes the fouling of a membrane in a MBR. It then goes on describe the results obtained from running the data obtained from various plant through this phenomenological model. Finally, the last Section of this Chapter details the results of using this plant data to calibrate and validate the time series input-output version of this fouling model.

4.1.1 Introduction - classical fouling models

Mathematical modelling of the fouling process can assist the engineer in improving the membrane operation and performance, i.e. better prediction of the fouling rate and optimisation of the corresponding retaliatory actions needed to reduce it. Several classical fouling studies (e.g. (Ho and Zydney 2000), etc.) use a three mechanism model for the biofouling process: a) pore constriction; b) pore blockage; and, c) cake filtration (see Fig. 4.1). These mechanisms can be directly related to the main bio-fouling processes observed in a MBR system. Mathematical expressions for the three mechanisms are shown in Table 4.1.

For a constant applied pressure, all the above equations can be derived from a general expression postulated by Hermia (1982), where the exponent n is used to differentiate between different mechanisms (Equation 4.1).

$$\frac{d^2t}{dV^2} = k \cdot \left(\frac{dt}{dV}\right)^n \tag{4.1}$$

Thus, the Duclos-Orsello et al. (2006) model was chosen for this study as it contains all three main fouling mechanisms as stated by Hermia (1982), and it is a more refined version of the original Ho and Zydney (2000) model, which itself is based on the classical fouling mechanisms outlined in Hermia (1982). In

n-value	Filtration model	Description	Differential equations
0	cake filtration	deposit of particles larger than the membrane pore size onto the membrane surface	$\frac{dR_p}{dt} = f'R'J_b \cdot C_b$
$\frac{3}{2}$	pore constriction	deposition of particles smaller than the membrane pore size onto the pore walls, reducing the pore size	$dA_b = -\alpha \cdot Q_u \cdot C_b$
2	complete blocking	occlusion of pores by particles with no particle superimposition	$dA_u = \alpha \cdot Q_u \cdot C_b$

Table 4.1: Mathematical expressions for classical fouling models

Section 2.5.1.7 a comparison of several current fouling models was also undertaken and the Duclos-Orsello et al. (2006) model was rated the best for this same reason. It is also felt that this formulation is sophisticated enough and with sufficient degrees of freedom for the type of analysis being carried out under this study, whilst still relatively simple in structure with a limited number of model parameters based on actual measurable membrane fouling quantities and/or properties. It is also a model which can be modified for a sidestream crossflow MBR plant with bioreactor and backwash mode.

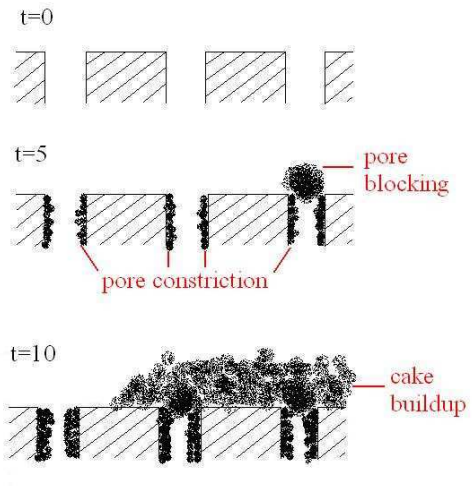

Fig. 4.1: Three mechanism fouling model using simplified membrane structure (Paul, 2006)

4.1.2 Duclos-Orsello's (2006) approach

In this model formulation, Duclos-Orsello et al. (2006) splits the total flow through the membrane into flow through the unblocked membrane surface area and flow through the blocked membrane surface area (Equation 4.2).

$$Q_t = Q_u + Q_b \tag{4.2}$$

He then proceeds to develop a solved differential equation solution which equates to the unblocked area flow, and also an integral expression which equates to the blocked area flow as shown in the combined Equation 4.3. The summation of these expressions gives the decline in total flow through the membrane. Using data obtained from several dead end filtration experiments described below, he tests his model formulation, and solves Equation 4.3 probably using numerical analysis techniques but this is not explicitly stated in his paper.

$$\begin{aligned} Q_t = & \frac{Q_0}{\left(1+\beta\cdot Q_0\cdot C_b\cdot t\right)^2}\cdot e^{-\frac{\alpha\cdot C_b\cdot J_0\cdot t}{(1+\beta\cdot Q_0\cdot C_b\cdot t)}} \\ & + Q_0\int_0^t \frac{\frac{\alpha\cdot C_b\cdot J_0}{(1+\beta\cdot Q_0\cdot C_b\cdot t_p)^2}\cdot e^{-\frac{\alpha\cdot C_b\cdot J_0\cdot t_p}{(1+\beta\cdot Q_0\cdot C_b\cdot t_p)}}}{\sqrt{(\frac{R_{p0}}{R_m}+(1+\beta\cdot Q_0\cdot C_b\cdot t_p)^2)^2+2(\frac{f'R'\cdot\Delta p\cdot C_b}{\mu\cdot R_m^2})(t-t_p)}}\cdot dt_p \end{aligned} \tag{4.3}$$

The data used to test his model formulation is obtained from several extensive constant TMP membrane filtration experiments in dead end mode using BSA solution as a model **SMP** solution, and polystyrene microspheres as a model particulate solution to mimic mixed liquor particulates (see Table 4.2).

Test	Model prediction is validated by comparing model prediction with experimental flux decline data[a] obtained from following experiments with fouling mechanisms isolated and/or combined:
1	0.25m polystyrene microsphere (external fouling will dominate) through $0.2\mu m$ MF membranes - *describes cake build up only*
2	prefiltered BSA solutions (pore blockage will be reduced by aggregates of BSA) - *describes pore constriction as dominate mechanism*
3	bovine serum albumin (BSA) solutions - *all three mechanisms involved*

[a] In this way, verify that results of this new model tend towards the single fouling mechanism case when experiment is designed to make that mechanism dominate the fouling process.

Table 4.2: Tests Carried out to Verify Duclos-Orsello Model

The molecular size of a single non-aggregated BSA colloid is smaller than the average pore size of the membrane used in his experiment. Therefore, filtration experiments using BSA in non-aggregated form were used to simulate the pore constriction mechanism in the model where single BSA colloids stick to the inside of the membrane pores.

The second mechanism, namely pore blockage, was tested experimentally using aggregated BSA colloids. These bigger, clumps of BSA colloids are deemed to plug the membrane pores. Subsequently the flux in this area declines at a faster rate than for pore constriction.

This leads sequentially to the testing of the third phenomenon that is modelled, namely cake filtration. In the model formulation, once the pores are blocked locally then pore constriction ceases in that area and particulate cake deposition begins. Thus in the model the unblocked membrane area reduces at the expense of a subsequent increase in blocked area.

The data obtained from these experiments was used to validate and calibrate the model parameter set, namely α (blockage parameter) and β (constriction parameter) for a range of normalised flow rates (e.g. $\frac{Q_0}{Q}$) and total resistance of membrane and deposit combined, R_{total}. Additional follow-up experiments measured the combined effects of all mechanisms on the parameter values, and also the membrane material properties such as hydrophobicity and hydrophilicity. In all these experiments the influence of cross flow, temperature and the design of the membrane module itself are entirely ignored. Fig. 4.2 and Fig. 4.3 detail the experiments conducted, and actual data values plotted against model simulation curves as reported in the Duclos-Orsello et al. (2006) paper. The parameters were analysed under four different bulk concentrations ranging from 1 g/l through to 8 g/l. This bulk concentration, C_b, is equivalent to MLSS in a wastewater treatment plant. The fit between experimental and theoretical is very good in these plots, which is probably due to the fact that only one fouling mechanism at a time is considered, and the model solutions are single phase only and filtration only occurs in simple dead end mode.

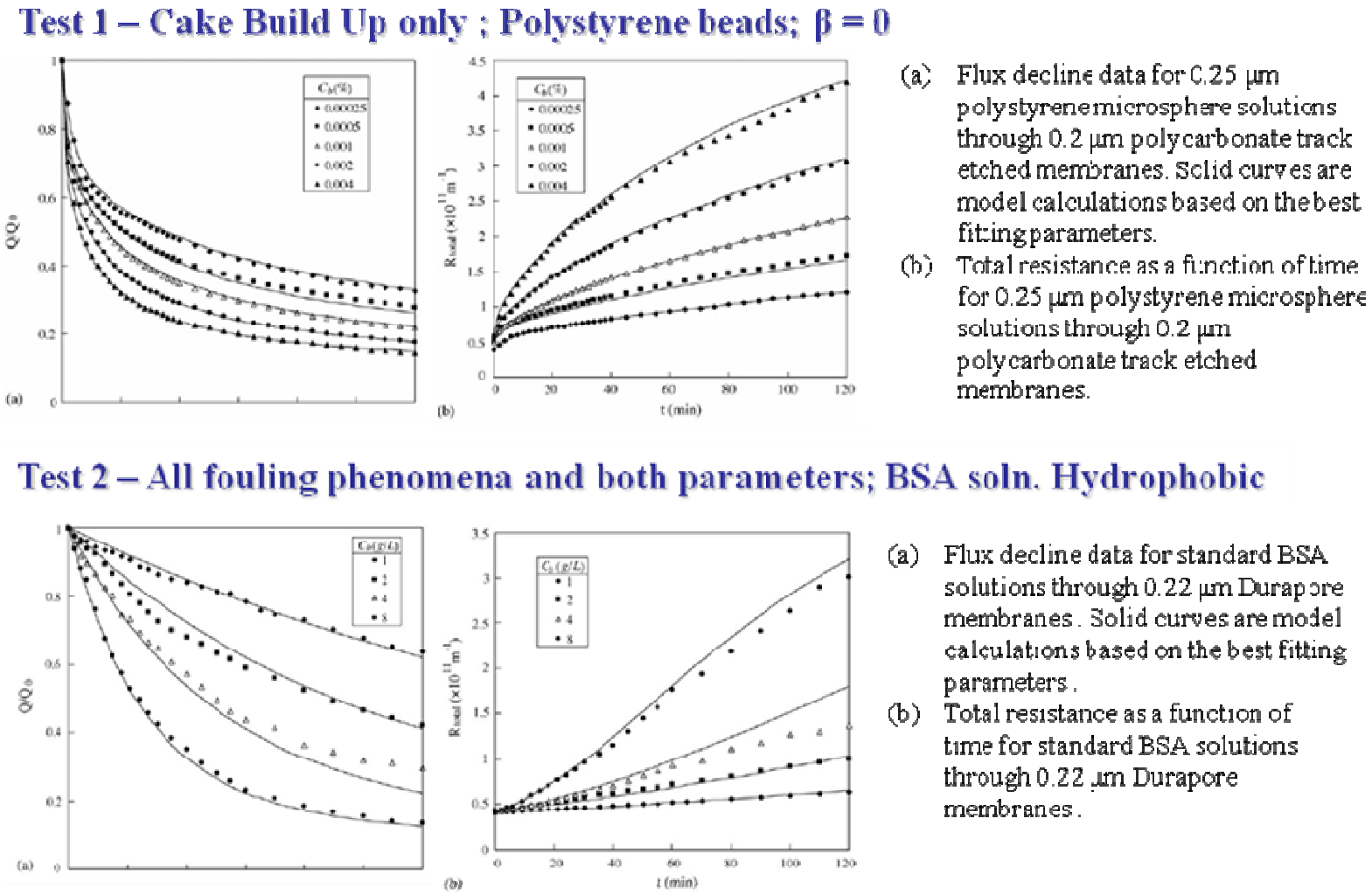

Fig. 4.2: Duclos-Orsello (2006) fouling model - experiments and model simulations 1.

(a) Flux decline data for 0.25 μm polystyrene microsphere solutions through 0.2 μm polycarbonate track etched membranes. Solid curves are model calculations based on the best fitting parameters.

(b) Total resistance as a function of time for 0.25 μm polystyrene microsphere solutions through 0.2 μm polycarbonate track etched membranes.

(a) Flux decline data for standard BSA solutions through 0.22 μm Durapore membranes. Solid curves are model calculations based on the best fitting parameters.

(b) Total resistance as a function of time for standard BSA solutions through 0.22 μm Durapore membranes.

Test 3 – Pore constriction only ; pre-filtered BSA soln.
Hydrophobic; Rp0 = 0 ; α = 0

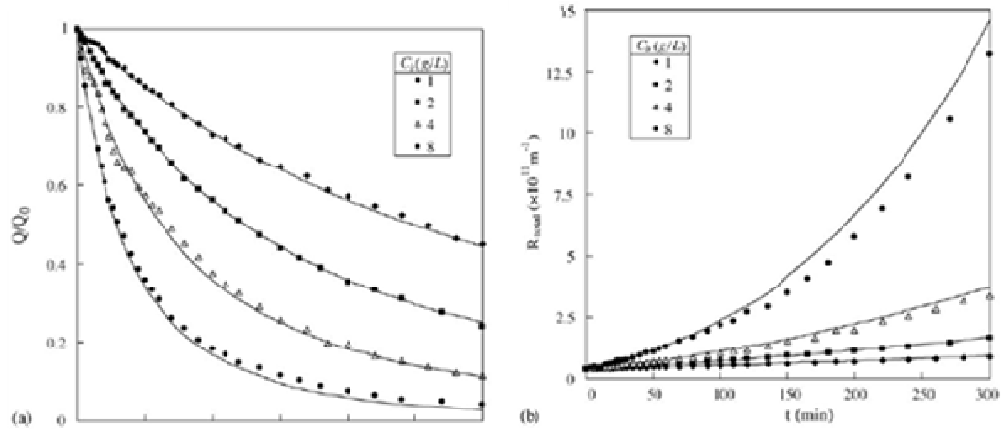

(a) Flux decline data for 0.1 μm prefiltered BSA solutions through 0.22 μm Durapore membranes. Solid curves are model calculations based on the best fitting parameters.

(b) Total resistance as a function of time for 0.1 μm prefiltered BSA solutions through 0.22 μm Durapore membranes.

Test 4 – All phenomena except Pore constriction; BSA soln.
Hydrophilic; β = 0

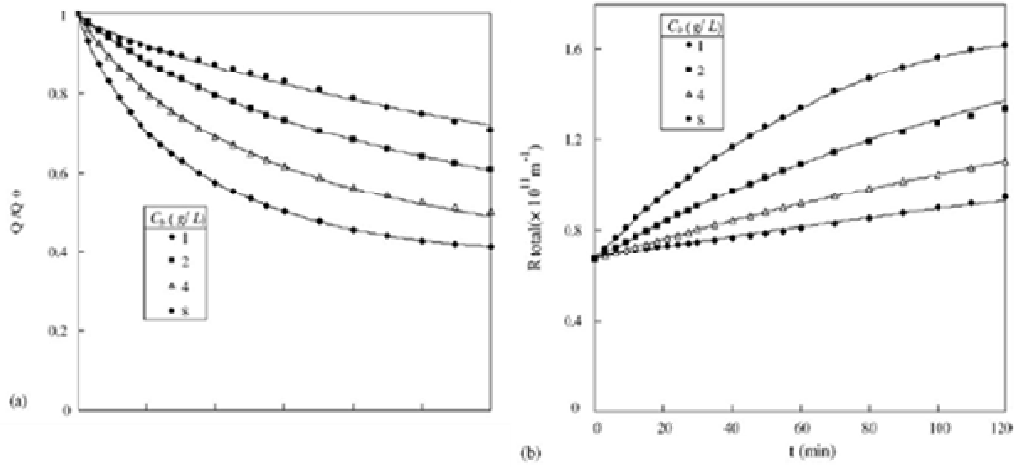

(a) Flux decline data for standard BSA solutions through 0.22 μm Durapore membranes. Solid curves are model calculations based on the best fitting parameters.

(b) Total resistance as a function of time for standard BSA solutions through 0.22 μm Durapore membranes.

Fig. 4.3: Duclos-Orsello (2006) fouling model - experiments and model simulations 2.

4.1.3 Improvements and modifications to Duclos-Orsello's approach

The following shortfalls listed below were found in the Duclos-Orsello et al. (2006) approach. Subsequently in a bid to make this model more practical and usable for a typical MBR plant situation, this approach was extensively modified under this study (Paul et al. 2007).

- Since he uses solutions from solved differential equations when calculating the flow through the un-blocked membrane area, the state variables in the study must remain constant during any simulation. In a real life plant this is not the case, with say the MLSS concentration which is analogous to the C_b parameter (bulk concentration) in this model, often changing significantly in time. So any altered model formulation procedure must allow for this fact.
- Since he uses an integral expression to calculate the flow through the blocked membrane area, the initial conditions in this study must remain fixed in any simulation, and any simulation must always commence from this point. In any useful simulation model, the user must be able to state different and varied initial conditions, and also be able to start a simulation from any point in time. So any altered model formulation must cater for this modelling issue.
- The integral expression means the TMP is kept constant during the simulation, and therefore the mathematical formulation of this model cannot be used for varying TMP situations which occur in many real life plant.
- This model formulation assumes pore constriction stops as soon as pore blockage occurs. This may not be the case as experienced in real life membrane fouling within a MBR system.

In order to overcome these deficits in the model formulation, the following modified mathematical solution was used:

1. When calculating the flow through the un-blocked membrane area, the model is formulated to use the original differential equations so that any state variables can be varied in time. This altered model formulation also has the further benefit of allowing parameter sets to be optimized using measured data values as is carried out in Section 4.1.4 below.

   Hence the change in flow rate through the open pores, Q_u, in the reducing unblocked membrane area, A_u, is calculated from Equation 4.4. This reduction in unblocked area is calculated from the differential Equation 4.5 where the unblocked flux, J_u, is itself determined from differential Equation 4.6.

$$Q_u = J_u \cdot A_u \tag{4.4}$$

$$\frac{dA_u}{dt} = -\alpha \cdot Q_u \cdot C_b = -\alpha \cdot J_u \cdot A_u \cdot C_b \tag{4.5}$$

$$\frac{dJ_u}{dt} = \frac{-2\beta Q_0 \cdot C_b}{\sqrt{J_0}} \cdot {J_u}^{3/2} \tag{4.6}$$

2. When calculating the flow through the increasingly blocked membrane area, the model is formulated so that once again the original differential equations are solved numerically rather than trying to solve an integral equation analytically. This means initial conditions can be varied and dynamic simulations can be run from any point in the simulation period.

The solving procedure is as follows. The change in flow rate through the closed pores, Q_b, in the increasing blocked membrane area, A_b, is calculated from Equation 4.7 which is based upon Darcy's Law, $J_b = \frac{\Delta p}{\mu \cdot (R_{total})}$. This increase in blocked area is calculated from the differential Equation 4.8 where the rate of change in blocked area is equal to the rate of change in unblocked area but negative.

The resistance of the membrane in Equation 4.7 is made up of the initial blocked membrane resistance, R_{inb}, and the growing external cake layer resistance, R_p. R_{inb} is calculated from Equation 4.9 where R_m is the clean membrane resistance, whilst R_p is determined from the differential Equation 4.10 where f' is the fraction of foulants in the mixed liquor that cause the build up of the cake layer and R' is the specific protein layer resistance.

$$Q_b = \frac{\Delta p}{\mu(R_{inb} + R_p)} \cdot A_b \tag{4.7}$$

$$\frac{dA_b}{dt} = \frac{-dA_u}{dt} = \alpha \cdot J_u \cdot A_u \cdot C_b \tag{4.8}$$

$$\frac{dR_{inb}}{dt} = \beta \cdot Q_0 \cdot C_b \cdot \sqrt{R_m} \cdot \sqrt{R_{inb}} \tag{4.9}$$

$$\frac{dR_p}{dt} = f' R' J_b \cdot C_b \tag{4.10}$$

3. It has been observed in practice that membrane pore constriction continues even after solids cake build up in a MBR system (Drews et al. 2007a). This is because in real life the range of particle size distribution of the mixed liquor particles and colloids is very large as well as the pore size distribution of the membrane pores themselves. This means smaller colloids can be transported through the poorly packed porous cake layer into larger pores even though they may be partially occluded by larger particles.

   Hence the blocked membrane resistance, R_{bl}, in this modified formulation is also composed of the pore constriction resistance which will continue even after the pore is blocked. R_{bl} is calculated from Equation 4.11 where the continuing pore constriction is added to the initial blocked membrane resistance, R_{inb}. The original model formulation of Duclos-Orsello et al. (2006) does not allow this process to happen.

$$R_{bl} = R_{inb} + R_p \tag{4.11}$$

The final modified and improved version of the Duclos-Orsello et al. (2006) approach can be summarised by Equation 4.12 which determines the total flow through the membrane while all three mechanisms take place.

$$Q_t = J_u \cdot A_u + \frac{\Delta p}{\mu(R_{inb} + R_p)} \cdot A_b \tag{4.12}$$

This new model formulation should allow it to be used for practical purposes such as for predicting the fouling rate on a real life MBR plant, and for the operation and automatic control of the plant. However any new MBR model would also need to include a plant layout with hydrodynamic regime, and would need calibration with actual measured data values.

4.1.4 Simulation and model calibration work using Duclos-Orsello data

The accuracy of this modified approach was confirmed using the experimental data from Duclos-Orsello et al. (2006) and by producing a Matlab/SIMULINK© model of this approach (as shown in Fig. 4.4). The Matlab/SIMULINK© platform is a good development tool for solving problems with differential equations. This SIMULINK© model would also allow dynamic simulations with parameters that are changeable in time. This further allows the utilisation of optimisation toolboxes in SIMULINK©. Parameter optimisation of this formulated model is a very important capability since some of these parameters in a real life MBR plant would relate to several operational influences on the fouling mechanisms like air-sparging, cross flow velocities, etc, which could then be reflected in these parameters.

Consequently the experimental data and parameter values from the Duclos-Orsello et al. (2006) paper were used in the modified model formulation. The solution was slightly different from the original paper's results. However by using the SIMULINK© Genetic Algorithm Toolbox, the pore blockage parameter, α, the pore constriction parameter, β, and the fractional foulant specific cake layer resistance, $f'R'$, were made to fit the normalised flow rate data as shown in Fig. 4.5. The fit between experimental and theoretical is very good in this plot again probably due to the fact that only one fouling mechanism at a time is considered and the model solution is single phase only and filtration only occurs in simple dead end mode.

In Fig. 4.5, the circles represent the measured normalised flow rate values and the lines the fitted dynamic model values using optimised parameters found by the genetic algorithm method. Hence this modified model formulation would allow the creation of a plant layout with a practical fouling model that could be validated and calibrated using the real life plant's own measured data. This is a huge improvement on the original model formulation which was set up only for a laboratory analysis situation.

4.1.5 Sensitivity analysis of model parameters

Following verification of the modified model formulation, a sensitivity analysis was carried out for the three main parameters in this fouling model, namely the pore blockage parameter, α, the pore constriction parameter, β, and $f'R'$ which is the fractional foulant layer specific resistance. This sensitivity analysis was carried out to see which model parameters were most responsive under different simulated operational conditions for a MBR plant. The parameters were analysed under four different bulk concentrations, C_b), ranging from 1 g/l through to 8 g/l. Several simulations were completed for different combinations of parameter values, however for the sake of brevity only some results can be commented on (Paul et al. 2007). Table 4.3 lists three of the most interesting simulations carried out.

Simulation No.	α	β	$f'R'$	$\frac{R_{p0}}{R_m}$
1) equivalent to: *normal MBR operation conditions.*	0.0001	0.1	4 x 10^9	0.5
2) equivalent to: *SMP formation conditions.*	0.1	10	4 x 10^{10}	0.7
3) equivalent to: *Extreme lab SMP formation conditions.*	10	300	4 x 10^{11}	0.9

Table 4.3: Simulation parameters for sensitivity analysis

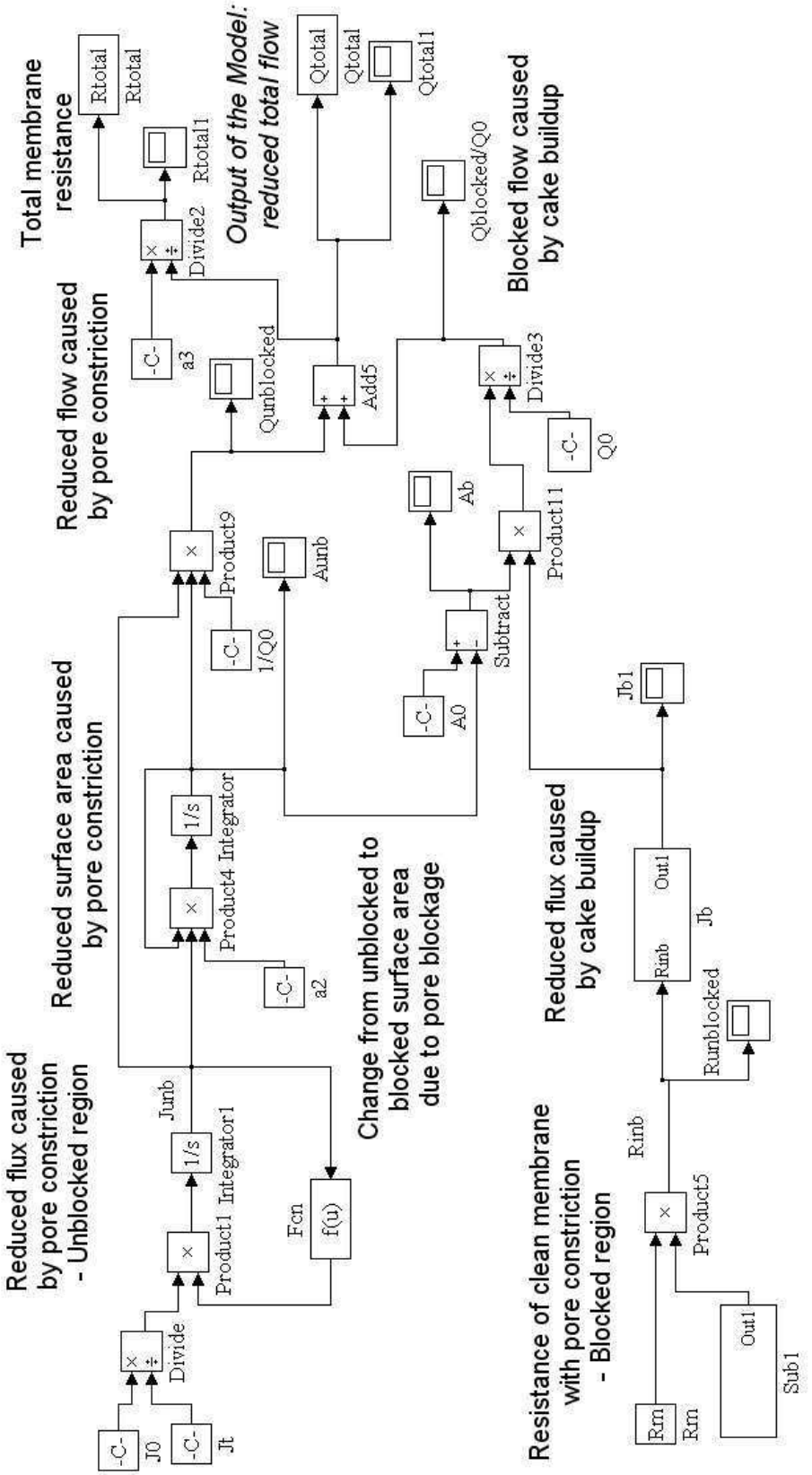

Fig. 4.4: Matlab/SIMULINK modified formulation of Duclos-Orsello (2006) fouling model of microfiltration membranes.

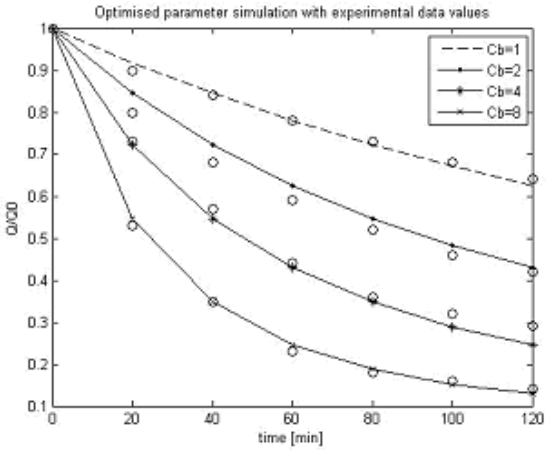

Fig. 4.5: Comparison of optimal parameter simulation plot with experimental data values from the Duclos-Orsello paper

In Simulation 1, the values of α and β are small with also a low specific resistance of the fraction of foulants on the membrane, $f'R'$. Fig. 4.6 shows there is a progressive almost linear increase in membrane fouling resistance.

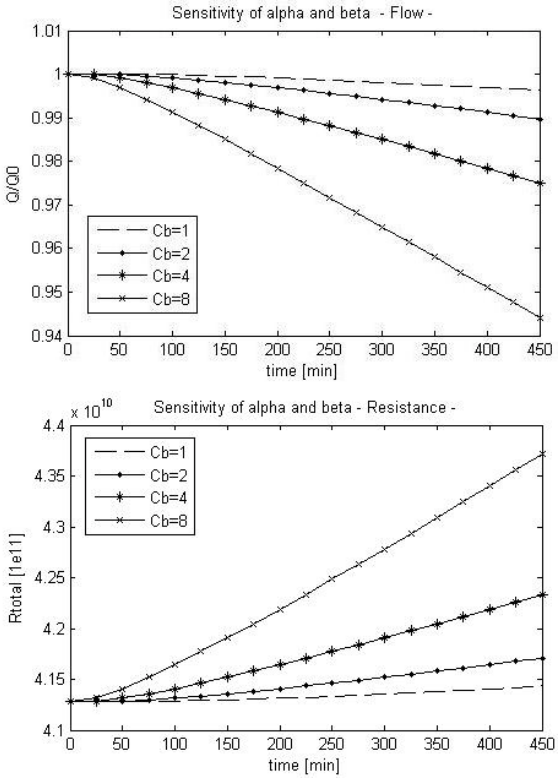

Fig. 4.6: Sensitivity analysis for small α, β and $f'R'$ values.

In Simulation 2, α and β values are large with a subsequent higher $f'R'$ value. Fig. 4.7 shows that the fouling resistance is very non-linear for high bulk concentrations.

In Simulation 3, α and β values are extremely large with a subsequent much higher $f'R'$ value. Fig. 4.8 shows a dramatic drop in the flow through the membrane with the fouling resistance being very non-linear for all bulk concentrations.

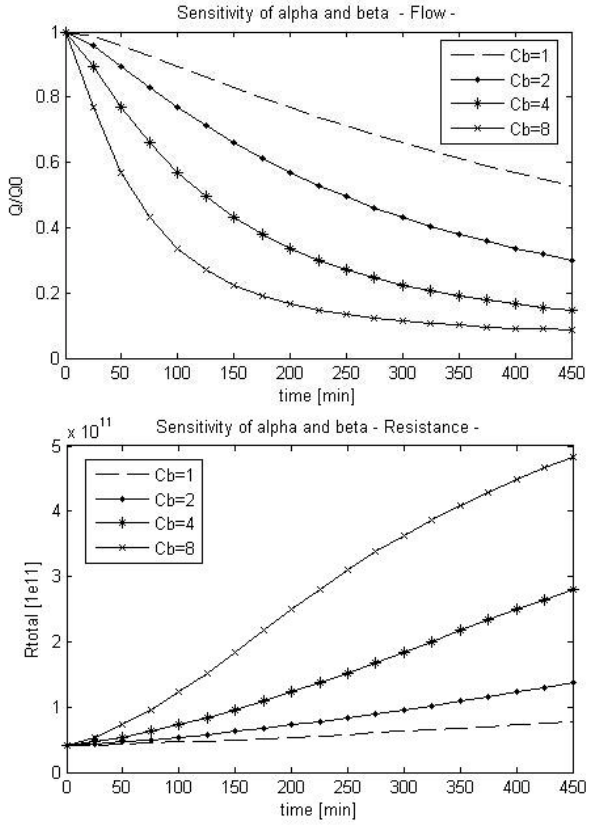

Fig. 4.7: Sensitivity analysis for large α, β and $f'R'$ values.

The outcomes of the sensitivity analysis seem to indicate that the Simulation 1 situation refers to the normal operational mode of a MBR membrane where effective CiP measures are limiting pore constriction and especially cake build up. Simulation 2 on the other hand is analogous to a situation when **SMP** builds up in the MBR reactor due to "stressed" microbial biomass producing it under unusual operational and environmental conditions, e.g. low temperatures, low DO conditions, high salinity of mixed liquor, etc. Here the CiP procedures are insufficient to arrest the membrane fouling and more drastic measures such as aggressive chemical cleans are needed to regain flux. Simulation 3 would not occur in practice unless in a laboratory situation since there is a dramatic loss in flux with instant clogging of the membranes by all three fouling mechanisms. However it does prove useful since it shows the model can be used to demonstrate the TMP jump experienced in practice under extreme conditions.

In purely physical terms the pore constriction parameter, β, clearly governs the intrinsic membrane fouling caused by colloidal and soluble protein material. In the case of a MBR, β would relate to the pore size distribution of the membrane, the membrane hydrophobicity, and the aggregation effect of proteins and polysaccharides as **SMP**. It must be remembered that the typical size of protein macro-molecules, colloids and colloidal aggregates range from nanometres to tens of nanometres whereas the microfiltration membrane pore size range varies from 100 to 200 nanometres. β would also slightly depend on the MLSS concentration, as large particles can impede the flow of colloids to the membrane surface and walls. It is worth noting that the majority of the experiments carried out to test the original model were conducted using model protein solutions ranging from concentrations of 1 g/l up to 8 g/l with no solids in the solution to impede pore constriction effects. Usually in a MBR the MLSS is much higher but is composed of mainly particulates while the **SMP** concentration varies from 100 to say 500 mg/l depending on microbial "stress" conditions. Hence the experimental measured rate of fouling is significantly higher than would ever be experienced in a real plant.

The parameter α refers to cake build up and in the sensitivity analysis includes for the effects due to the CiP mitigation measures and MLSS concentrations effects. This physically means the bulk concentration of solids in the solution and the types and extent of CiP measures would directly influence the α value. The

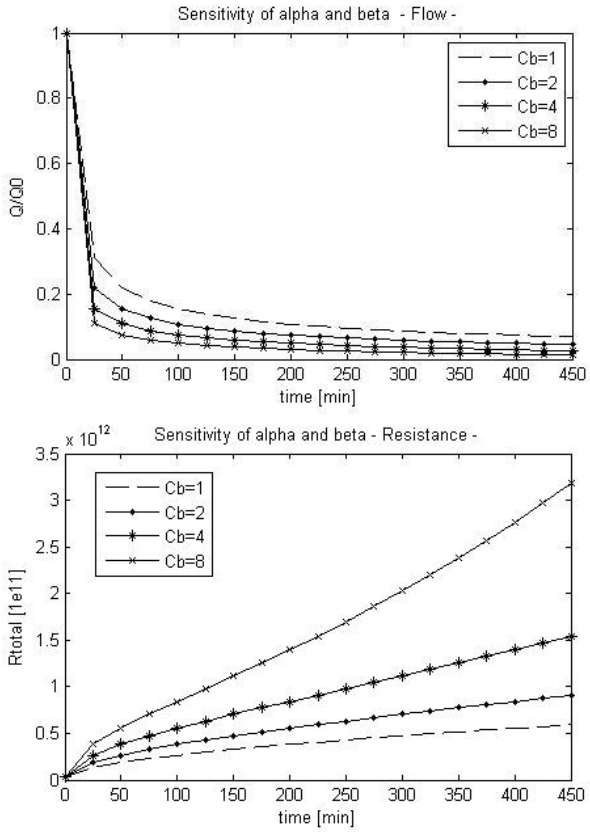

Fig. 4.8: Sensitivity analysis for extremely large α, β and $f'R'$ values.

α value would also indirectly include biomass floc size and species diversity, so that if filamentous bacteria predominated then cake build up would be more rapid with subsequent increased α values.

The combined parameter $f'R'$ could be correlated in real terms to the biofilm growth on the surface of the membrane. This parameter would then be influenced by the biofilm properties such as adhesiveness, thickness and porosity, and as well as the membrane surface roughness.

Consequently this modified fouling model described in Paul et al. (2007) is rich enough to be able to express within its main parameters the main effects found in a typical MBR membrane situation . However it would still need to be modified to match local MBR configurations and hydrodynamic operational conditions as detailed in Section 4.1.6.

4.1.6 Reformulation of Duclos-Orsello model for specific MBR plant layouts used in this study

This modified fouling model needs to include hydrodynamic effects for the various MBR plant (and the membrane filtration unit) used in this study that are used to generate the data needed to test this modified model. Hydrodynamically speaking this means inclusion of the following effects for specific plant as detailed in Section 4.1.6.1 and Section 4.1.6.2:

- Membrane surface scour which occurs in both submerged and crossflow sidestream MBR plant. In submerged plant this is usually a constant air scouring and sparging by coarse bubble aeration (as is the case with the ITT Sanitaire submerged pilot MBR plant operated at Coors UK Limited). For crossflow sidestream plant this membrane scouring effect is due to constant CFV from continually recirculating mixed liquors from the bioreactor (as is the case with all Aquabio's crossflow plant).
- A backwash mode which is used to remove material accumulated within the membrane by reversing the permeate flow rate. This is usually for a fixed periodic interval of constant duration and intensity (as is the case with the Aquabio crossflow pilot plant, and ITT Sanitaire's pilot membrane filtration unit operated in dead end mode at Cardiff Wastewater Treatment Works).

As mentioned in Section 2.2.1, all researcher's agree that the pore blocking and pore constriction mechanisms within a MBR are largely due to the build up of **SMP** and free EPS. This correlation can be catered for in this model by replacing the bulk concentration term with a new term which relates to **SMP** effects (see Section 4.1.6.3 below).

One final reformulation of the model outlined in Section 4.1.6.4 allows the model to be used for varying TMP operational conditions such as occurred with ITT Sanitaire's pilot membrane filtration unit.

4.1.6.1 Membrane surface scour effects inclusion

The following model equations are altered to cater for these specific hydrodynamic effects:

In Equation 4.10, an additional term for scour is added to reduce the cake build up accordingly. Again in this case C_b refers to MLSS of a MBR. This additional term which is the cake resistance multiplied by a constant term (which itself is a function of air sparging rate or CFV), allows cake to be removed.

$$\frac{dR_p}{dt} = f'R'J_b \cdot C_b - k_p(CFV) \cdot R_p \tag{4.13}$$

In Equation 4.5, an additional term for scour is added to increase the unblocked area of the membrane accordingly. In this case C_b refers to MLSS of a MBR. This additional term which is the blocked area (reset after a backwash interval) multiplied by an area constant term (which is a function of of air sparging rate or CFV), allows unblocked area to increase with increased scouring rate.

$$\frac{dA_u}{dt} = -\alpha \cdot J_u \cdot A_u \cdot C_b + k_b(CFV) \cdot (A_0(after_{backwash}) - A_u) \tag{4.14}$$

4.1.6.2 Backwash mode inclusion

The following model equations are added to the formulation to cater for these specific hydrodynamic effects:

For simplicity's sake, it is assumed that changing to the backwash mode does not take any time, i.e. it occurs instantaneously.

Equation 4.15 simply resets the cake resistance by a certain amount after the backwash step has occurred. This reset can be altered to cater for full membrane recovery or for complete membrane clogging.

$$R_p(after_{backwash}) = f_{rp} \cdot R_p(before_{backwash}) \tag{4.15}$$

where $R_p(after_{backwash})$ = cake resistance after backwash time.
where $R_p(before_{backwash})$ = cake resistance before backwash time.

when $f_{rp} = 1$ means no recovery (complete clogging);
and when $f_{rp} = 0$ means full recovery. Usually use a figure of 0.05 is used for an ideal system.

Equation 4.16 simply resets the blocked area by a certain amount after backwash has occurred. This reset can be altered to cater for full membrane area recovery or for complete membrane area surface covering.

$$A_0(after_{backwash}) = f_{rAU} \cdot A_0 + (1 - f_{rAU}) \cdot A_u(before_{backwash}) \tag{4.16}$$

where $A_0(after_{backwash})$ = Original unblocked area after backwash time.
where $A_u(before_{backwash})$ = Unblocked area before backwash time.

when $f_{rAU} = 0$ means no recovery;
and when $f_{rAU} = 1$ means full recovery. Usually use a figure of 0.95 is used for an ideal system.

4.1.6.3 SMP effects inclusion

In Equation 4.6, the C_b term which refers to MLSS is changed into the concentration of **SMP** (or EPS). This then directly takes into account the effect of the sludge water properties on pore constriction. The revised formula is:

$$\frac{dJ_u}{dt} = \frac{-2\beta Q_0 \cdot S_{SMP}}{\sqrt{J_0}} \cdot {J_u}^{3/2} \tag{4.17}$$

where S_{SMP} = concentration of **SMP** in the sludge water.

4.1.6.4 Reformulation of formulae for constant flux operation with variable TMP

This further reformulation allows data to be used which was collected under varying TMP with constant flux stepping conditions, such as is the case with the ITT Sanitaire membrane filtration plant operated at Cardiff WWTP which was operated under these specific conditions. This is as opposed to the Aquabio pilot MBR plant which was operated under constant TMP with variable flux conditions. It is worth remembering that since over 90% of MBRs operate in constant flux mode as they are submerged systems, then this model reformulation should reflect this situation.

Using Equation 4.18:

$$Q_b = J_b \cdot A_b = \frac{\Delta p}{\mu(R_{inb} + R_p)} \cdot A_b \tag{4.18}$$

Rearranging to Equation 4.19:

$$\Delta p = \mu(R_{inb} + R_p) \cdot J_b \tag{4.19}$$

Differentiating both sides, with μ taken as a constant and setting Δp = TMP, gives:

$$\frac{dTMP}{dt} = \mu \cdot \frac{d}{dt}(J_b \cdot R_{inb} + J_b \cdot R_p) \tag{4.20}$$

Then using the Product Rule (Leibniz's Law) to find the derivatives of the products of these functions gives:

$$\mu \cdot \frac{dTMP}{dt} = (J_b \cdot \frac{dR_{inb}}{dt} + R_{inb} \cdot \frac{dJ_b}{dt}) + (J_b \cdot \frac{dR_p}{dt} + R_p \cdot \frac{dJ_b}{dt}) \tag{4.21}$$

This can be simplified to the following:

$$\mu \cdot \frac{dTMP}{dt} = J_b \cdot (\frac{dR_{inb}}{dt} + \frac{dR_p}{dt}) + (R_{inb} + R_p) \cdot \frac{dJ_b}{dt} \tag{4.22}$$

Thus, Equation 4.22 allows the TMP to be a variable value for a constant flux, and replaces Equation 4.7 in the model formulation procedure.

4.2 *Phenomenological membrane fouling model - results and discussion*

The extensive phenomenological model formulation described in the previous section was tested by using real life plant data sets collated specifically for this purpose. Hence the model was calibrated and validated using the Matlab/SIMULINK© software package in order to investigate how accurate a formulation it proved for the specific model parameters involved, and how complex or simple a step this is when measured against other model types used later in this Chapter (see Section 4.3). Flux stepping data sets from the Aquabio pilot MBR plant and the ITT Sanitaire pilot membrane filtration unit were used in this regard. The next section details the model outputs and results obtained from utilising these data sets.

4.2.1 Simulation results from Aquabio pilot MBR plant

4.2.1.1 Data set used from Aquabio pilot MBR plant

As mentioned earlier flux stepping tests were carried out on the novel vertical air-lift sidestream MBR pilot plant detailed in Section 3.4.2.7 over a two day period for differing recirculation pump speeds and flux step duration periods. This included off-line tests measuring MLSS concentrations, as well as EPS and **SMP** levels in the sludge water which are the main foulants on the membrane (Drews et al. 2008). The flux stepping results were filtered to remove the major permeate flow oscillations associated with the backflushing procedure, and also to remove periods that occurred inadvertently during some flux steps when the plant automatically shutdown. These periods occurred when the throttle valve settings were either fully or almost fully open, or when fully closed or almost fully closed. When in the open valve setting position, it meant the inverter load on the recirculation pump exceeded high level load settings, which when exceeded automatically shutdown operations to protect the pump motor from excessive voltages. Conversely in the closed valve setting position, the very large pressure generated across the inlet and outlet of the membrane meant almost immediate enormous cake build up and pore blocking, leading to very reduced flux rates which then dropped below the automatic minimum shutdown level for the plant, thus triggering this automated shutdown event. The filtered data set is shown in Figs. 4.9 and 4.10.

For the flux steps used, not all the curves proved to have a realistic uniform drop suitable for a model formulation. All curves first dropped rapidly as expected due to the immediate cake build up mechanism (itself due to MLSS), but some instead of then dropping at a reduced rate due to more slower pore constriction effects (due to **SMP**), just remained steady state for the rest of the step period. This flat lining to a steady state means that time dependent fouling conditions no longer dominate, and thus cannot be modelled by a continuous time dependant model. More flux steps needed to be carried out to minimise these anomalistic results, but due to the limited availability of the plant under this research study, it was not possible to carry out any further tests over subsequent days. Consequently only part of the filtered flux step data obtained was suitable to be used to test the model formulation. This reduced data set that was actually used to test the formulated Duclos-Orsello model is shown in Figs. 4.11 and 4.12.

The vast uncertainty in this membrane's performance appears to be because of a range of reasons, the main ones being related to the need to change significantly the operating conditions of the plant before any flux step could be run. The operational changes responsible for this erratic membrane fouling behaviour appear to be as follows with the ones thought most responsible listed first:

- Obviously any flux stepping procedure extends the membrane performance beyond the normal operating range used during standard operation, albeit for a limited short duration. In fact critical flux may be exceeded, especially in localised areas nearer the membrane inlet.
- As stated the specific need to change the throttle valve setting for every flux step, and whether stepping up or down by opening and closing the valve respectively, meant no consistency of operation. This throttling affect varied the generated flux enormously which obviously impinged upon

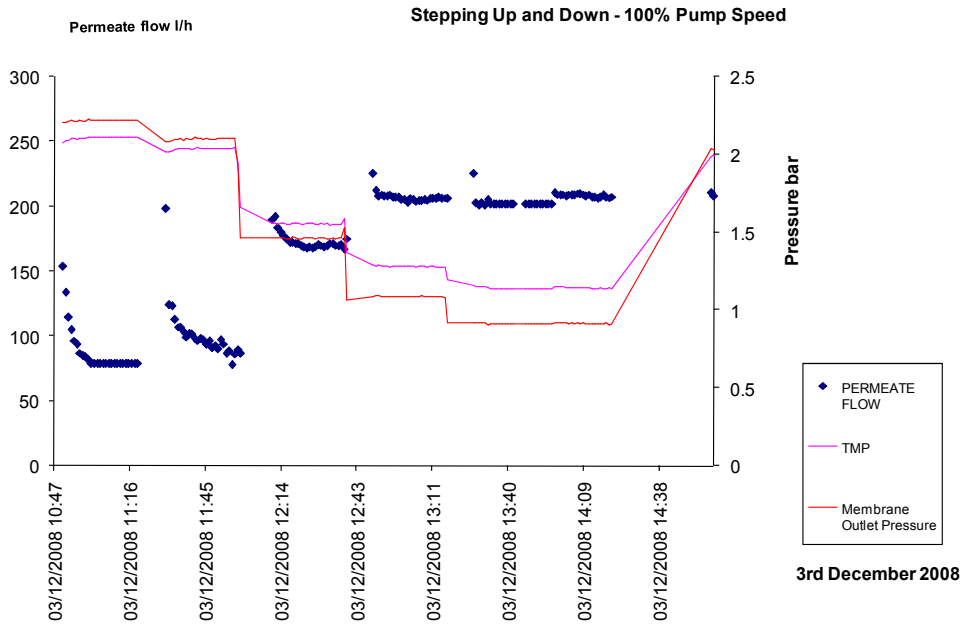

Fig. 4.9: Filtered flux stepping tests on 3rd December 2008

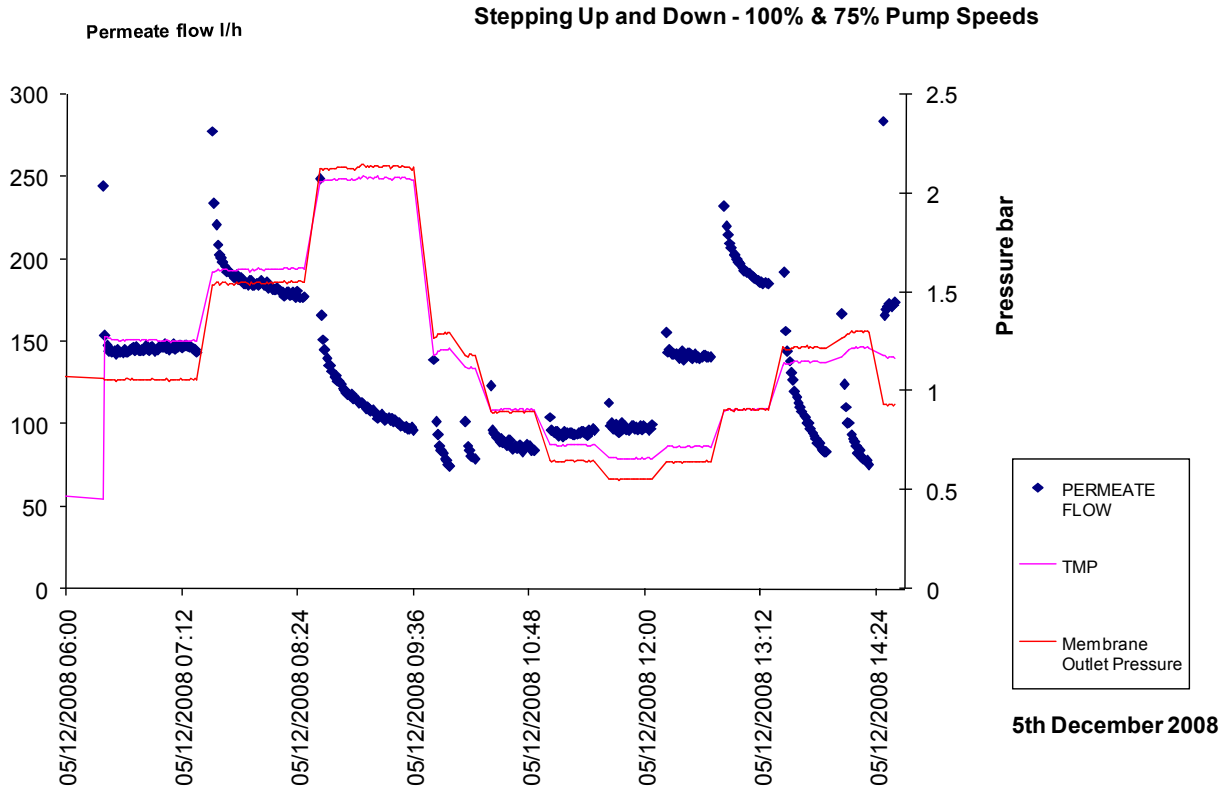

Fig. 4.10: Filtered flux stepping tests on 5th December 2008

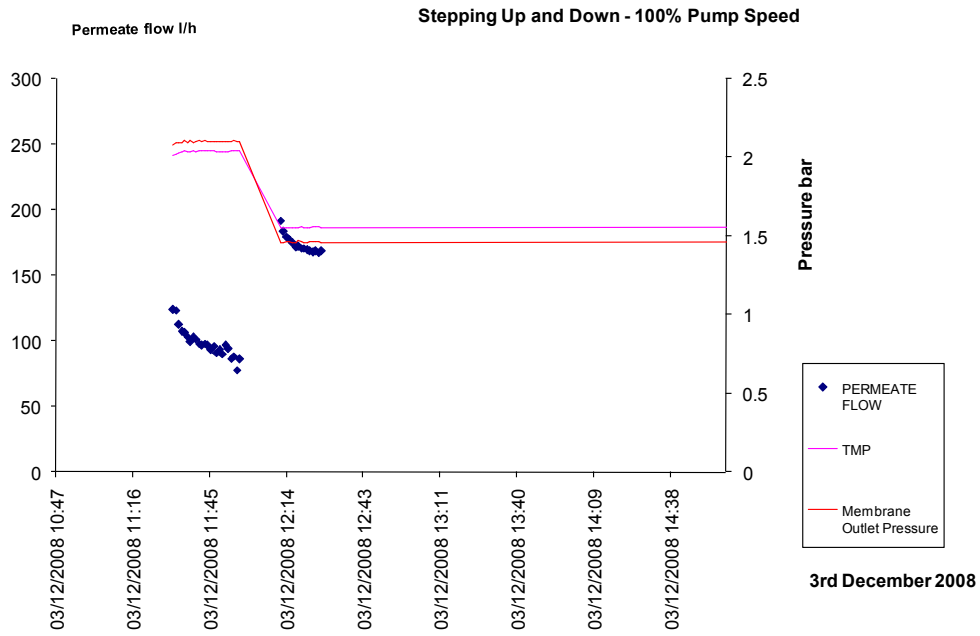

Fig. 4.11: Reduced flux stepping tests on 3rd December 2008

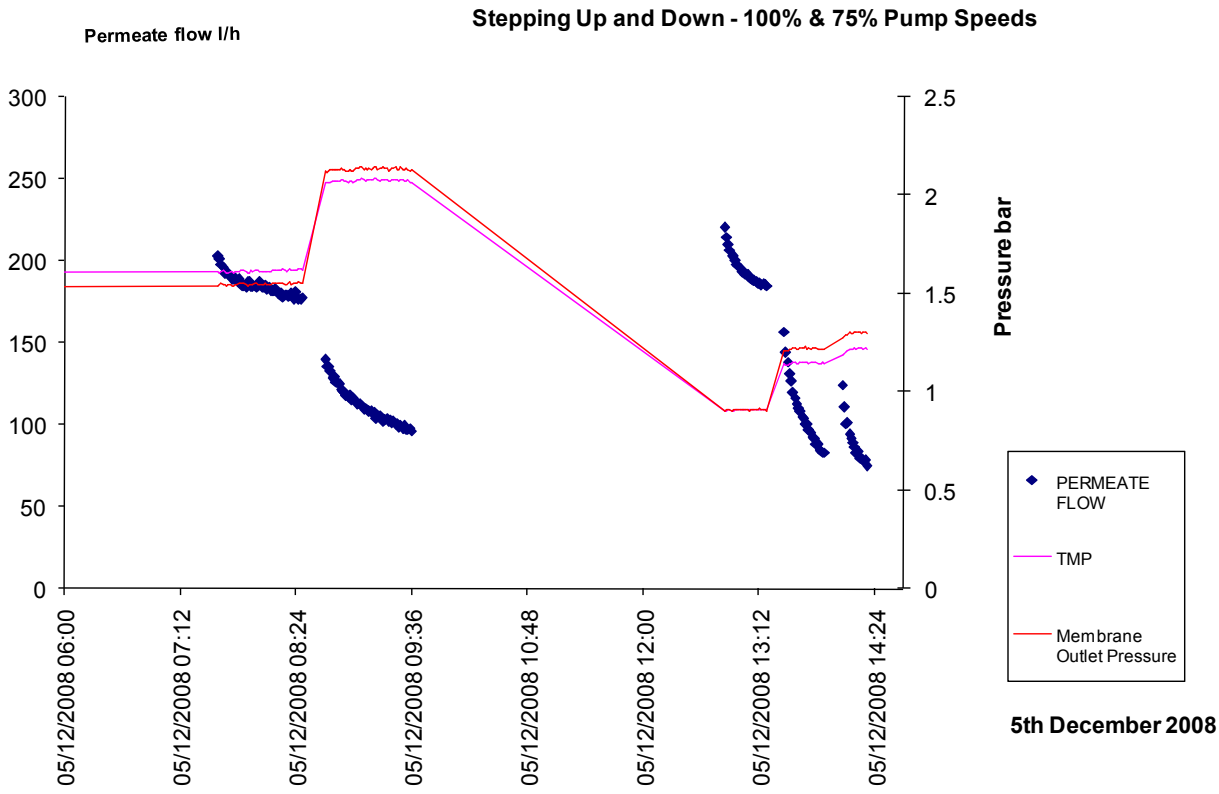

Fig. 4.12: Reduced flux stepping tests on 5th December 2008

the membrane modules hydrodynamic regime. Thus this constantly changing hydrodynamics greatly upset this plant's short term membrane performance, and led to increased performance instability due to greater localised sensitivities because of these constantly changing conditions. Conversely with a more standard constant flux operated plant which is the vast majority of MBR plant, the throttle valve settings are never altered, leading to consistent hydrodynamics.

- The changes in pump speed from 100% and 75% added further complexities to the hydrodynamic situation.
- The altering of the flux step duration from one hour to thirty minutes, again, added further complexities to the hydrodynamic situation.
- It appears that the previous membrane operating performance for that day before flux stepping began strongly influenced the results of the subsequent flux stepping tests. If under standard operation the membrane performance in terms of flux achieved proved consistent, then the follow-on flux step tests gave better results, especially in-line with fouling theory. This ability for the membrane to retain a "memory" of previous events by some sort of hysteresis of the fouling process even occurred from flux step to flux step. For instance if inadvertent automatic shutdown occurred due to the extreme valve settings described earlier, then the next flux step at the altered valve setting almost always proved not to give a smooth flux drop as expected with traditional fouling theory.
- Again alterations in backflushing regime carried out before the next step from two distinct 120 second backflushes running sequentially to a single equivalent backflush of 240 seconds length did not help the situation. Additionally the need to carry out the backflushes manually can also lead to discontinuities in the membrane performance.

For all these reasons, the membrane when under extreme operating conditions that occurred during some of the flux stepping procedure, did not perform consistently. As expected this erratic behaviour was more pronounced when the critical flux conditions were exceeded. For the flux steps, the flux rate could vary from anything like 25 $l/m^2/hr$ up to almost 60 $l/m^2/hr$. The bottom flux rate is well below a critical flux condition, whilst the top rate is close to or exceeding the critical flux rating, which if prolonged could eventually damage the membrane by introducing a permanent irreversible resistance which cannot be removed by chemical cleaning. The conclusion of this behaviour is that if the membrane is operated consistently and at a flux below critical, then performance was in-line with theory as occurred during normal standard operation before any flux steps were carried out. This means that any flux decline (or TMP increase) occurs only very slowly since fouling is minimised due to sub-critical flux operation.

4.2.1.2 Simulation results from all reduced flux stepping tests on 3rd December 2008

Fig. 4.13 shows the best of the measured data values that were used to calibrate and validate the model parameters. For the two flux steps selected, the first is close to exceeding critical flux, so that the α value that is calculated during the optimisation procedure is large as was the case during the sensitivity analysis scenarios described in Section 4.1.5 and in Table 4.3. In this figure, the first step has a high TMP and subsequent reduced permeate flow rate while the second step allows greater flow rate for a lower TMP. This is in line with theory as a higher TMP would cause greater membrane fouling.

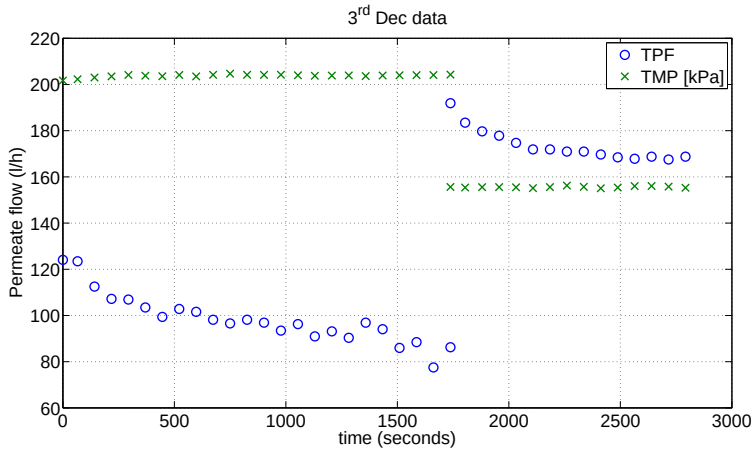

Fig. 4.13: Measured permeate flow for 2 flux steps on 3rd Dec 2008

Figs. 4.14 and 4.15 give the results from trying to fit the model using the calculated optimal parameter sets for both flux steps for the reduced data set for 3rd December 2008. The first figure shows the best fit for normalised permeate flow data so that a comparison can be made with the second day of flux stepping. The second figure shows the best fit using the actual permeate flow data. As can be seen, the fit is poor when using both flux step data simultaneously. This is since the GA fit value is too high at 15.8715 meaning a poor fit.

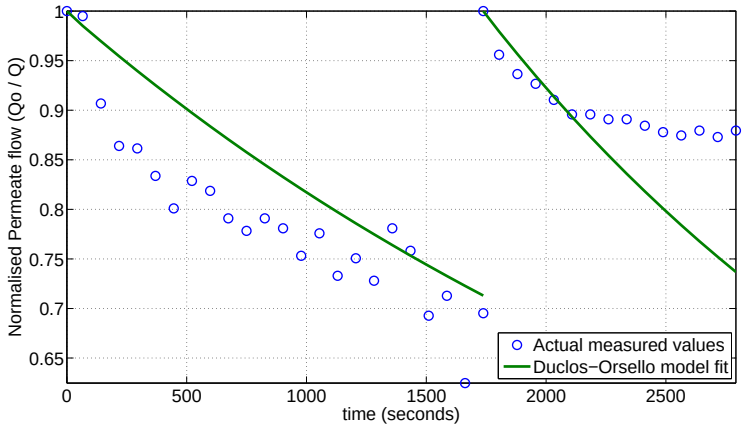

Fig. 4.14: Normalised permeate flow for 2 flux steps on 3rd Dec 2008 with best model fit

The poor fit is evidenced by the actual genetic algorithm run that was carried out to find the optimal parameter values as shown in Fig. 4.16. Hence the best and mean fits for the genetic algorithm run is still high when the procedure is completed for one hundred generations.

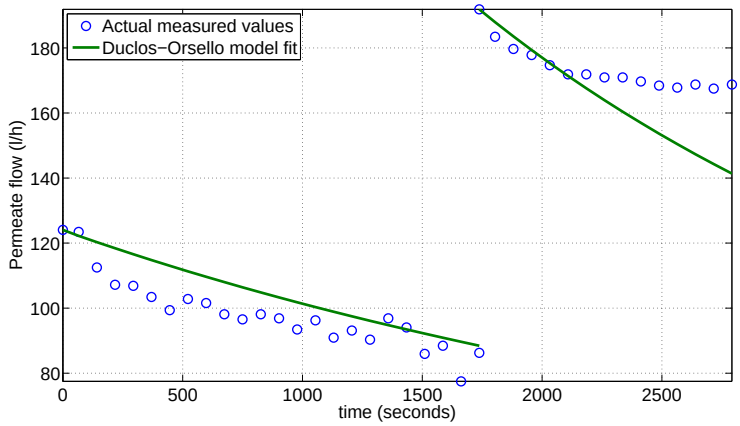

Fig. 4.15: Actual permeate flow for 2 flux steps on 3rd Dec 2008 with best model fit

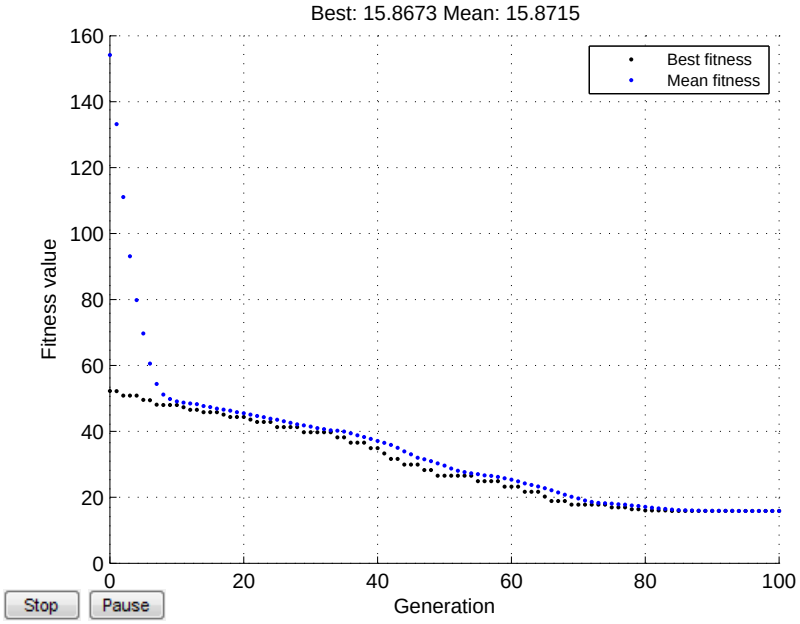

Fig. 4.16: Genetic algorithm run for 2 flux steps on 3rd Dec 2008 to find optimal model parameters

4.2.1.3 Simulation results from individual reduced flux stepping tests on 3rd December 2008

In an attempt to obtain a better fit to the data provided and also to take into account the huge operational differences between individual flux steps an altered optimisation procedure was used. Consequently instead of trying to fit both the chosen flux steps simultaneously, it was assumed that each flux step solution was unique due to the changing throttle valve setting significantly changing the hydrodynamics, etc.. This assumption would then mean that the data set used was discontinuous in time between flux steps, and therefore each step should be considered separately by the model on a individual data-by-data basis. This altered model optimisation procedure was tried to see if a better fit occurred.

Fig. 4.17 details the results from the first flux step of two for 3rd Dec 2008, which proved good. This is since the GA fit value is much lower at 4.4742 meaning a considerably improved fit.

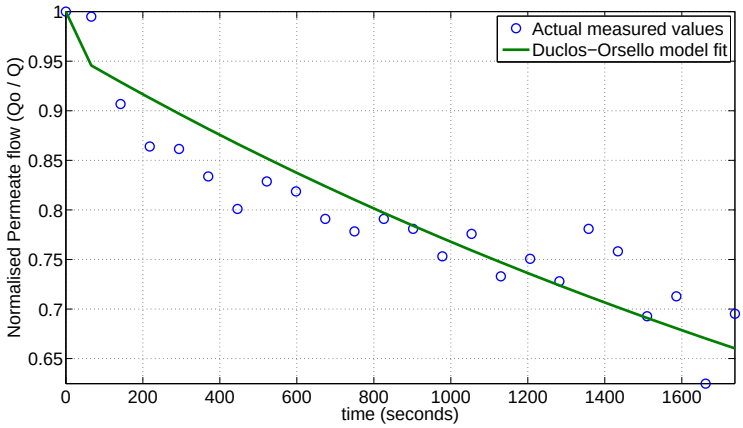

Fig. 4.17: Normalised permeate flow for first flux step of two on 3rd Dec 2008 with best model fit

The good fit is evidenced by the actual genetic algorithm run that was carried out to find the optimal parameter values as shown in Fig. 4.18. Hence the best and mean fits for the genetic algorithm run is low when the procedure is completed for one hundred generations.

Next, Fig. 4.19 details the results from the second flux step of two for 3rd Dec 2008, which proved an even better fit. This is as expected since the operational flux was well below critical. Again this is since the GA fit value is much lower at 3.0982 meaning a considerably improved fit.

This even better fit is evidenced by the actual genetic algorithm run that was carried out to find the optimal parameter values as shown in Fig. 4.20. Once again the best and mean fits for the genetic algorithm run is low when the procedure is completed for one hundred generations.

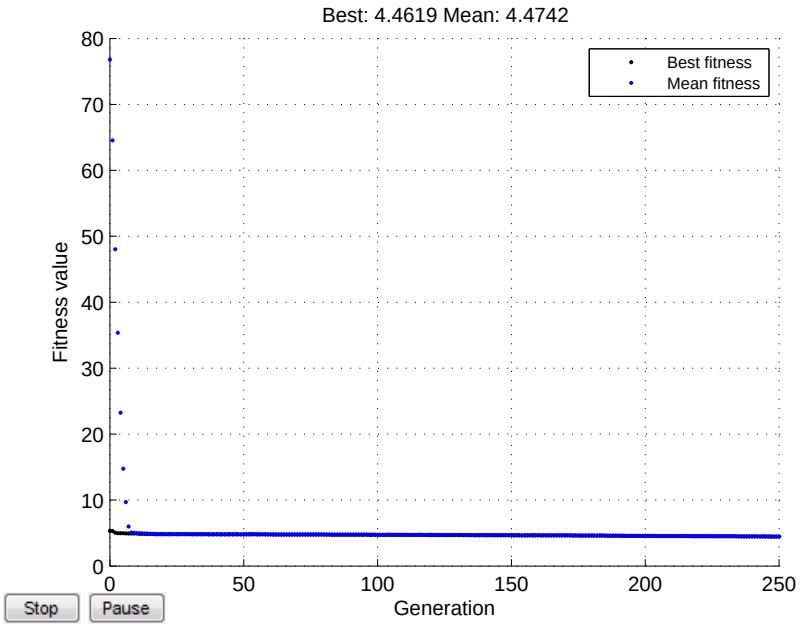

Fig. 4.18: Genetic algorithm run for first flux step of two on 3rd Dec 2008 to find optimal model parameters

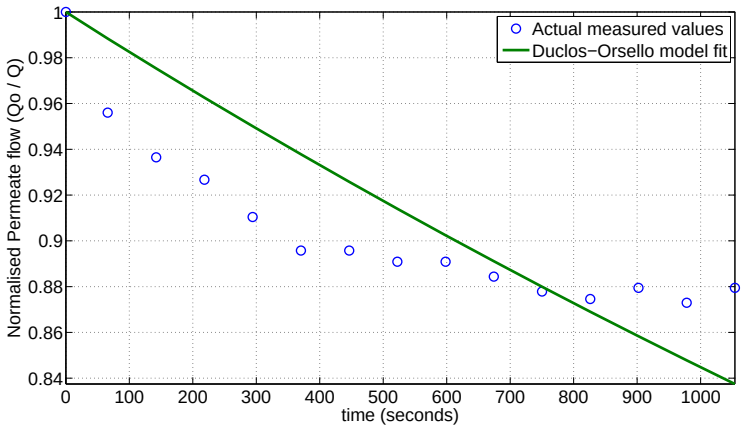

Fig. 4.19: Normalised permeate flow for second flux step of two on 3rd Dec 2008 with best model fit

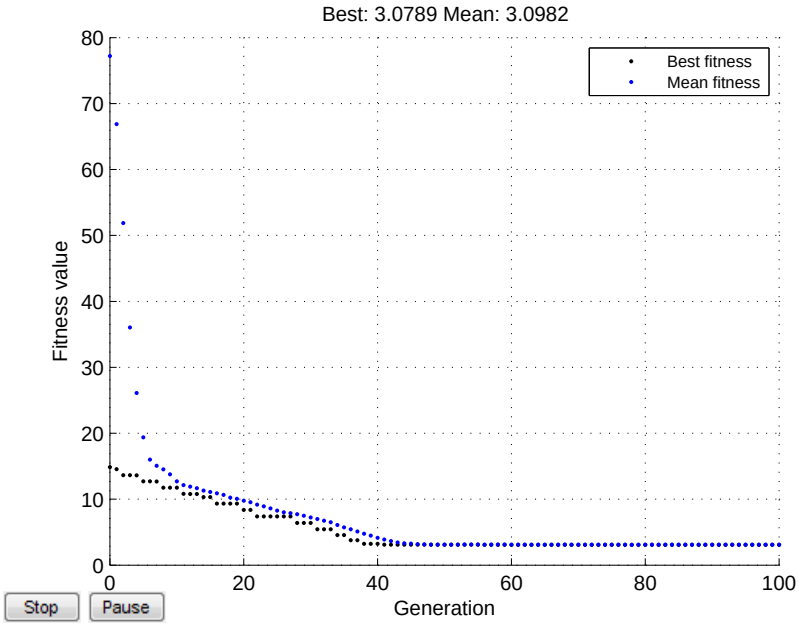

Fig. 4.20: Genetic algorithm run for second flux step of two on 3rd Dec 2008 to find optimal model parameters

4.2.1.4 Simulation results from all reduced flux stepping tests on 5th December 2008

For this second day of flux step testing, Fig. 4.21 shows the best of the measured data values that were selected and used to calibrate and validate the model parameters. For these five steps the variation in flux is considerable from anything like 27 $l/m^2/hr$ up to 55 $l/m^2/hr$.

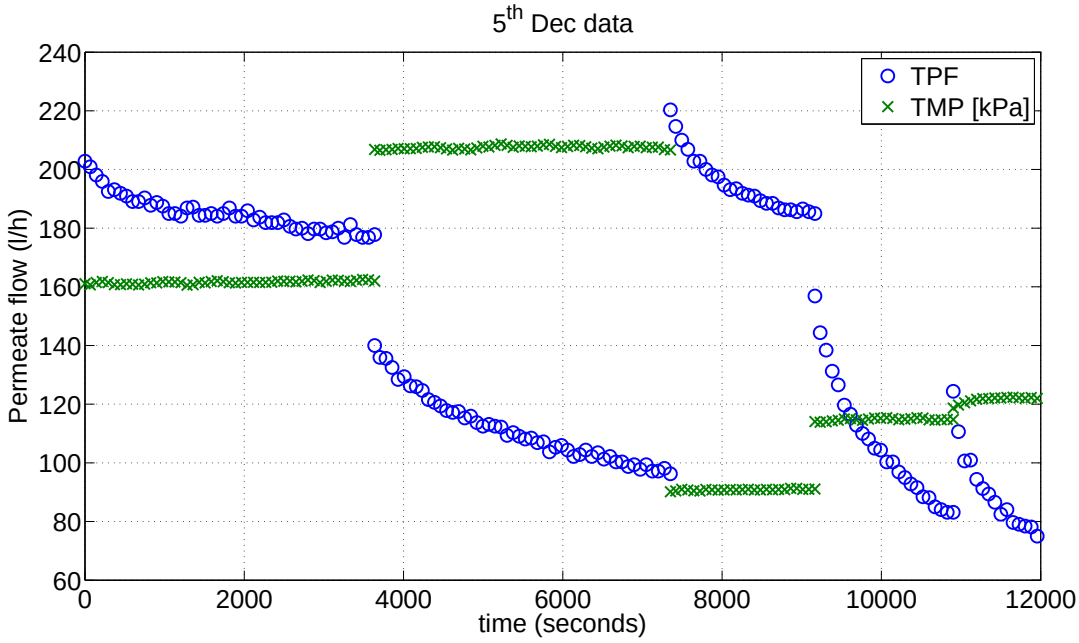

Fig. 4.21: Measured permeate flow for 5 flux steps on 5th Dec 2008

Once again like for the first day of testing, Figs. 4.22 and 4.23 give the results from trying to fit the model using the calculated optimal parameter sets for all flux steps for the reduced data set for 5th December 2008. The first figure shows the best fit for normalised permeate flow data so that a comparison can be made with the first day of flux stepping. The second figure shows the best fit using the actual permeate flow data. As can be seen, the fit is extremely poor when using all five flux step data simultaneously. This extremely poor fit seems to confirm the assumptions made earlier of regarding each flux step as a unique solution that should be tested separately.

Fig. 4.24 shows the genetic algorithm run to find optimal parameter values gave an extremely poor best and mean fit. This fit is still extremely poor even after two thousand generations have been run of the optimisation procedure.

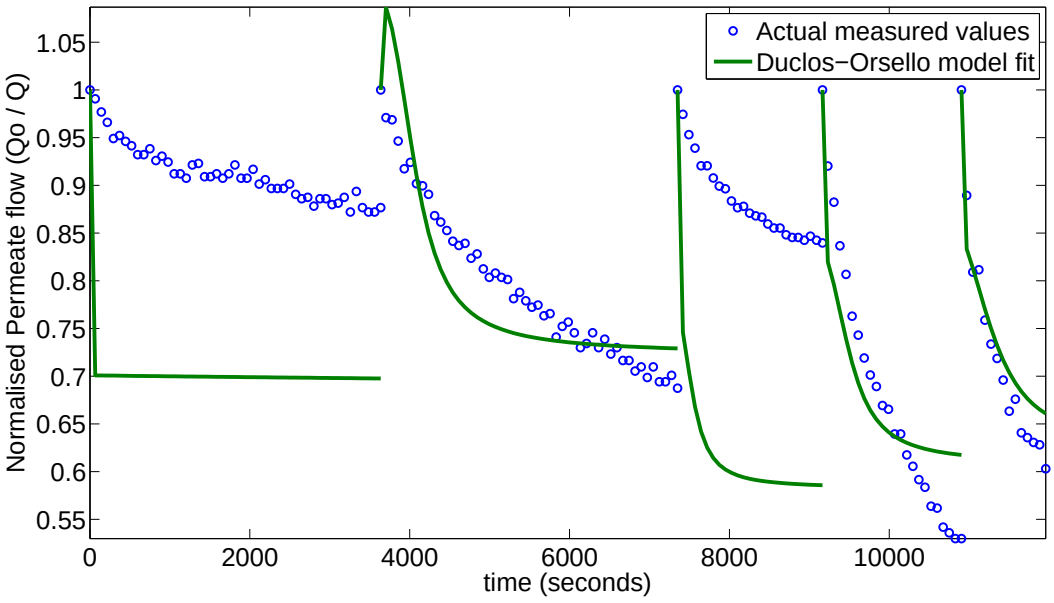

Fig. 4.22: Normalised permeate flow for 5 flux steps on 5th Dec 2008 with best model fit

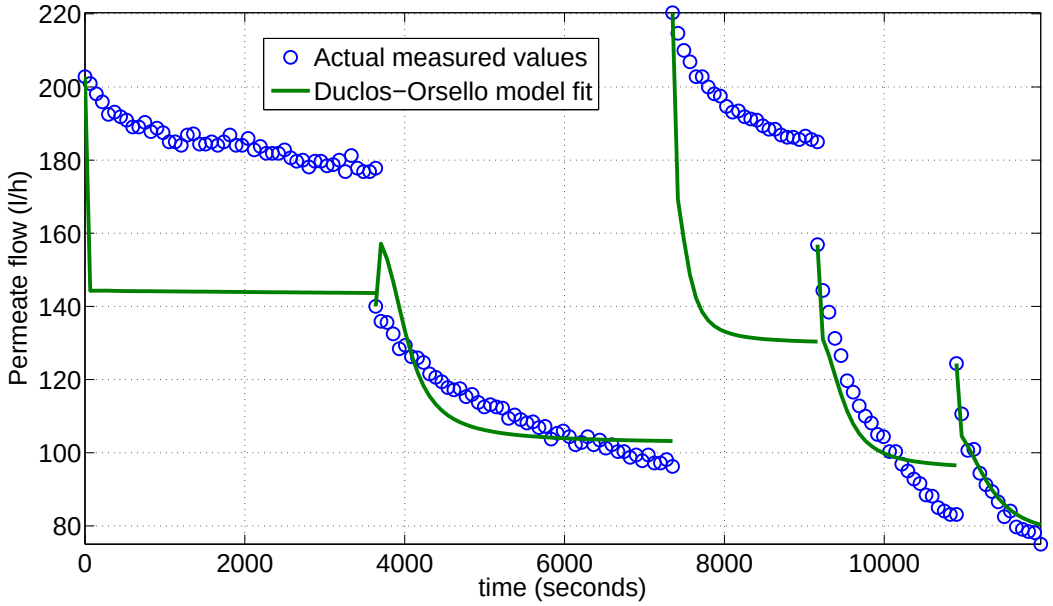

Fig. 4.23: Actual permeate flow for 5 flux steps on 5th Dec 2008 with best model fit

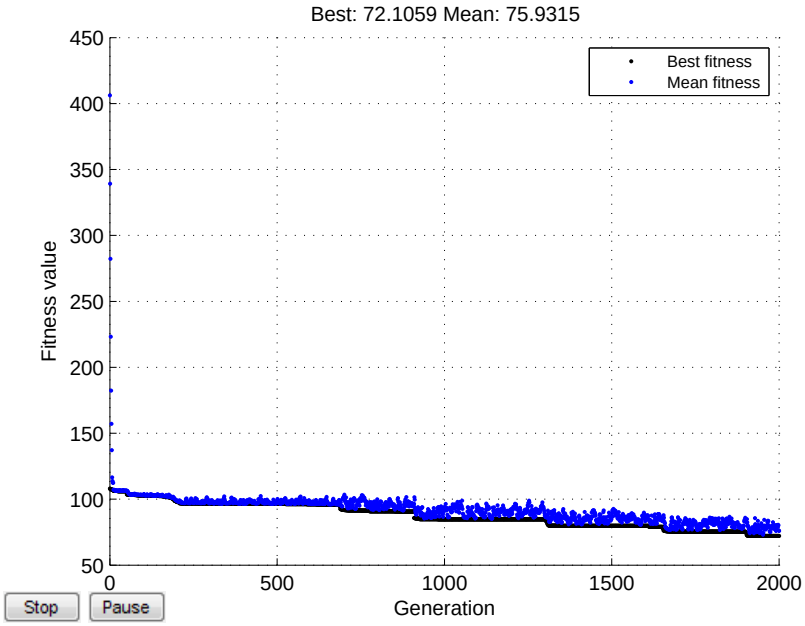

Fig. 4.24: Genetic algorithm run for 5 flux steps on 5th Dec 2008 to find optimal model parameters

4.2.1.5 Simulation results from individual reduced flux stepping tests on 5th December 2008

Again instead of trying to fit all five chosen flux steps simultaneously, it was assumed that each flux step solution was unique. This meant each step was considered separately by the model on a data-by-data basis. This procedure was carried out for each step and gave the results listed below. For the sake of brevity only limited comments are given, as the results were in-line with the assumptions made and the fit was in-line with theory.

So, for the first flux step of five on 5th Dec 2008 gives the result shown in Fig. 4.25. The genetic algorithm fit is good after only one hundred generations as shown in Fig. 4.26.

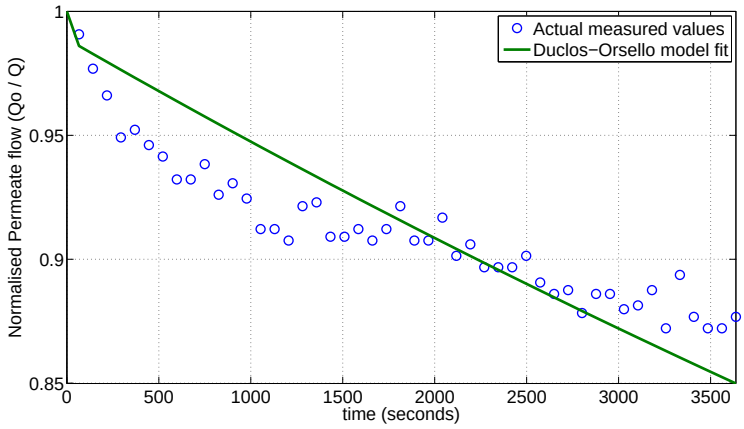

Fig. 4.25: Normalised permeate flow for first flux step of five on 5th Dec 2008 with best model fit

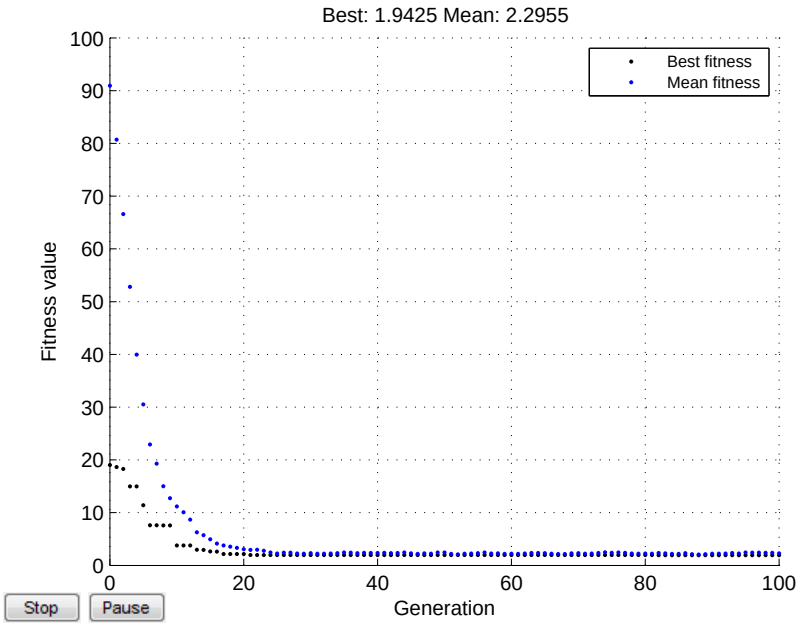

Fig. 4.26: Genetic algorithm run for first flux step of five on 5th Dec 2008 to find optimal model parameters

Next, for the second flux step of five on 5th Dec 2008 gives the result shown in Fig. 4.27. Again the genetic algorithm fit is good after only one hundred generations as shown in Fig. 4.28.

Next, for the third flux step of five on 5th Dec 2008 gives the result shown in Fig. 4.29. Again the genetic algorithm fit is good after only one hundred generations as shown in Fig. 4.30.

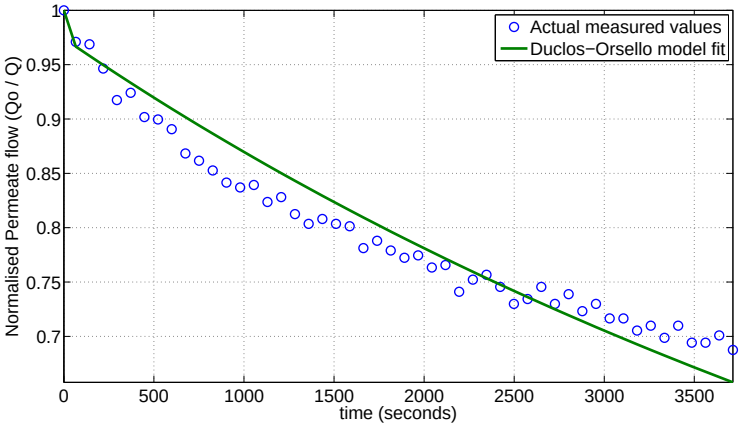

Fig. 4.27: Normalised permeate flow for second flux step of five on 5th Dec 2008 with best model fit

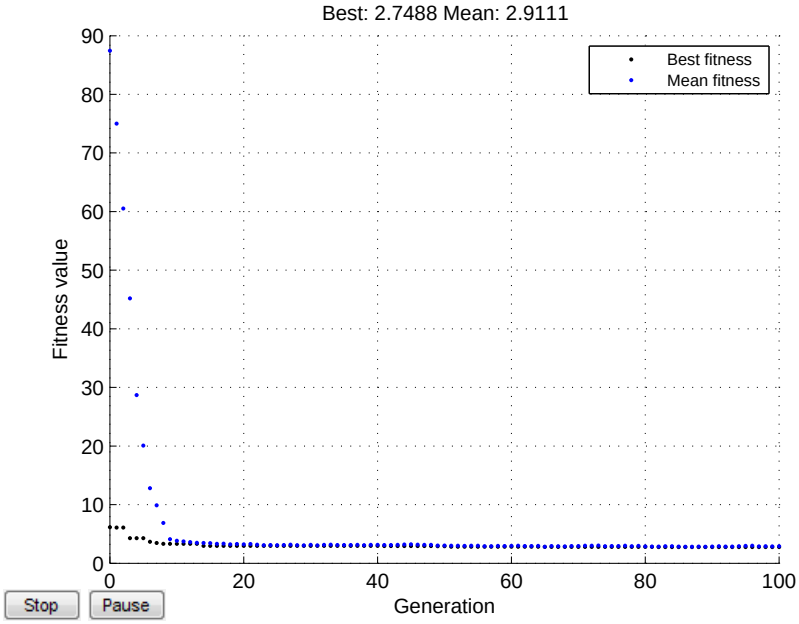

Fig. 4.28: Genetic algorithm run for second flux step of five on 5th Dec 2008 to find optimal model parameters

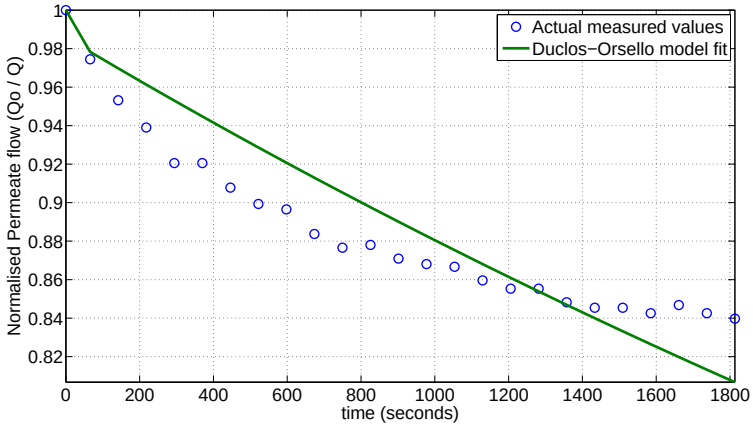

Fig. 4.29: Normalised permeate flow for third flux step of five on 5th Dec 2008 with best model fit

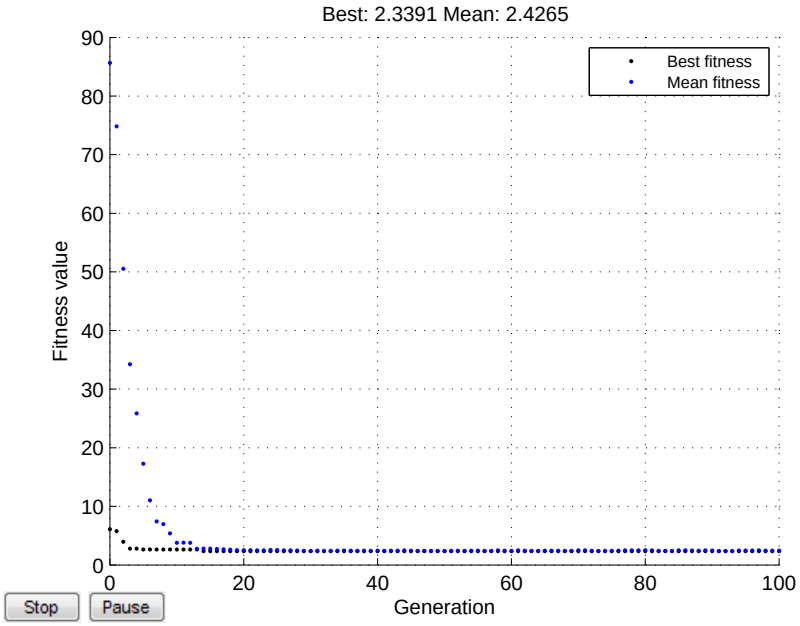

Fig. 4.30: Genetic algorithm run for third flux step of five on 5th Dec 2008 to find optimal model parameters

Next, for the fourth flux step of five on 5th Dec 2008 gives the result shown in Fig. 4.31. Again the genetic algorithm fit is good after only one hundred generations as shown in Fig. 4.32.

Finally, for the fifth flux step of five on 5th Dec 2008 gives the result shown in Fig. 4.33. Again in this finally run, the genetic algorithm fit is good after only one hundred generations as shown in Fig. 4.34.

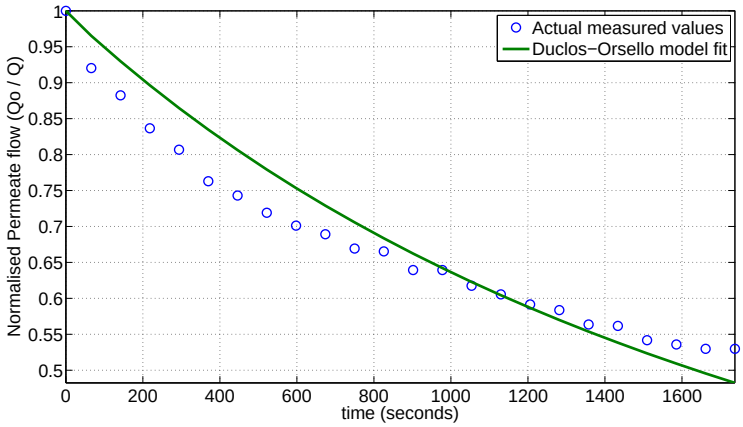

Fig. 4.31: Normalised permeate flow for fourth flux step of five on 5th Dec 2008 with best model fit

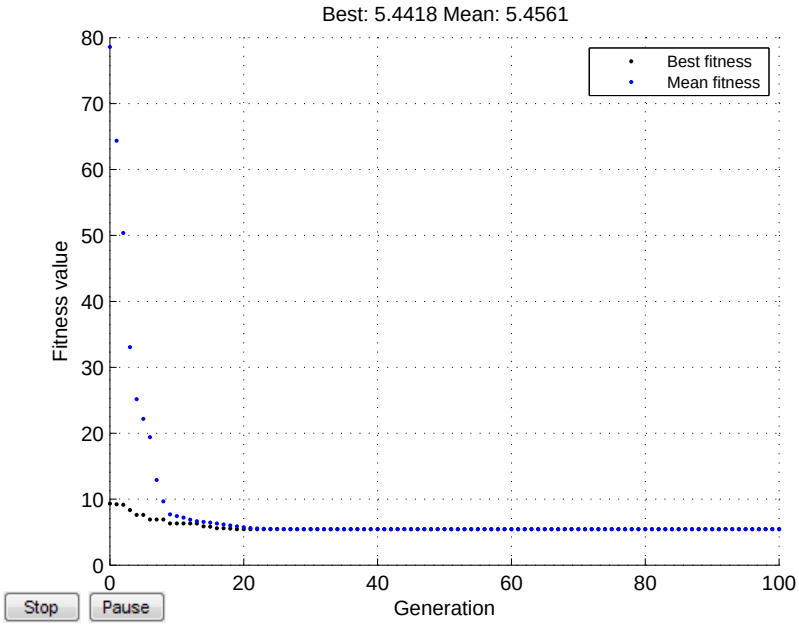

Fig. 4.32: Genetic algorithm run for fourth flux step of five on 5th Dec 2008 to find optimal model parameters

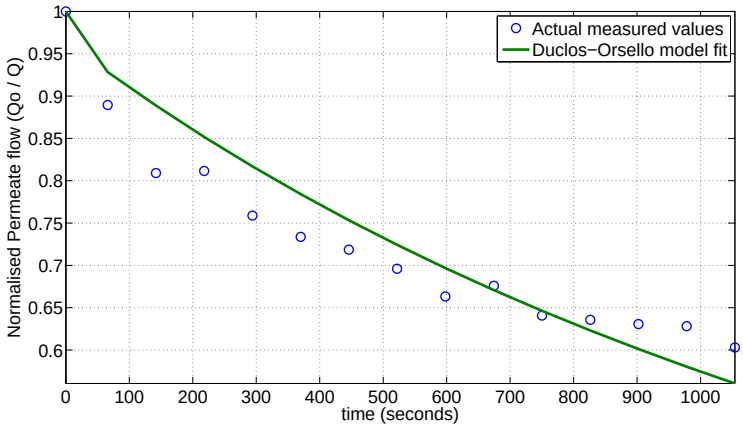

Fig. 4.33: Normalised permeate flow for fifth flux step of five on 5th Dec 2008 with best model fit

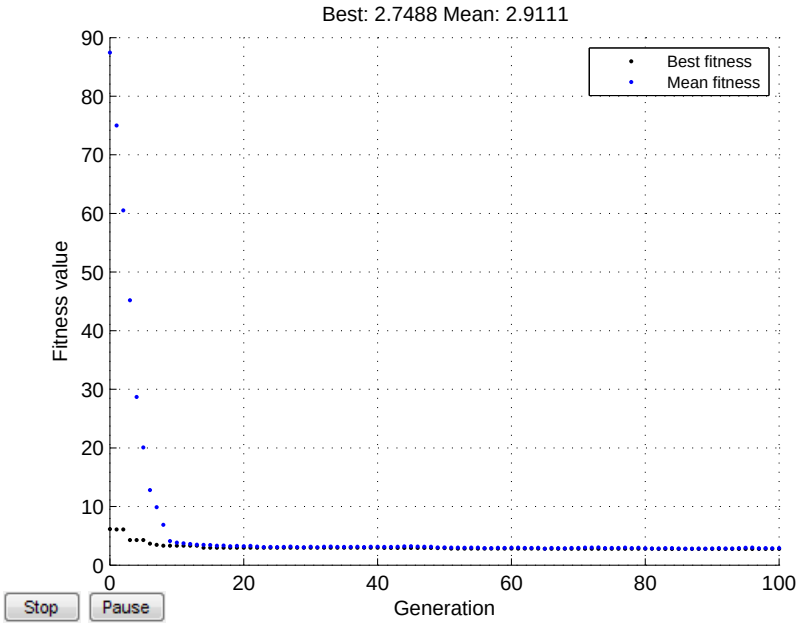

Fig. 4.34: Genetic algorithm run for fifth flux step of five on 5th Dec 2008 to find optimal model parameters

4.2.2 Simulation results from ITT Sanitaire pilot membrane filtration unit

Flux stepping tests carried out on the ITT Sanitaire pilot membrane filtration unit located at Cardiff WWTP were used to recalibrate and revalidate the reformulated Duclos-Orsello model. Unlike the Aquabio pilot MBR data, each flux step up for this membrane unit were carried out three times consecutively with backwashes in between, so that any membrane performance errors were minimised. This means this data is more consistent, and since the throttle valve settings remained untouched for a more standard constant flux plant, the hydrodynamics did not greatly vary. Further, as this is a much more simpler membrane unit with no bioreactor and significantly reduced mixed liquor concentrations (and subsequent **SMP** levels), this greatly simplified the situation and reduced the likelihood of anomalies. Hence the results reflect and fit membrane fouling theory.

Of the full set of steps both up and down, only a reduced data set was considered of steps up as shown in Fig. 4.35. This was because the stepping down procedure was done too rapidly and not consistently enough so that the measured data became very scattered and more prone to inaccuracies. In fact for the stepping up procedure only the middle flux step values of 40, 45 and 50 $l/m^2/hr$ were used as shown in Fig. 4.36, as they were deemed the best of the measured data values. Also of the three main fouling mechanisms under consideration, none of them dominated giving skewed results. The lower flux steps up of 30 and 35 $l/m^2/hr$ were rejected since they showed not enough variations for modelling purposes as they were below critical flux levels with only the cake build up mechanism dominating. Conversely the higher flux steps up of 55 and 60 $l/m^2/hr$ were rejected since they showed too large scatter for modelling purposes as they were above critical flux levels with the pore constriction mechanism dominating. This scatter is attributed to the higher suction pressure effects on permeate side due to the permeate suction pump speed increasing, meaning the chance of air coming out of solution increased with a subsequent knock-on effect on the sensitivity of the flow measurement devices and pressure sensors.

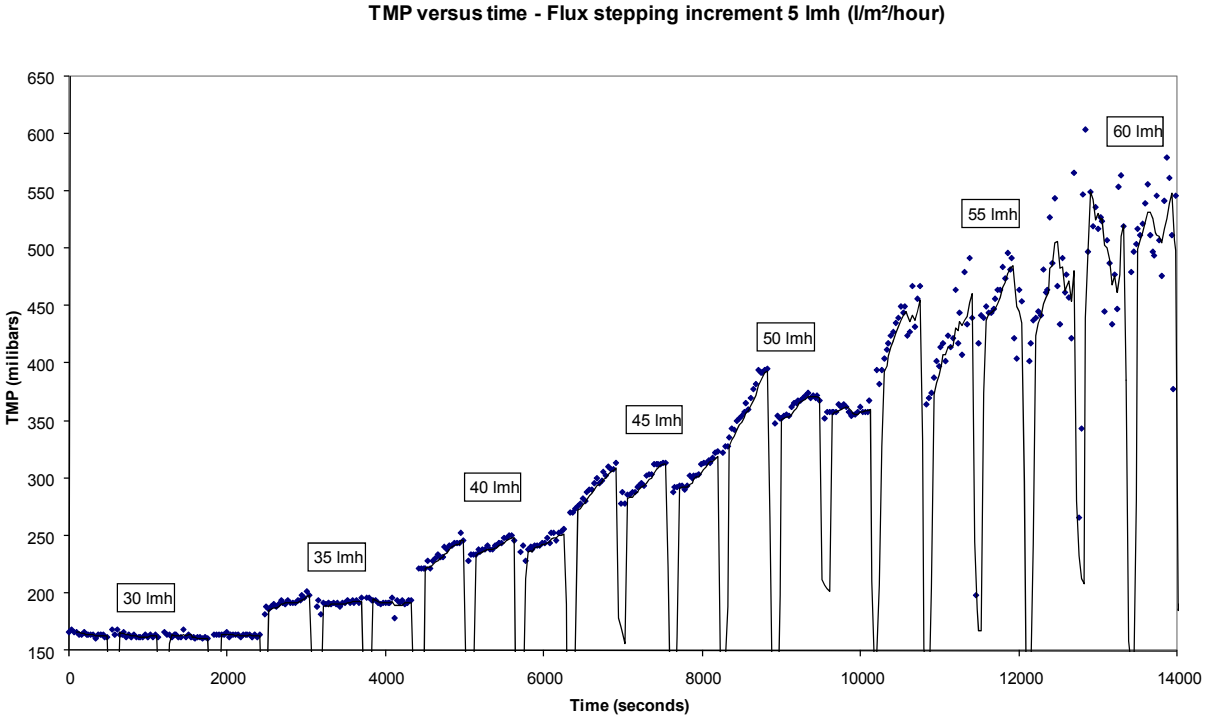

Fig. 4.35: Measured TMP data for all flux steps up at constant fluxes for ITT pilot unit at Cardiff

Using these middle flux step values of 40, 45 and 50 $l/m^2/hr$ of which the last flux step of three at 50 $l/m^2/hr$ was even rejected, the remaining eight steps up were collectively used to calibrate the formulated model by running a parameter estimation and optimisation procedure. Fig. 4.37 shows the results and the best fit when comparing model values with actual measured ones. The genetic algorithm routine which

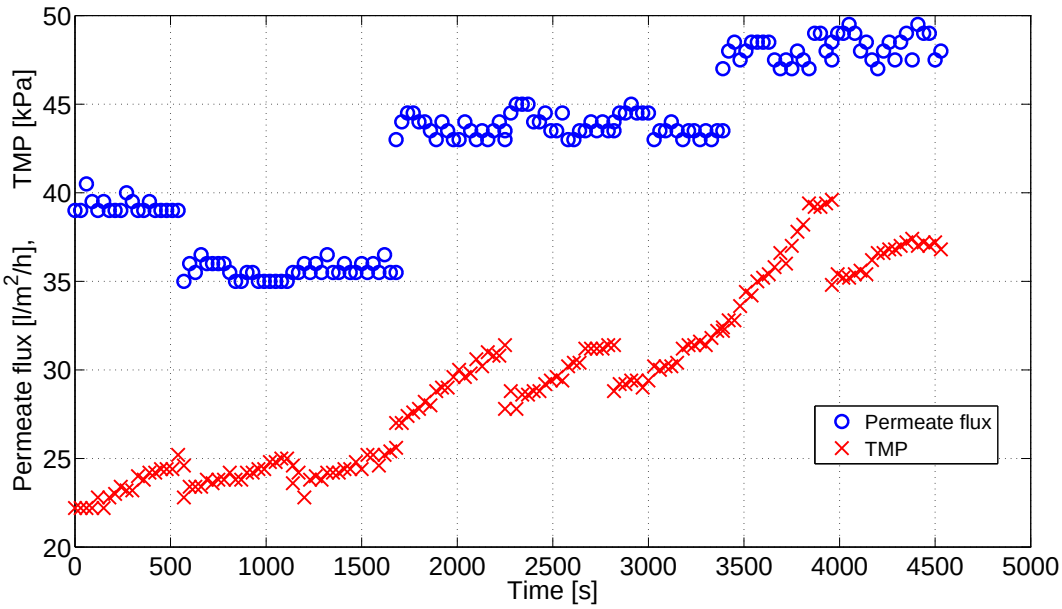

Fig. 4.36: Measured TMP data for 8 flux steps at constant fluxes for ITT pilot unit at Cardiff

calculated the optimal parameter values gave an extremely good fit after five thousand generations as shown in Fig. 4.38 for best and mean fits.

The reason for these exceptional results have already been mentioned, namely: very low mixed liquor concentrations (and subsequent very low **SMP** levels) give a extremely consistent membrane performance; a membrane unit only with no complex bioreactor (i.e. no significant biological and biochemical variations to worry about); and a simple plant flow train with automated backwash procedure. Other factors that influenced these exceptional results is this was a constant flux operation giving simpler hydrodynamics with no discontinuities in time. Also the plant had been operating consistently over a long period of time unlike the Aquabio pilot MBR plant. Further, the flux stepping tests occurred on the same day, and also the air-sparging procedure used to clean the membrane which was at a very high rate (i.e. much higher than for a full size commercial unit) occurred continuously even during the backwashes. This meant extreme membrane clogging was very unlikely. Finally, since the whole procedure was automated, no extreme events occurred such as voltage inverter levels being exceeded, so that no automatic shutdowns happened as inadvertently happened with the other plant.

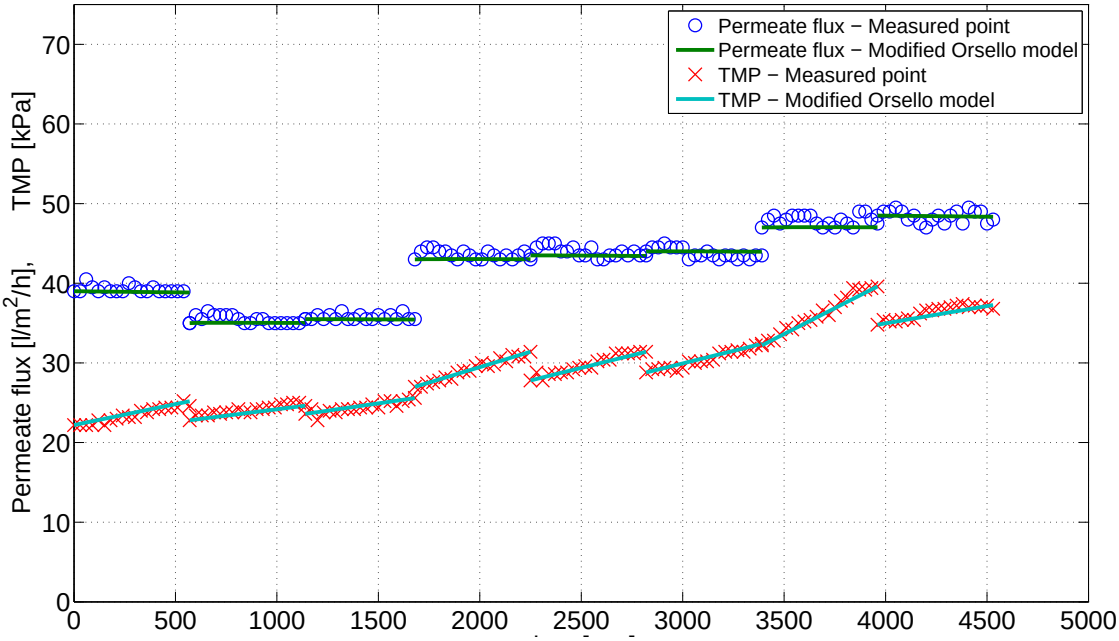

Fig. 4.37: Measured TMP data for 8 flux steps at constant fluxes for ITT pilot unit with best model fit

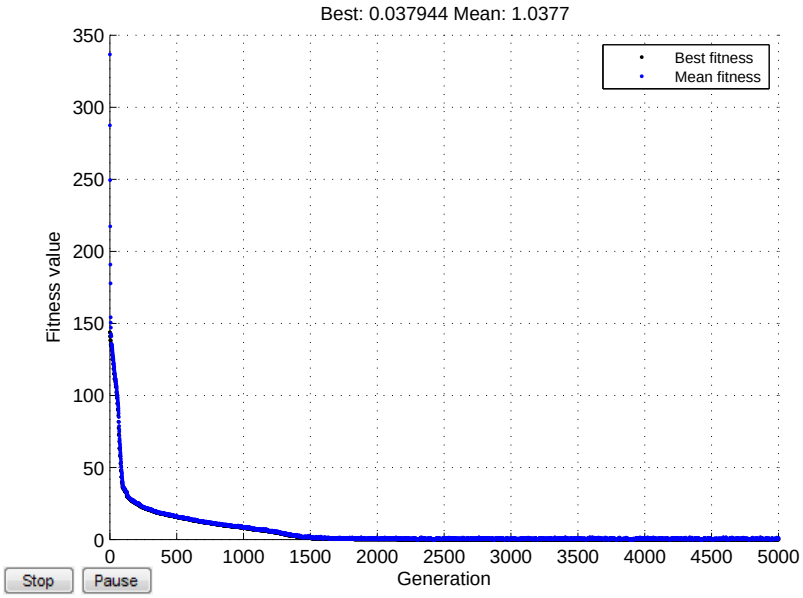

Fig. 4.38: Genetic algorithm run for 8 flux steps for ITT pilot unit to find optimal model parameters

4.2.3 Summarising results from phenomenological model

Table 4.4 compares the genetic algorithm fit for all the model runs carried out. It is clear that for the Aquabio pilot MBR plant, that the fit is very good when the flux steps are taken individually as unique solutions. Also the fit improves when the specific step regime produces fluxes and TMPs that are well below critical conditions, so that the membrane performance is not compromised and does not have a knock-on effect on the subsequent flux step due to the hysteresis "memory" of the membrane. In comparison the ITT membrane unit gives results even better than the best Aquabio pilot MBR plant results. This is as expected due to the factors already discussed in the previous sections.

Plant type and flux step combo	Best GA fit	Mean GA fit
Aquabio - both flux steps on 3rd Dec 2008	15.8673	15.8715
Aquabio - all 5 flux steps on 5th Dec 2008	72.1059	75.9315
Aquabio - 1^{st} flux step of two on 3rd Dec 2008	4.4619	4.4742
Aquabio - 2^{nd} flux step of two on 3rd Dec 2008	3.0789	3.0982
Aquabio - 1^{st} flux step of five on 5th Dec 2008	1.9425	2.2955
Aquabio - 2^{nd} flux step of five on 5th Dec 2008	2.7488	2.9111
Aquabio - 3^{rd} flux step of five on 5th Dec 2008	2.3391	2.4265
Aquabio - 4^{th} flux step of five on 5th Dec 2008	5.4418	5.4561
Aquabio - 5^{th} flux step of five on 5th Dec 2008	2.7488	2.9111
ITT pilot unit Cardiff - all 8 flux steps	0.037944	1.0377

Table 4.4: Comparison of GA fits for various plants for different flux step combinations modelled

When comparing the optimised parameter values shown in Table 4.5 that were determined by the genetic algorithm routine, a clear pattern again emerges. The pore blockage parameter, α, is high for all modelled data sets like the situations in the sensitivity analysis described as Simulations 2 and 3 when the **SMP** formation conditions predominate and it is not a normal MBR scenario (see Section 4.1.5). This is as expected because most of the flux steps are well above the normal operating range of the membranes under consideration. The pore constriction parameter, β, is of the same order as occurred in the sensitivity analysis procedure in Section 4.1.5 which is as expected. However the $f'R'$ parameter which is the product of fractional amount of total foulant contributing to deposit growth, f', and the specific protein layer resistance, R', is much reduced when compared to the sensitivity analysis values. This can be explained since the sensitivity analysis used pure protein solutions as BSA whilst the real life plant have mixed liquors of which only a small proportion consist of protein matter. The $\frac{R_{p0}}{R_m}$ parameter is of the same order for all flux steps as those determined under the previous sensitivity analysis. The four remaining parameters which refer to the extensive model reformulation to include membrane scour affects and backwash regimes cannot be compared. However the membrane scour terms, namely $k_p(CFV)$ and $k_b(CFV)$, appear to be of a sensible size, and the size of the backwash terms f_{rp} and f_{rAU} appear to make sense as well. The f_{rp} parameter value is quite high for most flux steps meaning that full recovery of the membrane is never achieved which is as expected for a membrane being stepped under fluxes beyond its normal operating range. Again for f_{rAU} parameter value is quite low for most flux steps meaning that full recovery of the membrane unblocked area after a backwash is never achieved which is as expected for a membrane being stepped under fluxes beyond its normal operating range, and without sufficient time to recover performance. In summary, this means most of parameter values are of the same order as stated in the Duclos-Orsello et al. (2006) paper, or for those new parameters they are of a size that make theoretical and mathematical sense. Consequently this model formulation does appear accurate enough to be used to model a membrane filtering mixed liquors and experiencing subsequent fouling and clogging.

Plant type and flux step combo	α	β	$f'R'$	$\frac{R_{p0}}{R_m}$	$k_p(CFV)$	$k_b(CFV)$	f_{rp}	f_{rAU}
Aquabio - both flux steps on 3rd Dec 2008	1736	14.25	7374	0.67	595	788	0.85	0.89
Aquabio - all 5 flux steps on 5th Dec 2008	6934	0.07	9184	0.17	43.50	12.50	0.98	0.013
Aquabio - 1^{st} flux step of two on 3rd Dec 2008	9528	16.58	2183	0.79	944	109	0.62	0.11
Aquabio - 2^{nd} flux step of two on 3rd Dec 2008	179	8.01	3158	0.94	857	894	0.55	0.28
Aquabio - 1^{st} flux step of five on 5th Dec 2008	5237	1.80	6909	0.66	83.94	359	0.53	0.73
Aquabio - 2^{nd} flux step of five on 5th Dec 2008	6486	7.36	2441	0.14	115	126	0.83	0.71
Aquabio - 3^{rd} flux step of five on 5th Dec 2008	9293	4.69	8455	0.56	800	516	0.26	0.046
Aquabio - 4^{th} flux step of five on 5th Dec 2008	2024	32.17	2983	0.86	936	422	0.93	0.41
Aquabio - 5^{th} flux step of five on 5th Dec 2008	9494	54.10	3900	0.76	701	93.31	0.51	0.95
ITT pilot unit Cardiff - all 8 flux steps	3469	0.14	8079	0.56	183	694	0.97	0.26

Table 4.5: Comparison of optimal parameter values for various plants for different flux step combinations modelled

4.3 *Behavioural membrane fouling model - input-output system identification approach*

4.3.1 Introduction - behavioural fouling model formulation

In order to directly compare the two different model types, namely the phenomenological Duclos-Orsello formulation against an input-output behavioural model based on system identification methods, the same plant data sets were used. The behavioural fouling model formulation is based upon the "Model Conceptualisation Procedure" described in Section 3.3 in which the plant data sets used are formatted for the Matlab's System Identification Toolbox© and CUEDSID software. The different system identification model formulations tested were:

1. Linear parametric ARX, ARMAX and state space models developed in the Matlab's System Identification Toolbox© with GUI. The same plant data sets were used as for the phenomenological model.
2. Alternative linear parametric subspace models developed in the CUEDSID software package and Matlab©. The same plant data sets were used as for the phenomenological model.
3. A bilinear parametric subspace model developed in the CUEDSID software package and Matlab©. In this case the data set was very long term membrane filtration data from ITT Sanitaire submerged pilot MBR plant using Coors UK Limited data which contained a sufficient change in fluid temperature due to the environment for the bilinearity effects to be investigated and measured. This bilinearity was probably affected by the changes in MLSS concentrations as well.

In summary, the more regular linear class of models are tested first on the data sets under consideration. The main feature of these linear system models is that they obey the laws of superposition of input-output variables, and are therefore relatively easy to deduce. Next the special class of non-linear systems, known as bilinear systems, is modelled in which superposition of variables would not apply. Non-linear systems can have time-dependant system coefficients (i.e. model parameters), unlike linear systems in which they are fixed. This means the non-linear coefficients are often difficult to deduce.

4.4 *Behavioural membrane fouling model - results and discussion*

4.4.1 Simulation results from Aquabio pilot MBR plant

4.4.1.1 Reduced data set of 7 best flux steps with simplified input/output model structure

The reduced data set of the seven best flux steps as depicted in Figs. 4.11 and 4.12 was used to test the proposed input-output model structures. At first only a very simple model formulation was tried by using the "Model Conceptualisation Procedure" outlined in Section 3.2. This simple model formulation was used to test whether input-output model structures were appropriate for the type of data sets available. Thus by applying the generic membrane model formulation described in Section 3.3.2 and using this same nomenclature, the following simple input-output structure was tested on this reduced data set.

Firstly, the very general case was considered as outlined below for a constant TMP varying permeate flux operation:

$$\mathbf{y_{12}'} = \mathbf{u_2} = \begin{bmatrix} S_{PS} \\ S_{PP} \\ X_{MLSS} \\ X_{EPS} \\ \mu(T) \end{bmatrix}; \mathbf{m_2} = \begin{bmatrix} \omega_{pump} \\ \nu_{throttle} \\ f_{bwash} \end{bmatrix}; \mathbf{x_2} = \begin{bmatrix} \\ irreversible\ fouling \\ reversible\ fouling \\ cake \end{bmatrix}; \mathbf{y_{21}'} = \begin{bmatrix} TMP \\ q_{perm} \end{bmatrix}$$

In the actual pilot plant layout and operation, since the flux stepping occurred over two days with little practical change in liquor viscosity, MLSS concentration, and **SMP** levels, then the input vector y_{12}' can be considered as a constant in this specific case, and therefore ignored. The internal state vector x_2 is part of the black box model so does not need to be determined explicitly. Thus the only changing input data sets are reflected in vector m_2 of which the backwash variations have already been removed from the reduced data set under consideration.

Hence in vector m_2, the pump and throttle valve settings are reflected in the flows into and out of the membrane module, and also the pressure experienced across this same module. These are in this case as follows:

- Q_1 flow rate into module.
- Q_2 flow rate out of module (on recirculation loop).
- Q_3 generated permeate flow rate, expressed as a permeate flux ($l/m^2/hr$).
- P_1 pressure into module.
- P_2 pressure out of module (on recirculation loop).
- P_3 generated permeate pressure.
- TMP generated TMP across membrane which equals $(P_1 + P_2)/2 - P3$.

The output vector for this simplified input-output model is only composed of the permeate flux, since the TMP in this case can be considered as one of the input variables for a constant pressure flux stepping system. Thus, in this specific case the simplified model reduces to the following vectors for the Matlab's

System Identification Toolbox© and CUEDSID software:

$$\mathbf{m_2} = \begin{bmatrix} Q_1 \\ TMP \end{bmatrix}; \mathbf{y_{21}}' = \begin{bmatrix} Q_3 \end{bmatrix}$$

When this simple model is run as a subspace formulation using the CUEDSID software, the best fit is for a 1^{st} order model with block size of 13 as shown in Fig. 4.40. By the way this fit is carried out by using the last three flux stepping cycles as the validation data set. The model order relates to the number of delayed inputs and outputs used in the corresponding linear difference equations, so a 1^{st} order model has the least number of equations required, and takes the smallest time to compute a solution. However, a larger model order may offer a better fit by increasing the degrees of freedom of the model equations, although this is not always true. In general, when fitting by trial and error, it is best to obtain the optimal fit for the smallest model order and largest block size possible. The block size, k, which refers to the size of the four block algorithm used to find a solution (Chen and Maciejowski 1999), should always be greater than the model order, otherwise a convergent solution is not obtainable. Hence the block size limits the largest model order available. The greater the block size, the greater the computing power needed to come up with a solution, but the better the potential model fit. However, a larger block size is also limited by the amount of data required, so there may be insufficient data to allow a solution for very large block sizes. Incidentally when using the CUEDSID software, its algorithm's automatically calculate the largest block size possible, and also can recommend a best fit model order as well as shown in Fig. 4.39 which suggest a best fit order of one.

In this case the best fit achievable is not very good at 55% as shown in Fig. 4.40. As can be the fit is poor since the model predicts the flux should increase over a flux step cycle when it should actually be decreasing. Thus the model is predicting that the membrane fouling reduces over time for the flux step which patently is not true as the pilot plant was not operating at a sufficiently high enough CFV or low enough mixed liquor concentration to prevent or even reduce cake build up. This obviously suggests that the incoming membrane flow and TMP are not sufficient in themselves to provide a good model fit for a subspace formulation for this particular plant layout.

The subspace model calculated by the CUEDSID software for this particular data set is as follows:

$$x(t + T_S) = A.x(t) + B.u(t) + K.e(t); \qquad x(0) = 0$$
$$y(t) = C.x(t) + D.u(t)$$

where:

$$A = \begin{bmatrix} 1.0149 \end{bmatrix}; B = \begin{bmatrix} -0.0067752 \\ -0.19319 \end{bmatrix}; C = \begin{bmatrix} -28.133 \end{bmatrix}; D = \begin{bmatrix} 15.919 \\ 417.98 \end{bmatrix}; K = \begin{bmatrix} -0.0019766 \end{bmatrix}$$

The same data and model structure was then run on Matlab's System Identification Toolbox© using its GUI, and the ARX and ARMAX model formulations. The state space model formulation was also tried in this case, but it gave a best fit of -246.7% so was ignored. The MISO ARX model calculated by Matlab's System Identification Toolbox© for this particular data set is as follows:

$$A(q) \cdot y(t) = B(q) \cdot u(t) + e(t)$$

where:

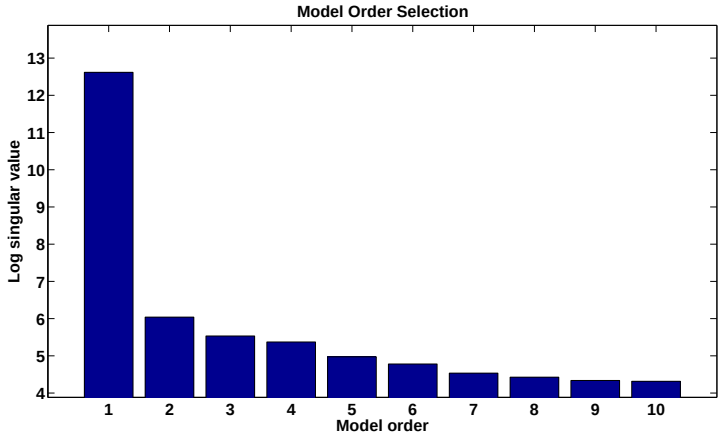

Fig. 4.39: Subspace formulation model for 7 best flux steps - Recommended model order

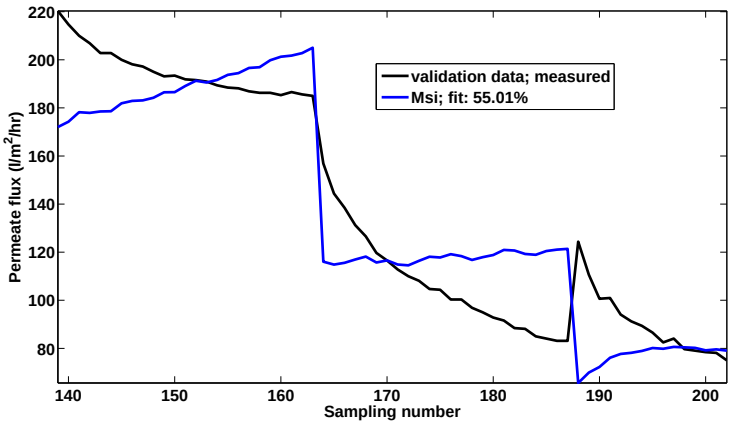

Fig. 4.40: Subspace formulation model for 7 best flux steps - best fit for permeate flux

$$A(q) = 1 - 0.9834 \cdot q^{-1} + 0.4587 \cdot q^{-2} - 0.4388 \cdot q^{-3} + 0.2298 \cdot q^{-4}$$
$$B_1(q) = -2.369 \cdot q^{-1} + 8.235 \cdot q^{-2} - 12.16 \cdot q^{-3} + 7.262 \cdot q^{-4}$$
$$B_2(q) = -73.21 \cdot q^{-1} + 211.6 \cdot q^{-2} - 348.6 \cdot q^{-3} + 205 \cdot q^{-4}$$

Once again the MISO ARMAX model calculated by Matlab's System Identification Toolbox© using its GUI for this particular data set is as follows:

$$A(q) \cdot y(t) = B(q) \cdot u(t) + C(q) \cdot e(t)$$

where:

$$A(q) = 1 - 1.659 \cdot q^{-1} + 0.6963 \cdot q^{-2}$$
$$B_1(q) = 0.1388 \cdot q^{-1} + 0.01811 \cdot q^{-2}$$
$$B_2(q) = -24.46 \cdot q^{-1} + 23.06 \cdot q^{-2}$$
$$C(q) = 1 - 0.8898 \cdot q^{-1} - 0.1102 \cdot q^{-2}$$

Incidentally for most of the remaining Section's in this Chapter the exact model vector values as given above will not be stated for the sake of brevity.

Figs. 4.41 and 4.42 show the input and output data used in the ARX and ARMAX model formulations. The calibration and validation data depicted has already had all the trends and mean values removed from it before it is used for the fitting procedure. Even though the validation data set in this case is much larger and is half the data available, Fig. 4.43 shows that the best fits for the ARX and ARMAX model formulations are 36% and 45% respectively, which is slightly worse than the subspace formulation in numerical terms. However, the shape of the fit is very good and in the same general direction. This means as the flux reduces at a slightly decreasing exponential rate due to the gradual switching in membrane blocking mechanisms from rapid pore constriction initially towards a more slower cake build up, the model formulations predict this same effect. This shows this simple input-output model structure for this particular plant layout is capable of predicting the correct direction of permeate flux decrease albeit using autoregressive iterative optimisation methods as opposed to the single shot algebraic subspace methods.

4.4.1.2 Reduced data set of largest flux step with simplified input/output model structure

In order to try and improve the fit, it was decided that the slightly poor fit obtained by both the subspace and more traditional autoregressive formulations could be re-attempted by using a single flux step data set. This would then eliminate any continuity errors occurring due to the truncation of data sets. In other words since some of the best selected flux steps (and flux step portions) did not occur exactly after each other and some occurred even on different days, therefore this discontinuity in data set would not take into account the membrane "memory" mechanism which seem to apply in which the future memory

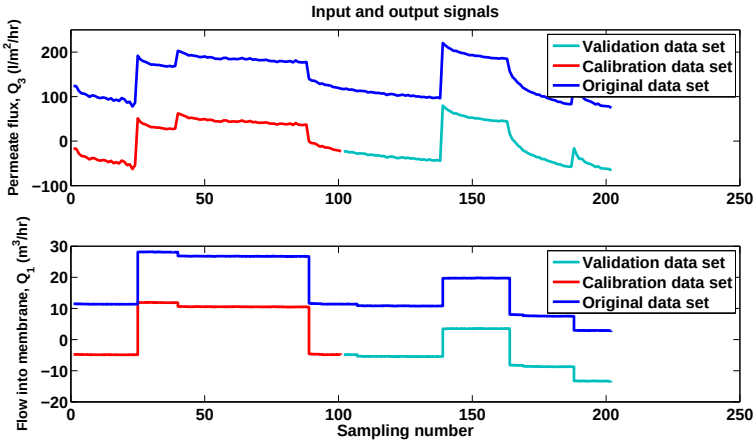

Fig. 4.41: ARX and ARMAX formulation model - 1) input and output data

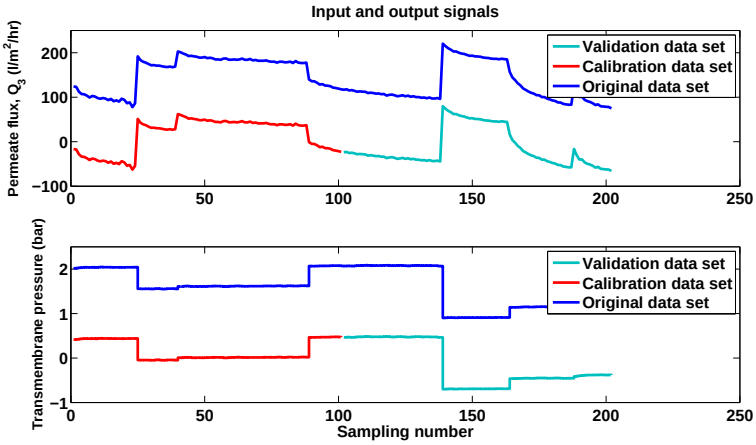

Fig. 4.42: ARX and ARMAX formulation model - 2) input and output data

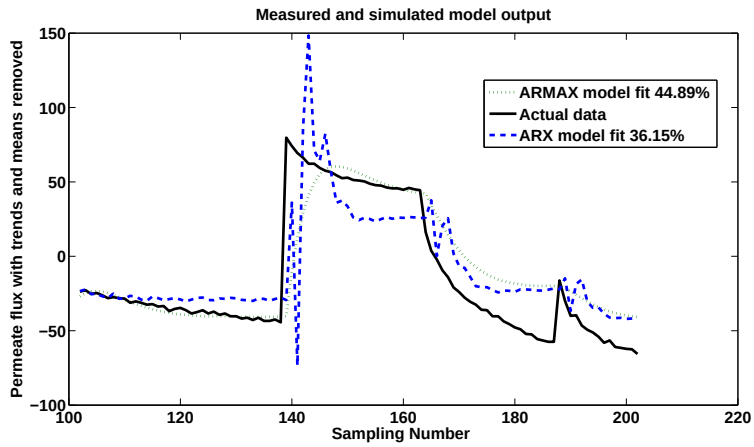

Fig. 4.43: ARX and ARMAX formulation model - best fit for permeate flux

performance appears to significantly depend on the previous operational state of the plant. The removal of backwash step data also could add to this discontinuity in the best selected data set.

A single flux step data set would not have this discontinuity in it and thus may offer a better fit, or at least eliminate this possible reason for a poor model fit. Thus in this case the largest flux step was chosen as the other six contained insufficient data points to allow either a subspace or a more traditional autoregressive formulation to be run. The same procedure as reported in the previous Section was carried out. The autoregressive formulations all gave extremely poor results ranging from the best for the ARX model of -132% up to the worst for the state space model of -162%. The subspace method gave better results although not as good as those reported in the previous Section. Fig. 4.44 shows that although the best fit was 43% for the subspace method, the shape of the fit is in the correct direction. It is likely that this degradation in model fit is primarily due to the limited data points for a single flux step cycle, even though the data variability and noise is greatly reduced for a single flux cycle. Consequently one of the main limitations of all these input-output model formulations are that they are data rich methods requiring considerable data to give optimal solutions and results. Another shortfall of these methods as proved by these results is that they require data sets with considerable variability in input data and preform better with noisy data. Therefore in this case of using almost constant TMP data to predict a varying permeate flux has proved difficult since the input data is so steady in nature. A longer data set including other input variables which do change fairly randomly, such as environmental temperature, should improve upon the model's predictability.

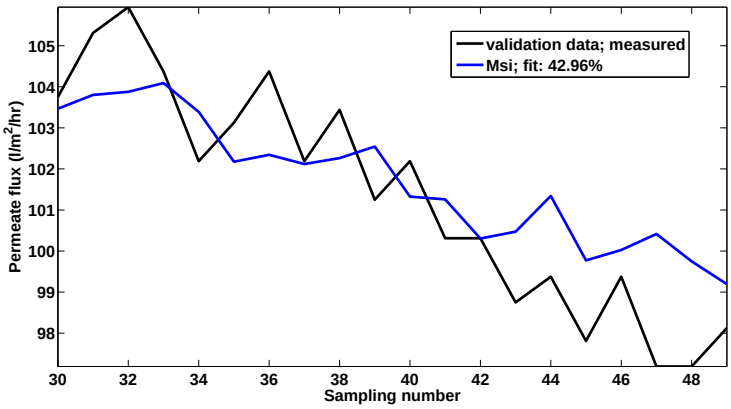

Fig. 4.44: Subspace formulation model for single flux step - best fit for permeate flux

Incidentally it may appear slightly odd that a negative fit can be obtained for some of these simulation runs when a standard fitting method usually reduces the square of the sum of the errors thus always giving positive fit values. This is due to the fact that the best model fit in percentage terms is defined in a slightly different way as follows:

$$ModelFit = [1 - \frac{Norm \cdot (Y - \bar{Y})}{Norm \cdot (Y - Mean(Y))}] \cdot 100 \tag{4.23}$$

where:
$Norm$ is a standard Matlab© function that calculates the length of the state vector.
Y is the real measured value.
$\bar{Y}$ is the simulated output value.
$Mean$ is a standard Matlab© function that calculates the average value of the state vector.

As can be seen from Equation 4.23, if the simulated output value is much larger than the mean of the measured output value, then the fit can go negative.

4.4.2 Simulation results from ITT Sanitaire pilot membrane filtration unit

4.4.2.1 Reduced data set of 8 best flux steps up with input/output model structure

In the previous Section, the results indicate that the approach used could be advocated for MBR plant in general, but this needs to be tested further on additional plant and increased data sets, especially those containing significant biochemical process data as well which may help to improve the model fit. Hence the data from the ITT Sanitaire pilot membrane filtration unit was tested. As the plant layout for this unit is very simple with no bioreactor to complicate matters, the selected input-output model structure should give a very high degree of accuracy.

For this pilot membrane filtration unit, out of the total of 29 flux steps completed both going up and down as shown in Fig. 3.51, only the eight best fitting ones were initially selected which exhibited a marked linear increase in TMP over the test period. They all happened to be flux steps going up from 35 to 45 $l/m^2/hr$ as depicted in Figs. 3.53 and 3.54. This reduced data set would mean the initial input-output model formulation to be tested should give good fits with the standard behavioural model formats being used here. The other steps which were rejected from this specific simulation run showed some very random behaviour without sufficient trend as well as a huge scatter especially at high fluxes.

Once again by applying the generic membrane model formulation described in Section 3.3.2 and using this same nomenclature, the following input-output structure was tested on this new reduced data set.

The very general case is slightly altered for this new plant layout and operation, and for the variation in data gathered. Thus this revised case is outlined below for a constant flux, increasing TMP forward suction pump operation of a submerged membrane system, with no throttle valve changes applicable and no measurement of viscosity and eEPS:

$$\mathbf{y_{12}'} = \mathbf{u_2} = \begin{bmatrix} S_{PS} \\ S_{PP} \\ X_{MLSS} \end{bmatrix}; \mathbf{m_2} = \begin{bmatrix} \omega_{suctionpump} \\ f_{bwash} \end{bmatrix}; \mathbf{x_2} = \begin{bmatrix} irreversible\ fouling \\ reversible\ fouling \\ cake \end{bmatrix}; \mathbf{y_{21}'} = \begin{bmatrix} TMP \end{bmatrix}$$

For this reduced data set, the general model case was run in three different ways as follows:

1. The input is the permeate flux only, with the output being the TMP.
2. The input is the permeate flux and measured **SMP** levels, with the output being the TMP. The **SMP** level is composed of the combined measured protein and polysacchrides concentrations.
3. The input is the permeate flux, the measured **SMP** levels, and the measured MLSS concentration, with the output being the TMP.

Thus, the data set for the input-output formulation becomes more comprehensive for each simulation run as another input state is added. If once again the internal state vector x_2 is ignored, and the backwash effect is not taken into account as it is deemed negligible, then the input-output structure which is actually tested on this reduced data set simplifies to the following for a constant flux varying TMP operation:

$$\mathbf{y_{12}'} = \mathbf{u_2} = \begin{bmatrix} S_{SMP} \\ X_{MLSS} \end{bmatrix}; \mathbf{m_2} = \begin{bmatrix} Q_3 \end{bmatrix}; \mathbf{y_{21}'} = \begin{bmatrix} TMP \end{bmatrix}$$

This input-output formulation was run using both the subspace formulation on the CUEDSID software, and then using the same data and model structure on Matlab's System Identification Toolbox© using its GUI and the ARX, ARMAX and state space model formulations. The results are outlined below.

For the subspace model run results, which are initially described here, the model order for each of the three simulations runs was kept fixed as well as the block size (i.e. a sixth order model with block size of four). Further, for all three runs, four flux steps (i.e. half the data set) was used for the validation exercise. Fig. 4.45 shows that the best fit achieved by having a single input variable is 79%, while Fig. 4.46 shows the fit improves to 90% by having two input variables. In Fig. 4.47 the fit is 89% percent respectively, which is for the simulation run with three input variables. This shows that further input data does not improve the fit appreciably. One interesting point to note is that the shape of the fit is extremely good and is in the right direction (i.e. TMP increases with time).

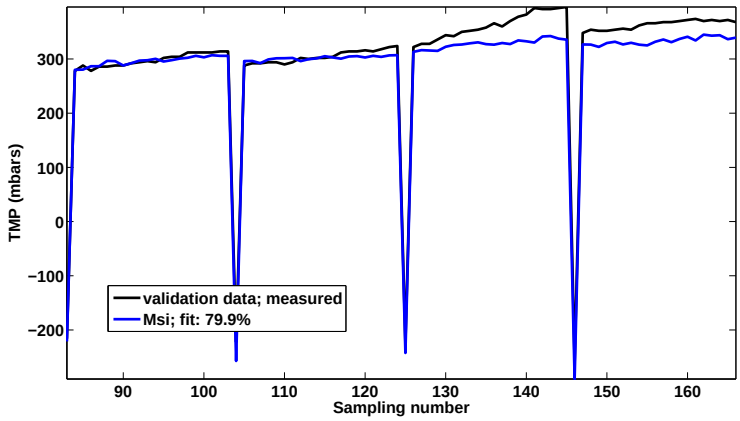

Fig. 4.45: Subspace formulation model for 8 best flux steps - best fit for TMP using flux only

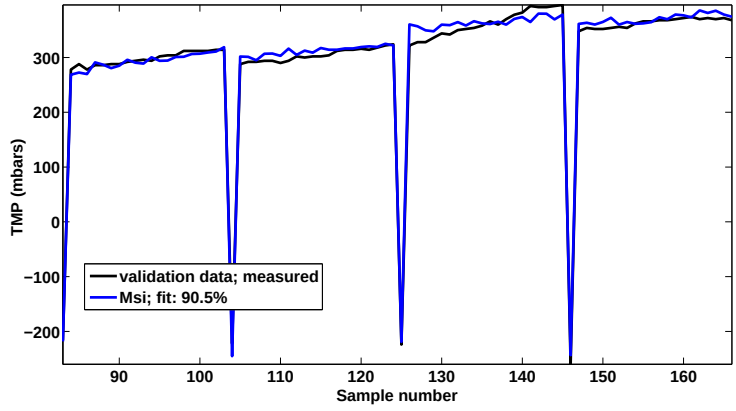

Fig. 4.46: Subspace formulation model for 8 best flux steps - best fit for TMP using flux and SMP levels

Fig. 4.48 shows the input and output data sets used in the other autoregressive methods tested here. Once again half the data set is used for validation purposes so theoretically the model fitting procedure should prove more accurate than the subspace method even if the actual individual fit may prove worse. Once again this calibration and validation data is thoroughly processed by extensive filtering (i.e. de-trended and de-meaned) before actual use.

Four basic autoregressive methods were used as described below:

1. A standard ARX model structure.
2. A standard ARMAX model structure.

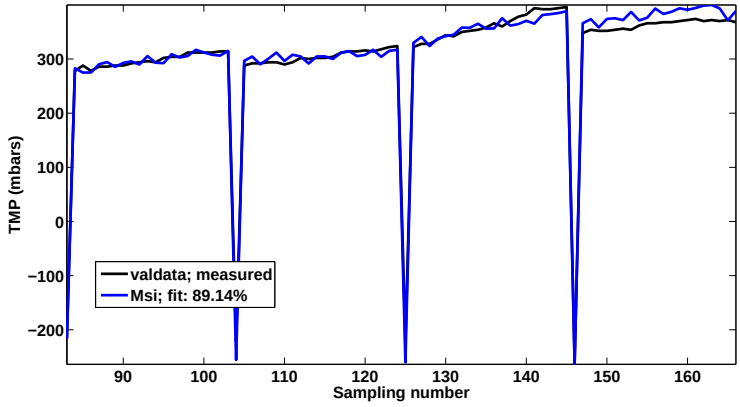

Fig. 4.47: Subspace formulation model for 8 best flux steps - best fit for TMP using flux, SMP and MLSS levels

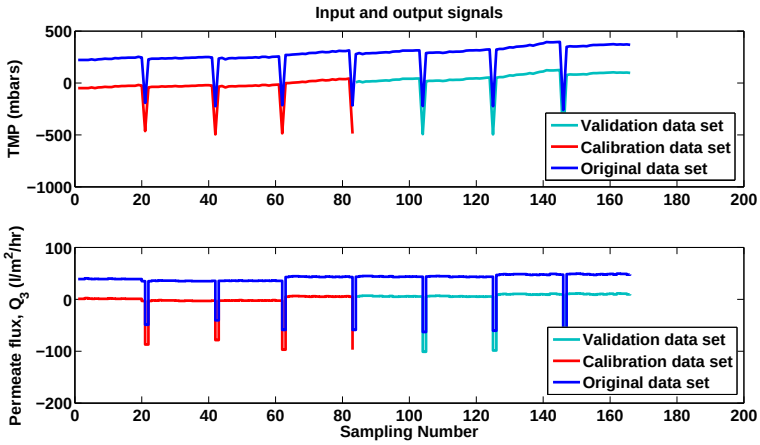

Fig. 4.48: ARX, ARMAX and state space formulation models - input and output data for 8 steps

3. A standard state space model structure using a very generalised *prediction error method* function in the iteration optimisation procedure. In Matlab's System Identification Toolbox© this is written as a "state space (pem) method".

4. A very basic subspace method which forms part of the standard Matlab System Identification Toolbox©. This extremely crude subspace method, known as the "n4sid function", uses a four block algorithm to find a solution. This means the input and output data is split into two blocks which can be thought of as "*past*" and "*future*". Therefore the basic version of this subspace method suffers from systematic errors (i.e. bias), and often fails to provide a solution. These errors are avoided by using algorithms of additional complexity such as the ones used in the CUEDSID software package, which splits the data into three blocks, namely the "*past*", "*current*" and "*future*" blocks (Chen and Maciejowski 1999). The result of using this improved approach is that the bias is greatly reduced and a solution is always obtainable.

Fig. 4.49, which is for the first simulation run, reveals that the fit is extremely poor for the two autoregressive methods that actually provided a positive solution. Additionally, the oscillating shape of the fit is very poor as it is in the wrong direction with the TMP decreasing with time. For the second simulation run with increased input data sets as shown in Fig. 4.50, the oscillating fit is still poor with only two methods providing a positive solution, albeit of the wrong shape for the first two flux steps. For the final simulation run with the most input data, Fig. 4.51 reveals that there is a deterioration in fit with only one method providing a positive solution (i.e. the state space (pem) method). However, the shape and direction of the fit is correct this time even though the simulated data is again prone to gradually attenuating fluctuations around a mean point (i.e. rapid but diminishing oscillations). These poor fits can be attributed to the regular backwash events that cause a sudden large negative drop in the TMP that the simulated models are unable to cope with. For these methods, it is clear that the data represents a different class of models from those utilised by the standard autoregressive methods. As can be seen in Table 4.6 which compares all these methods with the previous CUEDSID subspace method, this latter method proves superior for all occasions in this case. It can be concluded from these simulations, that increased input data sets do not necessarily improve a model fit but they can greatly improve the shape and direction of the fit.

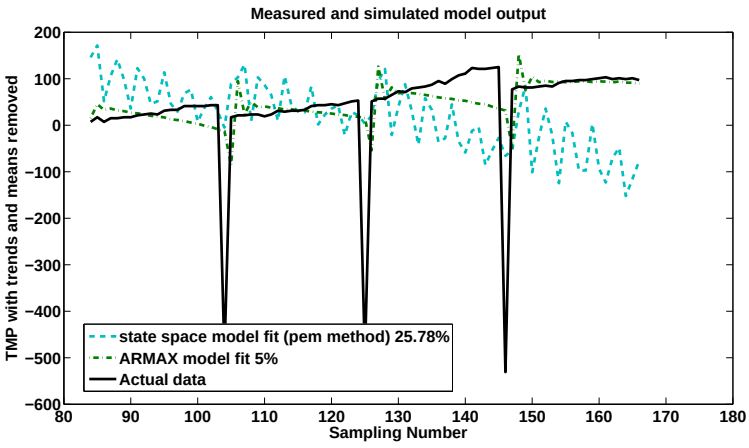

Fig. 4.49: ARMAX and state space formulation models - best fit for TMP with flux input only

Input data set type	CUESID Subspace	ARX	ARMAX	State space (pem)	State space (n4sid)
Permeate flux only	79.90%	-116.5%	5.00%	25.78%	-35.53%
Permeate flux and SMP	90.50%	-32.64%	-107.00%	5.38%	4.95%
Permeate flux, SMP and MLSS	89.14%	-1.39%	-33.32%	8.5%	-60.74%

Table 4.6: Reduced data set - comparison of best fits for various autoregressive model formulations

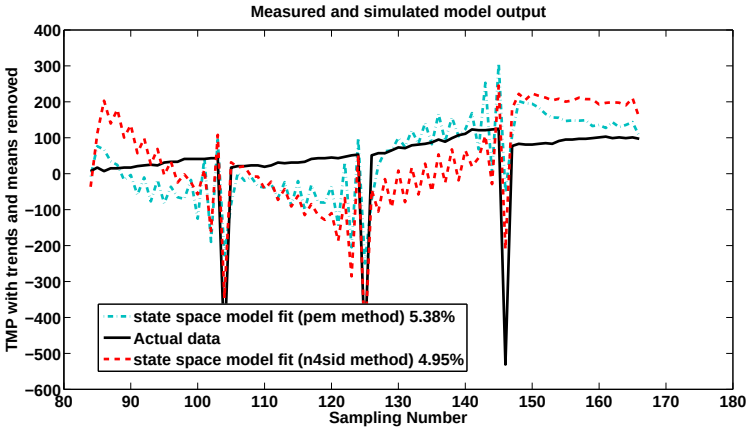

Fig. 4.50: State space formulation models - best fit for TMP using flux and SMP levels

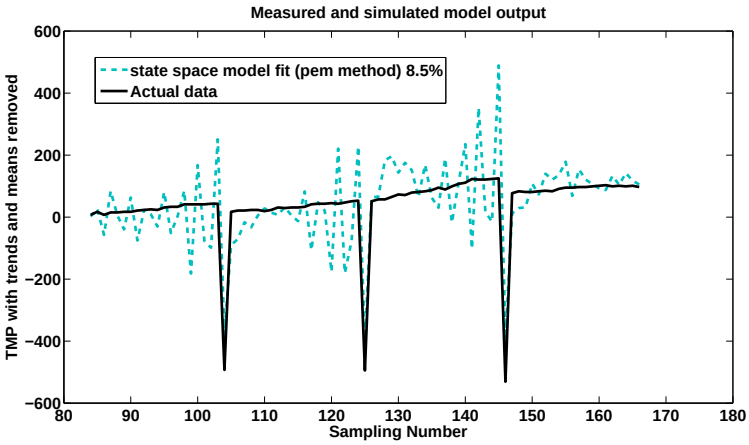

Fig. 4.51: State space formulation model - best fit for TMP using flux, SMP and MLSS levels

4.4.2.2 Full data set of all 29 flux steps up and down with input/output model structure

In an attempt to ascertain how good all these methods are at fitting data that has wide scatter and variability, it was decided to try to fit the various model structures to all 29 flux steps, both for those going up and down, as depicted in Figs. 3.51 and 3.52. This would rigourously test the robustness of each method against a much larger, albeit much more variable data set. In this attempt to fit a much larger data set, it was also thought a good idea to try to measure the effects of the regular and periodic backwashes on the various simulation models. This is since the backwash occurs over a very short period and produces a rapid and extreme change in flux direction that will obviously impact upon any model fit. Hence the following formulation with backwash included was given consideration in the basic input-output model structure:

$$\mathbf{y_{12}'} = \mathbf{u_2} = \left[X_{MLSS}\right]; \mathbf{m_2} = \begin{bmatrix} Q_3 \\ f_{bwash} \end{bmatrix}; \mathbf{y_{21}'} = \left[TMP\right]$$

This is the same formulation as previously except the **SMP** data is ignored here to keep the formulation simple and to keep it focused on the measurement of backwash effects as well as on the use of an increased data set with increased scatter. Nevertheless, the MLSS concentration was retained in this general formulation since based upon the results of the previous section, it appears this specific concentration yields some slight improvement in fit. For this full data set of all 29 flux steps, the general model case above was run in three different ways as follows:

1. The input is the permeate flux and the MLSS concentration, with the output being the TMP.
2. The input is the permeate flux, the MLSS concentration, and the previous backwash step initial conditions, with the output being the TMP.
3. The input is the permeate flux and the MLSS concentration, with the output being the TMP, while all the backwash steps are removed entirely so there is no discontinuities in the data and subsequent sudden large reversals in flux.

Of the three types of run described above, the second one refers to the inclusion of the backwash step initial conditions as an input variable. This was done to measure the effect of using the initial start point of the previous backwash step as an input variable to see if there is any improvement in fit. Theoretically speaking this means if after a certain backwash period only a moderate recovery in membrane permeability occurs, this should be reflected in the start point for the next flux step. In other words a poor recovery of flux caused by a previous backwash step, would mean that the next forward flux step would be more prone to quicker fouling, and hence its flux production for this flux step period would be poor in overall terms. This is also a very crude way of trying to introduce the concept of the membrane retaining a hysteresis "memory" of the previous operational event. Mathematically speaking this can be represented as follows:

$$BW_1 = TMP_{ratio} \cdot TMP_0 \tag{4.24}$$

where

TMP_1 TMP value for beginning of next forward flux step period.

TMP_0 TMP value for end of previous forward flux step period (before backwash commencement).

TMP_{ratio} The ratio of TMP_1 to TMP_0.

BW_1 Backwash initial condition held constant during TMP_1 step, and now used as an input variable.

Basically, Equation 4.24 uses the reset ratio of drop in TMP during the previous backwash period to determine the input value for the backwash initial condition for the next forward flux step. For the third type of simulation run envisaged all the backwash steps are entirely removed to see if the model fit improves, since the backwash itself is of little real interest in this analysis as only positive forward feed flux production is what really matters.

Initially a subspace formualtion was tested first using the CUEDSID software and approximately 15 flux steps for the validation process which is roughly half the data points. For all three runs a fourth order model with block size of 15 is used. By the way as the data used here was quite constant in nature with little variation, it meant that the subspace formulation did not provide a solution due to this data consistency. This was overcome by introducing a very slight randomness in the values, especially the more constant input ones, in order to get the subspace algorithm to work. This random number generator only varied real input numbers by less than 1%, but this slight introduction of white noise was sufficient to allow the subspace algorithms to function properly. Nonetheless, an unintended consequence of this was that slightly different results are given each time for the identical simulation runs using the same Matlab© coding. This unfortunate side effect could only be overcome by running the Matlab© script several times to get a feel for this random behaviour, and then selecting the best averaged fits for the run.

Fig. 4.52 reveals an inadequate fit especially for the stepping down procedure. There is a slight improvement in model correlation in the second run depicted in Fig. 4.53, and a very large improvement with the third run with all backwashes removed as shown in Fig. 4.54.

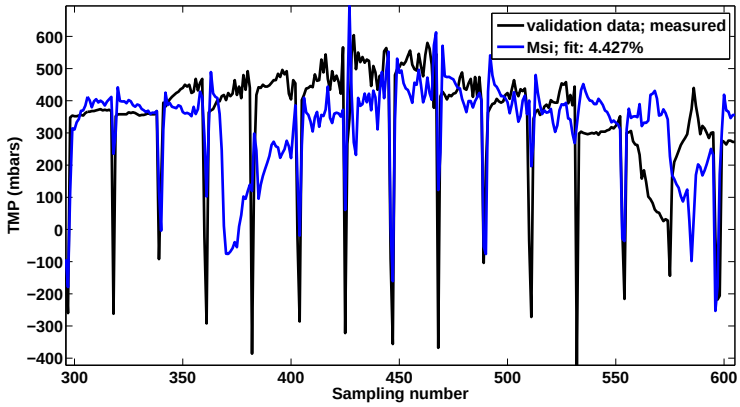

Fig. 4.52: Subspace formulation model for all 29 flux steps - best fit for TMP using flux and MLSS levels

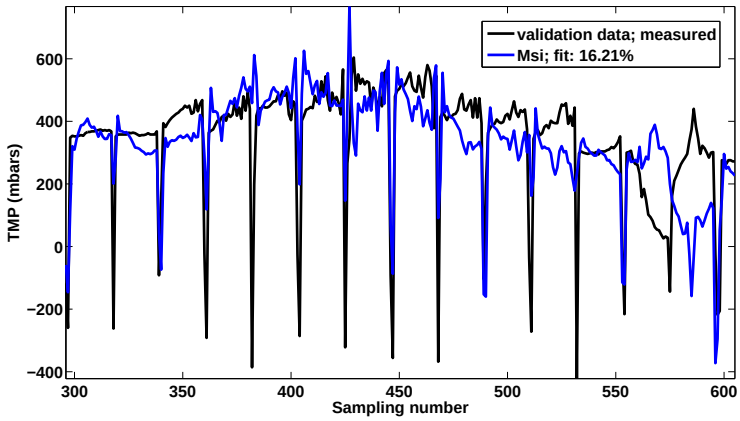

Fig. 4.53: Subspace formulation model for all 29 flux steps - best fit for TMP using flux, MLSS and backwash initial condition

Once again the other autoregressive model structures were also tested on these same formulations using the same input and output values. Again the input and output data sets, such as permeate flux, MLSS,

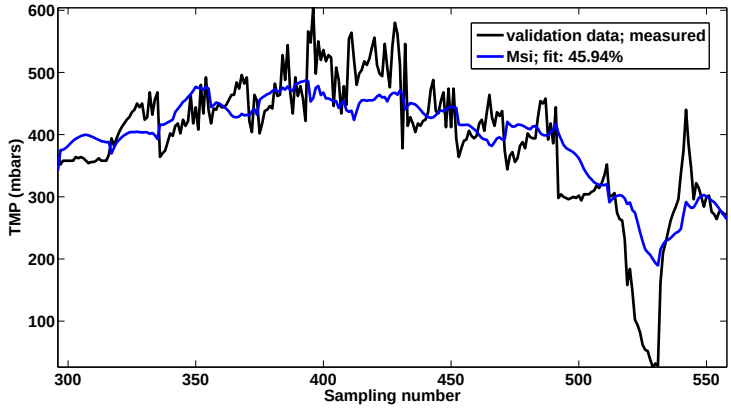

Fig. 4.54: Subspace formulation model for all 29 flux steps - best fit for TMP using flux and MLSS levels with backwash removed entirely

and backwash initial conditions, were de-trended and de-meaned as shown in Figs. 4.55, 4.56, and 4.57. In this respect, Fig. 4.57 proves interesting as it shows the change in backwash initial conditions as an input variable. It proves to have quite a variance trend even though it remains constant during a forward flux step.

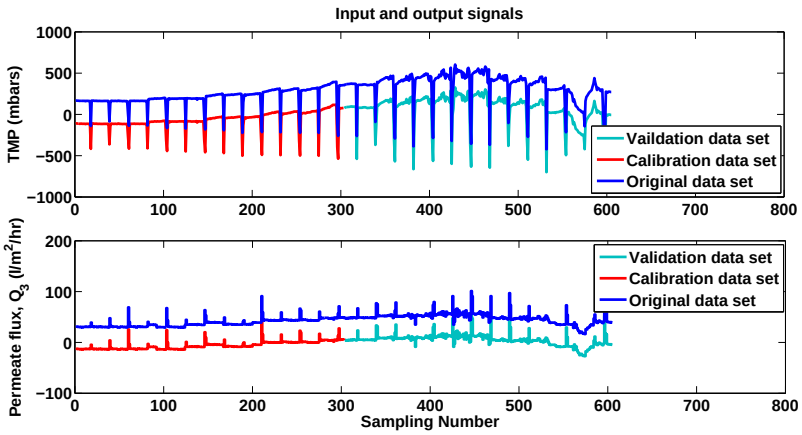

Fig. 4.55: ARX, ARMAX and state space formulation models - 1) input and output data for 29 steps

Figs. 4.58, 4.59, and 4.60 show similar results to the CUEDSID subspace method. Table 4.7 summarises all the results. From this table it is abundantly evident that the subspace method only proves slightly better than the other model structures. In fact all the model structures perform adequately for the runs with no backwash inclusion in them. In conclusion, both these real life plant data and those from the previous Section, both suggest model structures of this type are suitable for modelling of membrane fouling of MBR systems. On the other hand, they still need to be tested on much longer filtration data sets of several weeks if not months of values. Also a non-linear approach should also be tested, more especially when varying temperature data is also available, in order to establish whether a non-linear model gives a better fit even though it is a more complex formulation. This is tried in the next Section of this Chapter.

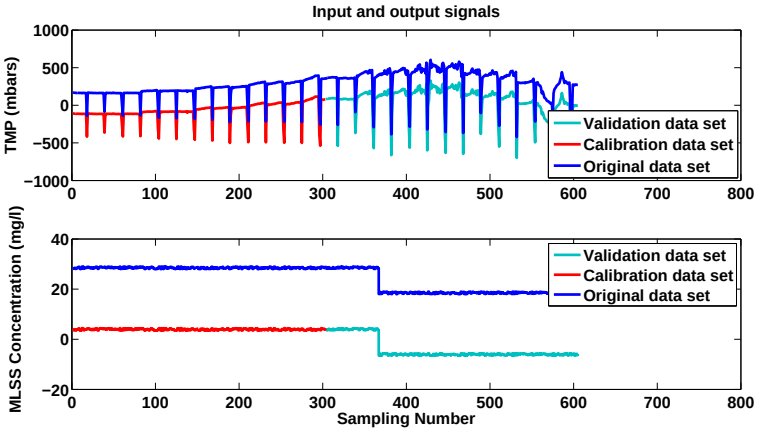

Fig. 4.56: ARX, ARMAX and state space formulation models - 2) input and output data for 29 steps

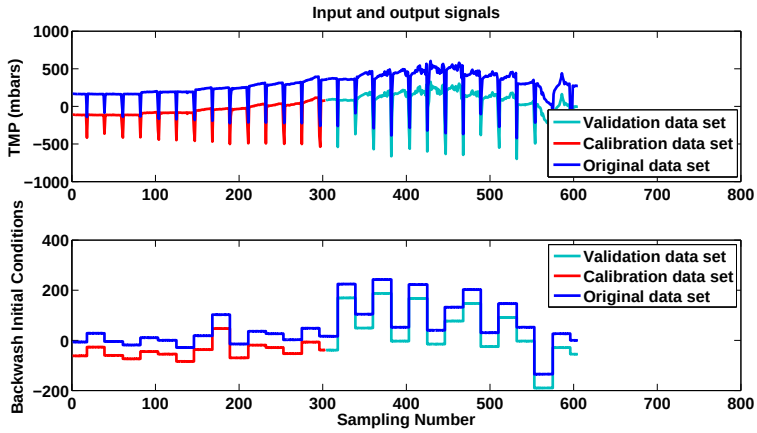

Fig. 4.57: ARX, ARMAX and state space formulation models - 3) input and output data for 29 steps

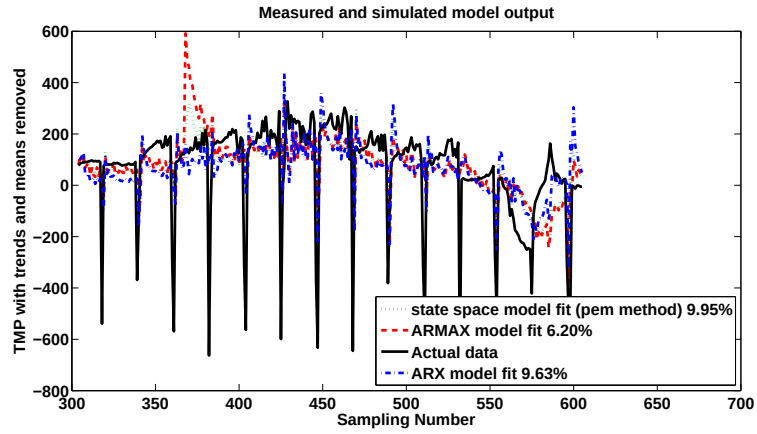

Fig. 4.58: ARX, ARMAX and state space formulation models - best fit for TMP using flux and MLSS levels

Input data set type	CUESID Subspace	ARX	ARMAX	State space (pem)	State space (n4sid)
Permeate flux and MLSS	4.427%	9.63%	6.20%	9.95%	no fit
Permeate flux, MLSS and backwash initial condition	16.21%	6.20%	6.46%	0.75%	3.14%
Permeate flux, MLSS and backwash initial removed	45.94%	45.24%	45.92%	43%	45.2%

Table 4.7: Full data set - comparison of best fits for various autoregressive model formulations

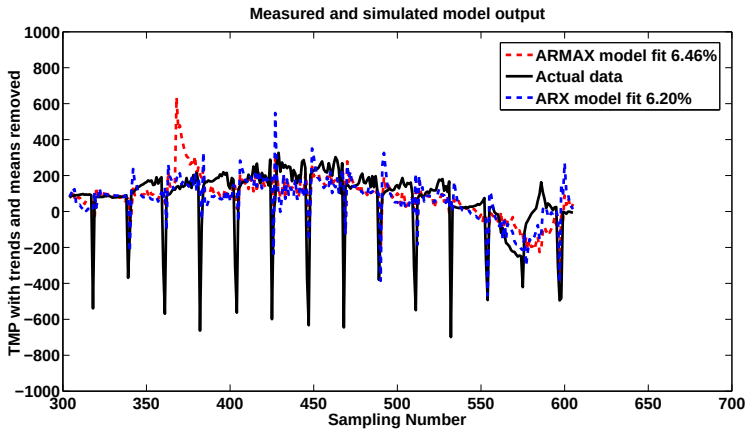

Fig. 4.59: ARX, ARMAX and state space formulation models - best fit for TMP using flux, MLSS and backwash initial condition

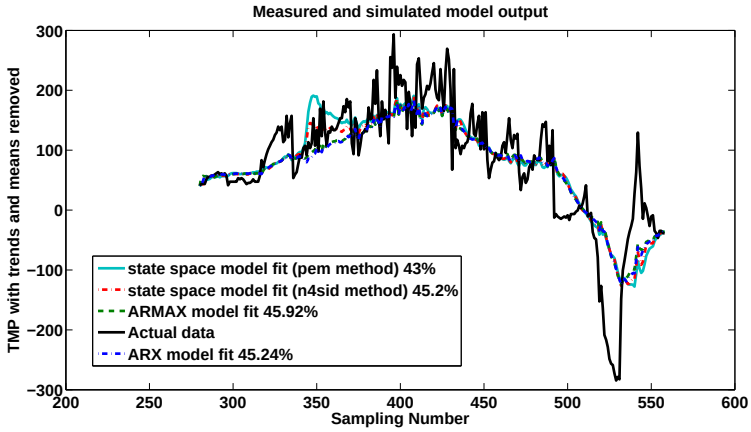

Fig. 4.60: ARX, ARMAX and state space formulation models - best fit for TMP using flux and MLSS levels with backwash removed entirely

4.4.3 Simulation results from ITT Sanitaire submerged pilot MBR plant

4.4.3.1 Reduced data set from November and December with input/output model structure

The ITT Sanitaire submerged pilot MBR plant that operated under a constant flux increasing TMP regime with regular fixed backwash steps was studied next. The advantage of its data set is that it was accumulated over several months and consisted of regular measurements taken on-line. Consequently, for a single month there are hundreds of thousands of data points that could be potentially used in any model simulation. Further, the mixed liquor temperature was regularly measured on-line so could be used as an input variable to see whether a bilinear model gave a representative fit for the data.

The best set of data was selected for this plant when it was operated at the Coors Limited (UK) site for the November to early December period when a very large variation in TMP was experienced. This was so that a larger variation in the data values would then allow a better fit to be obtained, as all these autoregressive methods appear to function better when there is greater variability in data, particularly as they were originally designed to fit extremely variable Econometric data. As the data set for even this vastly reduced period was still very extensive, only a few critical data sets were loaded. Otherwise the four-block algorithm used by the CUEDSID software is unable to cope with too large a data set and fails to implement.

Based on the results from the previous Section, the backwashing data has been removed from this data set as it is considered as non-essential in the correlation procedure. Incidentally, this pre-filtering out of the backflush steps also greatly simplifies the output plots and thereby makes them easier to discern. The input-output model formulation is as follows for this submerged MBR plant operated largely at constant flux with increasing TMP over a longer term period:

$$\mathbf{y_{12}}' = \mathbf{u_2} = \begin{bmatrix} X_{MLSS} \\ Temp_{liquid} \end{bmatrix}; \mathbf{m_2} = \begin{bmatrix} Q_3 \end{bmatrix}; \mathbf{y_{21}}' = \begin{bmatrix} TMP \end{bmatrix}$$

For this reduced data set, the general model case was run in three different ways as follows:

1. The input is the pre-filtered permeate flux only, with the output being the pre-filtered TMP.
2. The input is the pre-filtered permeate flux and the MLSS concentration, with the output being the pre-filtered TMP.
3. The input is the pre-filtered permeate flux, the MLSS concentration, and the liquid temperature, with the output being the pre-filtered TMP.

This last case allows the the testing of a bilinear model in temperature, and will be discussed and analysed further in the next Section. Only 40 points out of the many thousands available were initially used for the validation of the CUEDSID subspace method. This was done in order to speed up the computational process and so that a readable visual output plot could be prepared that would easily show any discernable model fit. At a later date another simulation run using up to 1000 points was used for validation of the subspace method and it gave largely similar results to those found previously. The other autoregressive methods were validated as usual with half the data set which amounted to over 19,000 points in this case.

Fig. 4.61 gives the plots for all the pre-filtered input and output operational data sets, and the plots for the process variables as well. It is evident that even though the permeate flux remained constant over this entire period, the TMP increased dramatically, more especially in early December. From the process variables it appears this increased TMP primarily correlates with rapid drops in MLSS concentrations for the same period in early December rather than the temperature variations which do not seem to directly

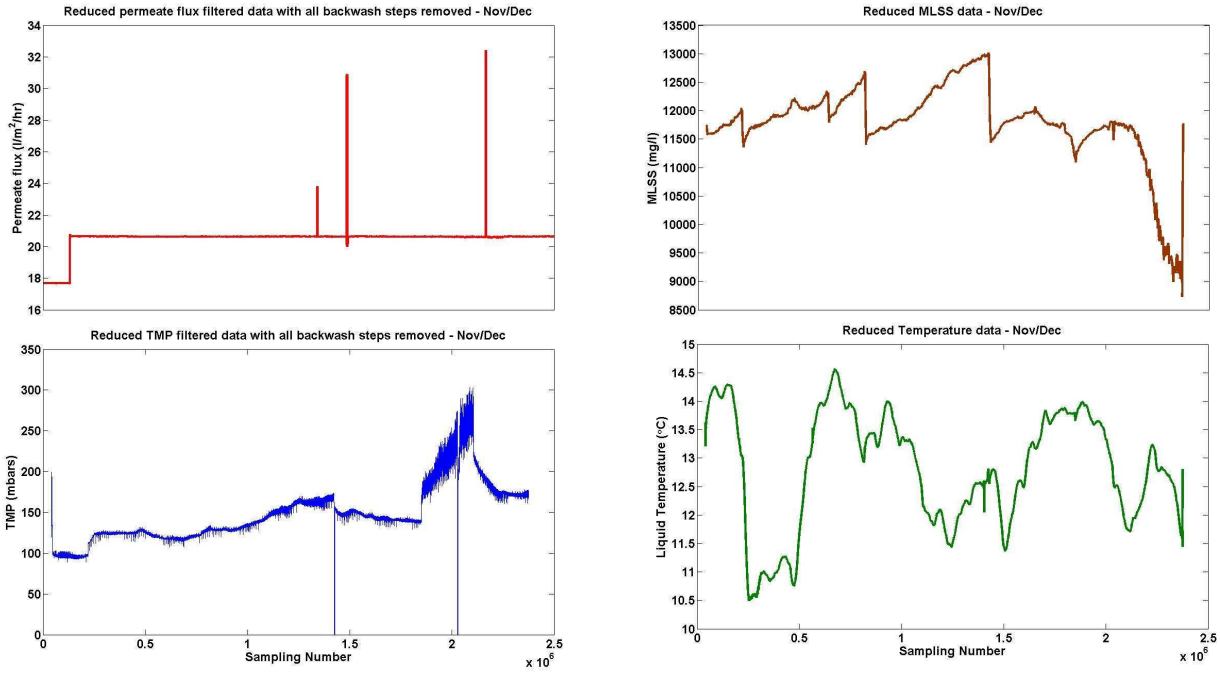

Fig. 4.61: Reduced data set for ITT pilot MBR - Nov/Dec

affect the TMP.

Fig. 4.62 is a plot of the first simulation run using the CUEDSID software for differing orders of model from one through to ten. It is evident that in this case as the model order increases the fit improves accordingly (i.e. first order model with fit of 73.54% up to a tenth order model with 90.80% fit). Also the shape and direction of the TMP plot improves as well to better reflect the real life data set.

Figs. 4.63, 4.64, and 4.65 are all three simulation runs for first order models with block sizes of one so that they all can be directly compared against each other. It is abundantly obvious that the fit gets better with the increased input data variables, and the shape and direction of the TMP increase per flux step also improves considerably until they almost closely match.

Following these simulations on the specialist subspace method advocated here, the other autoregressive methods were tried using over 19,000 points in the validation exercise. Table 4.8 summarise all the results. It shows that the other methods performed generally poorly compared to the CUEDSID method even though it was validated on a much reduced data set. Once again the ARX method proves reasonably robust while the state subspace (n4sid) method again gives either no fit or poor fit. In conclusion, it is recommended that the state subspace (n4sid) method should not be used for these data types and instead preference should always be given for the CUEDSID subspace method.

Input data set type	CUESID Subspace	ARX	ARMAX	State space (pem)	State space (n4sid)
Permeate flux only	73.24%	19.66%	20.09%	23.07%	no fit
Permeate flux and MLSS	72.75%	16.86%	17.34%	no fit	no fit
Permeate flux, MLSS and temp	73.24%	17.08%	17.61%	no fit	-151%

Table 4.8: Nov/Dec data set - comparison of best fits for various autoregressive model formulations

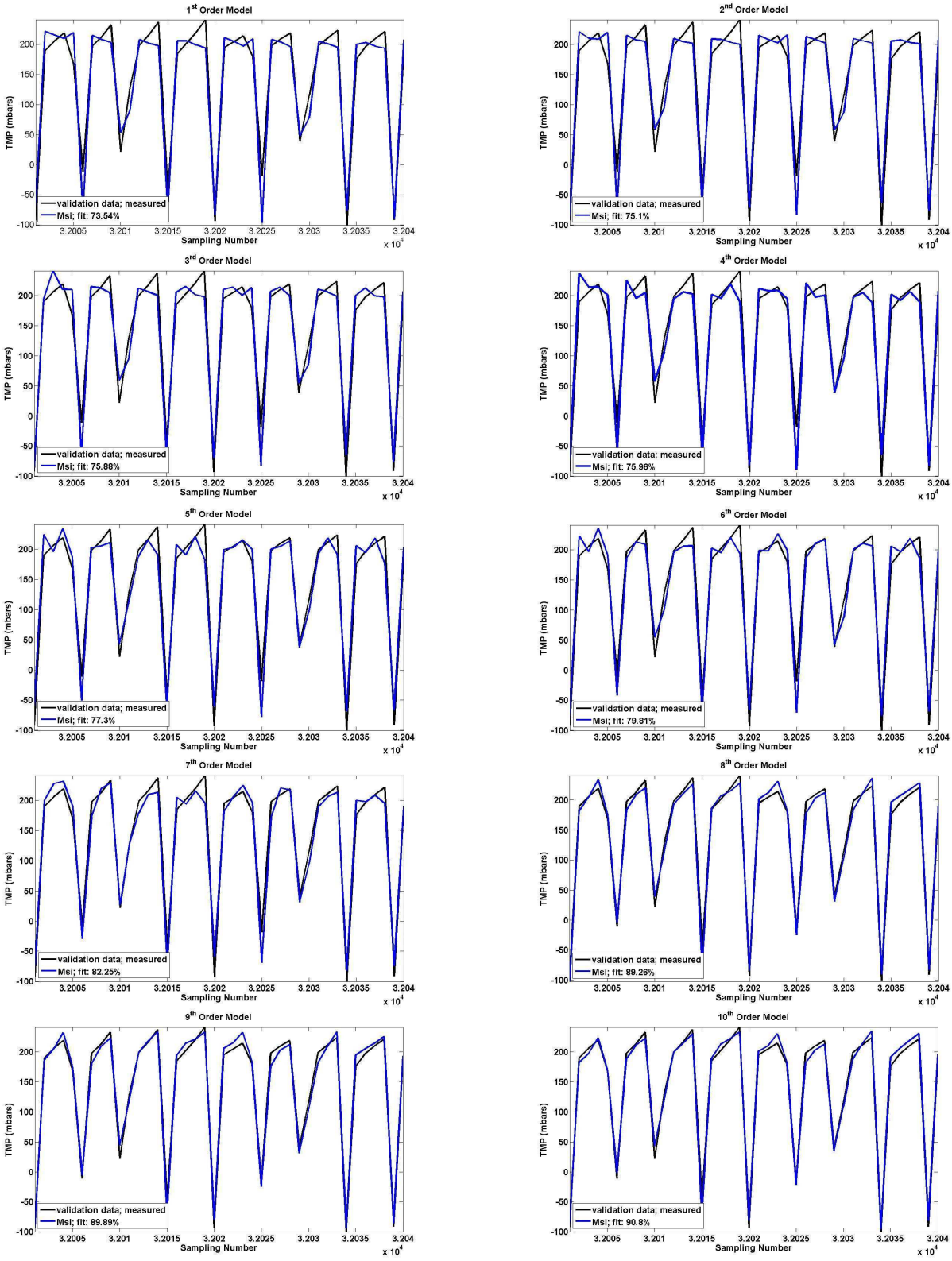

Fig. 4.62: Improvement of model fit with increasing model order

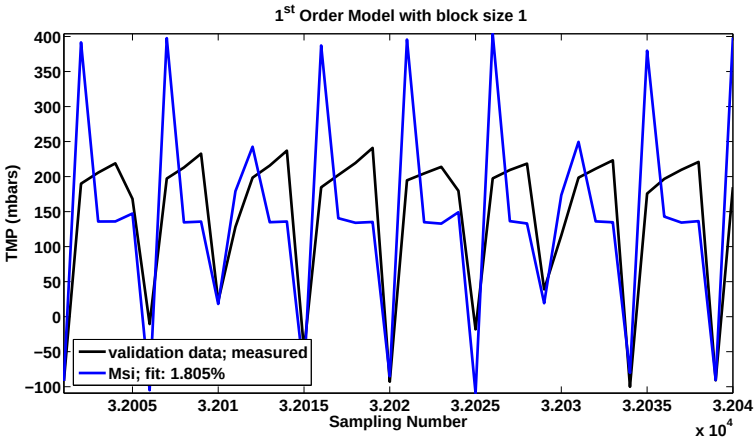

Fig. 4.63: Subspace formulation for Nov/Dec reduced data set - best fit for TMP with flux only

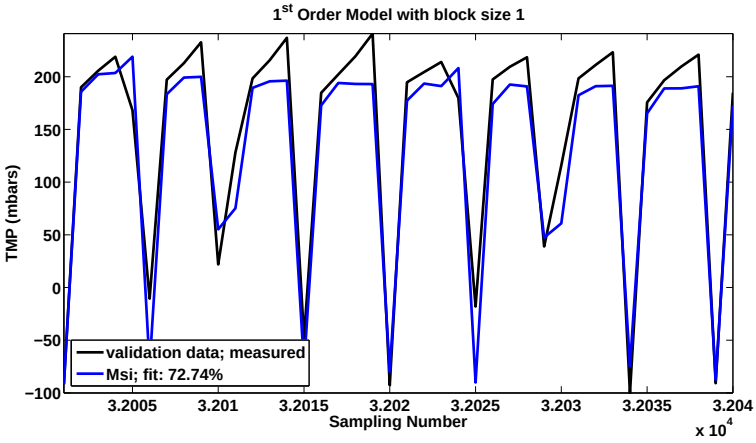

Fig. 4.64: Subspace formulation for Nov/Dec reduced data set - best fit for TMP with flux and MLSS levels

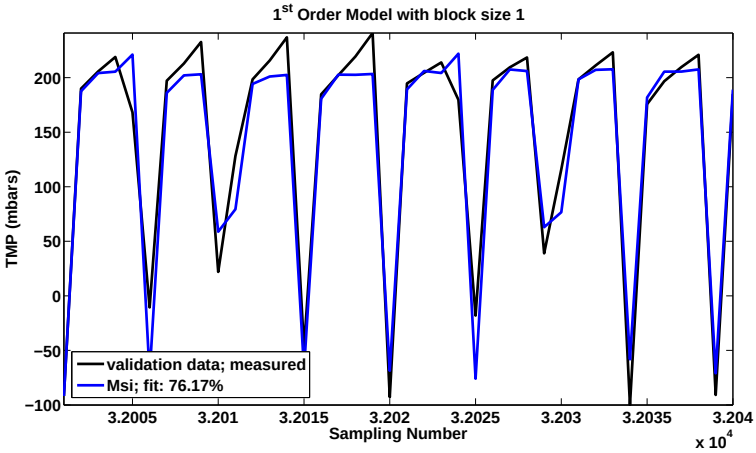

Fig. 4.65: Subspace formulation for Nov/Dec reduced data set - best fit for TMP with flux, MLSS levels and temperature

4.4.4 Bilinear model - Simulation results from ITT Sanitaire submerged pilot MBR plant

In order to test a non-linear model structure, a different reduced time period was used from the one used earlier for the extensive data set that was collated from running the ITT Sanitaire submerged pilot MBR plant. The different period that was selected was for the full month of January and consisted of nearly 24,000 data points. This month was chosen since the plant ran continuously for this period and also the MLSS was fairly constant for this same time period, so any bilinear model fit could only be attributed to the liquid temperature variations.

Once again as for the previous Section only a few critical data variables were used, namely the permeate flux, MLSS and temperature values as inputs with the output being the TMP. This was again done so that the four-block algorithm used by the CUEDSID software was able to handle the reduced data set. Additionally as before the backwashing data was removed from this data set by pre-filtering. Fig. 4.66 gives the plots for all the pre-filtered input and output operational data sets, and the plots for the process variables as well. As can be seen the MLSS concentration varies between a very limited range of 7,000 to 11,000 mg/l for the mixed liquor with an average value of 9,000 mg/l for the entire period, whilst the temperature of the wastewater varies considerably with a wide range of between 8 to 13.5 $^{\circ}C$. In terms of the operational variables, then both the permeate flux and TMP vary for the entire period, with the flux being ramped up and down and then up again. This variation in operational variables should assist the CUEDSID software's subspace algorithm in obtaining MISO model solutions.

In order to keep the analysis simple and straight forward the Matlab System Identification Toolbox© was not used in this Section even though it does have two non-linear model formulations that can be used in the GUI package, namely a non-linear ARX model and an alternative non-linear Hammerstein-Wiener model.

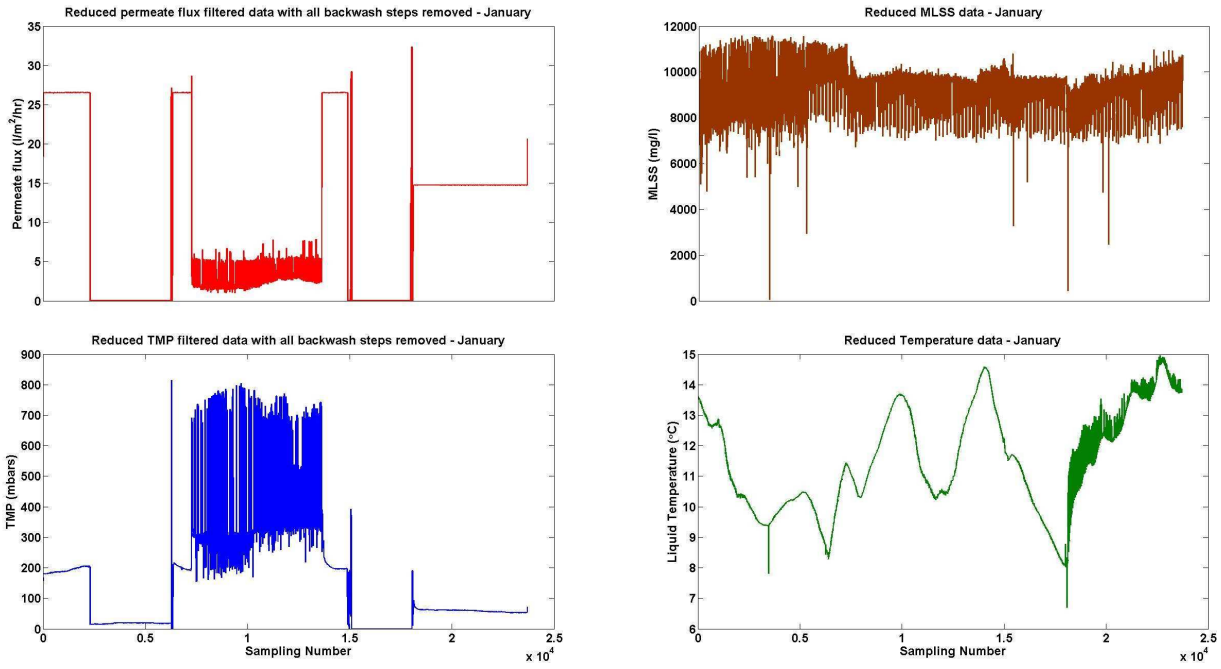

Fig. 4.66: Reduced data set for ITT pilot MBR - January

4.4.4.1 Model runs with linear subspace model formulation

Of the 24,000 points that were available only 2,000 were selected for this linear analysis. The CUEDSID software was run using 1,700 points to calibrate the 1st order subspace model formulation, with the remaining 300 points being used to validate the model. Fig. 4.67 shows that the best model fit for this first order model with block size of 46 was only 25.95%. The shape of the fit is quite poor as well with the model being incapable of producing accurately the regular step pulsing of the TMP during this reduced time period.

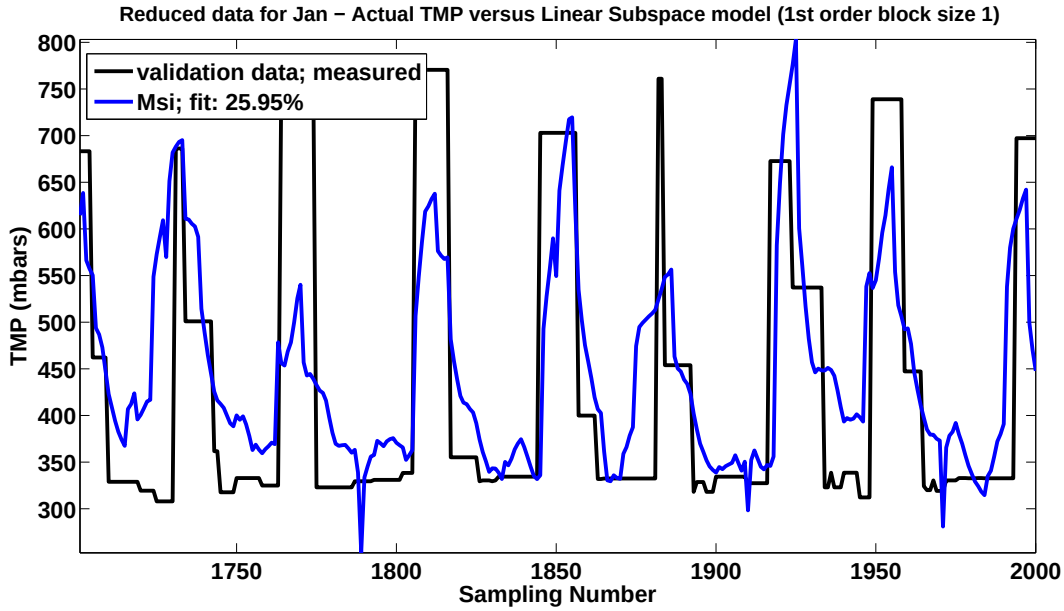

Fig. 4.67: Subspace formulation for Jan reduced data set - best fit for TMP with flux, MLSS levels and temperature

The subspace linear MISO model calculated by the CUEDSID software for this particular data set is as follows:

$$x(t+T_S) = A.x(t) + B.u(t) + K.e(t); \qquad x(0) = 0$$
$$y(t) = C.x(t) + D.u(t)$$

where:

$$A = \begin{bmatrix} 0.8712 \end{bmatrix}; B = \begin{bmatrix} -0.15849 \\ 0.00002638 \\ -0.00034283 \\ 0.76701 \end{bmatrix}; C = \begin{bmatrix} -85.336 \end{bmatrix}; D = \begin{bmatrix} 58.249 \\ 0.032973 \\ 26.428 \\ 471.71 \end{bmatrix}; K = \begin{bmatrix} -0.00016374 \end{bmatrix}$$

4.4.4.2 Model runs with bilinear subspace model formulation

In this case the specialised bilinear function that is incorporated into the CUEDSID software was used to ascertain if the previous linear fit could be improved upon by using a non-linear model. In this regard the

same reduced data set of 2,000 points was used with the identical number of 1,700 calibration points. This was done so that both types of model could then be directly compared against each other. The procedure that was developed to determine the best fit bilinear model was as follows:

1. The linear model developed in the previous Section is used as the start point for determining the eventual bilinear model. Hence it is slightly altered into a bilinear form with the N vector which represents the coefficients of the Kronecker product being initially set to zero.
2. The eigenvalue of the bilinear model's vector A is calculated and if it is less than one, then the model is assumed to be stable, and should run in a bilinear form. This stability condition must be satisfied otherwise the complex algorithm's in the bilinear model version will fail to implement. The closer this negative value of vector A's eigenvalue is to one, the more the bilinear formulation is prone to failure. If failure occurs, then another model structure needs to be used which meets this model sensitivity and stability criteria. This is one limitation of using this non-linear model formulation.
3. This "start point" bilinear model is then simulated using the same data set as before and the output from this simulation is saved.
4. This simulated output data is then used to run the subspace bilinear function using 1,700 points of data for the calibration step.
5. The validation step is then completed using only 100 points of the remaining 300 (to keep the computation time reasonable, and the output plots easy to read). The simulated output TMP is plotted against the new calculated values from the finalised bilinear model to show the best fit (see Fig. 4.68).
6. This final bilinear model is then simulated with the original data values to show the best fit for both model types on the same plot along with the original data values (see Fig. 4.69).

As can be seen in Fig. 4.68 the bilinear model formulation gives a better fit for the simulated output of 43.03%. It is worth remembering that this fit is improved even though a third of the number of validation points was used. It also means that the procedure developed above to determine the best fit bilinear model using the best fit linear model as a start point has been verified. In fact this procedure could be easily be automated for full MPC.

The actual subspace bilinear model calculated by the CUEDSID software for this particular data set is as follows:

$$x(t+T_S) = A.x(t) + N(u(t) \otimes x(t)) + B.u(t); \qquad x(0) = x0$$

$$y(t) = C.x(t) + D.u(t)$$

where:

$$A = \begin{bmatrix} 0.1112 \end{bmatrix}; B = \begin{bmatrix} -0.0121 \\ 0 \\ 0.0073 \\ -0.5041 \end{bmatrix}; C = \begin{bmatrix} -55.7901 \end{bmatrix}; D = \begin{bmatrix} 49.2111 \\ -0.0017 \\ 7.6624 \\ -43.0112 \end{bmatrix}; N = \begin{bmatrix} 0.0008 \\ 0 \\ -0.0002 \\ 0.0370 \end{bmatrix}$$

Fig. 4.69 is a plot of both types of model against the original TMP data. It clearly shows that the bilinear model performs much better by giving the optimal fit. In the plot both models preform badly at first with the linear model grossly under predicting values while the bilinear version slightly over predicts values.

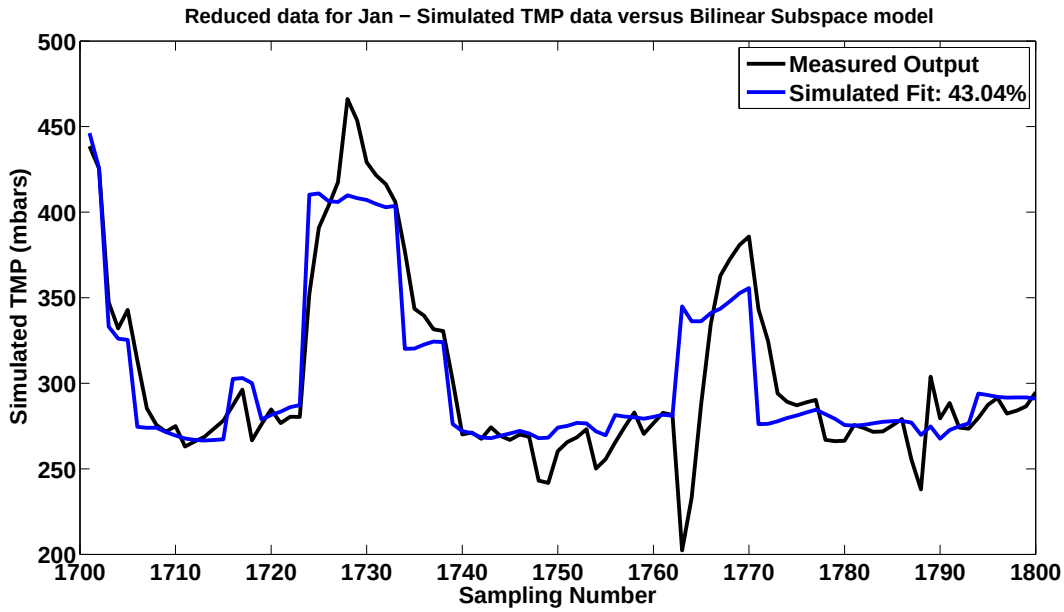

Fig. 4.68: Bilinear formulation for Jan reduced data set - best fit for simulated TMP with flux, MLSS levels and temperature

Both model types settle down, with however the linear model still giving a much larger scatter in predicted values as opposed to the bilinear model.

Since this data set was carefully selected to minimise the effects of the mixed liquor concentration on the operational TMP, the mixed liquor temperature can only be the other factor that determines the bilinearity of this data set. Consequently, this proves that this wastewater data types are suitable to be used to verify non-linear subspace model varieties.

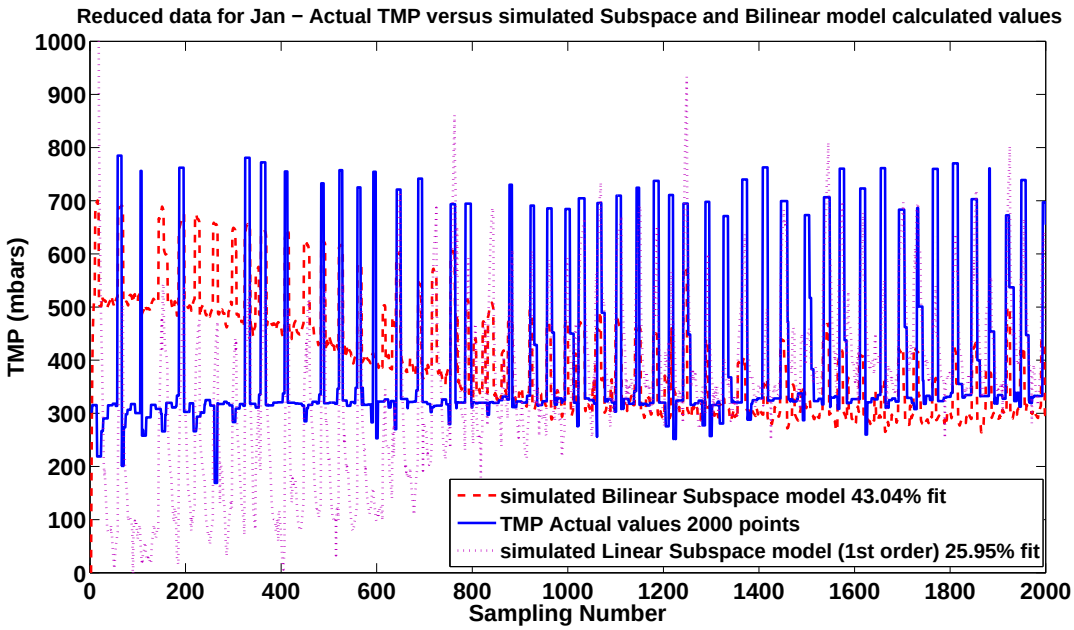

Fig. 4.69: Reduced Jan data - comparison of actual TMP with best fits from Linear and Bilinear Subspace simulated models

4.4.5 Summarising results from behavioural models

Table 4.9 summarises the results from some of the behavioural model runs for the data used from the three plant. It is clear that overall the subspace method developed in the CUEDSID software gives the superior fit results when compared to the other autoregressive methods. However, in the case of the Aquabio pilot plant, the other autoregressive methods give better shape of fit for each flux step with the flux reducing slightly exponentially with time.

Plant Type	CUESID Subspace	ARX	ARMAX	State space (pem)	State space (n4sid)
Aquabio pilot MBR plant - 7 best flux steps	55%	36%	45%	no fit	-246.7
ITT pilot membrane unit - 8 best flux steps	89.14%	-1.39%	-33.32%	8.5%	-60.74%
ITT pilot MBR plant - long term data	73.24%	17.08%	17.61%	no fit	-151%

Table 4.9: Comparison of model fits for various plants for different MISO data sets

The following summarised points can be made regarding behavioural model structures used in this Section:

- If the input-output model structure is not selected judiciously then the resulting model will prove of little predictive value. Therefore very careful thought has to be applied to develop appropriate and sensible input-output model structures that best reflect reality.
- Continuously gathered data sets gave better model fits then discontinuous data sets such as was proved when using the best flux stepping data from the Aquabio pilot plant.
- Different plant layout seem to favour different behavioural model formulations, so some achieve a better fit using state space and subspace formulations, whilst others are better reflected using autoregressive iterative formulations such as the ARX formulation. However, the subspace method developed in the CUEDSID software always performed adequately and so should always be tried first. Conversely, the Matlab© subspace method (n4sid) that consistently performed poorly so should not be used.
- It was found that when the backwash data was entirely removed from the data set, the fits for all methods considerably improved. It is recommended it is always discarded from a data set before use if at all possible, since it will negatively skew the fit especially the shape and direction of the fit.
- As expected, the bilinear subspace model gives a better fit than its linear version, although its formulation is more complex in nature, and the algorithm used is very sensitive and thus apt to fail or not be able to provide a solution.
- It is abundantly evident from these simulation results that behavioural input-output model structures can give useful predictive results when compared to a traditional phenomenological mechanistic approaches for wastewater treatment.

4.5 *Chapter Summary*

In this Chapter, a comprehensive phenomenological membrane fouling model was developed from a basic version initially produced by Duclos-Orsello et al. (2006). Once calibrated and validated, this modified model was then tested on data sets taken from real life plant that are described in the second half of Chapter 3. The results produced varied, although on the whole they proved generally very good. It was noted that phenomenological fouling models need to be made bespoke for each individual filtration system on a case-by-case basis, and thus will always prove time consuming to construct and will always require expert knowledge to be used properly. This is especially true for the hydrodynamics of the process and the membrane operational regime.

Using the same data sets used for the first model type, several behavioural fouling models based on the "Model Conceptualisation Procedure" outlined in the first half of Chapter 3 were tested as alternative model structures. This included both linear and non-linear input-output model structures. Out of the various linear input-output model structures tested, the subspace method developed in the CUEDSID software nearly always gave the best and most consistent results. Also the non-linear bilinear version of this subspace model proves not as accurate as the phenomenological model even though it uses a single shot fast algorithm for parameter estimation. It also was very fragile and prone to crashing.

Chapter 5

MBR model development work: Activated Sludge system

5.1 *Phenomenological Activated Sludge models - Lu and Oliveira models*

This Chapter firstly describes the development of phenomenological models to describe the Activated Sludge biological processes in bioreactor of a MBR especially in relation to extra-cellular polymeric substances (EPS) and **SMP**. It then goes on to detail the results obtained from running the plant data through these developed models. The last Section of this Chapter describes the results obtained from using both the actual plant data as well as the specially generated data to calibrate and validate the time series input-output version of these Activated Sludge models.

5.1.1 Introduction - Activated Sludge modelling for MBRs

As already mentioned in Section 2.3.2, there are several mathematical models available to describe the Activated Sludge processes in a MBR system. In this research study, only those models that consider the simple removal of both carbon substrate and Nitrogen nutrient are utilised. More complex models that also include biological Phosphorous nutrient removal are not considered, as their level of complexity is not required in this study in order to demonstrate the novel modelling ideas being scrutinised here.

The most widely known and used Activated Sludge model is the IWAs ASM1, which has become a major reference for many scientific and practical projects. It was first introduced in 1987 by Henze et al. (1987) and is still considered as a "state-of-the-art" global model with its kinetic and stoichiometric parameters having being extensively studied and calibrated on an international basis. This model contains seven soluble, S, and, six particulate, X, components in the wastewater. Each of the thirteen components represents an independent state and has different growth and decay processes that are given in the Peterson Matrix shown in Fig. 5.1 (Petersen et al. 2001). Each row of this matrix represents a process and each column refers to a specific component concentration. There are eight processes altogether which are interrelated to each other. Fig. 5.2 shows the major process interactions. For example the differential equation for the conversion of soluble biodegradable matter, which is one of the thirteen components is given in Equation 5.1. In this equation, S_S represents the concentration of the specific component, Y_H is a yield coefficient for biomass growth, and ρ_i are the process rates related to this component, with process number i.

$$\frac{dS_S}{dt} = \frac{-1}{Y_H} \cdot \rho_1 - \frac{1}{Y_H} \cdot \rho_2 + 1 \cdot \rho_7 \tag{5.1}$$

The eight process rates are based on simple Monod kinetics. For instance the process rate for the aerobic growth of heterotrophs, ρ_1, is shown in Equation 5.2, where X_H is the heterotrophic biomass concentration, μ_H is the maximum growth rate, and S_O is the dissolved oxygen concentration. The kinetic parameters are K_S and $K_{O,H}$, which are half-saturation constants that control the switching functions $\frac{S_S}{K_S+S_S}$ and $\frac{S_O}{K_{O,H}+S_O}$ respectively which determine the biomass growth. For example, for soluble biodegradable matter, the switching term equals the maximum value of 1 as S_S approaches infinity, and equates to a minimum of 0 if S_S is a zero concentration. Incidentally, if S_S equals K_S, then the value of the switching term is 0.5, and the process rate is halve of the normal value. Thus in Equation 5.2, both the switching functions control the takeup of soluble substrate by biomass and the utilisation of oxygen, which collectively determine the rate of the biomass growth process, ρ_1.

$$\rho_1 = \mu_H \cdot \frac{S_S}{K_S + S_S} \cdot \frac{S_O}{K_{O,H} + S_O} \cdot X_H \tag{5.2}$$

The IWAs ASM3 is another powerful and commonly used biological model (Gujer et al. 1999). It was formulated by the same international working group that initially created the ASM1. The basic idea of the ASM3 is to give a much clearer and easier distinction between the soluble and particulate components that practically reflect the reality faced by plant operators. The soluble matter is defined as having particle sizes that pass through a 0.45 μm GFC filter paper. In the ASM3, all the conversion processes of heterotrophs and nitrifiers are clearly separated in contrast to the ASM1 version. Additionally, all components are easy to determine by a simple influent characterisation procedure, as opposed to the ASM1 whose organic Nitrogen fractions are especially difficult to measure. One other main difference from the convoluted and interrelated ASM1 components, is that for the ASM3 components the interactions are in a single direction only. This means substrate and nutrient uptake, and biomass growth and decay (known as endogenous respiration) occur on a sequential basis only. Conversely, the ASM1 requires an iterative procedure in order to find a solution and some component states can go negative if the model is poorly set up, whilst the ASM3 is simpler to solve in a single-shot procedure and its component states always remain positive. However, the mathematical format of this model is similar to the ASM1 with thirteen components and twelve processes related to COD demand (with a thirteenth process related to TSS demand). Again, Fig. 5.2 shows the major processes interactions. These include the thirteen model component fractions, the thirteen process equations, and the stoichiometric and kinetic parameters in the full Petersen matrix. Incidentally, whereas the ASM1 has been widely used to provide a better understanding of wastewater treatment systems in both scientific and practical applications such as in extensive study of different plant carried out by Drews et al. (2007b), there are far fewer published papers about the use of ASM3 in pilot or full scale WWTP applications. The few papers that focus on the ASM3 model tend to use it more for its simplicity rather than its universal applicability (Hulsbeek et al. 2002).

5.1.1.1 Biological factors impacting on MBR fouling

The concentration of EPS in either bound or soluble/colloidal form is considered as the major cause of membrane fouling in a MBR system. EPS in its soluble/colloidal form that is found in the sludge supernatant is usually termed **SMP** and thought to play a more important fouling role than its bonded counterpart. The **SMP** concentration in the sludge water itself is highly dependent on various factors like the influent wastewater characteristics, the solids loading rate, the SRT, the MLSS concentration, mechanical stress on the biomass due to the hydrodynamic regime employed (e.g. CFV), and the microbial growth phase of the biomass. Further factors leading to an increase in **SMP** formation have been identified as unsteady plant operation due to intermittent feeding, toxic shock loads, irregular sludge wastage, shifts in the oxygen supply, and high salinity/acidity load conditions. All these additional factors are thought to cause the microbes in the biomass to become stressed which in turn leads them to produce EPS as a protective coating, e.g. cell encapsulation, with some of this dissolving into the supernatant as **SMP** (Drews et al. 2006). All these selectivity conditions not only affect the sludge supernatant's propensity for increased pore blockage

	S_I	S_S	X_I	X_S	X_H	X_A	X_P	S_O	S_{NO}	S_{NH}	S_{ND}	X_{ND}	S_{ALK}
1 Aerobic growth of heterotrophs		$-\frac{1}{Y_H}$			1			$-x_1$		$-i_{XB}$			$-z_1$
2 Anoxic growth of heterotrophs		$-\frac{1}{Y_H}$			1				$-y_2$	$-i_{XB}$			$-z_2$
3 Aerobic growth of autotrophs						1		$-x_3$	y_3	$-i_3$			$-z_3$
4 Decay of heterotrophs				$1-f_P$	-1		f_P					$-i_4$	
5 Decay of autotrophs				$1-f_P$		-1	f_P					$-i_5$	
6 Ammonification of soluble organic nitrogen										1	-1		1/14
7 Hydrolysis of entrapped organics		1		-1									
8 Hydrolysis of entrapped organic nitrogen											1	-1	

Fig. 5.1: Petersen Matrix for ASM1

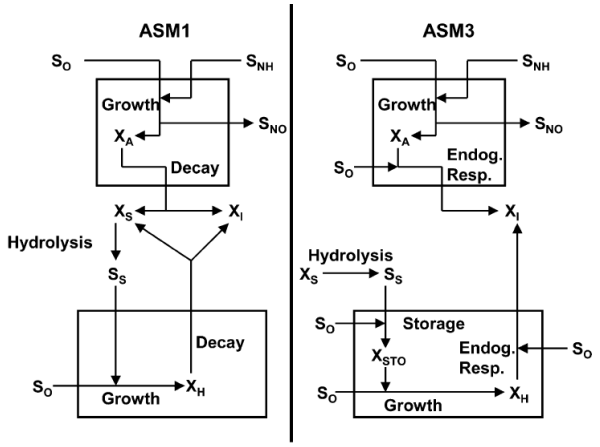

Fig. 5.2: Substrate flows for autotrophic and heterotrophic biomass in ASM1 and ASM3 models (Paul, 2006)

and constriction (i.e. irreversible fouling), but also impact on the liquor particulate's ability to cause cake build up (i.e. reversible fouling). For instance a poorly conditioned mixed liquor and sludge can allow the predominance of filamentous flocs which increase cake buildup and membrane clogging. Conversely a mixed liquor experiencing extreme hydrodynamic conditions (e.g. very high CFVs), would promote small pin flocs to predominate, which creates sludge that proves very hard to settle and dewater. Fig. 5.3 shows the relationship of MLSS concentration to sludge floc size distribution. It is clear from this plot, that higher MLSS concentrations lead to narrower floc size distributions which would give poorly packed, less dense membrane cakes, which at low CFV regimes would cause greater clogging.

Current research has also noted the following issues:

- The EPS concentration has a direct affect on sludge filterability and thus the specific cake resistance.
- The **SMP** deposits inside the membrane pores and then constricts the pores area and thereby increases the overall membrane resistance. This **SMP** deposition is governed by a **SMP** rejection parameter which in most models is assumed to remain constant even if in reality the fouling propensity of **SMP** changes in time.

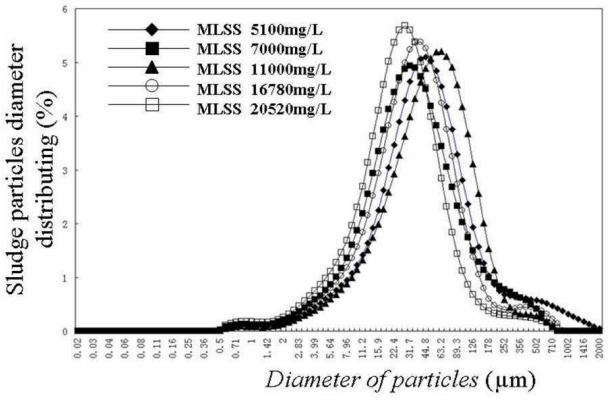

Fig. 5.3: Sludge floc size distribution for varying MLSS concentrations (Judd and Judd, 2006)

- Fouling is affected both by the floc size distribution of the Activated Sludge and the pore size distribution of the membrane.
- The CST of sludge deposits is affected by the polysaccharide content of the EPS, and thus EPS composition and not only its concentration.
- Not only bound EPS but also dissolved EPS as **SMP** is found to affect cake permeability.
- Fouling is negatively affected by the concentration of flocculent matter in the filtrate.
- Production of **SMP** and EPS are affected by the quantity of nutrients in the influent.

5.1.1.2 MBR biology - Selected modelling approaches

Two versions of a modified Activated Sludge model which take into account the production of EPS as **SMP**s were tested using the real life data produced from the full scale sidestream configuration Aquabio MBR plant which is owned and operated by Kanes Foods in Worcestershire. The first version of the modified biological model used the ASM1 (Henze et al. 1987) combined with a **SMP** model and is based on the work carried out by Lu et al. (2001). The second version of the modified biological model used the ASM3 (Gujer et al. 1999) combined with a MP model based on the work carried out by Oliveira-Esquerre et al. (2005). This comparison was carried out in order to see which version better predicted substrate removal efficiency and by inference the production of eEPS which would directly impinge upon membrane fouling rates by subsequent pore blocking.

As stated in the Literature Review Section, there have been a few models published that contain further processes and parameters that relate to protein and polysaccharide production, or that have been specifically developed for a MBR situation. Some are modified versions of the Activated Sludge variety model that have been adapted to a MBR situation (Gehlert and Hapke 2003), while others are stand alone varieties such as the one developed by Laspidou and Rittmann (2002) that do not relate directly to the methods used by IWAs Activated Sludge models but which still take into account **SMP** production. Some are very complex in structure with many new parameters needing calibration, such as the MBR model developed by Jang et al. (2006b) which is an Activated Sludge variety model that contains many new processes for specific fractional states of **SMP** and EPS production and degradation.

The best models were not necessarily chosen here and neither were the worst. The Lu et al. (2001) model was chosen since it contains the main **SMP** components that researchers consider important in membrane fouling by supernatant liquor. These variables are namely the BAP and the UAP. Hence this model is fairly complex but not too complex like the Jang et al. (2006b) one since it does not have additional EPS components. However it does have some additional parameters and processes due to formation and/or degradation of BAP and UAP.

The Oliveira-Esquerre et al. (2005) model was chosen simply because it has the easiest model structure available with only a single additional process and component, and only four additional parameters. So it was quite easy to calibrate having only a limited degree of freedom and thus many complex checks and simulations could be carried out for it. Also it was very easy to ascertain its shortfalls and any advantages, if any. Further it is only one of a few versions of ASM3 variety models developed by researchers since most use the ASM1 or its variants. Therefore it was ideal to be used here to fully study the model calibration procedure of an Activated Sludge variety model adapted for a MBR situation. This comprehensive testing procedure is as follows: a) mass balancing checks for Carbon fractions, Nitrogen fractions (and Phosphorous fractions if used), and then a charge balance; b) kinetic parameter estimation and optimisation; c) sensitivity analysis with respect to process variables; and, d) comparison of process outputs with existing bona fide Activated Sludge models, like ASM1 and ASM3. The Author is not necessarily suggesting that either of the two models used here should be used to model MBR processes since they have many limitations. However, as will be seen later, they are ideal for answering the research question of "how easy is it in practice to calibrate and validate a relatively simple Activated Sludge model for a real life MBR plant which is still rich enough in complexity to include the major biological / biochemical agents involved in the fouling of MBRs".

One aspect of both these models that was discovered was that neither model was fully tested as should have been done by their developers, so neither model as they original stand are accurate in predicting sludge yields, aeration demands, etc. Under the larger research project these models were extensively tested, and then modified to make them accurate as possible within the constraints of each model structure. This testing procedure is itemised below but not described in this thesis as it was carried out by other project staff. This severe testing procedure is especially carried out for the Oliveira-Esquerre et al. (2005) model (Janus and Paul 2009), and should be used for any future formulated biological / biochemical model.

- *Model and process descriptions:*
    1. Lu ASM1 based model (i.e. Reactions, Petersen Matrix, Issues, Modifications).
    2. Oliveira ASM3 based model (i.e. Reactions, Petersen Matrix, Issues).
    3. Modification of the Lu / Oliveira model processes (if any).
    4. Inclusion of processes into the ASM1 / ASM3 Petersen matrix.
    5. Stoichiometric links between original ASM1 / ASM3 and new **SMP** / EPS processes.
    6. Comparison between modified models and the original **SMP** process models.
- *Simulations with published model:*
    1. Simulation with a range of different steady state operating conditions.
    2. Comparison of sludge production and oxygen demand for all models.
    3. Other Sensitivity studies.
    4. Overview of published model issues.
- *New Model Calibration Procedures:*
    1. Linkages between biological and fouling models: **SMP**, EPS, MLSS.
    2. Links between COD and **SMP** / EPS - conversion equations.
    3. Parameter identification procedures (e.g. optimisation based calibration, identification of new **SMP** and EPS kinetic parameters).
- *Initial model simulations in Matlab©:*
    1. Simulation of existing models in Matlab/SIMULINK©.
    2. Identification of model deficiencies.
    3. New model development in Matlab/SIMULINK©.
    4. New model calibration procedures.
    5. Development of model calibration protocol for any future new models.

5.1.2 Model and process descriptions - Petersen Matrix

5.1.2.1 Combined ASM1 and SMP - Lu ASM1 model

Fig. 5.4 describes the Lu et al. (2001) mathematical model of **SMP** formation and degradation based on the ASM1 where the overall **SMP** consists of two specific types (Leudeking and Piret 1959). The first type, known as UAP, is comprised of the direct byproducts of substrate utilization and cell growth. The second type, known as BAP, can be considered as the byproducts of endogenous respiration of cell mass. The total **SMP** is the sum of UAP and BAP. Fig. 5.5 shows pictorially these additional two **SMP** states in the Lu et al. (2001) model when compared to the standard ASM1.

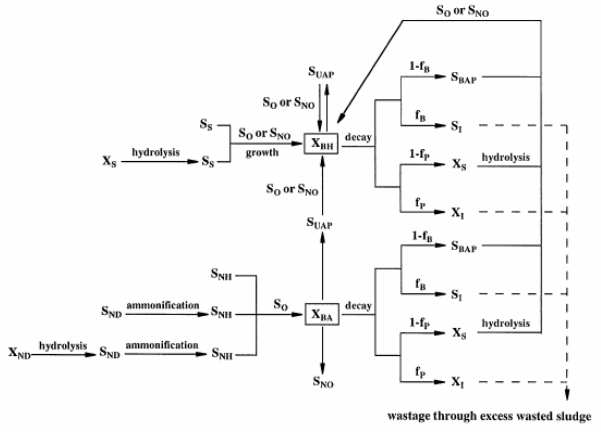

Fig. 5.4: Schematic description of Lu's SMP formation model based upon the ASM1 (Lu, 2001)

This extensively modified Lu ASM1 has the following additions.

- 4 new processes.
- 4 new stoichiometric parameters.
- 3 new kinetic parameters (to be estimated from measurements).
- 2 new Monod constants.
- 2 new variables.

The full list of processes is then:

1. Aerobic growth of X_H on S_S.
2. Aerobic growth of X_H on S_{BAP}.
3. Anoxic growth of X_H on S_S.
4. Anoxic growth of X_H on S_{BAP}.
5. Aerobic growth of X_A.
6. Particulate formation through decay of X_H.
7. S_{BAP} formation through decay X_H.
8. Particulate formation through decay of X_A.
9. S_{BAP} formation through decay of X_A.
10. Ammonification of soluble organic N.

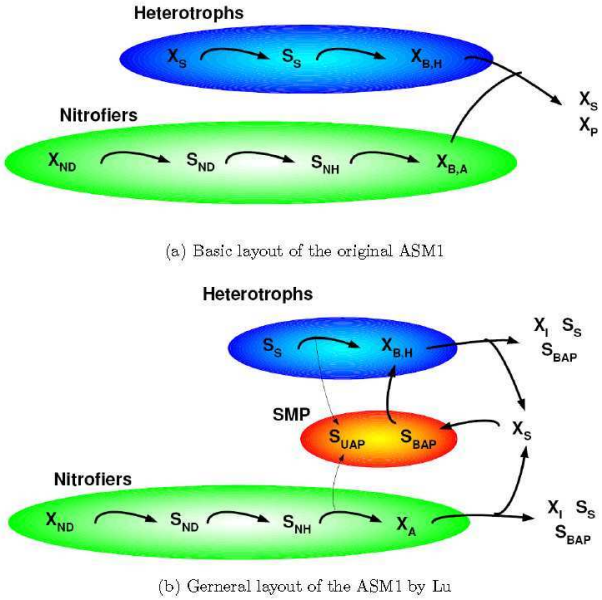

Fig. 5.5: Comparison of processes interactions between standard ASM1 and Lu ASM1 version (Paul, 2006)

11. Hydrolysis of entrapped organics.
12. Hydrolysis of entrapped organic N.

This new model is an extension of the ASM1 which means that the original processes of ASM1 were not changed. As mentioned earlier the new model introduces two new state variables, namely UAP and BAP and four new processes: both aerobic and anoxic growth of heterotrophs on UAP, and both aerobic and anoxic growth of heterotrophs on BAP. These new processes are also based on Monod kinetics.

Some of the stoichiometric coefficients in the original ASM1 model had to be modified in order to satisfy COD and Nitrogen mass balances, and charge balances in each process. This creates coupling between old and new transformation reactions and means that some of the original default set of stoichiometric parameters will need to be altered in order to create a model which is equivalent to the original ASM1 with its default parameters. The model introduces seven new stoichiometric and kinetic parameters associated with **SMP**. All other stoichiometric and kinetic parameters in the model follow the naming conventions introduced in the original ASM1.

UAP is produced directly by original substrate metabolism and BAP is derived from the decay of the active biomass. The formation rate of UAPs is proportional to the rate of substrate utilization, whereas the formation rate of BAPs is proportional to the amount of active biomass (Leudeking and Piret 1959).

5.1.2.2 Combined ASM3 and MP model - Oliveira ASM3 Model

Fig. 5.6 outlines Oliveira's modified ASM3 model which takes into account the MP as part of the biotransformation process. This MP is analogous to the BAP component in the Lu et al. (2001) ASM1 model version. Only the biomass decay products, BAP, were considered in this modified ASM3 model because they account for most of all microbial products as **SMP**; they represent the majority of soluble organic matter in the effluent; and, they exert a critical influence on the flux-rate achieved in the membrane filtration of Activated Sludge suspensions (Barker and Stuckey 1999). In fact Jiang et al. (2008) stated that the mixed liquor's propensity for fouling is caused solely by the BAP fraction and not by the UAP fraction.

1. Based on Activated Sludge Model No. 3 (ASM3).

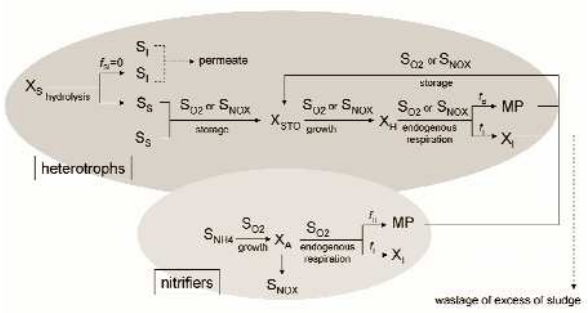

Fig. 5.6: Schematic describing metabolic pathway of Oliveira's modified ASM3 model (Oliveira-Esquerre, 2005)

2. Two additional processes and three parameters.
3. One additional state - MP (Microbial Products).
4. MP produced from lysis (f_B) and microbiological activity (γ_{MPh} and γ_{MPa})

- 2 new processes.
- 5 new stoichiometric parameters.
- 0 new kinetic parameters.
- 1 new Monod constant.
- 1 new variable.

The full list of processes is then:

1. Aerobic storage of S_S.
2. Aerobic storage of M_P.
3. Anoxic storage of S_S.
4. Anoxic storage of M_P.
5. Aerobic growth of X_H.
6. Anoxic growth of X_H.
7. Aerobic endogeneous respiration of X_H.
8. Anoxic endogeneous respiration of X_H.
9. Aerobic growth of X_A.
10. Aerobic endogeneous respiration of X_A.
11. Anoxic endogeneous respiration of X_A.

Hence this Oliveira-Esquerre et al. (2005) model adds one new state variable and two kinetic processes to the original ASM3 model. The state variable MP stands for Microbial Products which is a sum of **SMP** and EPS. Two new processes are:

1. Aerobic storage of MP.
2. Anoxic storage of MP.

The new parameters in this altered ASM3 model are:

- $Y_{SMP} = 0.5$ (taken from Lu et al. (2001) paper)
- $K_{MP} = 30$ (taken from Lu et al. (2001) paper)
- $MP_h = 0.4$ (taken from Lu et al. (2001) paper)
- $MP_a = 1.5$ (taken from Lu et al. (2001) paper)
- ${}_fB = 0.8$ (estimated from other sources)

5.1.2.3 Connections with MBR membrane fouling model

One aspect of this study is to begin the initial steps required in constructing an eventual integrated biological and fouling model for a MBR. In this respect, in Chapter 4 a modified membrane fouling model was developed based on the Duclos-Orsello et al. (2006) formulation which itself was based on the standard Darcy's Law and the main fouling mechanisms involved in MF and UF. In this model's expression there is a natural linkage to the Oliveira ASM3 model since it includes the MLSS concentration and **SMP** concentration in its base equation. The basic formulation is presented in Equations 4.9, 4.10 and 4.17 together with the model variables as used in the Oliveira ASM3 model. As can be seen the reversible fouling rate is dependent on the total particulate concentration produced by the biological model, whilst the irreversible fouling is determined by the **SMP** concentration calculated from the biological model as well as the volume of permeate passing through the membrane in the time period under consideration. Similar biological linkages can be made for the Lu's ASM1 version model with this membrane fouling model.

5.1.3 Model checking

The ASM1 has been extensively checked to ensure its accuracy in multiple situations with several distinguished articles checking the veracity of the parameter values used. Numerous calibration procedures are available to ensure that the is used properly for the specific WWTP under investigation. The COST Benchmark Simulation model was especially useful in this regard as it provided a way of checking variations in individual ASM1s components against specific anticipated parameter changes (Copp 1999, 2000).

On the other hand the ASM3 has no agreed benchmark model, and it has been less thoroughly checked. Therefore when developing a modified ASM3 like the one that Oliveira-Esquerre et al. (2005) produced, it is important that it has been chemically balanced to reflect reality. Oliveira-Esquerre et al. (2005) did not do this in his paper. This means a mass balancing in terms of Carbon and Nitrogen fractions is required followed by a subsequent charge balance of substances. This ensures the model obeys the laws of conservation of material by having realistic stoichiometric parameter values that produce and remove the correct proportion of all components in the model for each process, especially the newly introduced ones. A similar process has also to be conducted for the Lu's ASM1 version model.

The entire checking and calibration process involves undertaking the following steps:

- Formulate and check mass balance equations for conservation of Carbon, Nitrogen and Phosphorous fractions.
- Static parameter calibration gives the parameters controlling the large time constants.
- Dynamic parameter calibration gives the parameters responsible for small time constants (i.e. sufficient excitation required both in terms of variability of amplitude and frequency).

5.1.4 Process sensitivity analysis - Oliveira ASM3 Model

5.1.4.1 Biological, operational and environmental factors promoting EPS production

The following list summarises the major factors that are known to increase EPS and **SMP** production that in turn lead to associated gains in membrane fouling. However the exact nature of individual mechanisms that promote EPS production is still not known comprehensively (Drews et al. 2007b):

1. Low DO levels.
2. Low SRT with unacclimatised biomass.
3. Low F/M ratio i.e. low kg COD loading per kg MLSS content.
4. High mixed liquor viscosity.
5. Low environmental temperatures.
6. Low pH.
7. High salinity.
8. High local fluxes and/or short duration extreme fluxes beyond critical.
9. Low CFV in sidestream configurations or non-slug flow coarse bubble aeration in submerged systems.
10. Inadequate cleaning regime and/or other ineffective flux recovery methods.

In order to see whether the biological Activated Sludge models under investigation were sensitive to these main fouling factors, several sensitivity analysis simulations were carried out which are not described in this thesis as they were carried out by other researchers (Janus and Paul 2009).

5.2 *Phenomenological Oliveira ASM3 model - results and discussion*

5.2.1 Data selection for simulation runs

Once Lu's modified ASM1 model and Oliveira's modified ASM3 were both fully checked and tested in the previous Sections of this Chapter and under the larger project work, and further extensively modified to better reflect reality, they were used to run simulations using sampling programme data from a real life MBR plant, which in this case was the Aquabio's main plant located at Kanes Foods (Paul and Hartung 2008). This plant's data set was selected in this regard as it proved very accurate even though protein and polysaccharide measurements were never completed for it. Also an accurate mass balancing and influent characterisation was carried out for this trustworthy data set which is needed to fully calibrate and validate any phenomenological model. This means that any model run described later on in this Section can only infer the **SMP** levels and thus the predicted values cannot be compared against real ones. However, even inferred values could still prove useful if they appear to be of the right order of magnitude. The main issue here is that both models predict good values for all the other measured state variables, and also that their strengths and weaknesses can be fully examined without worrying about the use of any compromised data in the simulation runs.

The reason why the Aquabio pilot plant's data set was not used to run these simulations was that even though protein and polysaccharide measurements were completed, the other major wastewater state variables measured such as COD, Ammonia, etc., proved to be very inaccurate as an adequate mass balancing of values could not be achieved. In fact the collated biological data proved of limited use since it was probably corrupted and needed to be fully reconstructed to be of any use. It must be remembered that to obtain an accurate wastewater influent and sludge characterisation (i.e. breakdown of composite measured variables into component state variables), then the collated data must have a very high degree of precision that allows the SRT to determined to to at least 97% accuracy (Meijer et al. 2001). Therefore it was decided not to use this slightly untrustworthy data set for testing any phenomenological model as it was not of sufficient accuracy for these purposes especially when mass balancing the Carbon, Nitrogen and Phosphorous fractions. It is important to note that this unbalanced data set would likely produce very negative component states for the Lu's modified ASM1 model specifically for the unbalanced Nitrogen based components. Therefore it was a correct decision to reject this data set from the analysis being carried out here. On the other hand, this data set can be used in a behavioural modelling approach which does not have the limitations of a phenomenological model of the Activated Sludge variety. Hence this data set was used later in Section 5.4.2 to run a subspace procedure where data accuracy and mass balancing of component states is not an issue.

5.2.2 Sampling programme results from Aquabio main MBR plant

A schematic layout and picture of the full scale plant is presented in Figs. 5.7 and 5.8. In this layout in order to effectively separate the biomass, four banks of specialised UF membrane modules are used, fed by a recirculation system from the two bioreactor tanks, A and B. To allow a fully calibrated model to be produced measurements were taken at the following points in the flow train:

1. At the inflow.
2. In bioreactors tanks, A and B.
3. In the permeate tank.
4. At the wastage point (not used in the calibration procedure but just used as a check).

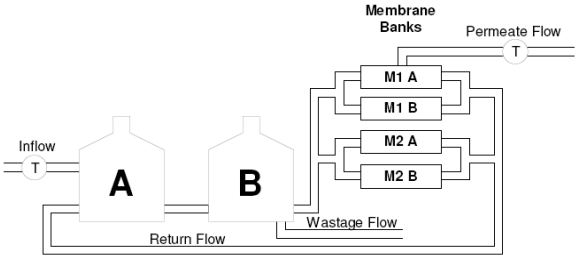

Fig. 5.7: Flow train of Kanes Foods full scale MBR plant (Paul and Hartung, 2008)

Fig. 5.8: Picture of Kanes Foods full scale MBR plant (Paul and Hartung, 2008)

5.2.2.1 Data set used from Aquabio main MBR plant

Table 5.1 summarises some of the typical biological and nutrient loading data that was collected from the plant during the intensive three weekly sampling programme. The figures are given as either a range or as an average with plus or minus the largest variance.

Measured Data	Inflow	Bioreactor	Permeate	Wastage
COD unfiltered (mg/l)	455 ± 179	7032 - 19240	8 - 30	1012 - 19600
TSS / MLSS (mg/l)	72 - 692	15250 ± 2000	4 - 68	820 - 22890
Total Nitrogen (mg/l)	22 ± 17	53 ± 19	0.7-16.9	12 - 204
Ammonia (mg/l)	0.2 - 4.8	5.2 ± 3.1	0 - 0.6	3.2 - 13.0
Total Phosphorous (mg/l)	2.4 - 8.4	3.9 - 22.4	0.2 - 4.4	4.0 - 25.3
Return Flow rate (m^3/hr)	254 ± 6	-	-	-
Viscosity (cP)	-	170 ± 63	-	177 ± 302

Table 5.1: Some of the Typical Averaged Biological, Nutrient and Other Measurements made during 3 week sampling period

Since **SMP** measurements such as for proteins and polysaccharides was unfortunately not carried out under this sampling programme, the closest measure of the mixed liquor's foulability on the membrane would then relate to the MLSS concentration and the fluid viscosity. Figure 5.9 is a plot of the MLSS concentration in Reactor B and the liquor viscosity. It shows that the MLSS concentration was largely constantly high

over the sampled period even though the liquor viscosity dropped slightly. The plants fluxes and TMPs remained consistent over this period as the high CFV of nearly 4 m/s would keep the membranes clean from cake build up even though the MLSS concentration was high. In fact the sludge itself was examined and found to be quite a healthy settleable mix having low SVI values as well.

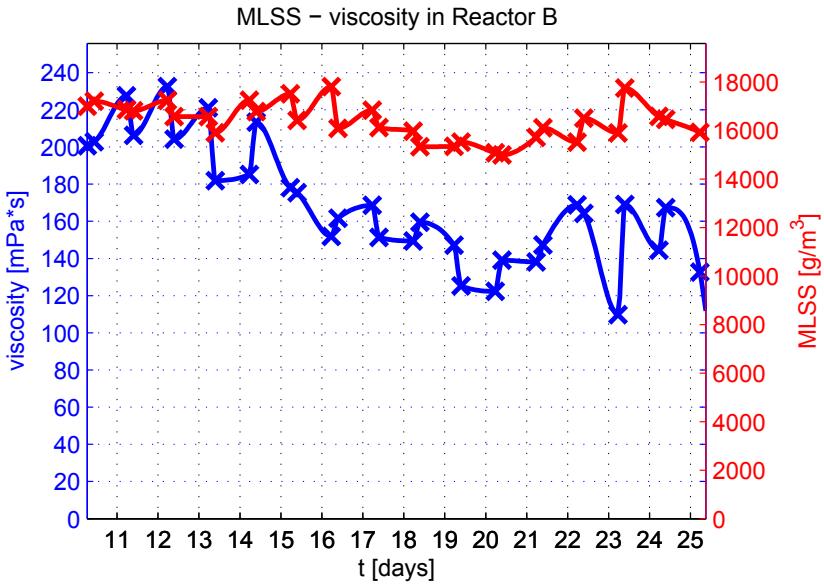

Fig. 5.9: Measured actual values of MLSS and viscosity in Reactor B

The measured data was used to carry out a full wastewater characterisation using the protocol developed in Hulsbeek et al. (2002) and then simulations were run on Matlab© for both Lu's modified ASM1 model and Oliveira's modified ASM3. Since it was beyond the scope of this study to determine by experimental means the exact kinetic parameter values for this particular plant, the values used in these dynamic simulations were the same as those quoted in the original papers by Henze et al. (1987) and Gujer et al. (1999). These steps are described further in follow-on Sections. Incidentally even if the eventually calculated **SMP** concentrations may be erroneous due to this gross assumption, since the difference in error is the same in each model, the overall results can be directly compared. Thus they can give by inference an indication of the fouling potential of the sludge supernatant.

5.2.3 Influent and sludge characterisation procedure

The next big challenge was to prepare the selected data set for utilisation in the phenomenological models by carrying out a thorough influent and sludge characterisation procedure. This was accomplished by initially fractionating the measured wastewater variables in the influent, bioreactor and outlet streams such as the COD and TN into the component state variables for both models such as the soluble substrate, S_S, and particulate substrate, X_S. Figs. 5.10 and 5.11 detail the relationship between these model component states and the actual measured COD and TN fractions.

Standard protocols have already been developed to allow this fractionating procedure to go ahead (Hulsbeek et al. 2002). It is worth noting that wastewater and sludge characterisation is an art in itself requiring a lot of experience in ensuring it is carried out properly, so for the sake of brevity only the major aspects of it can be mentioned here. The trial and error iterative protocol developed in this study used a combined approach taken from Meijer et al. (2001), Hulsbeek et al. (2002) and Baranao and Hall (2004). Again for the sake of brevity, the Nitrogen fractions are not considered here but a similar procedure was completed to determine them.

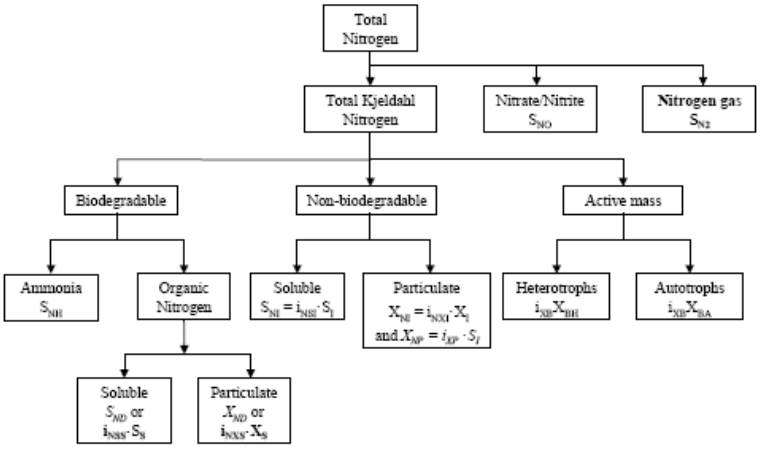

Fig. 5.10: How ASM1 components in the bioreactor relate to actual measured COD and N fractions (Paul, 2006)

$$\mathrm{CODtot} = S_I + S_S + X_I + X_S + X_{BH} + X_{BA} + X_P$$

$$\mathrm{Ntot} = S_{NH} + S_{ND} + S_{NO} + X_{ND} + X_{NI} + i_{XB} \cdot (X_{BH} + X_{BA}) + i_{XP} \cdot X_P$$

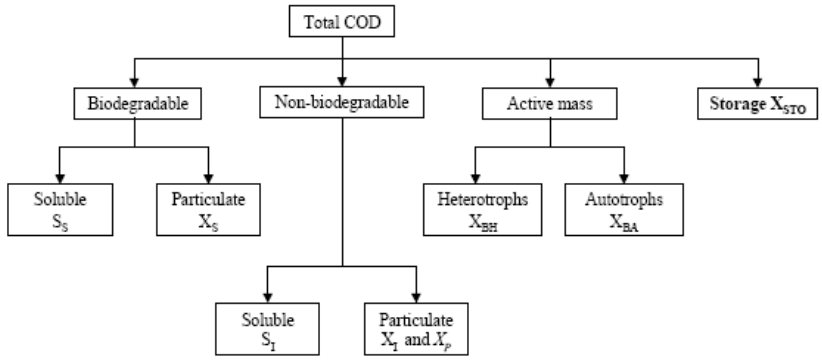

Fig. 5.11: How ASM3 components in the bioreactor relate to actual measured COD and N fractions (Paul, 2006)

$$\mathrm{CODtot} = S_I + S_S + X_I + X_S + X_H + X_A + X_{STO}$$

$$\mathrm{Ntot} = S_{NH} + S_{NO} + S_{N2} + i_{NSI} \cdot S_I + i_{NSS} \cdot S_S + i_{NXS} \cdot X_S + i_{NBM} \cdot (X_H + X_A) + i_{NXI} \cdot X_I$$

The basic procedure applied here for the fractions determined from the COD does not require complex, expensive and time-consuming laboratory respirometric batch tests but proves simple to apply and leads to a high degree of accuracy in the fractionating procedure. It is as follows:

5.2.3.1 Known measured quantities

Assume $XCOD_{in}/VSS_{in}$ ratio is equal to 1.6. Assume standard book values for b_H and Y_H.

Measured values:

- Inflow Q_{in}
- Incoming chemical oxygen demand, COD_{in}
- Incoming filtered chemical oxygen demand, $COD_{in,FIL}$
- Incoming total suspended soilds, TSS_{in}
- Incoming volatile suspended soilds, VSS_{in}
- Incoming total Phosphorous, TP_{in}
- Bioreactor tank volume, V_T

- Bioreactor chemical oxygen demand, COD_{bio}
- Bioreactor mixed liquor suspended soilds, $MLSS_{bio}$
- Bioreactor mixed liquor volatile suspended soilds, $MLVSS_{bio}$
- Bioreactor total Phosphorous, TP_{bio}

- Outlet chemical oxygen demand, COD_{out}
- Outlet filtered chemical oxygen demand, $COD_{out,FIL}$
- Outlet Phosphate level, $PO^{+}_{4,out}$

5.2.3.2 Unknown model fractions

Assume $X_{H,in} = 0$ and $X_{A,in} = 0$ and $S_O = 0$.

Need to determine:

- Soluble unbiodegradable substrate, $S_{I,in}$
- Soluble rapidly biodegradable substrate, $S_{S,in}$
- Particulate slowly biodegradable substrate, $X_{S,in}$
- Particulate unbiodegradable substrate, $X_{I,in}$

5.2.3.3 Determining $S_{I,in}$ and $S_{S,in}$ fractions

It is known that all fractions added up must equal incoming COD, thus:

$COD_{in} = S_{I,in} + S_{S,in} + X_{S,in} + X_{I,in}$

But $S_{I,in}$ = 0.9 x $COD_{outlet,FIL}$ taken from Hulsbeek et al. (2002).

And $COD_{in,FIL} = S_{I,in} + S_{S,in}$

Therefore $S_{S,in}$ = $COD_{in,FIL}$ - (0.9 x $COD_{outlet,FIL}$)

Also, $XCOD_{in} = COD_{in}$ - $COD_{in,FIL} = X_{S,in} + X_{I,in}$

5.2.3.4 Determining $X_{I,in}$ and $X_{S,in}$ fractions

The Activated Sludge models used here are very sensitive to modifications in the influent composition especially the inert particulate fractions, $X_{I,in}$, which will affect the sludge production (Brdjanovic et al. 2000). Therefore, first the SRT needs to be calculated with a high degree of accuracy.

The best way of doing this is to use the Phosphorous fractions for the mass balancing and SRT calculation, since the Phosphorous balance is closed as there is no Phosphorous fractions in the gaseous phase (i.e. all solids are conserved).

Therefore the SRT can be expressed in terms of MLSS:

SRT = [V_T x $MLSS_{bio}$] / Sludge production

In terms of COD this equates to:

SRT_{COD} = [V_T x COD_{MLSS}] / Sludge production in COD terms, where COD_{MLSS} = COD_{bio} - $COD_{out,FIL}$

In terms of a Phosphorous mass balance (without needing wastage sludge excess values) this equates to:

SRT_{COD} = [V_T x (TP_{bio} - $PO^{+}_{4,out}$] / [Q_{in} x (TP_{in} - $PO^{+}_{4,out}$]

So, SRT is now known accurately, and the Sludge production in COD terms, $SLUDGE_{prod,COD}$, can be found. To determine X_I use the following Equation from Baranao and Hall (2004):

$$SLUDGE_{prod,COD} = Q_{in} \cdot [X_I + \frac{(1 + f_{XI,in} \cdot b_H) \cdot Y_H \cdot (COD_{in} - S_I - X_I)}{(1 + b_H \cdot SRT_{COD})}] \tag{5.3}$$

where:

$$f_{XI,in} = \frac{X_{I,in}}{S_{I,in} + S_{S,in} + X_{S,in} + X_{I,in}} = \frac{X_{I,in}}{COD_{in,FIL} + COD_{in} - COD_{in,FIL}} \tag{5.4}$$

Then $X_{S,in}$ can simple be determined from $XCOD_{in}$ = COD_{in} - $COD_{in,FIL}$ = $X_{S,in}$ + $X_{I,in}$

And a check can be made using the relationship of $XCOD_{in}/VSS_{in}$ = 1.6 = ($X_{S,in}$ + $X_{I,in}$) / VSS_{in}

A similar but altered procedure can be developed to calculate the Nitrogen fractions in the influent, and all bioreactor tank fractions. The tank fractions can also be determined by running the plant simulation for at least 100 days at steady state so that the micro-organisms can grow until they reach representative mixed liquor concentrations as per the method used in (Copp 1999, 2000) for the COST Benchmark Simulation model.

5.2.4 Discussion of simulation results

Several simulations were run using the fractionated component state data on both the original ASM1 and ASM3 models followed by runs using Lu's modified ASM1 model and Oliveira's modified ASM3 models. All outputs from each simulation run were plotted on the same graphs so results could be directly compared. Figs. 5.12 to 5.14 are plots of measured values against simulated values of COD, Ammonia and Nitrates concentration in Reactor B for the four model runs. Fig. 5.15 is a plot of simulated **SMP** levels in Reactor B for the two modified model runs.

It is clearly evident from the results of all four model type simulation runs, that the original untouched models overall performance it nearly always better than the modified versions that include **SMP** components. This is as would be expected due to the increased parameter sets which in themselves have not been properly verified by extensive global research as is the case with the those for the original untouched Activated Sludge model varieties.

In Fig. 5.12 all the simulation plots over predict the COD level in the reactors by a considerable amount, especially Lu's modified ASM1 model. This can probably be attributed to inaccuracies in the influent and sludge characterisation procedure especially in the determination of the soluble inert component level, $X_{I,bio}$, in the reactor. If this very sensitive component is underestimated by errors in the calculation of the SRT, then the COD level is easily over predicted by all models. These inert fractions can build up quite rapidly and are only controlled by regular sludge wastage. However the plant operators at the Kanes Foods site did not accurately record sludge wasting regimes properly, so it would be easy to introduce errors in the stated wastage rates.

In terms of Ammonia levels in the reactors, then Fig. 5.13 illustrates that the ASM1 based models gave better predictions than their ASM3 counterparts which grossly underestimate levels. This is as expected since the ASM1 models give a comprehensive process degradation of bound organic Nitrogen which seems to give a better approximation of Ammonia concentration in the bioreactor tank than the ASM3 models. Although it must be remembered that from a practical point of view this organic Nitrogen is very difficult to determine in reality so the ASM3s model's structural simplicity may still give them some preference.

Fig. 5.14 shows that all the simulation plots greatly under predict the Nitrate levels. This again can probably be attributed to errors in the wastewater influent and sludge characterisation whose second most sensitive component, namely the readily biodegradable substrate fraction, S_S, will be over predicted if the particulate inert fraction, X_S, is under predicted. This increased S_S fraction affects the denitrification rate by increasing it considerably since there is additional rapidly utilisable substrate to allow full breakdown of the Nitrates to occur. This means final Nitrate levels will be predicted to be much lower than they actually are. It is also worth noting that there may be some simultaneous nitrification and denitrification occurring within the structure of a biological floc that none of the models are strictly geared up to predicting. This may also affect results.

In fact researchers have found that often the most error prone area of the model prediction procedure occurs first and is in using incorrect system data which in turn affects the characterisation procedure which then gives rise to inaccurate model predictions. Hence the critical primary data, such as SRT, plant recycle flow rates, DO levels, etc., needs to be thoroughly reconciled and checked for accuracy (Hulsbeek et al. 2002). Meijer et al. (2001) found that a proper wastewater characterisation is no guarantee for a successful model calibration as good data reconciliation is needed. In fact he deduced by using a sensitivity analysis that the relatively large influence of operational data (such as internal flow rates) on the model output was much larger when compared to variations in many kinetic Activated Sludge model parameters.

Fig. 5.15 demonstrates that the predicted **SMP** and MP for both model types, which should be largely responsible for most of the COD in the effluent (and hence by inference foulant pore blocking potential), was either slightly underestimated in the case of the Lu ASM1 model or grossly underestimated in the case of the Oliveira ASM3 model. This is most likely due to the use of standard kinetic parameter values in the models which should have been calibrated to be more site specific.

Figs. 5.16 to 5.18 are plots of measured values against simulated values of COD, filtered COD, and Ammonia concentration in the final effluent for the four model runs. Fig. 5.19 is a plot of simulated **SMP** levels in the final effluent for the two modified model runs.

Fig. 5.16 shows all models over predict COD levels in the final effluent, although the Lu's modified ASM1 greatly over predicts. Conversely Fig. 5.17 shows that the filtered COD levels in the effluent are very accurately predicted by both ASM3 model versions, with an overestimation by ASM1 versions particularly with Lu's modified ASM1.

Similar results are obtained for the effluent Ammonia as depicted in Fig. 5.18 which again shows the accurate prediction by both ASM3 model versions, with the ASM1 versions particularly Lu's modified ASM1 over estimating values. This over estimation by both ASM1 models can explained by their more complex processes which have greater degrees of freedom especially Lu's modified model which contains a whole host of new parameters. Thus accuracy is sacrificed for greater model complexity with improved process

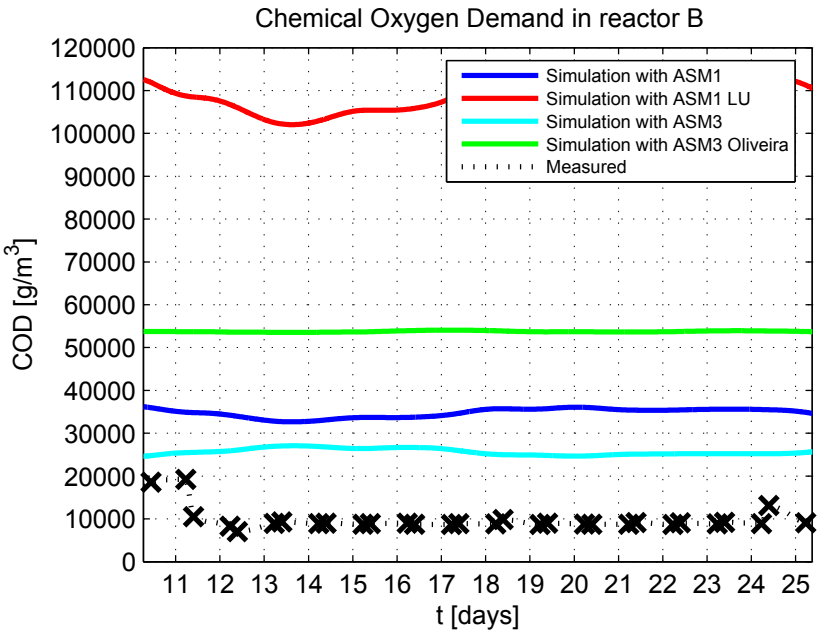

Fig. 5.12: Measured COD in Reactor B plotted against simulated values from ASM1, Lu ASM1, ASM3, Oliveira ASM3

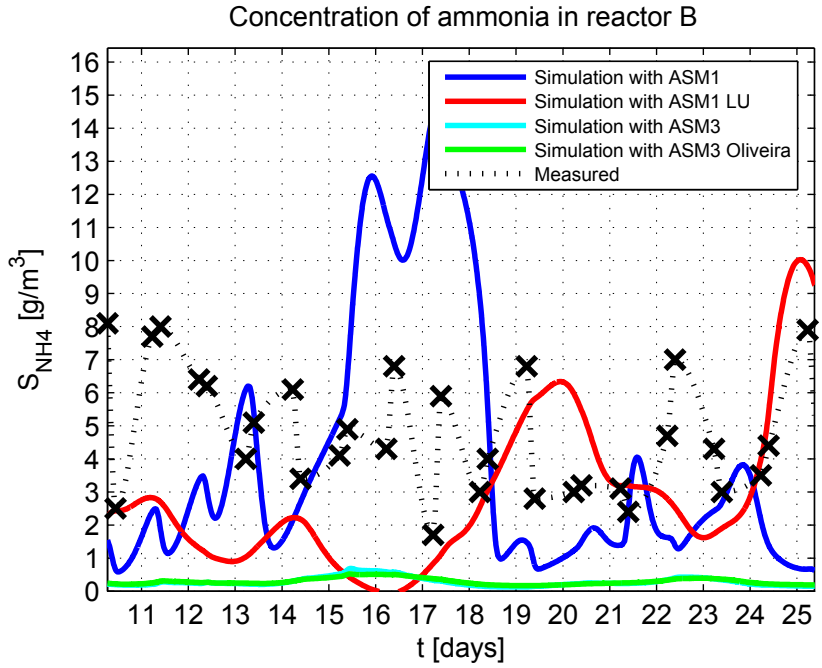

Fig. 5.13: Measured Ammonia in Reactor B plotted against simulated values from ASM1, Lu ASM1, ASM3, Oliveira ASM3

descriptions. On the other hand the ASM3 model have simpler structures with component states that can never go negative.

Fig. 5.15 shows the prediction of **SMP** and MP levels. Once again the MP levels are much lower than expected and can be attributed to both poorly selected kinetic parameter values, and also inherent problems with the Oliveira ASM3 model structure whose process description in this regard is much too simplistic. In other words this under prediction is due to the really guestimated parameter values being used here that have not been tested globally. However it is worth noting that the overall trend of the MP curve largely follows the actual effluent COD concentration, whilst the **SMP** curve shows a much greater fluctuation

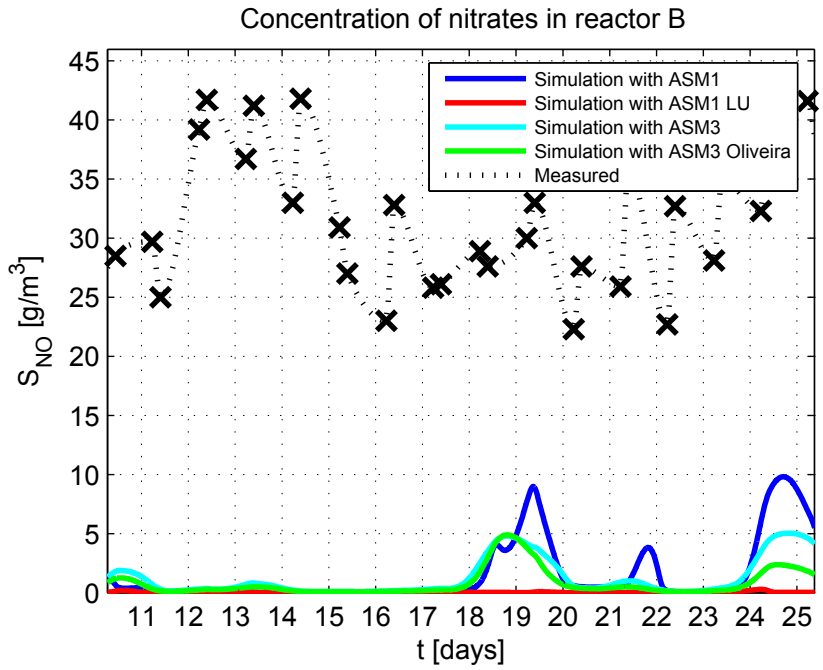

Fig. 5.14: Measured Nitrates in Reactor B plotted against simulated values from ASM1, Lu ASM1, ASM3, Oliveira ASM3

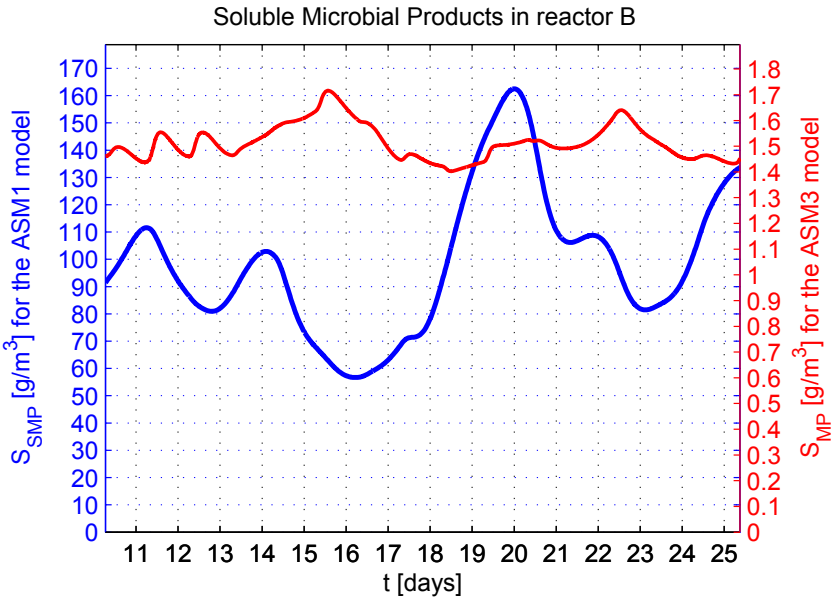

Fig. 5.15: Simulated model values of SMP in Reactor B for Lu ASM1 and Oliveira ASM3

which is not apparent in the real measurement data.

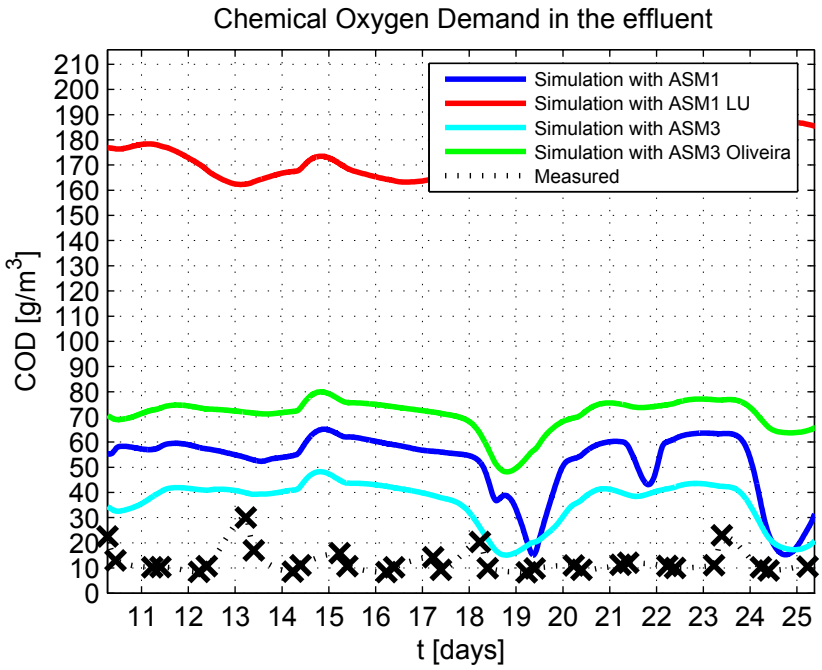

Fig. 5.16: Measured effluent COD plotted against simulated values from ASM1, Lu ASM1, ASM3, Oliveira ASM3

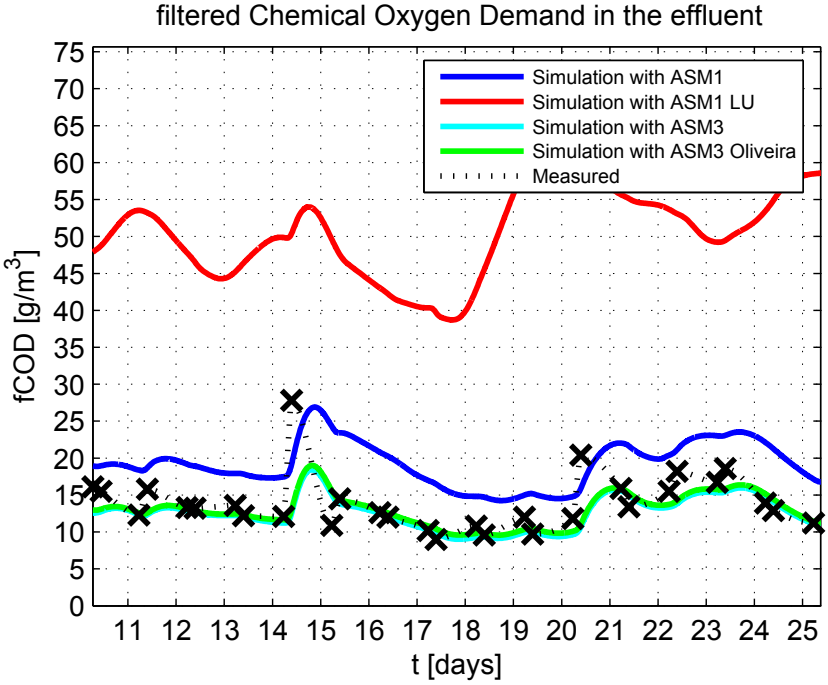

Fig. 5.17: Measured filtered effluent COD plotted against simulated values from ASM1, Lu ASM1, ASM3, Oliveira ASM3

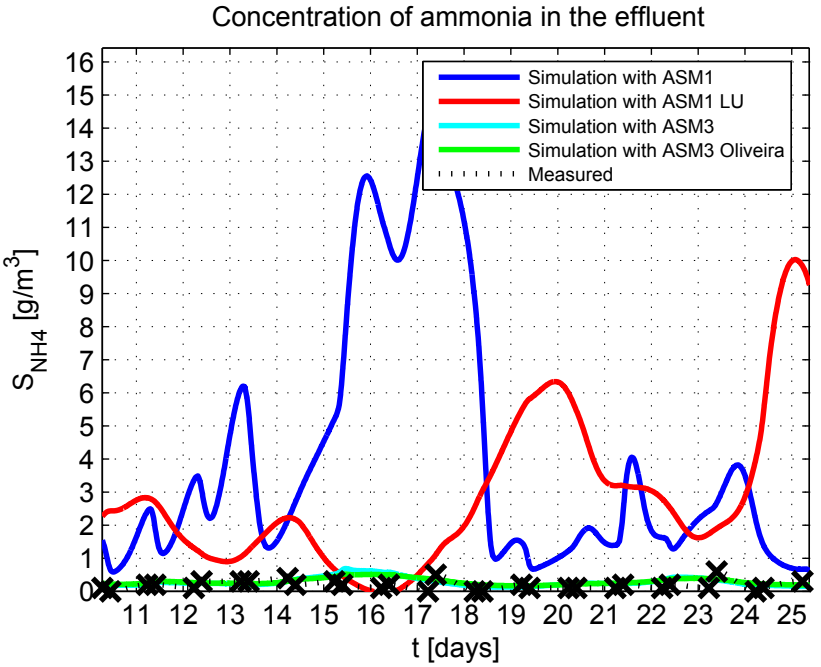

Fig. 5.18: Measured filtered effluent Ammonia plotted against simulated values from ASM1, Lu ASM1, ASM3, Oliveira ASM3

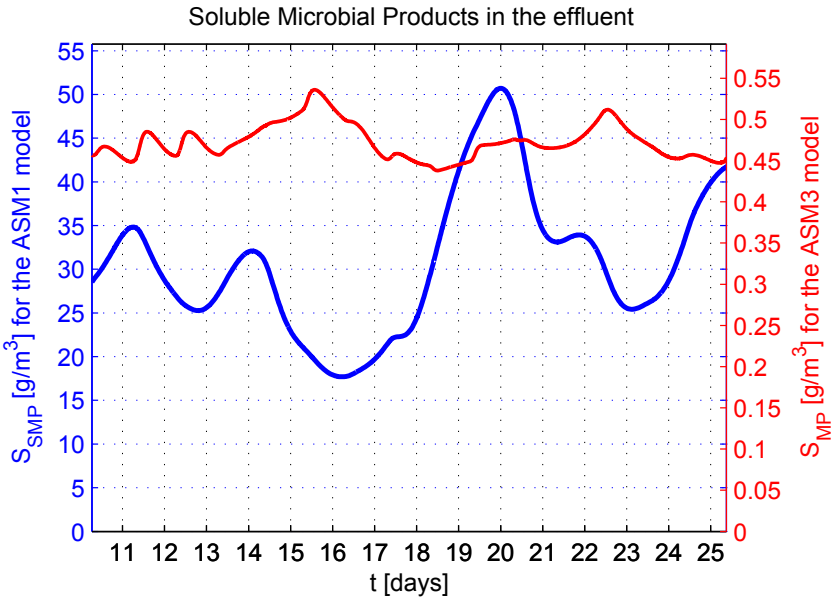

Fig. 5.19: Simulated model values of effluent SMP for Lu ASM1 and Oliveira ASM3

5.2.5 Summarising results from phenomenological models

The following summarised points can be made regarding phenomenological model structures:

- More complex model structures with numerous processes that attempt to accurately describe the biological and biochemical processes occurring in the bioreactor, especially those that impact upon membrane fouling, will obviously have numerous parameter values that require determination. Conversely simpler model structures with reduced parameter sets may be easier to calibrate, but their predictive capabilities may suffer as a consequence. Further, the addition of MP into the modified Oliveira ASM3 model only adds one additional process, whereas the Lu's modified ASM1 model includes four new **SMP** processes and their subsequent estimated kinetic parameters. These factors all impact on the eventual model identifiability which in layman's terms means too few measurements for too many processes will lead to many unidentified parameters.
- The two altered biological Activated Sludge models used here both have straight forward and easily established biological and membrane fouling model connections allowing eventual model integration.
- It is worth noting that the ASM3 is a sequential model that was originally proposed by the IWA not only as a way to correct some defects of ASM1 but also to take into account the advances in experimental evidence on storage of organic compounds (Gujer et al. 1999). It is also based upon a much simpler influent characterisation protocol making it much more practical for modellers and operators.
- Since EPS is composed of proteins and polysaccharides, standard chemical assays to measure these components would need to be carried out for any altered models that contained these components. However these assays could not be performed regularly as they are expensive and time consuming. They also are not standardised in wastewater treatment measurement protocols like other biochemical components.
- After conducting the various simulations (not shown in thesis for the sake of brevity), results showed that both modified models could be made to predict very closely to the original Activated Sludge models for all state and composite variables under this study. This is as opposed to the original published Oliveira and Lu models whose results diverge. This only proves the generality of this model development approach.
- It is suggested that the modified Oliveira ASM3 model could be further tested by having its **SMP** metabolism equations being totally decoupled from its ASM3 equations in order to mitigate against the model calibration and identification issues raised earlier. This may prove an intermediate solution until other approaches such as the behavioural methods advocated in the next Section are fully developed.
- Although the modified Oliveira ASM3 model is too simplistic a formulation, it is just being used here to demonstrate the relative complexity of a full calibration and validation procedure even for a relatively simple phenomenological model. This then can be compared against the complexity of the calibration procedure for the behavioural time series models described later in this Chapter. However it could still prove to be a relatively useful model when used judiciously and with care in certain situations.

5.3 *Behavioural Activated Sludge model - input-output system identification approach*

5.3.1 Introduction - behavioural Activated Sludge model formulation

Again as was carried out in Chapter 4, in order to directly compare the two different model types, namely the modified phenomenological ASM1 and ASM3 formulations against an input-output behavioural model based on system identification methods, the same plant data set were used (i.e. Aquabio's main MBR plant). This behavioural biological model formulation is based upon the "Model Conceptualisation Procedure" described in Section 3.3 in which the plant data set used is formatted for the Matlab's System Identification Toolbox© and CUEDSID software. The different system identification model formulations that were tested are as follows:

1. Linear parametric ARX, ARMAX and state space models developed in the Matlab's System Identification Toolbox© with GUI. The same plant data set was used as for the phenomenological model.
2. Alternative linear parametric subspace models developed in the CUEDSID software package and Matlab©. The same plant data set was used as for the phenomenological model.

These are described in Section 5.4.1. An alternative data set was also used to test the applicability of these empirical input-output behavioural models on biological Activated Sludge systems (i.e. Aquabio's pilot MBR plant). The output from this alternative data set is described in Section 5.4.2.

Since both these real life plant data sets did not allow a complete MIMO model to be run, a fictitious WWTP based upon the modified COST Benchmark simulation model and which is described in Section 3.4.6 was used to generate sufficient data points. This fictitious WWTP with an ideal point settler acting as the membrane unit provided nearly 20,000 data points for a varying temperature mixed liquor. Thus it would allow the full testing of a MIMO model structure.

Since the MIMO model structure gave acceptable results, it was decided that possibly a combination of both types of model might prove useful as a way of reducing the need to carry out complex protein and polysaccharide determination tests. These additional tests need expertise to run, can prove time consuming, and are usually prohibitively expensive to be run on numerous occasions, so any alternative proposed procedure which gave similar **SMP** accuracy could prove advantageous. In other words if a MBR plant had a full set of data including protein and polysaccharide measurements (which are thought to be the main agents responsible for fouling), and another MBR plant of similar layout had only conventional data sets, then the behavioural model could be used to predict the **SMP** levels in this second plant without the need for the complex **SMP** tests to be conducted. The full **SMP** prediction procedure would be as follows:

1. Collate the full data set including **SMP** levels for MBR plant No. 1.
2. Ideally run this full data set on a modified phenomenological Activated Sludge model so that actual and predicted **SMP** levels can be compared.
3. Run this full data set on a MBR plant No. 1 layout using an input-output behavioural model formulation. If the fit is good, then from this run the best input-output model structure is determined.
4. Collate the full data set excluding **SMP** levels for MBR plant No. 2.
5. Using the best input-output model structure determined from MBR plant No. 1 with the data set from MBR plant No. 2 to predict the **SMP** levels of plant No. 2.

6. Using the full data set including predicted **SMP** levels for MBR plant No. 2, run this full data sets on a modified phenomenological Activated Sludge model.

It is hoped this judicious use of both model types in combination will allow future researchers to take advantage of each model type while minimising their negative aspects. This means that input-output model structures could be used for rapid and easy prediction of **SMP** levels for plant operation and control without the need for constant complex **SMP** measurements. It also means that standard Activated Sludge models which have already been extensively tested in the field by numerous researchers could be used with only limited alteration for intensive MBR processes to predict the mixed liquor concentration and the more usual effluent quality indices.

5.4 *Behavioural Activated Sludge model - results and discussion*

5.4.1 Simulation results from Aquabio main MBR plant

Since the number of sampling points from the original sampling programme was insufficient to even allow the most basic input-output model structure to be implemented (i.e. 32 points only), it was doubled up by repeating the same results for a second similar length period. This meant that the autoregressive model structures could then be tested as there was just about enough points to allow the simulations to occur. However, the output from these runs can only be thought of as indicative as some of the sampling points are slightly concocted. The main issue here for the system identification protocols being tested, is to ascertain whether they will work on a biological model formulation. Later sections will actually deal with the accuracy and appropriateness of such methods, and which are the best of the various biological model structures being tested.

The input data was as follows based on the nomenclature described in Chapter 3 and for the wastewater components that were measured for this plant:

$$\mathbf{z_1} = \begin{bmatrix} q_{in} \\ COD_{in} \\ COD_{fil,in} \\ TSS_{in} \\ TN_{in} \\ NH_{3,in} \\ NO_{3,in} \\ TP_{in} \\ PO_{3,in} \\ pH_{in} \end{bmatrix}; \qquad \mathbf{m_1} = \begin{bmatrix} q_{waste} \\ DO \end{bmatrix}; \qquad \overset{'}{\mathbf{x_1}} = \begin{bmatrix} X_{MLSS} \\ \mu \end{bmatrix}$$

Disturbance matrix, m_1, is ignored as wastage did not occur over the short sampling period, and for simplicities sake DO can be thought of as an input state in the approximate bioreactor model as per the "Model Conceptualisation Procedure". Additionally, the incoming flow is ignored as it does not effect the daily load in kg/day, only its dilution. This simplifies the MIMO input-output model structure to the following:

$$\mathbf{z_1} = \begin{bmatrix} COD_{in} \\ COD_{fil,in} \\ TSS_{in} \\ TN_{in} \\ NH_{3,in} \\ NO_{3,in} \\ TP_{in} \\ PO_{3,in} \\ pH_{in} \\ DO \end{bmatrix}; \qquad \overset{'}{\mathbf{x_1}} = \begin{bmatrix} X_{MLSS} \\ \mu \end{bmatrix}$$

This structure was run for a subspace formulation using the CUEDSID software package and the best fit

was for a second order model with block size of one as depicted in Fig. 5.20. As can be seen the fit is positive for the MLSS concentration, but negative for the viscosity. By the way a quarter of the overall data points were used for the validation step.

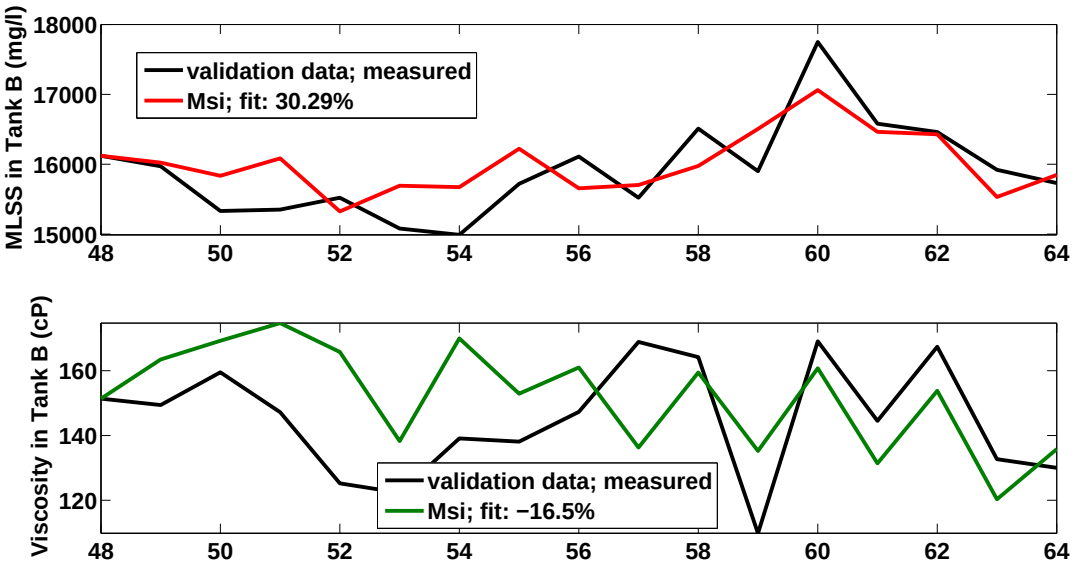

Fig. 5.20: Increased data set - all biological variables as inputs with MLSS and viscosity levels in bioreactor as outputs

Next the following reduced input-output model structure was tried in an attempt to improve the fit:

$$\mathbf{z_1} = \begin{bmatrix} q_{in} \\ COD_{in} \\ DO \end{bmatrix}; \qquad \overset{'}{\mathbf{x_1}} = \begin{bmatrix} X_{MLSS} \\ \mu \end{bmatrix}$$

Fig. 5.21 shows that the fit improves for the MLSS concentration but at the expense of the viscosity which actually deteriorates. Incidentally, this best fit is for a sixth order model with block size of five.

Finally for this increased data set, the following reduced formulation was used with only a single input of the COD:

$$\mathbf{z_1} = \begin{bmatrix} q_{in} \\ COD_{in} \end{bmatrix}; \qquad \overset{'}{\mathbf{x_1}} = \begin{bmatrix} X_{MLSS} \\ \mu \end{bmatrix}$$

This was again run as a subspace formulation, with the best being for a ninth order model with block size of seven. Fig. 5.22 shows the improve in fit for both the MLSS concentration and the viscosity.

Similar runs were carried out using the more standard autoregressive model structures (i.e. ARX, ARMAX, standard state space) using Matlab's System Identification Toolbox© with GUI. For the sake of brevity, Table 5.2 summarises the best fits for all runs.

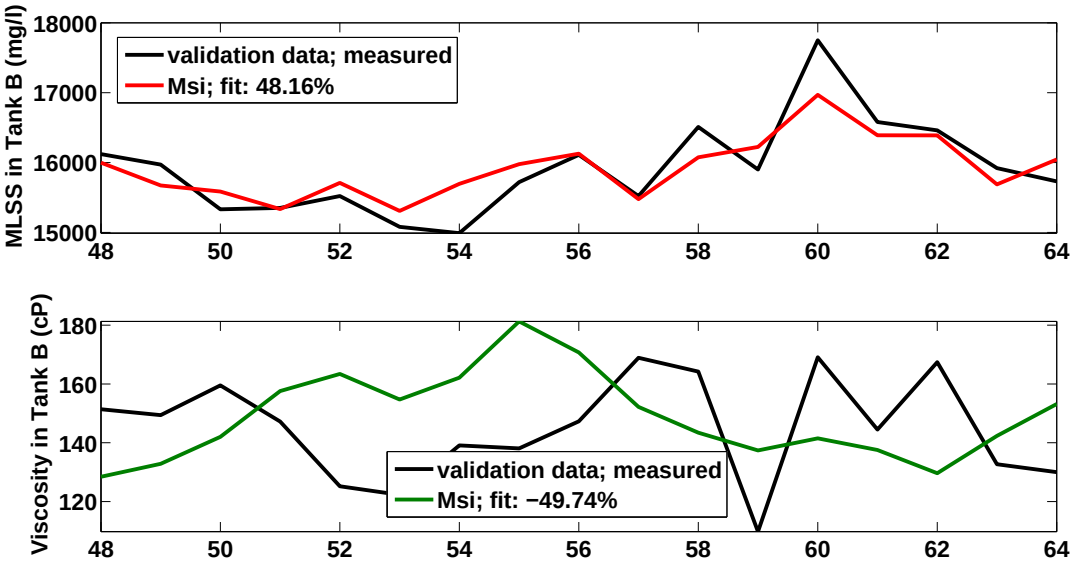

Fig. 5.21: Increased data set - COD and DO as inputs with MLSS and viscosity levels in bioreactor as outputs

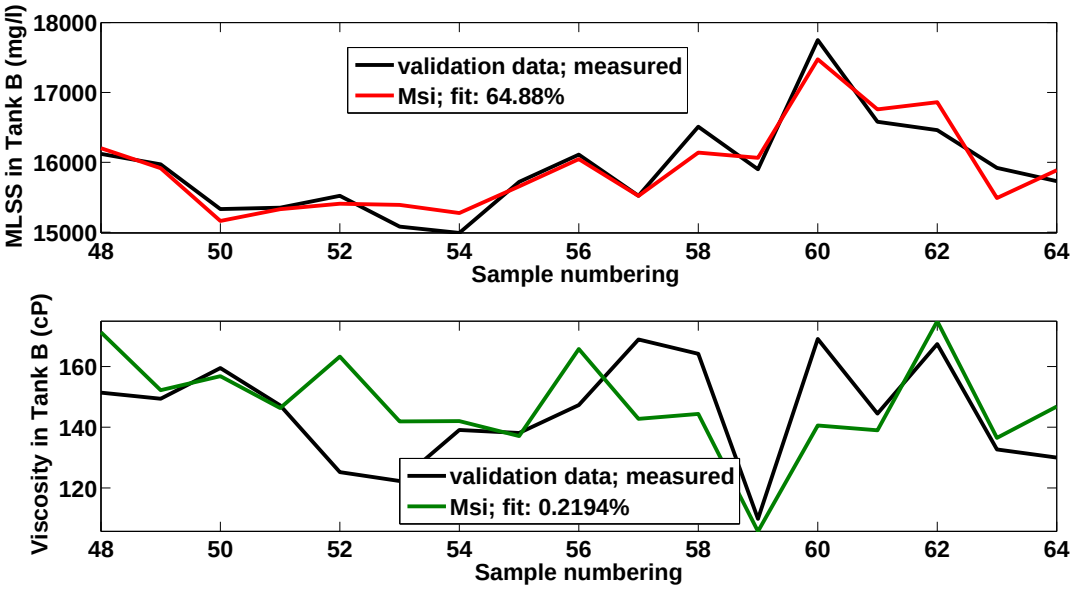

Fig. 5.22: Increased data set - COD only as input with MLSS and viscosity levels in bioreactor as outputs

Input data set type	CUESID Subspace	ARX	ARMAX	State space (pem)	State space (n4sid)
All input data	30.29% MLSS -16.50% μ	59.26% MLSS 55.48% μ	did not run	too few data	too few data
COD and DO as inputs	48.16% MLSS -49.74% μ	9.055% MLSS 13.13% μ	did not run	5.127% MLSS 5.672% μ	-13.83% MLSS -5.876% μ
Only COD as input	64.88% MLSS 0.2194% μ	10.60% MLSS 18.01% μ	did not run	no fit	no fit

Table 5.2: Aquabio main plant - comparison of best fits for various autoregressive model formulations

All of the simulation runs that worked proved that an autoregressive model structure can be used for biological data of this type. In this particular plant's case, the ARX model structure proved the best fit when used for the truly MIMO data set. It gave fits of over 50% for both outputs. In comparison to the results from the phenomenological model (i.e. ASM3 Oliveira), the results are comparable in terms of fit magnitude, even though the amount of work needed to calibrate and validate the autoregressive models is greatly reduced. However, due to the slightly manufactured nature of the input data set, further data is needed from a different MBR plant to test these autoregressive models in a more rigourous manner. In the next section of this Chapter this step is carried out for the data collated from Aquabio's pilot MBR plant. Ideally this data set should contain **SMP** and temperature data as well so that the model structure could be linked at a later date to a membrane fouling model, whether a linear or bilinear subspace formulation.

5.4.2 Simulation results from Aquabio pilot MBR plant

In this case the simulation could go ahead with the available data set since there were 100 sampling points. This proved just sufficient to allow a solution to be evaluated for an input-output model structure without the need to resort to the generation of further fictitious plant data. The MIMO input-output model structure used is as follows:

$$\mathbf{z_1} = \begin{bmatrix} COD_{in} \\ S_{SMP,in} \\ Temp \end{bmatrix}; \qquad \mathbf{x_1}' = \begin{bmatrix} X_{MLSS} \\ \mu \\ S_{SMP,bioreactor} \end{bmatrix}$$

Even though much more data was available for testing on this model structure such as TN values, Ammonia values, etc., only these few were selected to keep the procedure simple, and also to investigate the fit for the two new variables not fitted in the previous section, namely the **SMP** level and the liquid temperature. These new variables also prove useful when linking a biological model with a membrane fouling model. For this data set, this input-output model case was run in three different ways as follows to determine the optimal solution:

1. All the three input variables were run with the output being the **SMP** level only.
2. All the three input variables were run with the output being MLSS and **SMP** levels.
3. All the three input variables were run with the output being MLSS, viscosity and **SMP** levels.

A subspace formulation using the CUEDSID software package was initially tried to ascertain the optimal fit. Hence the best fit for the first subspace run is given in Fig. 5.23 with a second order model with a block size of four. A 38% fit is obtained.

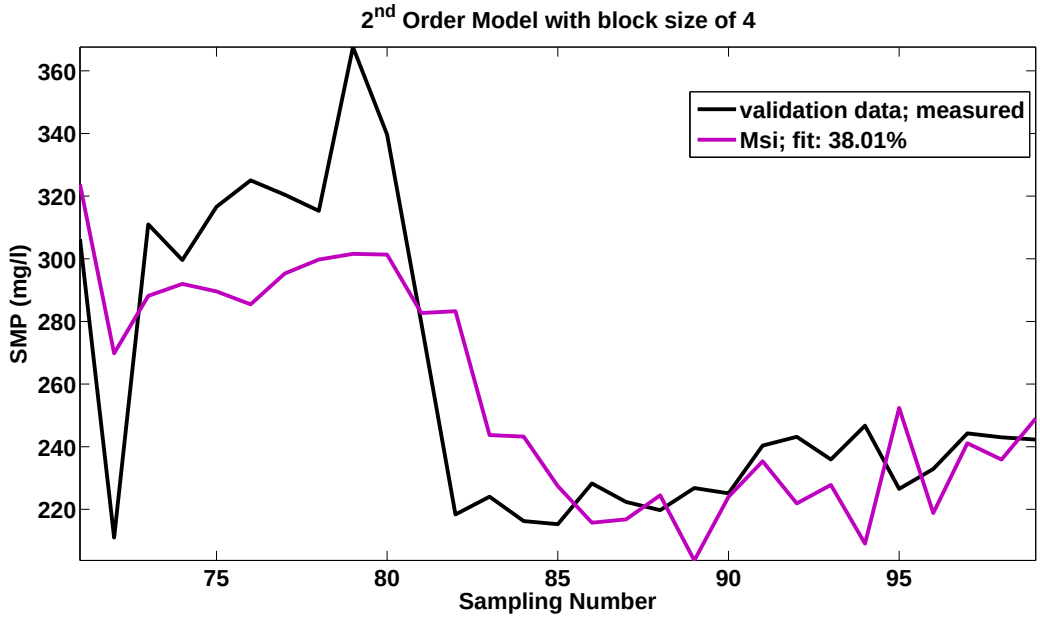

Fig. 5.23: Full data set - COD, SMP and temperature as inputs with SMP level in bioreactor as output

The best fit for the second run is given in Fig. 5.24 with a first order model with a block size of three. In this case the **SMP** fit deteriorates down to approximately 18.5% with a poor fit for MLSS concentration

of approximately 20%.

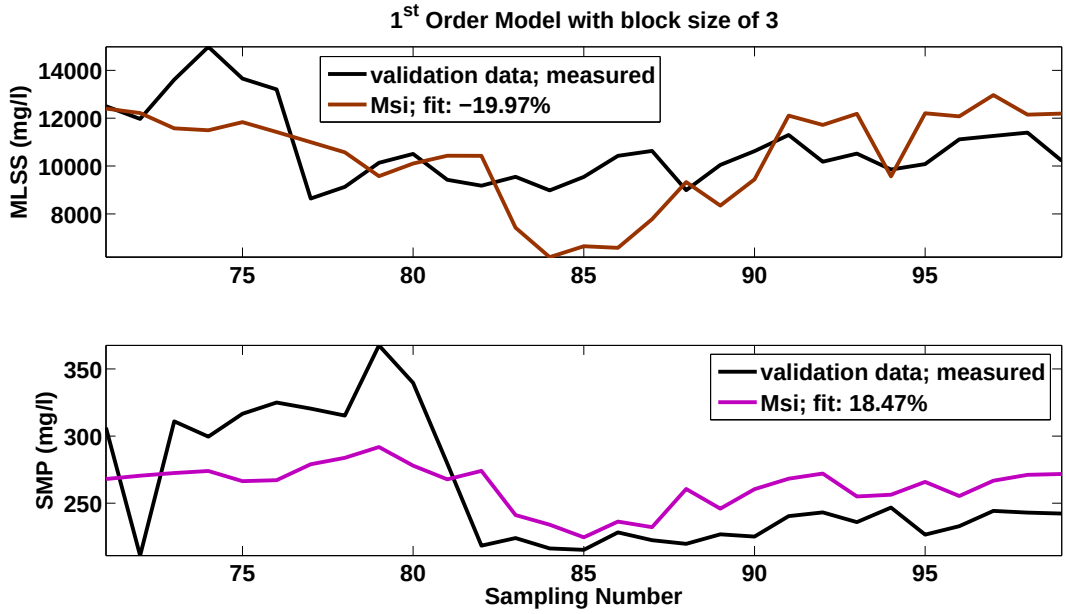

Fig. 5.24: Full data set - COD, SMP and temperature as inputs with MLSS and SMP levels in bioreactor as outputs

The best fit for the final run is given in Fig. 5.25 with a fifth order model with a block size of five. In this final case the **SMP** fit improves slightly to approximately 24% with a poor fit for MLSS concentration and viscosity of approximately 39% and 22% respectively. All of these three simulation runs clearly show that the fit reduces with an increased number of output variables as would be expected. The only way of overcoming this potential limitation of these autoregressive model structures is by increasing the number of data points.

Once again similar runs were carried out using the more standard autoregressive model structures (i.e. ARX, ARMAX, standard state space) using Matlab's System Identification Toolbox© with GUI. For the sake of brevity, Table 5.3 summarises the best fits for all runs.

Input data set type	CUESID Subspace	ARX	ARMAX	State space (pem)	State space (n4sid)
SMP output data only	38.01% SMP	-1.915% SMP	-1.495% SMP	8.341% SMP	no fit
SMP & MLSS outputs	18.47% SMP -19.97% MLSS	2.237% SMP -111% MLSS	did not run	-22.36% SMP -23.22% MLSS	very poor fit
SMP, MLSS & viscosity outputs	24.26% SMP -39.24% MLSS -21.63% μ	1.339% SMP -133.4% MLSS -4.191% μ	did not run	-95.07% SMP -162.3% MLSS -8.688% μ	-881.4% SMP -136.7% MLSS -32.7% μ

Table 5.3: Aquabio pilot plant - comparison of best fits for various autoregressive model formulations

Table 5.3 shows that the subspace formulation gives the best fit when compared to the other autoregressive model structures, although even its best fit is still relatively quite poor. In comparison a well structured and verified phenomenological model will give an enhanced fit if the data accuracy is kept high. However, the auto regressive methods may still prove useful for a biological model, but need testing on a much more extensive data set then the ones already used. In the next section, several thousand data points are used in the calibration and validation exercise to ascertain if a better fit is possible.

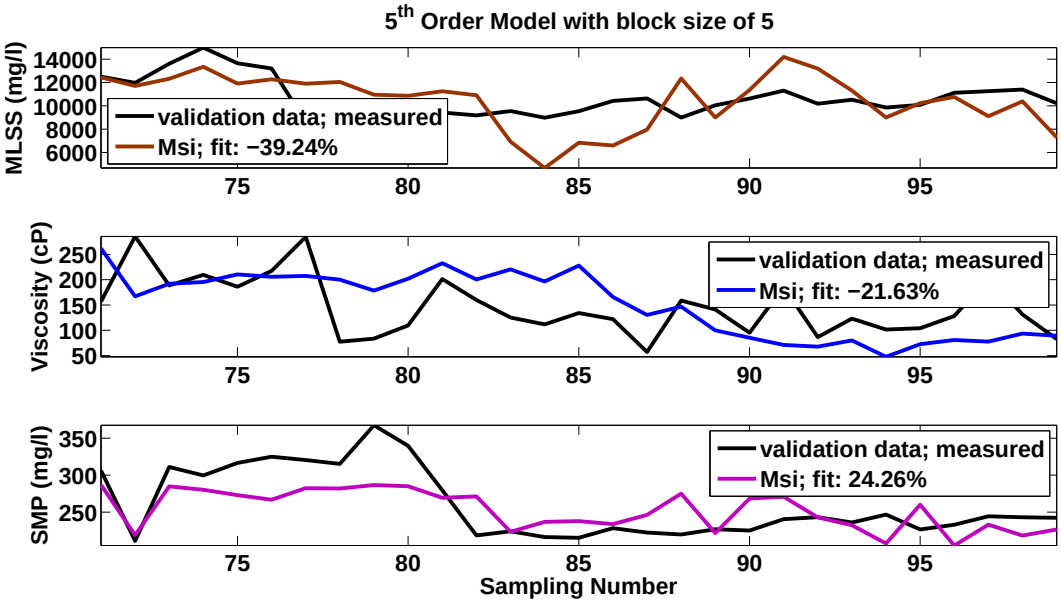

Fig. 5.25: Full data set - COD, SMP and temperature as inputs with MLSS, viscosity and SMP levels in bioreactor as outputs

5.4.3 Simulation results from Costbench mark model with temperature variation

Since the Aquabio main and pilot plant had insufficient data sets to allow an adequate testing of the system identification procedure for a MBR biological model, especially the subspace formulation, it was decided to use a much larger data set that could be relied upon. This would mean a true MIMO biological model could be tested as well as a MISO model. In order to give more realistic results, the data set should ideally be over a long enough time and take into account the temperature variations experienced during the day and at night. Incidentally these temperature variations especially impact on the nitrification and denitrification rates.

Accordingly the COST Benchmark simulation model, as described in Copp (1999, 2000) and which was modified to take into account temperature effects, was used to generate the required data set needed to test the structure of the proposed biological input-output model. How exactly this special data set was generated is fully described in Section 3.4.6. By the way almost 20,000 data points were generated by this COST Benchmark simulation which allowed a full system identification procedure to proceed for a true MIMO model set up. Obviously, since this modified Benchmark is based on the standard ASM1 model it does not include any **SMP** and/or EPS states, so it cannot be directly linked to a membrane fouling model.

The modified COST Benchmark simulation model was run using the varying temperature data on the ASM1 model, and the various bioreactor variable states were determined and saved for each of the five tanks in the fictitious plant layout. Out of this plant layout, the state variables were selected from those produced by the fully aerated tank four. This was since they would mean the DO level and its controller would not play a significant part in the model thus simplifying matters. Hence the input-output model structure would use the influent data file as the input vector with the output vector being the calculated states from fully aerated tank four.

5.4.3.1 Full data set - MIMO model set up

In this true MIMO model set up the following general formulation was used based upon the ASM1 nomenclature:

$$\mathbf{z_1} = \begin{bmatrix} Q_{in} \\ X_{S,in} \\ X_{ND,in} \\ X_{I,in} \\ X_{BH,in} \\ S_{S,in} \\ S_{NH,in} \\ S_{ND,in} \\ Temp \end{bmatrix}; \qquad \mathbf{x_1}' = \begin{bmatrix} X_{S,bio} \\ X_{P,bio} \\ X_{ND,bio} \\ X_{I,bio} \\ X_{BH,bio} \\ X_{BA,bio} \\ S_{S,bio} \\ S_{NO,bio} \\ S_{NH,bio} \\ S_{ND,bio} \\ S_{ALK,bio} \end{bmatrix}$$

The input states for autotrophic bacterial concentrations, the nitrate concentration, and the alkalinity are taken as negligible. The DO level in the influent is assumed to be zero whilst in the bioreactor is assumed to be kept fairly constant for a fully aerated tank. Other simplifications that are made include ignoring the wastage rate because it is very low when compared to the influent flow rate. Also, since the

simulation period is only for a 14 day duration when only limited wastage can take place. This greatly simplifies the input-output structure whilst still retaining the main component variables that are important.

Initially, a subspace formulation was tried with a full set of input-output variables using the CUEDSID software package. By the way the validation procedure used 2,000 points to obtain its best fit. Following this, the same procedure was carried out for the other autoregressive model structures using Matlab's System Identification Toolbox© with GUI. Table 5.4 summarises the best model fit results for all these various simulation runs.

Output variable best fit	CUESID Subspace	ARX	ARMAX	State space (pem)	State space (n4sid)
$X_{S,bio}$	-15.41%	31.20%	did not run	very poor fit	-27.37%
$X_{P,bio}$	-216.50%	41.01%	did not run	very poor fit	3.59%
$X_{ND,bio}$	-15.16%	24.05%	did not run	very poor fit	-53.30%
$X_{I,bio}$	-30.84%	53.14%	did not run	very poor fit	-239.70%
$X_{BH,bio}$	37.45%	45.60%	did not run	very poor fit	-87.92%
$X_{BA,bio}$	-146.30%	-48.00%	did not run	very poor fit	-517.80%
$S_{S,bio}$	26.61%	46.88%	did not run	very poor fit	-19.49%
$S_{O,bio}$	49.04%	80.04%	did not run	very poor fit	-0.51%
$S_{NO,bio}$	-197.04%	9.60%	did not run	very poor fit	-304.70%
$S_{NH,bio}$	-76.47%	40.92%	did not run	very poor fit	-12.83%
$S_{ND,bio}$	31.96%	40.22%	did not run	very poor fit	-12.07%
$S_{ALK,bio}$	-86.07%	44.19%	did not run	very poor fit	-69.45%

Table 5.4: Full data MIMO - comparison of best fits for various autoregressive model formulations

In the above table, it is clear that the ARX model gives the superior correlation results with only one state being a negative fit. The next best results were for the subspace model structure whose fit is generally negative for most state variables. The other methods performed even worse than this, especially the ARMAX model structure. It must be remembered that the standard autoregressive methods used half the total number of data points when attempting to achieve a best fit while only 2,000 points were used in the subspace validation exercise (in a bid to keep the computing time down to a reasonable length). Therefore the subspace method may improve with a much larger validation data set.

5.4.3.2 Reduced data set - MIMO model set up

In a bid to obtain a better model correlation than previous, the number of input and output variables were reduced to those thought to be the major ones involved in the substrate utilisation processes. In other words most of the minor variables that related to the nitrification and denitrification processes were ignored. Since the CUEDSID software package gives equal weighting to all variables, which should not really be the case for most wastewater variables, it was hoped that this reduction in variables to the most crucial ones would allow the major process relationships to be more easily and apparently discernible.

This reduced MIMO model was based upon the following general formulation:

$$\mathbf{z_1} = \begin{bmatrix} Q_{in} \\ X_{S,in} \\ X_{I,in} \\ X_{BH,in} \\ S_{S,in} \\ S_{NH,in} \\ Temp \end{bmatrix}; \qquad \overset{'}{\mathbf{x_1}} = \begin{bmatrix} X_{S,bio} \\ X_{I,bio} \\ X_{BH,bio} \\ S_{S,bio} \\ S_{NH,bio} \end{bmatrix}$$

Once again a subspace model structure was run using the CUEDSID software (with 2,000 points for validation) followed by simulation runs of the other autoregressive model structures using Matlab's System Identification Toolbox© with GUI. The best model correlations are summarised in Table 5.5.

Output variable best fit	CUESID Subspace	ARX	ARMAX	State space (pem)	State space (n4sid)
$X_{S,bio}$	-15.09%	37.04%	did not run	19.50%	10.96%
$X_{I,bio}$	-29.65%	27.37%	did not run	7.82%	35.33%
$X_{BH,bio}$	44.86%	46.86%	did not run	24.27%	21.96%
$S_{S,bio}$	26.72%	54.15%	did not run	9.14%	-0.04%
$S_{NH,bio}$	-76.35%	49.40%	did not run	-191.40%	-161.60%

Table 5.5: Reduced data MIMO - comparison of best fits for various autoregressive model formulations

It is evident from Table 5.5 that a reduced data set in general gives much better correlations for all model structures apart from the ARMAX model which again did not run. Additionally, the ARX model also gives the best fit followed by the state space (pem) method, and then the subspace formulation. In a bid to see whether model fits could be further improved upon, it was suggested that a MISO formulation may prove even more efficient.

5.4.3.3 Full data set - MISO model set up

In this case each of the main outputs were run as MISO model structures and the best fit ascertained for all methods. Fig. 5.26 depicts the simulation runs only for the subspace formulations, while Table 5.6 summarises the results in general for all the autoregressive methods.

Output variable best fit	CUESID Subspace	ARX	ARMAX	State space (pem)	State space (n4sid)
$X_{S,bio}$	34%	45.63%	40.81%	43.52%	no fit
$X_{I,bio}$	7.76%	48.63%	34.31%	no fit	no fit
$X_{BH,bio}$	45.94%	30.42%	43.5%	-243.10%	no fit
$S_{S,bio}$	17.75%	63.30%	62.67%	62.00%	no fit
$S_{NH,bio}$	-29.00%	41.87%	30.24%	31.45%	no fit

Table 5.6: Full data MISO - comparison of best fits for various autoregressive model formulations

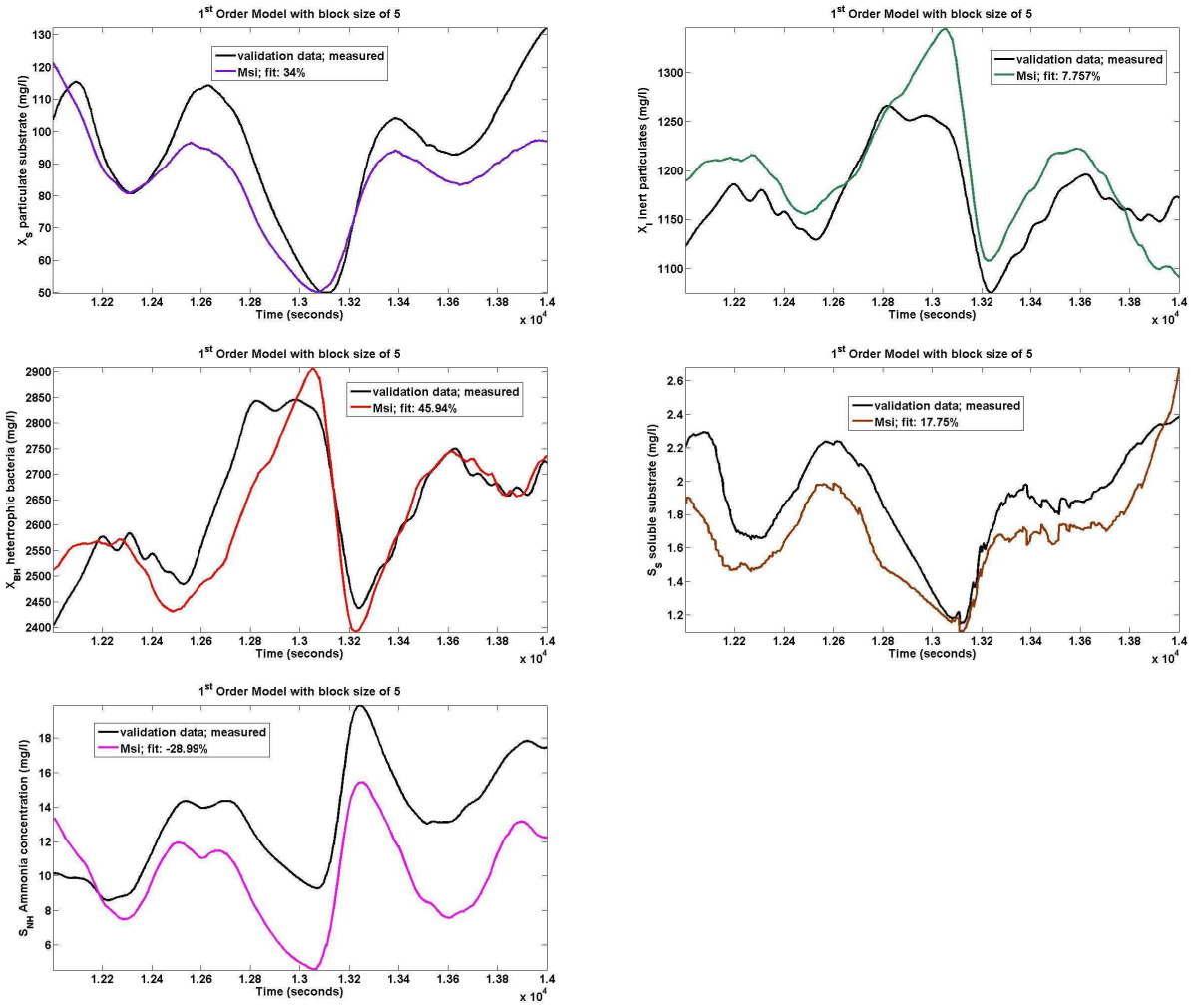

Fig. 5.26: MISO model formulations of 1st order with block size of 5 - X_S, X_I, X_{BH}, S_S, and S_{NH}

It is again evident from these simulations that the ARX model structure gave the best fit for all the MISO models, followed closely by the ARMAX model structure. The subspace formulation gave a slightly worse fit, with the state space (pem) method giving a relatively poor fit. The subspace (n4sid) method produced no fit in this case.

5.4.4 Using the input-output model structure to predict SMP levels for other plant

The previous sections of this Chapter have proved that the beauty of this input-output modelling approach is that models can be rapidly developed and verified without needing an prior process knowledge. The limitations of this approach are also clearly self-evident in that sometimes poor fits are achieved. Hence it is suggested that if the best of both the phenomenological and behavioural approaches could possibly be combined to give a procedure that would allow rapid but accurate model development without having to conduct extensive sampling programmes and numerous new sampling tests and measurements.

Consequently in this regard it was proposed that a times series model formulation could be utilised to predict the **SMP** values in a MBR bioreactor without actually having to regularly measure them. These could then be linked to the membrane fouling model if so required. In terms of the biological model, a standard IWA Activated Sludge models could be used without it needing any new **SMP** and/or EPS state variables (with their additional complex parameters as well). This judicious combination of both model types would mean savings in the types of measurements needed, and also in model calibration and validation procedures. It could also prove the best way forward to developing a truly integrated but accurate MBR model. However, much more research work is needed in this area.

As a first step to validate this recommended approach, the following modelling steps were completed based upon the available data under this study:

1. A very simple SISO input-output behavioural model formulation was developed. In this structure the input was the influent COD with the output being the **SMP** concentration.
2. This structure was implemented utilising the full data set from the Aquabio pilot MBR plant. The best fit model for all autoregressive structures was saved for later use. In this case it proved clearly to be the CUEDSID subspace formulation.
3. This saved subspace model structure was then implemented using the influent COD from the Aquabio main MBR plant in order to predict the **SMP** levels for this new plant which were unknown. By the way the increased data set was used in this regard.
4. Next Lu's modified phenomenological ASM1 model was used to also predict the **SMP** levels for the Aquabio main MBR plant using the same data set.
5. Both methods were then compared on the same plot to ascertain the variations in **SMP** values. If reasonable results were obtained, then this approach could be recommended for other plant.

The best fit for the SISO CUEDSID subspace method was 38.78% for a tenth order model with a block size of ten as outlined in Fig. 5.27. This model was validated on approximately a quarter of the data points available. All the results from the other autoregressive methods proved to be very poor and were subsequently rejected from potential further use. They were respectively: an ARX model best fit of -19.02%; an ARMAX model best fit of -21.99%; a state space (pem) model best fit of -34.88%; and, a state subspace (n4sid) model best fit of -17.56%.

Hence the SISO subspace formulation for this system was determined to be as follows:

$$x(t+T_S) = A.x(t) + B.u(t) + K.e(t); \qquad x(0) = x0$$

$$y(t) = C.x(t) + D.u(t) + e(t)$$

where:
$u(t)$ is input vector of the system

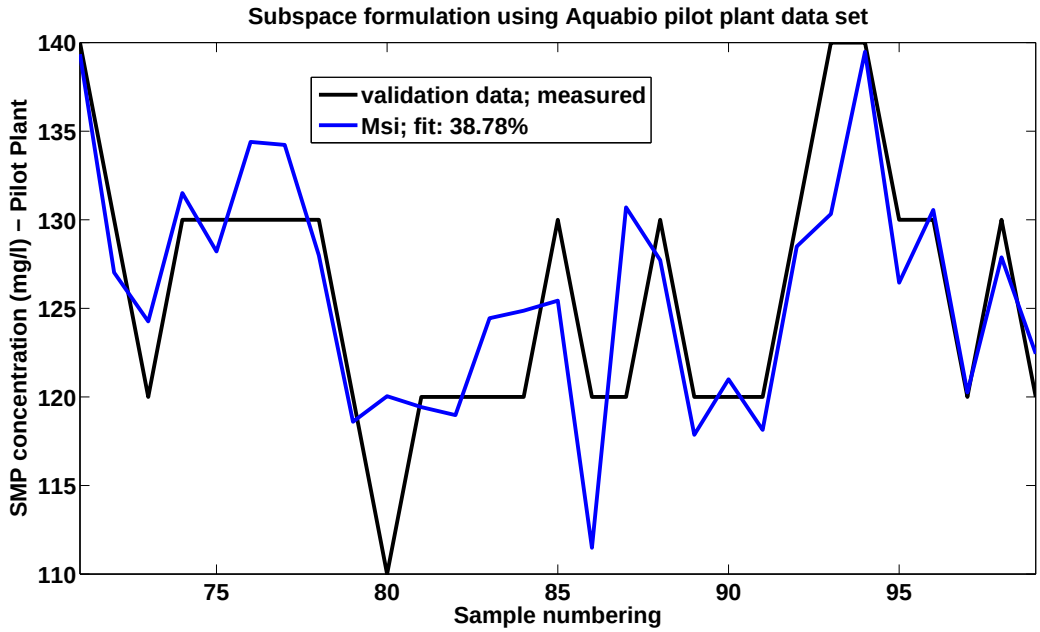

Fig. 5.27: SISO model formulations of 10th order with block size of 10 - COD is input with SMP level as output

$y(t)$ is the output vector of the system
$e(t)$ is the disturbance (control) vector of the system
$x(t)$ is the (unobserved) state vector of the system
A, B, K, C and D are the coefficients of the individual vectors respectively

Fig. 5.28 below shows the coefficients of this tenth order subspace model.

Next this best fit model was used together with the influent COD values from the Aquabio main plant increased data set to determine the predicted **SMP** levels in the bioreactor Tank B. Fig. 5.29 shows the results from this simulation run. The predicted **SMP** levels are between 100 to 700 mg/l which would be near to those expected in reality if the protein and polysaccharide concentrations were combined into a single value.

Finally, one of the modified phenomenological models developed earlier, namely Lu's modified ASM1 model, was run using this same data set. The **SMP** values determined from this alternative model were then plotted on the axis as for those of from the subspace model as shown in Fig. 5.30. This plot shows that although the subspace method predicts a much wider spread of **SMP** values, they are of the same order of magnitude as those predicted by Lu's modified ASM1 model, which in any case should prove the more accurate method as it was specifically calibrated earlier for this plant layout. In conclusion, this developed procedure shows that the combination of both approaches can prove very beneficial when trying to obtain optimal modelling results with the minimum of time and effort. It would also allow the more rapid take-up of modelling methods for the design, operation and control of MBR plant.

A =

	x1	x2	x3	x4	x5	x6	x7	x8	x9	x10
x1	0.98701	0.024397	0.0010642	-0.0036585	0.0069031	0.017282	0.0093709	-0.009471	0.0054204	-0.0092891
x2	0.53928	0.3893	-0.48828	0.0037817	0.017719	-0.34334	0.12667	-0.41315	-0.21284	0.064332
x3	-0.26264	0.63778	0.3774	0.65337	-0.17055	0.0063934	-0.099134	0.20295	0.039016	0.031946
x4	-0.41498	0.34325	-0.69458	-0.08241	-0.14587	0.2843	-0.10152	0.38701	0.14468	0.030179
x5	0.25971	-0.32082	-0.27371	0.51655	0.68311	-0.021343	-0.22792	0.20843	0.031932	-0.051701
x6	0.21075	-0.23285	-0.053465	0.033212	-0.34349	-0.73557	-0.1976	0.39457	0.30498	-0.18074
x7	0.46009	-0.46013	-0.27504	0.40959	-0.50683	0.23908	-0.35346	-0.58392	0.032381	-0.0095777
x8	0.37301	-0.36576	-0.18815	0.36288	-0.2095	0.074344	0.85091	0.064231	0.03256	0.01581
x9	0.26284	-0.21471	-0.098221	0.11467	-0.23726	-0.064554	-0.057868	0.25292	-0.8844	-0.071732
x10	0.0043037	-0.076125	-0.054861	0.10262	0.01575	-0.26205	0.06284	-0.13109	0.1342	0.6409

B =

	u1
x1	-0.0010912
x2	0.038164
x3	-0.019202
x4	-0.028452
x5	0.025278
x6	0.015414
x7	0.036181
x8	0.025753
x9	0.026688
x10	0.0046892

C =

	x1	x2	x3	x4	x5	x6	x7	x8	x9	x10
y1	-10.503	1.0749	-1.3938	3.3561	1.1129	-0.37269	1.7002	-1.5312	1.5207	-3.5998

D =

	u1
y1	0.88706

K =

	y1
x1	-0.0043146
x2	0.019827
x3	0.025154
x4	0.01278
x5	0.025778
x6	0.0070157
x7	0.011778
x8	0.036446
x9	-0.020632
x10	0.0025164

x(0) =

x1	0
x2	0
x3	0
x4	0
x5	0
x6	0
x7	0
x8	0
x9	0
x10	0

Fig. 5.28: SISO model formulations of 10th order with block size of 10 - coefficients of vectors

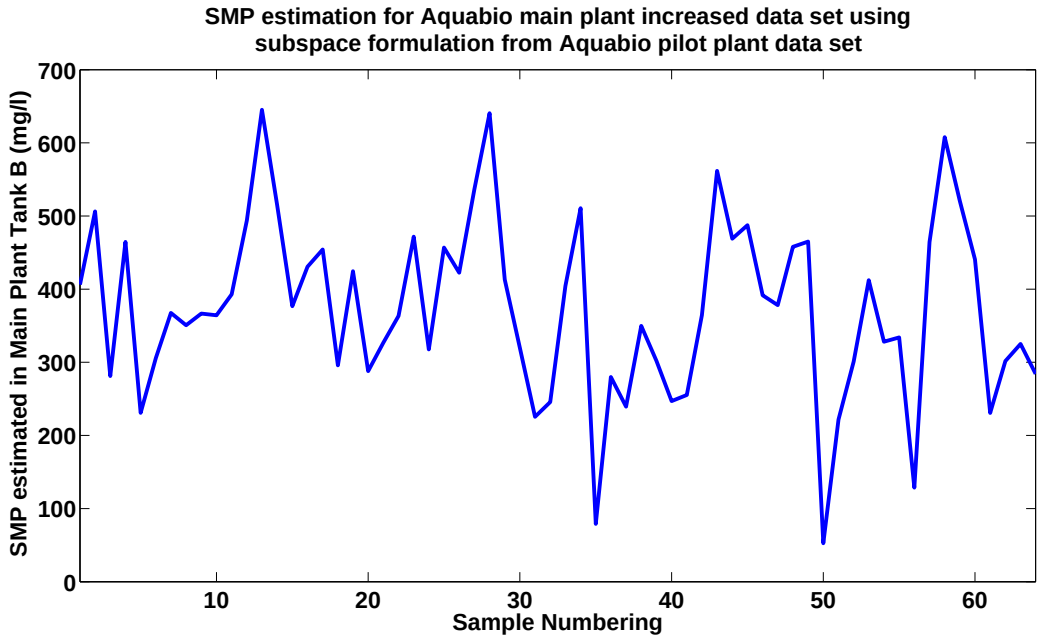

Fig. 5.29: Simulated SMP values for Aquabio main plant using subspace model

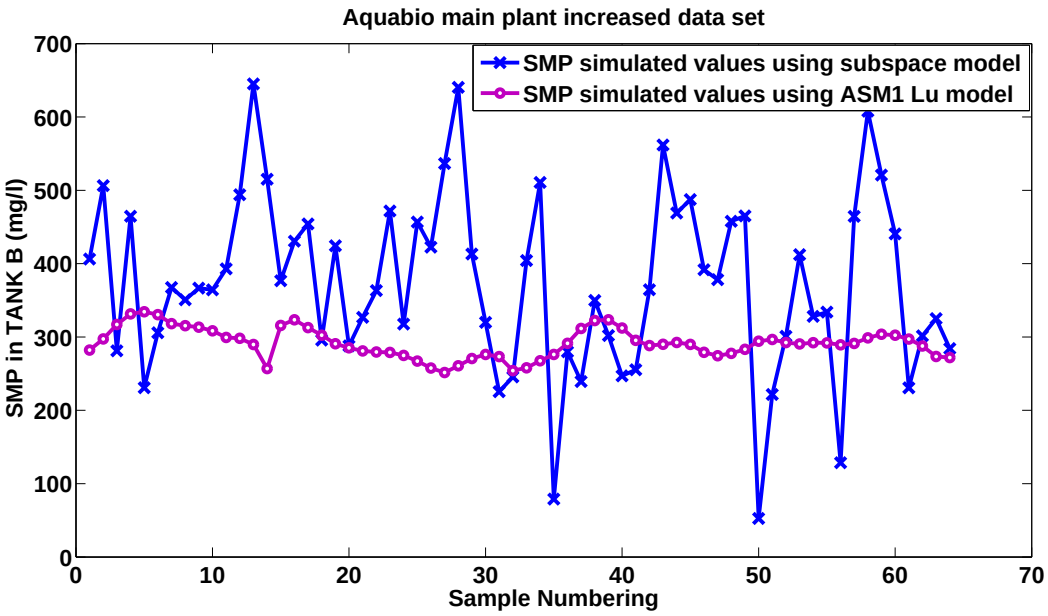

Fig. 5.30: Comparison of simulated SMP values for Aquabio main plant using subspace model and Lu's modified ASM1 model

5.4.5 Summarising results from behavioural models

The following summarised points can be made regarding behavioural model structures:

- A significant amount of collated data is required to allow these structures to be set up and fully tested.
- Although a subspace formulation based upon the CUEDSID software package always provides a solution that is reasonable for the real life plant data sets, it is not always the best fit as was the case for the fictitious WWTP data set.
- The other model structure that proves fairly robust and almost always provides a fairly decent solution is the ARX model. This is especially the case for the MIMO models with numerous inputs for the fictitious WWTP data set.
- The ARMAX structure often fails to provide a solution, or gives a extremely poor correlation for the real life plant data sets. However, it gave the second best model fits for the fictitious WWTP data set.
- Of the two state space model structures, the general state space (pem) method always out performs the state subspace (n4sid) method.
- The overall model fits for the behavioural models proved reasonably acceptable especially for large data sets. This correlation also improved with MISO structures as opposed to MIMO structures.
- The CUEDSID software's subspace algorithm proved far superior in all cases when compared to the standard subspace method (n4sid) employed by the Matlab's System Identification Toolbox©. In fact it always provided a solution, whereas conversely the subspace (n4sid) method proved very unrobust and frequently failed to give any solution.
- The procedure that was tested earlier that utilised both the phenomenological and behavioural model structures to account for shortfalls in plant data, proved to give reasonable results. This means that combinations of both model types could be used in future which can simplify the overall data collation, parameter estimation, and model verification procedures.

5.5 *Chapter Summary*

In this Chapter, two Activated Sludge models that included **SMP** components were further developed from basic versions. Once calibrated and validated, these modified models were tested on data taken from a real life plant. Using this data and other data obtained from similar plant described in the second half of Chapter 3, several behavioural biological models were tested as alternative model structures. Since the behavioural biological models required extensive data sets to allow a complete testing, data was also used from a fictitious plant specially developed for this purpose. In the last part of this Chapter an attempt was made to use both model types, namely phenomenological Activated Sludge models and behavioural biological models, in combination in order to predict **SMP** levels in plant in a quick, easy and cost effective manner.

It was found that the results from both modified phenomenological models could be made to predict very closely to the original Activated Sludge models for all state and composite variables. This is as opposed to the original published Oliveira and Lu models whose results diverge. This proves the generality of this model development approach.

For the behavioural model type, although a subspace formulation based upon the CUEDSID software package gave a solution that was reasonable for the real life plant data sets it was not always the best fit as was the case for the fictitious WWTP data set. The other model structure that proved fairly robust and almost always provided a fairly decent solution was the ARX model. This was especially true for the MIMO models for the fictitious WWTP data set.

Chapter 6

Conclusion and further work

6.1 *Conclusion and summary*

This Chapter summarises the conclusions of this research study and then suggests some follow-on work that needs to be carried out.

6.1.1 Executive Summary

MBRs are a recent innovation that combines a membrane filtration unit with a biological process technology in order to treat a wastewater. Compared to conventional Activated Sludge systems which are commonly used to treat wastewaters, MBRs produce excellent quality effluent, have a small footprint, and due to the dramatic reduction in membrane costs in recent years are now even becoming a viable alternative to conventional Activated Sludge systems.

The down side of MBRs is that operationally speaking membrane replacement costs are still high and the hydrodynamic control of membrane fouling is still an energy intensive process whether with air-sparging, backflushing, relaxation, crossflow velocities, chemical cleans or a combination of each. Additionally, membrane fouling occurring on the membrane surface and within the pores reduces the long term stability of the flux performance. Understanding by researchers of the nature of and the factors contributing to this fouling process is still currently limited.

Research into MBR technology requires an interdisciplinary approach which combines biological process knowledge with physical-chemical knowledge of membrane filtration. Many researchers currently tend to focus solely on one issue, either the biology or on the membrane itself. In this study an attempt was made to eventually allow the development of a combined predictive computer model of a MBR which would integrate both the process biology and the membrane fouling process. In this regard, two different model types, namely a phenomenological model structure and a behavioural model structure, were tested to ascertain which gave the best results for both biology and membrane filtration processes, and proved the most effective to allow eventual integration.

6.1.1.1 Synopsis of research work carried out

In Chapter 4, a comprehensive phenomenological membrane fouling model was developed from a basic version initially produced by Duclos-Orsello et al. (2006). Once calibrated and validated, this modified model

was then tested on data sets taken from real life plant that are described in the second half of Chapter 3. Using these same data sets, several behavioural fouling models based on the "Model Conceptualisation Procedure" outlined in the first half of Chapter 3 were tested as alternative model structures. This included both linear and non-linear input-output model structures.

In Chapter 5, two Activated Sludge models that included **SMP** components were further developed from basic versions initially produced by Oliveira-Esquerre et al. (2005) and Lu et al. (2001) respectively. Once calibrated and validated, these modified models were tested on data taken from a real life plant that was described in the second half of Chapter 3. Using this data and other data obtained from similar plant described in the second half of Chapter 3, several behavioural biological models based on the "Model Conceptualisation Procedure" outlined in the first half of Chapter 3 were tested as alternative model structures. Since the behavioural biological models required extensive data sets to allow a complete testing, data was also used from a fictitious plant specially developed for this purpose. In the last part of Chapter 5 an attempt was made to use both model types, namely phenomenological Activated Sludge models and behavioural biological models, in combination in order to predict **SMP** levels in plant in a quick, easy and cost effective manner.

6.1.1.2 Summary of research outcomes

The larger TSB projects aim was to improve the design, operation and control of MBR plant by using modelling techniques coupled with laboratory analysis methods. At the end of this project, only some limited in-roads had been made to this high level goal as it was deemed too lofty for a project of this level of financing, resourcing and scope. Hence the project had made some positive contributions in model development but only in a limited manner.

In terms of this PhD work, the overall goals were less ambitious, namely looking at how complex or simple phenomenological models of both the Activated Sludge and membrane fouling process were to create, verify and use in practice, and how accurate they were as well. Then an attempt was made to try and develop a totally different model type for both the Activated Sludge and membrane fouling process using methods that apparently addressed the deficiencies of the traditional phenomenological model type. Again for these alternative model types, the research work would look at how easy it was to create, verify and use them in practice, and how accurate they were as well.

Summary of membrane fouling models - both model types A very good correlation was shown between the measured and the expected flux decline/recovery for the phenomenological model, although a complex genetic algorithm procedure was needed for parameter estimation. The subspace model was almost as accurate as the phenomenological model even though it only used a single shot fast algorithm for parameter estimation. Further and longer historical data sets are needed to ascertain whether this second simpler modelling approach can be improved upon.

It initially looks like this novel approach has many advantages over traditional mechanistic models while giving comparable results for some input-output structures. It even has many advantages over other more traditional non-mechanistic models such as ANN and FNN methods. Early simulation results described in this study prove this, especially for subspace methods. However these methods can prove very fragile particularly the ARMAX formulation which is prone to crashing. Additionally a comprehensive "Model Conceptualisation Procedure" is required to tie it into reality which needs expert know-how to set up. They also require very large data sets to produce accurate formulations, and these linear models are only useful around a very narrow operating range or operating point. Non-linear model versions can improve the predictive accuracy but are even more fragile.

Summary of Activated Sludge models - both model types A poor model fit was shown for the modified Oliveira and Lu Activated Sludge models, although their parameters were changed from

the original models' values to reflect an MBR system. In comparison the subspace and ARX formulated biological models were reasonably accurate when compared to the Activated Sludge version, although a much longer historical data set is needed to confirm these initial findings.

It initially looks like this novel approach has many advantages over traditional mechanistic models while giving comparable results for some input-output structures. Early simulation results described in this study prove this especially for subspace methods. However these methods can prove very fragile particularly the ARMAX formulation which is prone to crashing. They also require very large data sets to produce accurate formulations, and these linear models are only useful around a very narrow operating range or operating point.

When answering the research questions posed, then generally speaking the overall performance of both the phenomenological models and the input-output models proved similar. All the phenomenological models proved difficult to set up and run for reasons already discussed earlier, while all the input-output model forms proved the opposite. The optimal way ahead in this area of research may be the prudent use of a combination of both model types. Hence this means using a conventional phenomenological Activated Sludge model to predict most process states while using a reduced input-output model structure to predict the process states that impinge directly on membrane fouling (i.e. SMP levels). This has the advantage of using well defined existing standard IWA models with all their benefits, with the SMP state components/s only being used in the input-output model version which would be easy to calibrate. In conclusion, further research is required using longer historical data sets to definitively ascertain whether this autoregressive modelling approach can be further developed and improved upon.

6.1.2 Summary of outputs and achievements in Chapter 4

The main research questions asked in terms of this Chapter were as follows:

- How easy is it in practice to calibrate and validate a relatively simple phenomenological membrane fouling model for a real life MBR plant which is still rich enough in complexity to express the major membrane fouling mechanisms involved?
- Is a system identification procedure using time series analysis a simpler, quicker behavioural modelling approach to use to determine membrane fouling within a real life MBR plant? Can it give the same degree of accuracy as a phenomenological model?

6.1.2.1 Phenomenological membrane fouling model

The following specific points can be made regarding the phenomenological model structure developed in this Section of Chapter 4:

- A basic phenomenological dead-end filtration model (Duclos-Orsello et al. 2006) that includes the three classical fouling mechanisms mentioned in Hermia (1982) (i.e. pore constriction, pore blocking and cake filtration) and that was based on a constant TMP operation was extensively modified. Modifications and add-ons to this basic model included:
  1. Alteration so that it could be used for constant flux and varying TMP operations.
  2. Inclusion of a backwash mode.
  3. It described pore constriction (i.e. irreversible fouling) in relation to the concentration of EPS and **SMP** in the liquor which are the main culprits deemed to instigate membrane fouling.
  4. It could be used in a crossflow scenario by the addition of scouring terms in the model formulation.
- Using data collected from the Duclos-Orsello et al. (2006) paper and Aquabio's pilot plant, this modified deterministic model was calibrated and validated in Matlab/SIMULINK©. A very good correlation was shown between the measured and the expected flux decline/recovery for this phenomenological model, although a complex genetic algorithm procedure was needed for parameter estimation. This model was then further tested using data from the ITT Sanitaire pilot membrane filtration unit operated at Cardiff WWTP.
- The links between the biological model described later in Chapter 5 and this fouling model are:
  1. *Connection with MLSS* - The MLSS concentration defines the solids mass flux rate towards the membrane surface and thus the propensity of cake buildup.
  2. *Connection with* **SMP** - The **SMP** material deposits inside the membrane pores reducing porosity and increasing TMP. The **SMP** was also found to affect cake permeability by cake voidage occlusion.
  3. *Connection with viscosity* - Permeate viscosity affects pressure loss during membrane filtration. Mixed liquor viscosity levels may correlate with EPS and **SMP** concentrations.
  4. *Connection with EPS* - The EPS concentration affects cake permeability.
- Attributes of this model:
  1. Dependant on either constant flux or constant TMP operation, it is able to predict the evolution of TMP increase or flux decrease in time for any new plant under given operational conditions.
  2. The model predicts both short-term (cake buildup) and long-term (pore constriction) fouling effects.

3. It can be used for control purposes to prevent fouling (i.e. determines optimum operating range for state variables and other parameters).
4. It can be linked to a biological reactor model and is easy to calibrate using a simple standard sampling method.

- Purposes of this fouling model:

1. *Optimisation* - needs a relation between cake buildup and CFV/scouring rate and flux and **SMP** deposition. This allows optimal throughput for minimal energy requirements.
2. *Monitoring membrane operation* - diagnostics. This allows troubleshooting for unforeseen events.
3. *Membrane filtration control* - This allows a better understanding of how to operate the membrane for this specific plant configuration.
4. *Model accuracy* - It proved reasonably accurate as a model especially for plant filtering low concentration mixed liquors and for simpler flow trains. Obviously its accuracy is also dependent on the quality of measured data supplied. Since these models only look at the biology in a very simplistic macroscopic way and only measure gross biochemical values, they cannot obviously describe the real affects of the biology on the membrane in a microscopic way as this is too complex a process and is prone to localised clogging effects.

Further points that can be made regarding this particular membrane fouling model, and phenomenological fouling models in general are:

- As membrane fouling is in reality a very complex and very little understood process at this moment in time, it is difficult to make a generalised fouling model that can adequately address all the issues and specific nuances involved.
- Phenomenological fouling models need to be made bespoke for each individual filtration system on a case-by-case basis. This is especially true for the hydrodynamics of the process (e.g. the type of sparging system in use), and the membrane operational regime (e.g. submerged or sidestream or vertical air-lift).
- Even though the model is unlikely to be used on plant intentionally operating for long periods above critical flux conditions, it should still be able to perform adequately under these conditions.
- Any model should be flexible enough to account for, in simple terms, periodic backflushing, relaxation, and chemical dosing mechanisms.
- Ideally, any model should have a dynamic backwash cycle. The current version only contains a simple reset mode following a backwash cycle, while a dynamic backwash would actually try to predict the permeability recovery based on the data collected and by using additional differential equations formulated for this specific purpose. These equations would describe the cake removal and pore unblocking based on backwash frequency, duration and intensity. This would make the model formulation much more complex but more comprehensive.

6.1.2.2 Behavioural membrane fouling model

Based upon the results of the simulation runs and general outcomes in Chapter 4, the following specific points can be made regarding behavioural model structures:

- Behavioural models based on standard mathematical formulations such as ordinary differential equations or difference equations of various orders can be used as a quick method for model prediction as no prior process knowledge is required for model calibration and validation. This was comprehensively proved by the various simulations run in this Chapter. The procedure automatically selects the best order of model based on the best number of lags in output data that give the optimal prediction. Little skill is needed by the simulator to obtain the best fit, and a significant amount of time is saved when compared to the complex needs of verifying a typical mechanistic model. Additionally, many of the complex tests, both laboratory based and in-situ, that are required to valid the numerous model parameters are not needed, or the need to carry out extensive literature reviews of parameter values used by previous reputable researchers.
- However, it is recommended if these model types are used as real practical alternatives to phenomenological approaches, extreme care should be taken in selecting appropriate variables when forming the input-output model structure. This is where a "Model Conceptualisation Procedure" developed by prior researchers will prove invaluable as it underpins the basic knowledge needed by a lay person when developing models of this type. This procedure means that various input-output structures are already developed and tested based on biochemical and hydrodynamic process knowledge, and the user only has to implement them.
- An input-output model structure seems appropriate to be used both for flux stepping data sets as well as long term standard filtration data sets. Additionally, an input-output model structure can be used irrespective of the membrane filtration unit's configuration or operational regime i.e. constant flux/varying TMP or constant TMP/varying flux; sidestream crossflow or submerged systems.
- In order to see whether a non-linear model could be formulated for advanced control purposes, which was based wholly upon measured historical data sets, a further conceptual model was developed based on non-linear system identification procedures and empirical times series analysis methods (Ljung 1999). This model was based upon a bilinear subspace state-space formulation with temperature being the other global variable. This alternative model was calibrated and validated in Matlab©, and gave improved fits when compared to its linear subspace alternatives. This suggests that other more complex non-linear model formulations need to be tested as they may give even better fits.

It is recommended that these input-output model structures should be used as follows:

- The models should only be used for automated plant control purposes, as they are linear ones which means they give acceptable results around a narrow operating range or point. They are of less use operationally speaking in a broad sense and a phenomenological model should always be preferred. This situation may change if non-linear model forms can be developed by future researchers which prove applicable for a much wider operational range.
- In terms of design purposes, they should never be used as they are not based on sound laws of physics, so design simulations of possible plant layout based on predicted flows and loads would never be reliable enough when putting together a tender bid for a Client.
- They need to be constantly updated with fresh data on a very regular basis, as they would be prone to becoming obsolete very quickly. This is also so that their accuracy and predictability remains high. This means a constant need to validate and calibrate them on fresh data. This could be automated in a MPC system which utilised on-line data gathered from sensors and other measurement devices. Telemetry or dedicated cabling would periodically and automatically transmit the fresh data to the model predictive controller which would update its model accordingly.
- In these models the backwash data that is used is taken as of the same importance as the forward filteration process when the weighting of data should really be different as it is of lesser significance.

This means the behavioural models should contain a mechanism to allow various aspects of the total data set to be weighted differently according to their importance in meeting the overall operational objectives. Thus as the main objective of the plant is to produce the greatest daily volume of permeate liquid, the forward flux data should be accorded greater significance. Since the backwash actually reduces the daily permeate volume, then it is of lesser importance. As they stand the behavioural models do not currently allow any weighting as they are developed for equally weighted data sets like for financial data taken from stock markets. This needs to be altered for future process models.

- This same concept could be extended as well to cover different variables in the data set since the current model forms used in this research work gives equal weight to all the various data variables which is obviously not the case in real life. This means a more significant weighting would be given to flows and pressure information, and less importance to biochemical process variables such as liquor concentrations, **SMP** levels, viscosities, and temperature.
- Since these are methods that require a plant that is data rich to produce good model fits, this can be perceived as a limitation of them when they are used for new plant or for those with limited sensors and measurement devices and/or limited prior off-line sampling measurements.
- Overall the bilinear subspace model does prove not as accurate as the phenomenological model even though it only used a single shot fast algorithm for parameter estimation. A much longer historical data set is probably needed to ascertain whether this bilinear modelling approach can be improved upon by utilising other non-linear model structures.

6.1.2.3 Comparing both model types

In terms of addressing the two original research questions that were posed, then Table 6.2 is a summary of the outputs from both model types which can be directly compared albeit in a subjective way.

1. Since both model types were formulated in different ways and with different constraints, it proved difficult in directly correlating model outputs with one another for both model types. This could only be done in a qualitative manner rather than using a more exacting quantitative method such as statistical analysis.

2. It was clear when answering the first research question, then the phenomenological model's performance far exceeded all the behavioural input-output model forms for all plant data sets. It also proved far superior in having greater flexibility in addressing different plant configurations especially in terms of hydraulics and hydrodynamics. On the negative side, the overall model development with additional modifications to cover all possible plant layout and operation proved very complex and onerous to complete. The same was the case for the model calibration and validation procedure which involved running complex genetic algorithm routines.

3. All the behavioural input-output model forms proved very quick to set up and run although their output proved generally poor apart from the subspace method developed in the CUEDSID software. In fact this specialised subspace method gave results of comparable accuracy for some of the data sets used.

4. A major constraint of the input-output model types proved to be that initial work needed to be carried out in providing a framework for developing them such as the "Model Conceptualisation Procedure" for a MBR system that was produced under this study. One other constraint was that they required large data sets to run, and some of them proved quite fragile for some data sets. This fragility was more pronounced for the non-linear model versions.

5. In conclusion, this study proves that a subspace procedure such as the specialised one developed under the CUEDSID software can give comparable accuracy when directly compared to a comprehensive phenomenological model. Therefore they can be used as fast alternatives to the traditional modelling approaches if used with care.

	PHENOMENOLOGICAL FOULING MODEL	BEHAVIOURAL FOULING MODELS					
RESULTS FROM PLANT DATA	Duclos-Orsello	CUESID Subspace	ARX	ARMAX	State space (pem)	State space (n4sid)	Bilinear model
Aquabio pilot MBR plant - flux stepping individual	Very good fit	Reasonable fit	-	-	-	-	-
Aquabio pilot MBR plant - flux stepping multiple	Poor fit	Poor shape fit	Poor fit	Poor fit	No fit	Very poor fit	-
ITT pilot membrane unit - flux stepping multiple	Excellent fit	Excellent fit	Poor fit	Poor fit	Poor fit	Very poor fit	-
ITT pilot MBR plant - long term data	-	Reasonable fit	Poor fit	Poor fit	No fit	Very poor fit	Reasonable fit

Table 6.1: Answering the research questions - summary of comparison of model types

6.1.3 Summary of outputs and achievements in Chapter 5

The main research questions asked in terms of this Chapter were as follows:

1. How easy is it in practice to calibrate and validate a relatively simple phenomenological biological Activated Sludge model for a real life MBR plant which is still rich enough in complexity to include the major biological / biochemical agents involved in the fouling of MBRs?
2. Is a system identification procedure using time series analysis a simpler, quicker behavioural modelling approach to use to accurately determine the biological interactions within the bioreactor of a real life MBR plant? Can it give the same degree of accuracy as a phenomenological model?

6.1.3.1 Phenomenological Activated Sludge models

The following summarised points can be made regarding phenomenological Activated Sludge model structures:

- A purely mathematical and automated optimisation of Activated Sludge variety model can prove problematic due to the complexity and resulting unidentifiable nature of the highly non-linear processes involved, especially for the ASM1 which has its circular death regeneration concept. Hence mathematical optimisation should always be supported by sufficient expert process knowledge, since an optimisation algorithm cannot differentiate between more defined (i.e. stoichiometric parameters) or less defined parameter values, and will often end up producing rather small modifications to a considerable number of parameters.
- Another major problem encountered in calibration of these models is the lack of identifiability of the model parameters since often more than one combination of influent characteristics and model parameters can give a reasonable fit based on the available data. Hence expert knowledge is required for these model types, so that all obtained information is carefully assessed, and so that the model parameters are constrained within realistic boundaries for the specific wastewater treatment processes under investigation.
- Another limitation of Activated Sludge models is that due to the generally highly effective removal capabilities of modern WWTP, there is limited effluent dynamics that can be used during the calibration of full scale installations. This can be overcome to some extent by taking additional (but costly) in-process measurements at several points in the bioreactor flow train.
- A proper Activated Sludge model that introduces new **SMP** processes to include mechanisms for membrane fouling requires considerable expertise and process knowledge to fully develop. This expertise in model development ranges from checks to the model processes to ensure balancing of components, through to parameter estimation and performance of the model calibration and validation procedures. It also includes extensive knowledge to carry out a proper influent and sludge characterisation procedure to determine the state components for the model.
- The complexity of this variety of phenomenological models means they require specialist knowledge to set up and often prove difficult to use in practice especially for existing plant operation and control. In the main, they have tended to be used for research purposes or for the concept design of new plant.

6.1.3.2 Behavioural Activated Sludge models

The following summarised points can be made regarding behavioural input-output Activated Sludge variety model structures:

- Unlike the counterpart membrane fouling input-output model structures, the behavioural Activated Sludge variety models have intuitively much more easily determined structures as they mainly represent the various state variable components in the model. For the membrane fouling input-output models, it often means mixing process model state components (i.e. MLSS) with operational variables such as TMP which may not make much sense in real terms unless the input-output structure is part of a rigorous framework that has been conceived like the "Model Conceptualisation Procedure". Conversely the Activated Sludge input-output model structures are fairly obvious in most instances.
- In these autoregressive model structures the weighting of state components is taken as being equal, although in process terms this is not the case with some state components being of significantly more importance than others. Hence it is suggested that a mechanism is introduced to allow different weightings for each component based on process knowledge. A simple of doing this way maybe to use two separate input-output models, one for Carbon based components with the other being for Nitrogen based components, with the former's results being given greater significance than those from the latter.
- A major limitation of a behavioural Activated Sludge variety model is that it requires a considerable amount of data taken over a long time period to run adequately which increases greatly when using large MIMO structures.
- It is debatable whether a behavioural Activated Sludge variety model could be easily linked to its counterpart membrane fouling model. In this regard, it may prove better to have a single input-output model that describes the whole MBR system as a black box process with a single error term.
- The optimal way ahead in this area of research may be the prudent use of a combination of both model types as was tried in the final part of Chapter 5. Hence this means using a conventional phenomenological Activated Sludge model to predict most process states while using a reduced input-output model structure to predict the process states that impinge directly on membrane fouling (i.e. **SMP** levels). This has the advantage of using well defined existing standard IWA models with all their benefits, with the **SMP** state components/s only being used in the input-output model version.

6.1.3.3 Comparing both model types

Once again in terms of addressing the two original research questions that were posed, then Table 6.2 is a summary of the outputs from both model types which can be directly compared albeit in a subjective way.

1. As in the case of the previous Chapter, since both model types were formulated in different ways and with different constraints, it proved difficult in directly correlating model outputs with one another for both model types. This could only be done in a qualitative manner rather than using a more exacting quantitative method such as statistical analysis.

2. When answering the research questions posed, then generally speaking the performance of both the phenomenological model and the behavioural input-output model proved similar. Both the original Activated Sludge models gave good results whilst the models that included **SMP** processes performed poorly overall. In a similar manner, the subspace method developed in the CUEDSID software and the ARX method gave good results for all the data sets used (including those from the fictitious plant), whilst the other autoregressive model structures either failed to run or gave very poor results.

3. All the phenomenological models proved difficult to set up and run for reasons already discussed earlier, while all the behavioural input-output model forms proved the opposite.

4. In conclusion, this study proves that a subspace procedure such as the specialised one developed under the CUEDSID software and a standard ARX method can give comparable accuracy when directly compared to the two main unaltered IWA Activated Sludge models. Therefore they could be used as fast alternatives to the traditional modelling approaches, although more research work is required in this area to confirm this assertion.

5. In conclusion, a sensible use of both model types in combination might be the best solution. This means that existing IWA Activated Sludge models can be used in an unaltered manner to determine most of the process states. This would only require a limited calibration procedure of a few kinetic parameters while the stoichiometry would remain unchanged. The process states responsible for membrane fouling such as the **SMP** levels would then be predicted by a simple-to-calibrate behavioural model.

	PHENOMENOLOGICAL BIOLOGICAL MODELS				BEHAVIOURAL BIOLOGICAL MODELS				
RESULTS FROM PLANT DATA	Original ASM3	Oliveira ASM3	Original ASM1	Lu ASM1	CUESID Subspace	ARX	ARMAX	State space (pem)	State space (n4sid)
Aquabio main MBR plant - sampling programme	Good fit	Poor fit	Good fit	Very poor fit	Reasonable fit	Reasonable fit	Failed to run	No fit	No fit
Aquabio pilot MBR plant - sampling programme	-	-	-	-	Reasonable fit	Poor fit	Failed to run	Poor fit	Failed to run
Fictitious COST Benchmark model with temp. MIMO	-	-	-	-	Reasonable fit	Good fit	Failed to run	Very poor fit	Poor fit
Fictitious COST Benchmark model with temp. MISO	-	-	-	-	Reasonable fit	Good fit	Good fit	Poor fit	No fit
Combining model types using Aquabio main and pilot data	-	-	-	Reasonable prediction	Reasonable fit	-	-	-	-

Table 6.2: Answering the research questions - summary of comparison of model types

6.1.4 Summary of novel research outcomes

This study managed to produce several models of the phenomenological and behavioural type to separately describe the membrane filtration process and the Activated Sludge processes in the bioreactor of a MBR system. The main novel aspect of this research work is that the use of behavioural models especially of the subspace variety has never been carried out before for a MBR system, either for the membrane fouling mechanisms or the biological processes in the bioreactor. Additionally, the creation of a thorough "Model Conceptualisation Procedure" has not been produced before for a MBR system.

On a related note, it is unlikely that an integrated behavioural model could be fully developed which gave the same degree of accuracy as its counterpart phenomenological version. One difficulty would be in trying to integrate the two different input-output model structures which may not have any relationship to each other particular in terms of the different time constants for the individual processes. For the phenomenological models this is not a concern as the mechanistic nature of the processes mean that relationships between different time constants for various processes are already known or easy to establish.

It is anticipated that the best and easiest way of fully expressing a MBR system in modelling terms, whether integrated or not, would largely depend on the the objectives of the modelling exercise:

Objective 1. – *Checking optimal biological performance.* The model would be used to run the plant in an optimal manner to gain the healthiest Activated Sludge with properties of reduced liquor foulability. This would produce excellent effluent quality, limit foaming events (which are still a problem in MBR systems), and indirectly maximise the generated flux throughput. It appears this could be accomplished by firstly using an unaltered conventional Activated Sludge model with book values for stoichiometry, and a few alterations to some kinetic parameters to cater for a MBR scenario. This would predict effluent quality levels and mixed liquor properties. The standard ASM1 or ASM3 would be recommended. This would then be judiciously used with a separate behavioural input-output model structure to predict the **SMP** states responsible for membrane fouling. These predicted **SMP** values would be compared against historically measured **SMP** levels and a saving could be made on this complex and frequent additional testing. These models would be both based on long time constants for the processes as they would use mainly off-line data.

Objective 2. – *Optimal plant operation and control.* It is anticipated that a behavioural input-output membrane fouling model would be the quickest and easiest model that could be used to check operational ranges for state and process variables, and to be used in control loops (such as in a MPC algorithm) in order to reduce energy usage whilst maximising membrane permeability. It would be used to achieve optimal permeate throughput and to predict the generalised trend for the drop in membrane permeability. However this model would not be capable of predicting specific membrane clogging events. Also the model would only be applicable for a very narrow operating range particularly if it was used with a linear autoregressive model structure. This model would need to be re-calibrated frequently with further on-line data. This re-calibration step could be automated to allow real time control. This model would be based on short time constants for the processes as it would use mainly on-line data.

Objective 3. – *Investigating optimal membrane performance.* A fully calibrated phenomenological membrane fouling model would be the best one to use in order to measure the membrane under more rigourous or non-standard operating conditions. This model would have to be site specific in terms of plant layout and membrane configuration. There obviously would be an overlap between these competing objectives, and the different model outputs could be used to assist in reaching these alternative objectives. However, much more research work is required to confirm these assertions.

6.2 *Proposed future work*

The outcomes of this research study can be usefully applied in several areas described below. Some of these areas involve direct follow-up on research and development work carried out here, while others are in related fields.

1. *Further phenomenological model development* - Both the membrane fouling and Activated Sludge models developed here can be further tested and expanded to improve their accuracy and precision.
2. *Further behavioural model development* - To improve upon their accuracy and precision, different input-output structures can be tested particularly new non-linear forms.
3. *Continuation of R&D work on Aquabio pilot plant* - Significant work is still required to measure the full capabilities of this plant, as well as using it to derive further practical data sets to continue research into membrane permeability issues.
4. *MBR Benchmark development* - In order to effectively measure in a truly independent fashion the possible gains in operational efficiency reported by researchers, a globally applicable MBR Benchmark is required. This would be analogous to the existing COST Benchmark simulation model which is used for conventional Activated Sludge WWTP. Incidentally this is a novel idea that has not been proposed before.
5. *Integrated MBR model development* - The ultimate aim of this initial research would be to create a truly integrated MBR model that included all the major Activated Sludge biological mechanisms involved in membrane fouling.
6. *MBR plant control strategy development based upon MPC* - One of the key objectives of any MBR system model is improved operation and control of plant. This can be achieved by using standard control methods (i.e. on/off control, step-control, PI control, etc.,) or alternatively by using modern MPC control algorithms.
7. *Commercialisation of MBR research outputs* - The outcomes of this research study, namely the developed models, could be commercialised into a MBR software package that would be sold to prospect Client's wishing to design and operate their plant more effectively.

6.2.1 Further phenomenological model development

Since there was a significant amount of work still remaining unfinished for both the biological models and membrane fouling models, the overall phenomenological modelling work can be continued in order to produce improved model versions. In terms of the membrane fouling model the following can be continued:

- Even though the model proved reasonably accurate for some plant layouts and liquors, the model should be tested on several different plant layouts with larger more diverse data sets particularly with extended flux stepping tests. The optimal model parameter sets from these simulation runs can then be compared against the existing ones to see if there are any correlations.
- Using different plant layouts, such as for a submerged MBR system, would mean that a modification to include for membrane scour by coarse bubble aeration would need to be developed. This would need to be optimised for slug-flow.
- A dynamic backflush procedure needs to be developed and tested for this model version. Again the kinetic parameter values from this altered model can be compared with the existing model's values.
- Using the same data set, a comparison needs to be made with other existing membrane fouling models such as the ones proposed by Liang et al. (2006) or by Ognier et al. (2004). This would test the modified Duclos-Orsello model's accuracy against other common models in this area.

In terms of the Activated Sludge models the following can be continued:

- Both the modified Oliveira ASM3 model and the modified Lu ASM1 model should be tested on several different plant layouts with larger more diverse data sets that particularly contain influent and bioreactor **SMP** concentrations. The optimal kinetic parameter sets from these simulation runs can then be compared against the existing ones to see if there is any correlation.
- A more complex simulation based on both **SMP** production and usage and EPS release and degradation can be incorporated into the existing processes for both models. This would be followed by an extensive model testing phase. These new process interactions can be based on the initial work carried out by Laspidou and Rittmann (2002) on EPS release and degradation. This should give a clearer mechanistic model that matches more closely the real biochemical conversion mechanisms that take place in the bioreactor.
- A modified version of an ASM2 or an ASM2d biological Phosphorous uptake and release model can be developed based upon similar process equations found in the Oliveira ASM3 model and in the Lu ASM1 model. These new models would need extensive testing.
- An alternative non-IWA model can be developed such as the Laspidou and Rittmann (2002) model albeit with a reduced set of process equations. This alternative model would only focus on the **SMP** components that are responsible for fouling while other less critical state components would be entirely omitted.

6.2.2 Further behavioural model development

Further testing is required of the conventional phenomenological Activated Sludge model in combination with a limited input-output behavioural model structure for **SMP** components only. This should be carried out for both the ASM1 and ASM3 models, and with different **SMP** components (i.e. UAP, BAP, MP, etc.) in the input-output model structure.

Continuation of this behavioural modelling work for both the membrane fouling and biological model versions could be expanded to include other autoregressive model structures not tested as yet. This could include the ARIMA model structures as well as other general non-linear approaches that already are included in Matlab's System Identification Toolbox©. Both the membrane fouling and biological model versions need to be further tested on different plant layouts and extended data sets. This could also include data taken from submerged industrial MBR plant, municipal MBR plant and also from more conventional WWTP both industrial and municipal.

This further behavioural model development work can also include trying out of other input-output black box approaches such as ANN methods and FNN methods for a MBR system using the existing "Model Conceptualization Procedure" to underpin this new model development work.

References

Abusam, A. A. 2001. Development of a benchmarking methodology for evaluating oxidation ditch control strategies. Ph.D. thesis, Wageningen University, Netherlands. 131

Agrimet. 2004. The pacific northwest cooperative agricultural weather network. URL `http://www.usbr.gov/pn/agrimet/webagdayread`. 130, 132

Akyurek, Evrim, Mehmet Yuceer, Ilknur Atasoy, Ridvan Berber. 2009. Comparison of control strategies for dissolved oxygen control in activated sludge wastewater treatment process. Jacek Jezowski, Jan Thullie, eds., *19th European Symposium on Computer Aided Process Engineering*, vol. Volume 26. Elsevier, 1197–1201. URL `http://www.sciencedirect.com/science/article/B8G5G-4WKSB5W-73/2/e9eb77d0815dc2e6f7f02e286607b054`. 48

Arabi, Sara, George Nakhla. 2008. Impact of calcium on the membrane fouling in membrane bioreactors. *Journal of Membrane Science* **314**(1-2) 134–142. URL `http://www.sciencedirect.com/science/article/B6TGK-4RRFN9G-2/2/d293dc3344efcaee8dd92a6d159e3f58`. 30

Baker, R. W. 1991. Membrane and module preparation. R. W. Baker, E. L. Cussler, W. Eykamp, W. J. Koros, R. L. Riley, H. Strathmann, eds., *Membrane separation systems: Recent developments and future directions*. Noyes Data Corporation, New Jersey, USA. 10

Baker, R. W. 2004. *Membrane technology and applications*. Wiley and Sons Ltd., NY, USA. 9, 10

Baranao, P.A., E.R. Hall. 2004. Modelling carbon oxidation in pulp mill activated sludge systems: calibration of activated sludge model no. 3. *Wat. Sci. & Tech.* **50(3)** 1–10. 214, 217

Barker, D. J., D. C. Stuckey. 1999. A review of soluble microbial products (smp) in wastewater treatment systems. *Wat. Res.* **33** 3063–3082. 29, 33, 208

Berthouex, P. M., George E. Box. 1996. Time series models for forecasting wastewater treatment plant performance. *Water Research* **30**(8) 1865–1875. URL `http://www.sciencedirect.com/science/article/B6V73-3VW7SB5-G/2/23959bcd6890c112a75e5156d4290a96`. 45

Berthouex, P. M., W. G. Hunter, Lars Pallesen, C. Y. Shih. 1978. Dynamic behavior of an activated sludge plant. *Water Research* **12**(11) 957–972. URL `http://www.sciencedirect.com/science/article/B6V73-48CFS3V-RV/2/cdd432b53206a7ff240011c30177c271`. 45

Blocher, C., M. Noronha, L. Funfrocken, J. Dorda, V. Mavrov, H. D. Janke, H. Chmiel. 2002. Recycling of spent process water in the food industry by an integrated process of biological treatment and membrane separation. *Desalination* **144(1-3)** 143–150. 12

Box, George E.P., Gwillym M. Jenkins, Gregory C. Reinsel. 2008. *Times series analysis: forecasting and control*. Wiley, Hoboken, New Jersey. 25, 27

Brdjanovic, D., M.C.M. van Loosdrecht, P. Versteeg, C.M. Hooijmans, G.J. Alaerts, J.J. Heijnen. 2000. Modeling cod, n and p removal in a full-scale wwtp haarlem waarderpolder. *Wat. Res.* **34(3)** 846–858. 216

Broeckmann, A., J. Busch, T. Wintgens, W. Marquardt. 2006. Modeling of pore blocking and cake layer formation in membrane filtration for wastewater treatment. *Desalination* **189**(1-3) 97–109. URL `http://www.sciencedirect.com/science/article/B6TFX-4J9X4KP-G/2/907489fbda94cc70cdcbd466e8ac337f`. 29, 36, 37, 40

Busch, Jan, Andreas Cruse, Wolfgang Marquardt. 2007. Modeling submerged hollow-fiber membrane filtration for wastewater treatment. *Journal of Membrane Science* **288**(1-2) 94–111. URL `http://www.sciencedirect.com/science/article/B6TGK-4MCDK0H-2/2/79e86069ae3a9b470afde7a05e7104ed`. 37, 40

Chaize, S., A. Huyard. 1991. Membrane bioreactors on domestic wastewater treatment sludge production and modeling approach. *Wat. Sci. Tech.* **23** 1591–1600. 41

Chang, In-Soung, Simon J. Judd. 2002. Air sparging of a submerged mbr for municipal wastewater treatment. *Process Biochemistry* **37**(8) 915–920. URL `http://www.sciencedirect.com/science/article/B6THB-44W2JRV-C/2/417189526a07e143c28548f52bd358cf`. 82

Chang, S., T.G. Fane, T.D. Waite. 2005. Effect of coagulation within the cakelayer on fouling transitions with dead-end hollow fiber membranes. *Proceedings of the International Congress on Membranes and Membrane Processes (ICOM)*. Seoul, Korea. 36

Chen, H., J.M. Maciejowski. 1999. A new subspace identification method for bilinear systems. Technical Report CUED/F-INFENG/TR.357, University of Cambridge, UK. 70, 176, 184

Cho, B.D., A.G. Fane. 2002. Fouling transients in nominally sub-critical flux operation of a membrane bioreactor. *J.Membr. Sci.* **209** 391–403. 36

Choi, H., K. Zhang, D.D. Dionysiou, D.B. Oerther, G.A. Sorial. 2005a. Effect of permeate flux and tangential flow on membrane fouling for wastewater treatment. *Sep. Purif. Technol.* **45** 68–78. 30

Choi, Hyeok, Kai Zhang, Dionysios D. Dionysiou, Daniel B. Oerther, George A. Sorial. 2005b. Influence of cross-flow velocity on membrane performance during filtration of biological suspension. *Journal of Membrane Science* **248**(1-2) 189–199. URL `http://www.sciencedirect.com/science/article/B6TGK-4DTKP0V-6/2/e4e8ed0aba8daefe58d4c89e965e1f5a`. 38, 40

Choi, Jung-Goo, Tae-Hyun Bae, Jung-Hak Kim, Tae-Moon Tak, A. A. Randall. 2002. The behavior of membrane fouling initiation on the crossflow membrane bioreactor system. *Journal of Membrane Science* **203**(1-2) 103–113. URL `http://www.sciencedirect.com/science/article/B6TGK-44VX084-T/2/d99cbdc8b762dbb5bd711cc9c0b89d10`. 31

Christodoulatos, Christos, David A. Vaccari. 1993. Correlations of performance for activated sludge using multiple regression with autocorrelation. *Water Research* **27**(1)

51–62. URL http://www.sciencedirect.com/science/article/B6V73-48BDRVK-X2/2/0acf4536cb8e793a844a75e8cdfbbed0. 45

Copp, J. B. 1999. Development of standardised influent files for the evaluation of activated sludge control strategies. internal report., IAWQ Scientific and Technical Report Task Group: Respirometry in Control of the Activated Sludge Process. 6, 51, 75, 130, 210, 217, 233

Copp, J. B. 2000. Defining a simulation benchmark for control strategies. *Water 21* **April** 44–49. 6, 51, 75, 130, 210, 217, 233

Debelak, Kenneth A., Carl A. Sims. 1981. Stochastic modeling of an industrial activated sludge process. *Water Research* **15**(10) 1173–1183. URL http://www.sciencedirect.com/science/article/B6V73-48BC69K-3H/2/3c47c467769c7d84cad66b9e1d7b0af8. 45

Dellana, Scott A., David West. 2009. Predictive modeling for wastewater applications: Linear and nonlinear approaches. *Environmental Modelling & Software* **24** 96–106. 24, 47

Di Bella, Gaetano, Giorgio Mannina, Gaspare Viviani. 2008. An integrated model for physical-biological wastewater organic removal in a submerged membrane bioreactor: Model development and parameter estimation. *Journal of Membrane Science* **322**(1) 1–12. URL http://www.sciencedirect.com/science/article/B6TGK-4SM1TCB-5/2/807c50ae8bdf55e5c9795acae2cbbdb2. 43, 44

Dixon, A., D. Butler, A. Fewkes, M. Robinson. 1999. Measurement and modelling of quality changes in stored untreated grey water. *Urban Water* **Vol.1** 293–306. 131

Drew, D. A., J. A. Schonberg, G. Belfort. 1991. Lateral inertial migration of a small sphere in fast laminar flow through a membrane duct. *Chem. Eng. Sci.* **46** 3219–3244. 20

Drews, A., M. Vocks, U. Bracklow, V. Iversen, M. Kraume. 2008. Does fouling in mbrs depend on smp? *Desalination* **231**(1-3) 141 – 149. doi:DOI:10.1016/j.desal.2007.11.042. URL http://www.sciencedirect.com/science/article/B6TFX-4T84F90-P/2/a9fd91171bfeda481acfddd57ccd406e. Selected Papers Presented at the 4th International IWA Conference on Membranes for Water and Wastewater Treatment, 15-17 May 2007, Harrogate, UK. Guest Edited by Simon Judd; and Papers Presented at the International Workshop on Membranes and Solid-Liquid Separation Processes, 11 July 2007, INSA, Toulouse, France. Guest edited by Saravanamuthu Vigneswaran and Jaya Kandasamy. 14, 29, 30, 152

Drews, Anja, Harvey Arellano-Garcia, Jan Schöneberger, Jana Schaller, Matthias Kraume, Günter Wozny. 2007a. Improving the efficiency of membrane bioreactors by a novel model-based control of membrane filtration. Valentin Plesu, Paul Serban Agachi, eds., *17th European Symposium on Computer Aided Process Engineering*, vol. Volume 24. Elsevier, 345–350. URL http://www.sciencedirect.com/science/article/B8G5G-4RWNRMW-24/2/0c4e4c3d6b8277b65c88d72219b12ec1. 143

Drews, Anja, Chung-Hak Lee, Matthias Kraume. 2006. Membrane fouling - a review on the role of eps. *Desalination* **200**(1-3) 186–188. URL http://www.sciencedirect.com/science/article/B6TFX-4KKPCN1-2M/2/225421b1f92e0b389bea5f0e391f580f. 203

Drews, Anja, Jan Mante, Vera Iversen, Martin Vocks, Boris Lesjean, Matthias Kraume. 2007b. Impact of ambient conditions on smp elimination and rejection in mbrs. *Water Research* **41**(17) 3850

– 3858. doi:DOI:10.1016/j.watres.2007.05.046. URL http://www.sciencedirect.com/science/article/B6V73-4NWKCM4-1/2/f2cd3013f47ee9b23bb18efc0553b72e. Membranes. 203, 211

Drioli, E., L. Giorno. 1999. *Biocatalytic membrane reactors*. Taylor and Francis Ltd., London, UK. 9, 10

Duclos-Orsello, Chase, Weiyi Li, Chia-Chi Ho. 2006. A three mechanism model to describe fouling of microfiltration membranes. *Journal of Membrane Science* **280**(1-2) 856 – 866. doi:DOI:10.1016/j.memsci.2006.03.005. URL http://www.sciencedirect.com/science/article/B6TGK-4JFH6T1-1/2/4268a5846d6747e11b830133eed0b886. 4, 38, 39, 40, 136, 137, 138, 139, 142, 143, 144, 172, 201, 210, 244, 247

EUROMBRA. 2007. D13 - characterisation and comparison of monitoring techniques applied to the selected mbrs operated by involved partners. *Membrane bioreactor technology (MBR) with an EU perspective for advanced municipal wastewater treatment strategies for the 21st century*. EC 6th Framework Programme, IBET - Instituto de Biological Experimental e Tecnológica. 15, 29

Eykamp, W. 1995. Microfiltration and ultrafiltration. R. D. Noble, S. A. Stern, eds., *Membrane separations technology: Principles and applications*, *Membrane science and technology series*, vol. Vol. 2. Elsevier, Amsterdam, The Netherlands. 10

Fenu, A., G. Guglielmi, J. Jimenez, M. Sperandio, D. Saroj, B. Lesjean, C. Brepols, C. Thoeye, I . Nopens. 2010. Activated sludge model (asm) based modelling of membrane bioreactor (mbr) processes: A critical review with special regard to mbr specificities. *Wat. Res.* **Accepted Manuscript**. 41

Freixo, M. R., M. N. de Pinho. 2002. Enzymatic hydrolysis of beechwood xylan in a membrane reactor. *Desalination* **149(1-3)** 237–242. 12

Futselaar, Harry, Henk Schonewille, Dick de Vente, Lute Broens. 2007. Norit airlift mbr: side-stream system for municipal waste water treatment. *Desalination* **204**(1-3) 1–7. URL http://www.sciencedirect.com/science/article/B6TFX-4MY8797-3/2/2110df342a4e0b99ce54ceb5ae9ef0b0. 79, 82

Gehlert, Gunther, Mariati Abdulkadir, Jan Fuhrmann, Jobst Hapke. 2005. Dynamic modeling of an ultrafiltration module for use in a membrane bioreactor. *Journal of Membrane Science* **248**(1-2) 63–71. URL http://www.sciencedirect.com/science/article/B6TGK-4DS6VTW-2/2/530f882b477439a512161a38ff6bc7ca. 37, 40

Gehlert, Gunther, Jobst Hapke. 2003. Rigorous approach to modeling of a continuous aerobic membrane bioreactor. *Eng. Life. Sci.* **3(7)** 292–298. 205

Gekas, V. 1986. Terminology for pressure driven membrane operations. *Desalination* **68** 77–92. 8

Gernaey, Krist V., Mark C.M. van Loosdrecht, Mogens Henze, Morten Lind, Sten B. Jørgensen. 2004. Activated sludge wastewater treatment plant modelling and simulation: state of the art. *Environmental Modelling & Software* **19** 763Ű783. 24

Grelier, P., S. Rosenberger, A. Tazi-Pain. 2006. Influence of sludge retention time on membrane bioreactor hydraulic performance. *Desalination* **192(1-3)** 10–17. 29

Guglielmi, Giuseppe, Daniele Chiarani, Devendra Prakash Saroj, Gianni Andreottola. 2010. Sludge filterability and dewaterability in a membrane bioreactor for municipal wastewater treatment. *Desalina-*

tion **250**(2) 660–665. URL http://www.sciencedirect.com/science/article/B6TFX-4XG3D6G-B/2/574e0d5a105301c8cb479ca107116484. 32

Gujer, W., M. Henze, T. Mino, M. van Loosdrecht. 1999. Activated sludge model no. 3. *Wat. Sci. Tech.* **39(1)** 183–193. 44, 203, 205, 214, 223

Henze, M., C. P. L. Jr. Grady, W. Gujer, G. v. R. Marais, T. Matsuo. 1987. Activated sludge model no. 1. 23, 42, 44, 202, 205, 214

Hermanowicz, S. W. 2004. Membrane filtration of biological solids: a unified framework and its applications to mbr. *Proceedings of the Water Environment-Membrane Technology Conference*. Seoul, Korea. 36, 39

Hermia, J. 1982. Constant pressure blocking filtration law: application to power law non-newtonian fluids. *Trans. Inst. Chem. Eng.* **60:** 183. 19, 38, 136, 247

Ho, Chia-Chi, Andrew L. Zydney. 2000. A combined pore blockage and cake filtration model for protein fouling during microfiltration. *Journal of Colloid and Interface Science* **232**(2) 389 – 399. doi:DOI:10.1006/jcis.2000.7231. URL http://www.sciencedirect.com/science/article/B6WHR-45FC66Y-T/2/00615fe08267bc950dc4659f19c0cbd3. 38, 40, 136

Ho, Chia-Chi, Andrew L. Zydney, Wei Yuan. 2003. Chapter 2 fouling phenomena during microfiltration: Effects of pore blockage, cake filtration, and membrane morphology. Dibakar Bhattacharyya, D. Allan Butterfield, eds., *New Insights into Membrane Science and Technology: Polymeric and Biofunctional Membranes*, *Membrane Science and Technology*, vol. 8. Elsevier, 27 – 44. doi:DOI:10.1016/S0927-5193(03)80005-0. URL http://www.sciencedirect.com/science/article/B8G6W-4NRK355-5/2/c04e896246570045535be37dc53cac17. 14

Hoa, P.T., L. Nair, C. Visvanathan. 2003. The effect of nutrients on extracellular polymeric substance production and its influence on sludge properties. *Water SA* **29(4)** 437–442. 29

Hoffmann, E. J. 2003. *Membrane separation technology: Single-stage, multistage and differential permeation*. Gulf Professional Publishing (Elsevier), NY, USA. 8

Honga, Yoon-Seok, Rao Bhamidimarri. 2003. Evolutionary self-organising modelling of a municipal wastewater treatment plant. *Water Research* **37** 1199Ũ1212. 47

Hsieh, K.M., G.A. Murgel, L.W. Lion, M.L. Shuler. 1994. Interactions of microbial biofilms with toxic trace metals: 1. observation and modeling of cell growth, attachment, and production of extracellular polymer. *Biotech. Bioeng.* **44** 219–231. 29

Huang, Ming-zhi, Jin-quan Wan, Yong-wen Ma, Wei-jiang Li, Xiao-fei Sun, Yan Wan. 2010. A fast predicting neural fuzzy model for on-line estimation of nutrient dynamics in an anoxic/oxic process. *Bioresource Technology* **101**(6) 1642–1651. URL http://www.sciencedirect.com/science/article/B6V24-4XJ13PS-1/2/898146a1bc4f63a1ca4baa1bd9d1941b. 46

Huang, R. Y. M. 1991. Pervaporation membrane separation processes. *Membrane science and technology series*, vol. Vol.1. Elsevier, Amsterdam, The Netherlands. 9

Hulsbeek, J. J. W., J. Kruit, P. J. Roeleveld, M. C. M. van Loosdrecht. 2002. A practical protocol for dynamic modelling of activated sludge systems. *Wat. Sci. Tech.* **45(6)** 127–136. 203, 214, 216, 218

Jang, Namjung, Xianghao Ren, Jaeweon Cho, In S. Kim. 2006a. Steady-state modeling of bio-fouling potentials with respect to the biological kinetics in the submerged membrane bioreactor (smbr). *Journal of Membrane Science* **284**(1-2) 352–360. URL `http://www.sciencedirect.com/science/article/B6TGK-4KKNDW4-5/2/f1044157479c01af351fc1be02c65c15`. 42

Jang, Namjung, Xianghao Ren, Jaeweon Cho, In S. Kim. 2006b. Steady-state modeling of bio-fouling potentials with respect to the biological kinetics in the submerged membrane bioreactor (smbr). *Journal of membrane science* **284** 352–360. 205

Janga, Namjung, Xianghao Ren, Geontae Kim, Changhyo Ahn, Jaeweon Cho, In S. Kim. 2007. Characteristics of soluble microbial products and extracellular polymeric substances in the membrane bioreactor for water reuse. *Desalination* **202**(1-3) 90–98. URL `http://www.sciencedirect.com/science/article/B6TFX-4MG7BS6-H/2/2dc2c83b7b652ebcbe6e10663324a3db`. 42

Janus, T., P. Paul. 2009. Final project presentations at quarterly steering committee meeting. *Unpublished work as part of TSB Project No. TP/3/DSM/6/I/15123*. De Montfort University, Queens Building, The Gateway, Leicester. 89, 122, 206, 211

Jeong, Tae-Young, Gi-Cheol Cha, Ik-Keun Yoo, Dong-Jin Kim. 2007. Characteristics of bio-fouling in a submerged mbr. *Desalination* **207**(1-3) 107–113. URL `http://www.sciencedirect.com/science/article/B6TFX-4N9NM3D-F/2/3ededb4391ae0d98f49cf3b1383dd54b`. 43

Jeppson, U. 1996. Modelling aspects of wastewater treatment processes. Ph.D. thesis, Lund University. 21, 131

Jiang, Tao, Silvie Myngheer, Dirk J.W. De Pauw, Henri Spanjers, Ingmar Nopens, Maria D. Kennedy, Gary Amy, Peter A. Vanrolleghem. 2008. Modelling the production and degradation of soluble microbial products (smp) in membrane bioreactors (mbr). *Water Research* **42**(20) 4955–4964. URL `http://www.sciencedirect.com/science/article/B6V73-4TN82DS-1/2/51f58ce5ec66fca2fc4b4fe5341faf6b`. 42, 43, 208

Jimenez, Julie, Patricia Grelier, Jens Meinhold, Annie Tazi-Pain. 2010. Biological modelling of mbr and impact of primary sedimentation. *Desalination* **250**(2) 562–567. URL `http://www.sciencedirect.com/science/article/B6TFX-4XCY403-F/2/4c3caf39c5d37bb853ca7ab88a1be10e`. 41

Judd, Simon, Claire Judd. 2006. Case studies. Simon Judd, Claire Judd, eds., *The MBR Book*. Elsevier Science, Oxford, 207 – 272. doi:DOI:10.1016/B978-185617481-7/50007-6. URL `http://www.sciencedirect.com/science/article/B85JB-4P6V93K-B/2/a8490d21547a7180d4c9234dd28d9db6`. 15, 29

Kim, Jeonghwan, Francis A. DiGiano. 2009. Fouling models for low-pressure membrane systems. *Separation and Purification Technology* **68**(3) 293–304. URL `http://www.sciencedirect.com/science/article/B6THJ-4WC119P-1/2/90aa0c3a50e6f8eca2ed8eb5b201a8d1`. 36

Kim, Jun-Young, In-Soung Chang, Hun-Hwee Park, Chang-Yong Kim, Jong-Bum Kim, Ji-Hyun Oh. 2008. New configuration of a membrane bioreactor for effective control of membrane fouling and nutrients

removal in wastewater treatment. *Desalination* **230**(1-3) 153–161. URL http://www.sciencedirect.com/science/article/B6TFX-4T553P3-J/2/46fb2a2552295f6396861f1357691794. 31

Knutsen, J. S., R. H. Davis. 2004. Cellulase retention and sugar removal by membrane ultrafiltration during lignocellulosic biomass hydrolysis. *Appl. Biochem. Biotech.* **114(1-3)** 585–599. 12

Koch, K. M., K. J. Habermann. 2005. *Membrane structures: the fifth building material*. Prestel Publishing, London, UK. 8

Kosvintsev, S., I. Cumming, R. Holdich, D. Lloyd, V. Starov. 2003. Sieve mechanism of microfiltration separation. *Colloids and Surfaces A: Physicochemical and Engineering Aspects* **230**(1-3) 167–182. URL http://www.sciencedirect.com/science/article/B6TFR-4B3M4HB-3/2/b8132061d23179ee878e0f56d88b9a36. 36, 40

Kosvintsev, S., R. G. Holdich, I. W. Cumming, V. M. Starov. 2002. Modelling of dead-end microfiltration with pore blocking and cake formation. *Journal of Membrane Science* **208**(1-2) 181–192. URL http://www.sciencedirect.com/science/article/B6TGK-462BHB7-1/2/326ccb9bffa27183c377abccbb6dcf2e. 40

Laspidou, Chrysi S., Bruce E. Rittmann. 2002. A unified theory for extracellular polymeric substances, soluble microbial products, and active and inert biomass. *Water Research* **36** 2711Ű2720. 42, 205, 257

Le-Clech, Pierre, Vicki Chen, Tony A.G. Fane. 2006. Fouling in membrane bioreactors used in wastewater treatment. *Journal of Membrane Science* **284**(1-2) 17 – 53. doi:DOI:10.1016/j.memsci.2006.08.019. URL http://www.sciencedirect.com/science/article/B6TGK-4KR4C05-1/2/25aaa253506e24829d7d8ea64446260b. 33

Lee, K. S., P. J. Lin, K. Fangchiang, J. S. Chang. 2007. Continuous hydrogen production by anaerobic mixed microflora using a hollow-fiber microfiltration membrane bioreactor. *Int. J. Hydrogen Energ.* **32(8)** 950–957. 12

Lee, Yonghun, Jinwoo Cho, Youngwoo Seo, Jae Woo Lee, Kyu-Hong Ahn. 2002. Modeling of submerged membrane bioreactor process for wastewater treatment. *Desalination* **146**(1-3) 451–457. URL http://www.sciencedirect.com/science/article/B6TFX-46WM7M0-7G/2/0737e6225616d9fddc473b89efe323e8. 37, 40, 43

Lesjean, B., S. Rosenberger, C. Laabs, M. Jekel, R. Gnirss, G. Amy. 2004. Correlation between membrane fouling and soluble/colloidal organic substances in membrane bioreactors for municipal wastewater treatment. *Water Environment Membrane Technology*. Seoul. 29

Leudeking, R., E. L. Piret. 1959. A kinetic study of lactic acid fermentation: Batch process at controlled ph. *J. Biochem. Microbiol. Technol. Engng.* **1** 393–412. 207, 208

Li, K. 2007. *Ceramic membranes for separation and reaction*. Wiley and Sons Ltd., Wiltshire, UK. 8

Li, S. L., K. S. Chou, J. Y. Lin, H. W. Yen, I. M. Chu. 1996. Study on the microfiltration of escherichia coli-containing fermentation broth by a ceramic membrane filter. *J. Membrane Sci.* **110** 203–210. 12

Liang, Shuang, Lianfa Song, Guihe Tao, Kiran Arun Kekre, Harry Seah. 2006. A modeling study of fouling

development in membrane bioreactors for wastewater treatment. *Water Environ. Res.* **78(8)** 857–863. 40, 256

Ljung, L. 1999. *System Identification: Theory for the User*. Prentice Hall. 25, 249

Loeb, S., S. Sourirajan. 1963. Sea water demineralization by means of an osmotic membrane. *Adv. Chem. Ser.* **38** 117–123. 8

Lu, S.G., T. Imai, M. Ukita, M. Sekine, T. Higuchi, M. Fuka-gawa. 2001. A model for membrane bioreactor process based on the concept of formation and degradation of soluble microbial products. *Wat. Res.* **35(8)** 2038–2048. 42, 44, 205, 207, 208, 210, 245

Makinia, J., S. A. Well. 2000. A general model of the activated sludge reactor with dispersive flow Ű 1. model development and parameter estimation. *Wat. Res.* **16(34)** 3987–3996. 131

Meijer, S.C.F., M.C.M. van Loosdrecht, J.J. Heijnen. 2001. Metabolic modelling of full-scale biological nitrogen and phosphorus removing wwtp's. *Wat. Res.* **35(11)** 2711–2723. 212, 214, 218

Melin, T., B. Jefferson, D. Bixio, C. Thoeye, W. De Wilde, J. De Koning, J. van der Graaf, T. Wintgens. 2006. Membrane bioreactor technology for wastewater treatment and reuse. *Desalination* **187**(1-3) 271–282. URL `http://www.sciencedirect.com/science/article/B6TFX-4J444DP-10/2/9966a783f1d346fb3a1b66388eac5a11`. 84

Meng, F., F. Yang. 2007. Fouling mechanisms of deflocculated sludge, normal sludge, and bulking sludge in membrane bioreactor. *J. Membr. Sci.* **305** 48–56. 30, 39

Ömer Faruk, Durdu. 2010. A hybrid neural network and arima model for water quality time series prediction. *Engineering Applications of Artificial Intelligence* **23**(4) 586–594. URL `http://www.sciencedirect.com/science/article/B6V2M-4XJN4R2-2/2/5b0ad8a29118e9a7738e7c8db902e050`. 47

Mjalli, Farouq S., S. Al-Asheh, H.E. Alfadala. 2007. Use of artificial neural network black-box modeling for the prediction of wastewater treatment plants performance. *Journal of Environmental Management* **83** 329Ű338. 46

Mugnier, N., J. A. Howell, M. Ruf. 2000. Optimisation of a backflush sequence for zeolite microfiltration. *Journal of Membrane Science* **175(2)** 149–161. 30

Mulder, M. 1996. *Basic principles of membrane technology*. Kluwer Academic Publishers, Dordrecht, The Netherlands. 8, 10

Munoz, Carlos, Daniel Rojas, Oscar Candia, Laura Azocar, Cristian Bornhardt, Christian Antileo. 2009. Supervisory control system to enhance partial nitrification in an activated sludge reactor. *Chemical Engineering Journal* **145** 453Ű460. 48

Nancy, University of. 2010. Cost 682/624 action website. URL `http://www.ensic.u-nancy.fr/COSTWWTP`. 130

Ng, Aileen N.L., Albert S. Kim. 2007. A mini-review of modeling studies on membrane bioreactor (mbr) treatment for municipal wastewaters. *Desalination* **212**(1-3) 261–

281. URL http://www.sciencedirect.com/science/article/B6TFX-4NX9C8D-Y/2/d1e39b2b929541185311b092e9993013. 33, 36, 41

Ni, Bing-Jie, Fang Fang, Wen-Ming Xie, Min Sun, Guo-Ping Sheng, Wei-Hua Li, Han-Qing Yu. 2009. Characterization of extracellular polymeric substances produced by mixed microorganisms in activated sludge with gel-permeating chromatography, excitation-emission matrix fluorescence spectroscopy measurement and kinetic modeling. *Water Research* **43**(5) 1350–1358. URL http://www.sciencedirect.com/science/article/B6V73-4V70N89-3/2/e19d179486e020bf8603144065ab9e70. 43

Nielsen, P. H., A. Jahn. 1999. *Microbial Extracellular Polymeric Substances*. Springer, Berlin. 29

Nielsen, P.H., A. Jahn, R. Palmgren. 1997. Conceptual model for production and composition of exopolymers in biofilms. *Wat. Sci. Tech.* **36** 11–19. 29

Novotny, Vladimir, Andrea G. Capodaglio. 1992. Strategy of stochastic real-time control of wastewater treatment plants. *ISA Transactions* **31**(1) 73–85. URL http://www.sciencedirect.com/science/article/B6V3P-47XN4SG-C/2/c7e48c587b1e1b0cd00334e44013b2ee. 48

Nuengjamnong, Chackrit, Ji Hyang Kweon, Jinwoo Cho, Chongrak Polprasert, Kyu-Hong Ahn. 2005. Membrane fouling caused by extracellular polymeric substances during microfiltration processes. *Desalination* **179**(1-3) 117–124. URL http://www.sciencedirect.com/science/article/B6TFX-4HBRP0N-F/2/f1b1f794de433c568031547cae33dd54. 29, 30, 31

Ognier, S., C. Wisniewski, A. Grasmick. 2004. Membrane bioreactor fouling in sub-critical filtration conditions: a local critical flux concept. *Journal of Membrane Science* **229**(1-2) 171–177. URL http://www.sciencedirect.com/science/article/B6TGK-4B9D83R-3/2/3fc89edc6a7d4156f3934cfbe7334e93. 34, 37, 38, 40, 256

Oliveira-Esquerre, K. P., H. Narita, N. Yamato, N. Funamizu, Y. Watanabe. 2005. Modeling of a conventional mbr for wastewater treatment. *21st Center of Excellence Program Publication*. Department of Urban and Environmental Engineering, Hokkaido University. 42, 44, 205, 206, 209, 210, 245

Olsson, Gustaf, Bob Newell. 1999. *Wastewater treatment systems: modelling, diagnosis and control*. IWA Publishing. 24

Paul, P. 2006. Improving the design and efficiency of mbr plant by using modelling and simulation. *"Biofouling in membrane systems" EUROMBRA Project Seminar, MBR-Network Programme, Norwegian University of Science & Technology*. 43

Paul, P., S. Prescott, B. Ulanicki. 2005. Assessing the influence of large diurnal temperature variations in non-temperate zones on denitrification/nitrification rates using the cost benchmark asm no.1 simulation. *IWA Specialised Conference "Nutrient Management in Wastewater Treatment Processes and Recycle Streams"*. Lemtech, Krakow, Poland. 130

Paul, P., B. Ulanicki, F. Lueder. 2007. Development of a microfiltration fouling model to be linked to the biology of an mbr system. *7th Aachen Membranes and Water Conference*. Department's of Chemical Engineering and Environmental Engineering, RWTH Aachen University, Germany. 142, 144, 148

Paul, Parneet, Christoph Hartung. 2008. Modelling of biological fouling propensity by inference in a side stream membrane bioreactor. *Desalination* **224**(1-3) 154 – 159. doi:DOI:10.1016/j.desal.2007.02.087. URL http://www.sciencedirect.com/science/article/B6TFX-4RSBPRX-Y/2/2ae7ee73b76b220c4ce4fc1c580d3328. Issues 1 and 2: 11th Aachener Membran Kolloquium, 28-29 March 2007, Aachen, Germany - Issue 3: Aqua 2006, 2nd International Conference on Water Science and Ttechnology - Integrated Management of Water Resources, November 2006, Athens, Greece. 212

Peinemann, K. V., S. P. Nunes. 2001. *Membrane technology in the chemical industry*. Wiley-VCh, Weinheim, Germany. 8, 10

Petersen, B., K. Gernaey, P.A. Vanrolleghem. 2001. Practical identifiability of model parameters by combined respirometric - titrimetric measurements. *Water Science and Technology* **43(7)** 347–356. 22, 202

Pollice, Alfieri, Adam Brookes, Bruce Jefferson, Simon Judd. 2005. Sub-critical flux fouling in membrane bioreactors – a review of recent literature. *Desalination* **174**(3) 221 – 230. doi:DOI:10.1016/j.desal.2004.09.012. URL http://www.sciencedirect.com/science/article/B6TFX-4GT7MHY-1/2/91614a8c5470cb370e7db0f9092a0291. 15

Porter, M.C. 1972. Concentration polarization with membrane ultrafiltration. *Ind. Eng. Chem., Prod. Res. Dev.,* **11(3)** 234. 20

PSE. 2004. gproms introductory user guide and gproms advanced user guide. URL http://www.psenterprise.com/gPROMS. 132

Psoch, C., S. Schiewer. 2006. Resistance analysis for enhanced wastewater membrane filtration. *Journal of Membrane Science* **280**(1-2) 284–297. URL http://www.sciencedirect.com/science/article/B6TGK-4J9N0SS-1/2/fe4c655a129fe5ac5e53345675007313. 30, 38, 40

Qiaoa, Junfei, Huidong Wang. 2008. A self-organizing fuzzy neural network and its applications to function approximation and forecast modeling. *Neurocomputing* **71** 564–569. 46

Raťduly, B., K.V. Gernaey, A.G. Capodaglio, P.S. Mikkelsen, M. Henze. 2007. Artificial neural networks for rapid wwtp performance evaluation: Methodology and case study. *Environmental Modelling & Software* **22** 1208–1216. 46

Reichl, G. 2004. Wastewater: a library for modelling and simulation of wastewater treatment plants in modelica. URL http://www.systemtechnik.tu-ilmenau.de/~fg_opt/wastewater/help/WasteWater_ASM1.html/WasteWater.ASM1. 131, 132

Rosenberger, S., C. Laabs, B. Lesjeanc, R. Gnirssd, G. Amy, M. Jekelb, J.-C. Schrottera. 2006. Impact of colloidal and soluble organic material on membrane performance in membrane bioreactors for municipal wastewater treatment. *Water Research* **40** 710 –720. 14, 15, 104, 105

Rosenberger, Sandra, Matthias Kraume. 2002. Filterability of activated sludge in membrane bioreactors. *Desalination* **146(1)** 373–379. 29

Sarioglu, M., G. Insel, N. Artan, D. Orhon. 2009. Model evaluation of simultaneous nitrification and denitrification in a membrane bioreactor operated without an anoxic reactor. *Journal of Membrane Sci-*

ence **337**(1-2) 17–27. URL http://www.sciencedirect.com/science/article/B6TGK-4VXTSJT-8/2/ec729101da646d4c493766258358522e. 31

Saroj, Devendra P., Giuseppe Guglielmi, Daniele Chiarani, Gianni Andreottola. 2008. Modeling and simulation of membrane bioreactors by incorporating simultaneous storage and growth concept: an especial attention to fouling while modeling the biological process. *Desalination* **221**(1-3) 475–482. URL http://www.sciencedirect.com/science/article/B6TFX-4RMGVXR-24/2/e331aab07c115b2321ae69077f507f5f. 42

Seminario, Luis, Roberto Rozas, Rodrigo Bórquez, Pedro G. Toledo. 2002. Pore blocking and permeability reduction in crossflow microfiltration. *Journal of Membrane Science* **209(1)** 121–142. 39

Sin, G., A. Guisasola, D.J.W. De Pauw, J.A. Baeza, J. Carrera, P.A. Vanrolleghem. 2005. A new approach for modelling simultaneous storage and growth processes for activated sludge systems under aerobic conditions. *Biotech. Bioeng.* **92(5)** 600–613. 42

Smets, I. Y., J. V. Haegebaert, R. Carrette, J. F. Van Impe. 2003. Linearization of the activated sludge model asm1 for fast and reliable predictions. *Wat. Res.* **37** 1831–1851. 131

Stare, Aljaz, Nadja Hvala, Darko Vrecko. 2006. Modeling, identification, and validation of models for predictive ammonia control in a wastewater treatment plantŮa case study. *ISA Transactions* **45(2)** 159–174. 48

Stephenson, Tom, Simon Judd, Bruce Jefferson, Keith Brindle. 2000. *Membrane bioreactor for wastewater treatment*. IWA Publishing. 19, 41

Strathmann, H. 1986. Preparation of microporous membranes by phase inversion processes. E. Drioli, M. Nakagaki, eds., *Membranes and membrane processes*. Plenum Press, NY, USA. 9

Takacs, I., G. G. Patry, D. Nolasco. 1991. A dynamic model of the clarification-thickening process. *Wat. Res.* **25** 1263–1271. 21, 130, 133

Tan, P. C., C. S. Berger, K. P. Dabke, R. G. Mein. 1991. Recursive identification and adaptive prediction of wastewater flows. *Automatica* **27**(5) 761–768. URL http://www.sciencedirect.com/science/article/B6V21-47WTGJJ-WB/2/a473c72df854144d3d0652b2b76697cd. 45

Tardieu, E., A. Grasmick, V. Geaugey, J. Manem. 1998. Hydrodynamic control of bioparticle deposition in a mbr applied to wastewater treatment. *Journal of Membrane Science* **147(1)** 1–12. 30

Ulbricht, M., A. Papra. 1997. Polyacrylonitrile enzyme ultrafiltration membranes prepared by adsorption, cross-linking, and covalent binding. *Enzyme Microb. Tech.* **20(1)** 61–68. 12

van Veldhuizen, H. M., M. C. M. van Loosdrecht, J. J. Heijnen. 1999. Modelling biological phosphorus and nitrogen removal in a full scale activated sludge process. *Wat. Res.* **33(16)** 3459–3468. 131

Vela, Vincent, María Cinta, Silvia Álvarez Blanco, Jaime Lora-García, Enrique Bergantiños-Rodríguez. 2006. Application of a dynamic model that combines pore blocking and cake formation in crossflow ultrafiltration. *Desalination* **200**(1-3) 138–139. URL http://www.sciencedirect.com/science/article/B6TFX-4KKPCN1-20/2/13d0cff71fb94e89657341af9b7803c5. 38, 40

Vocks, Martin, Ute Bracklow, Anja Drews, Boris Lesjean, Jan Mante, Matthias Kraume.

2006. Comparison of polysaccharide concentration and fouling rates in different membrane activated sludge systems. *Desalination* **199**(1-3) 381 – 383. doi:DOI:10.1016/j.desal.2006.03.211. URL http://www.sciencedirect.com/science/article/B6TFX-4KKPCMX-54/2/4d74f8af614755d4b486f3f81bd87744. Euromembrane 2006. 15

Wang, Zhan, Yin Song, Mei Liu, Jinmiao Yao, Yuanyuan Wang, Zhang Hu, Zhaohui Li. 2009. Experimental study of filterability behavior of model extracellular polymeric substance solutions in dead-end membrane filtration. *Desalination* **249**(3) 1380–1384. URL http://www.sciencedirect.com/science/article/B6TFX-4XC973H-2/2/24313c0f19bf719b2025b09364121eb1. 32

Wintgens, T., M. Gallenkemper, T. Melin. 2002. Endocrine disrupter removal from wastewater using membrane bioreactor and nanofiltration technology. *Desalination* **146(1-3)** 387–391. 12

Wintgens, T., J. Rosen, T. Melin, C. Brepols, K. Drensla, N. Engelhardt. 2003. Modelling of a membrane bioreactor system for municipal wastewater treatment. *Journal of Membrane Science* **216** 55–65. 37, 40

Wisniewski, C., A. Grasmick. 1998. Floc size distribution in a membrane bioreactor and consequences for membrane fouling. *Colloids Surf. A Physicochem. Eng. Aspects* **138** 403–411. 30

Yang, Wenbo, Nazim Cicek, John Ilg. 2006. State-of-the-art of membrane bioreactors: Worldwide research and commercial applications in north america. *Journal of Membrane Science* **270**(1-2) 201–211. URL http://www.sciencedirect.com/science/article/B6TGK-4GX1J16-4/2/0f0848412134b17948e3c54127d76331. 15

Ye, Y., V. Chen, A.G. Fane. 2006. Modeling long-term subcritical filtration of model eps solutions. *Desalination* **191**(1-3) 318 – 327. doi:DOI:10.1016/j.desal.2005.04.128. URL http://www.sciencedirect.com/science/article/B6TFX-4JTNDNN-1H/2/a6d188c61c6bdf479a1142754288a658. International Congress on Membranes and Membrane Processes. 38

Ye, Y., P. Le Clech, V. Chen, A.G. Fane. 2005a. Evolution of fouling during crossflow filtration of model eps solutions. *Journal of Membrane Science* **264**(1-2) 190 – 199. doi:DOI:10.1016/j.memsci.2005.04.040. URL http://www.sciencedirect.com/science/article/B6TGK-4GCX0BR-3/2/4ff4b40d18204a9c44ee763bd466fca7. 33, 34, 36

Ye, Y., P. Le Clech, V. Chen, A.G. Fane, B. Jefferson. 2005b. Fouling mechanisms of alginate solutions as model extracellular polymeric substances. *Desalination* **175**(1) 7 – 20. doi:DOI:10.1016/j.desal.2004.09.019. URL http://www.sciencedirect.com/science/article/B6TFX-4GT7MJ0-3/2/0cf2db496447bef0ee0d92a89181ea52. Conference on Fouling and Critical Flux: Theory and Applications. 33, 40

Yoo, Chang Kyoo, Peter A. Vanrolleghem, In-Beum Lee. 2003. Nonlinear modeling and adaptive monitoring with fuzzy and multivariate statistical methods in biological wastewater treatment plants. *Journal of Biotechnology* **105** 135–163. 24, 46

Yujun, W., X. Jian, L. Guansheng, D. Youyuan. 2008. Immobilization of lipase by ultrafiltration and cross-linking onto the polysulfone membrane surface. *Bioresource Technol.* **99(7)** 2299–2303. 12

Zarragoitia-González, Alain, Sylvie Schetrite, Marion Alliet, Ulises Jáuregui-Haza, Claire Albasi.

2008. Modelling of submerged membrane bioreactor: Conceptual study about link between activated slugde biokinetics, aeration and fouling process. *Journal of Membrane Science* **325**(2) 612–624. URL http://www.sciencedirect.com/science/article/B6TGK-4TC34W7-2/2/37a448862130804b2cee198a18b3871c. 37

Zydney, A. L., C. K. Colton. 1987. A concentration polarisation model for the filtrate flux in crossflow microfiltration of particulate suspensions. *Chem. Eng. Commun.* **47** 1–27. 20